Ph.D. Thesis

Université de Limoges

University of Limoges

ED 652 - Biologie, Chimie, Santé (BCS)

XLIM - UMR CNRS 7252

A thesis submitted to University of Limoges

in partial fulfillment of the requirements of the degree of

Doctor of Philosophy (PhD)

Recherche clinique, innovation technologique et thérapeutique, santé publique

Code course: ED615

Presented and defensed by

Francesco DIANA

On December 12, 2025

Rosuvastatin for intracranial aneurysms treated with flow diverter: preclinical study in rabbits

Thesis supervisor: Prof. Aymeric ROUCHAUD and Prof. Charbel MOUNAYER

JURY:

President of jury

M. Charbel MOUNAYER, Professor, Service de Neuroradiologie, CHU Limoges, France

M. Aymeric ROUCHAUD, Professor, Service de Neuroradiologie, CHU Limoges, France

Reporters

M. Maxime GAUBERTI, Professor, Service de Radiologie Diagnostique et Interventionnelle, Centre Hospitalier Universitaire de Caen Normandie, France

M. Sébastien SOIZE, Professor, Department of Intervention Neuroradiology, Reims University Hospital, Reims, France

Examiners

M. Nicolas PICARD, Professor Pharmacogénétique, Service de Pharmacie, CHU Limoges, France

Mme. Voahirana RATSIMBAZAFY, Professor, Service de Pharmacie, CHU Limoges, France

Mme. Graciela PAVON-DJAVID, Professor, U1148 INSERM, Laboratory for Vascular Translational Science, Université Sorbonne Paris Nord, France

Guests

M. Francesco DI SALLE, Professor, Department of Medicine, Surgery and Dentistry, Scuola Medica Salernitana, Section of Neurosciences, University of Salerno, Salerno, Italy

License CC BY-NC-ND 4.0



UNIVERSITÀ DEGLI STUDI DI SALERNO
DIPARTIMENTO DI MEDICINA, CHIRURGIA E ODONTOIATRIA
"SCUOLA MEDICA SALERNITANA"

CORSO DI DOTTORATO DI RICERCA IN
MEDICINA TRASLAZIONALE DELLO SVILUPPO E
DELL'INVECCHIAMENTO ATTIVO

MARCATORI MOLECOLARI, RADIOLOGICI, CLINICI E COGNITIVO-COMPORTAMENTALI DELLO SVILUPPO E DEL DECLINO FUNZIONALE - 88031-03

TESI DI DOTTORATO

Rosuvastatin for intracranial aneurysms treated with flow diverter: preclinical study in rabbits

Il Tutor
Ch.mo Prof
Francesco Di Salle

Il Co-Tutor
Ch.mo Prof
Aymeric Rouchaud

Candidato
Francesco Diana
Matr. 8803100025

ANNO ACCADEMICO 2023 - 2024

License CC BY-NC-ND 4.0

Acknowledgements

I would like to thank Professor Aymeric ROUCHAUD for having agreed to supervise this thesis. Thank you infinitely for your trust and your support. Your big personality is a guide for the entire EMIS Lab. I hope we will have the opportunity to continue working together on many projects. Please accept here the expression of my sincere gratitude for all that you have given me, and my deepest respect.

I would like to thank Professor Charbel MOUNAYER, for his trust in the project. The deep sense of admiration I felt while listening your lectures is what inspired me to carry out the project in the EMIS lab. The depth of your understanding of complex neurovascular diseases is, for me, a goal to aspire to. Please accept my gratitude and admiration.

I would like to thank the Professors Maxime GAUBERTI, Sébastien SOIZE, and Graciela PAVON-DJAVID who kindly accepted to be reviewers or examiners of this thesis. Thank you for your efforts. I hope that we will have the opportunity to collaborate on future research projects.

I would like to thank all the people directly and indirectly connected with the EMIS Lab: Professors Nicolas PICARD and Voahirana RATSIMBAZAFY and their respective teams, Géraud FORESTIER, Maxime BAUDOUIN, Romain CHAUVET, Faraj TERRO, Jeremy MOUNIER, Aurélien LE FLAHEC, Sylvia BARDET, Kevin JANOT, Jon CORTESE, Alexis BELGACEM, Florence BOSSELUT, the Xray technicians, Delphine TARNAUD, Claude COUQUET, Caroline CROGUENNEC. Without your valuable help, this project would not have been completed.

I would like to thank all the companies that supported the study, particularly Balt for generously providing the flow diverters. A special thanks to Mohamed Bahri for your direct support. Thank you to all the funders who contributed to the financial support of the study.

I would like to thank Professor Francesco DI SALLE for giving me the opportunity to link this project to the University of Salerno through a dual degree PhD. Your commitment to

License CC BY-NC-ND 4.0

neuroscience, which I was able to appreciate during the three years spent at “San Leonardo”, is a model to follow. Please accept my sincere gratitude.

Finally, I thank those who have always watched over me, trusted me, and supported me unwaveringly in all my projects. I want to thank my parents from the bottom of my heart for being there and supporting me all these years. I will never thank you enough for everything you do for me.

To my grandparents, who would have been proud of me even without any academic achievement.

To my friends, for whom I am nothing more than Francesco, for your presence, loyalty, and all the time spent together.

To those whose names do not appear here, but who accompanied, guided, and supported me throughout my journey!

License CC BY-NC-ND 4.0

Rights

This creation is available under a Creative Commons contract:

« Attribution-Non Commercial-No Derivatives 4.0 International »

online at https://creativecommons.org/licenses/by-nc-nd/4.0/



Table of Contents

Acknowledgements 4
Rights 6
Table of Contents 7
List of Figures 10
List of Tables 12
Abstract 13
Abbreviation list 15
Chapter I. Introduction to Intracranial Aneurysms 17
I.1. Epidemiology 18
I.2. Pathophysiology 19
I.3. Biological mechanisms 20
I.4. Treatment 23
I.4.1. Endovascular treatment 24
Chapter II. Improve the outcome of the treated IA 30
II.1. Definition of Complex IA 30
II.2. Creation of a morbidity and mortality risk score 31
II.3. Alternative technique for ruptured IA 33
Chapter III. Flow Diverter 36
III.1.1. History of FD stent 36
III.1.2. Mechanism of action and biology of flow diversion 38
III.2. Clinical evidences on FD efficacy and safety 43
III.3. Limits of the treatment 46
III.4. Risks of FD treatment 51
III.4.1. Aneurysm patency 51
III.4.2. Risk of delayed rupture 52
III.4.3. Distal intracerebral hemorrhage 53
III.4.4. Covered branches and risk of occlusion 54
Chapter IV. Antiplatelet therapy and FD coatings 56
IV.1. Double antiplatelet therapy 56
IV.2. Single antiplatelet therapy 58
IV.3. Antiplatelet therapy and FD healing 58
Chapter V. Wall-oriented treatment strategies 60

License CC BY-NC-ND 4.0

V.1. Biological optimization of FDs 60
V.2. Stimulation of proliferative response 63
V.3. Prevention of aneurysm wall cell injury 64
V.4. Inhibition of inflammation and oxidative stress 65
V.5. Inhibition of extracellular matrix degradation 68
Chapter VI. Statins as wall-oriented treatment 70
VI.1. Pleiotropic effect of statins 70
VI.1.1. Statin and endothelium 73
VI.1.2. Statin and smooth muscle cells 74
VI.1.3. Statin and platelets 75
VI.2. Rosuvastatin as wall-oriented strategy 76
Chapter VII. Rationale for Rosuvastatin therapy to enhance FD healing 79
VII.1. Main thesis questions 80
Chapter VIII. Preparation of the rabbit model 83
VIII.1. Rabbit model creation and FD deployment 83
VIII.2. FD deployment 85
VIII.3. Rosuvastatin and Aspirin administration 88
VIII.4. Timeline of the follow-up 89
VIII.5. Aneurysm occlusion assessment 90
VIII.6. Patency of covered branches assessment 91
VIII.7. Histological analysis 92
VIII.8. Rosuvastatin serum concentration measurement 96
VIII.9. Correlation between Rosuvastatin serum concentration and FD struts coverage 97
VIII.10. Budget and resources 97
Chapter IX. Effect of Rosuvastatin on FD treatment 99
IX.1. Summary of the study design 99
IX.2. Main results of the study 100
IX.2.1. Aneurysm occlusion 101
IX.2.2. Branches covered by the FD 102
IX.2.3. Composite outcome 104
IX.2.4. Histomorphological analysis FD/stent coverage by neotissue 105
IX.2.5. MPM in stented aorta: endothelial cells and collagen 107
IX.2.6. Rosuvastatin concentration and endothelialization 109
IX.3. Discussion 110

License CC BY-NC-ND 4.0

IX.4. Future scenarios 113
IX.5. Translation of these results in a RCT 115
IX.6. Statin therapy and FDSM 118
IX.7. Rosuvastatin coated FD 119
IX.8. Oral Rosuvastatin vs Rosuvastatin coated FD 120
Conclusion 123
Bibliography 125
Appendices 150
Appendix 1. DELPHI consensus on CIA 151
Appendix 2. MARTA score 160
Appendix 3. IFD-assisted coiling 175
Appendix 4. FD with or without coils 185
Appendix 5. Article Rosuvastatin 194
Appendix 6. Article P8RI-coated Silk Vista versus Pipeline Vantage (Shield) 204

License CC BY-NC-ND 4.0

List of Figures

Figure 1. Examples of intracranial aneurysms 17

Figure 2. Schematic outlining the inflammatory mediators involved in aneurysm formation and progression to rupture 21

Figure 3. How hemodynamics plays into intracranial aneurysm dynamics 22

Figure 4. Role of high and low WSS in aneurysm initiation, growth, and rupture 23

Figure 5. Treatments of the intracranial aneurysms previously described in Figure 1 25

Figure 6. Intrasaccular devices actually available 26

Figure 7. Stents most commonly used for the treatment of intracranial aneurysms 28

Figure 8. Pointplot for risk of combined primary outcome EVT and NT 33

Figure 9. Cases of intrasaccular flow disruptor-assisted coiling (IFD-AC) 34

Figure 10. Some flow diverters commercialized 37

Figure 11. Mechanism of flow diversion 38

Figure 12. Relation between porosity and hemodynamic changes 40

Figure 13. Cellular and molecular mechanisms underpinning device endothelialization follow flow diversion treatment of cerebral aneurysms 42

Figure 14. Examples of shear-driven and inertia-driven types 49

Figure 15. Intrasaccular flow alteration induced by different stents 50

Figure 16. Forest plots of tailored dual antiplatelet therapy (DAPT) vs conventional DAPT . 57

Figure 17. Chart showing the approaches taken by various surface modifications to reduce or eliminate the need for dual antiplatelet therapy (DAPT) 61

Figure 18. Principal functions of CD31 63

Figure 19. Inflammatory reaction associated with intracranial aneurysm (IA) formation 67

Figure 20. Pleiotropic effects and mechanisms of statins in various organs or systems 71

Figure 21. Mechanism of the pleiotropic effects of statins 72

Figure 22. Pleiotropic effects and mechanisms of statins in cerebrovascular ECs 74

Figure 23. Statins as antithrombotic drug 76

Figure 24. Elastase-induced aneurysm model in the rabbit 85

Figure 25. Protocol of FD implantation 86

Figure 26. High-Frequency Optic Coherence Tomography 87

Figure 27. Schematic illustration of modified O'Kelly-Marotta scale 91

Figure 28. Covered branch patency 92

Figure 29. Histology of the aneurysmal neck 93

Figure 30. Multiphoton microscopy 96

License CC BY-NC-ND 4.0

Figure 31. Study protocol 100

Figure 32. DSA controls 101

Figure 33. HF-OCT controls 103

Figure 34. Effects of Rosuvastatin on strut coverage by neotissue 106

Figure 35. Multiscale analysis of neotissue formation and extracellular matrix remodeling following flow-diverter stent (FD) implantation in rabbit arteries 108

Figure 36. Pearson's correlation between Rosuvastatin concentration and DAPI-positive nuclei endothelial cells, Collagen SHG-positive fibers, and collagen directionality score 110

Figure 37. PLGA-Rosuvastatin-loaded stent 120

License CC BY-NC-ND 4.0

List of Tables

Table 1. MARTA score 32
Table 2. Parameters related to the stent design. 48
Table 3. Histomorphological analysis protocol. 94
Table 4. DSA and HF-OCT outcomes. 104

License CC BY-NC-ND 4.0

Abstract

Intracranial aneurysms (IAs) are pathological dilatations of the cerebral arterial wall, affecting 2-3% of the adult population. Their rupture leads to subarachnoid hemorrhage, a devastating condition associated with high morbidity and mortality. Flow diverters (FD) have changed aneurysm treatment by reconstructing the parent artery and promoting aneurysm exclusion through progressive endothelialization. However, FD therapy has limitations, including thromboembolic events, incomplete aneurysm occlusion in up to 20% of cases, and risk of occlusion of covered side branches.

Statins, have pleiotropic vascular effects that can optimize the FD healing. In addition to cholesterol lowering effect, statins enhance nitric oxide (NO) bioavailability, mobilizes endothelial progenitor cells (EPCs), reduces inflammation, and improves endothelial repair. These mechanisms could promote FD struts endothelialization, leading to faster and complete aneurysm occlusion with higher side branch patency.

This thesis investigated the effect of Rosuvastatin on FD healing in a preclinical rabbit model. Elastase-induced aneurysms were created in the right common carotid artery of 22 rabbits. Four weeks later in each rabbit, FDs were implanted in the subclavian artery, covering the elastase-induced aneurysm (efficacy assessment), and in the descending aorta, covering the lumbar branches (assessment of covered branches patency). Rabbits were randomized to receive either Rosuvastatin plus Aspirin (Rosu+ASA, n=13) or Aspirin alone (ASA, n=9). After two weeks, aneurysm occlusion was assessed angiographically with the O'Kelly-Marotta (OKM) scale, side branches patency with high-frequency optical coherence tomography (HF-OCT), and struts coverage with histology and Multiphoton Microscopy (MPM). Serum Rosuvastatin concentration was correlated with endothelialization.

Results showed a trend toward higher complete aneurysm occlusion in the Rosu+ASA group (84.6% vs 66.6%). Side branch patency was significantly improved, both for vessels ≥1 mm (94.4% vs 46.1%, p=0.007) and <1 mm (95.4% vs 73.4%, p=0.036). The composite outcome

License CC BY-NC-ND 4.0

(complete occlusion with all branches patent) favored Rosuvastatin (76.9% vs 22.2%, p=0.011). Histology demonstrated a tendency toward increased strut coverage and neointimal thickness with Rosu+ASA, and the amount of endothelial covering stent strut (assessed with the MPM) had a strong positive correlation with the Rosuvastatin serum levels (r=0.92, p=0.02).

In conclusion, in this elastase-induced aneurysm model Rosuvastatin therapy enhanced FD treatment by promoting aneurysm occlusion, preserving side branch patency, and supporting endothelialization. These findings support the hypothesis that Rosuvastatin may enhances flow diversion efficacy and safety, needing further preclinical validation and potential clinical trials.

License CC BY-NC-ND 4.0

Abbreviation list

ACA	Anterior Cerebral Artery
ACoA	Anterior Communicating Artery
bFGF	Basic Fibroblast Growth Factor
CCA	Common Carotid Artery
CFA	Common Femoral Artery
CFD	Computational Fluid Dynamics
CIA	Complex Intracranial Aneurysm
DAPI	4′,6-diamidino-2-fenilindolo
ECs	Endothelial Cells
ECM	Extracellular Matrix
eNOS	Endothelial NO Synthase
EVT	Endovascular Treatment
EPCs	Endothelial Progenitor Cells
ETBR	Endothelin B Receptors
FD	Flow Diverter
FDSM	Flow Diverter with Surface Modification
GGPP	geranylgeranyl pyrophosphate
H&E	Hematein and Eosin
HMG-CoA	Hydroxymethylglutaryl Coenzyme A
HO-1	Heme Oxygenase-1
IAs	Intracranial Aneurysms
ICA	Internal Carotid Artery
IFD	Intrasaccular flow disruptors
IL-1β	Interleukin-1β
iNOS	Inducible Nitric Oxide Synthase
KLF2	Kruppel-like Factor-2
LC-MS/MS	Liquid Chromatography-tandem Mass Spectrometry

License CC BY-NC-ND 4.0

LDL-C	Low-Density Lipoprotein Cholesterol
MCA	Middle Cerebral Artery
MCP-1	Monocyte Chemoattractant Protein-1
MMP	Matrix Metalloproteinases
NADPH	Nicotinamide Adenine Dinucleotide Phosphate
NIT	NeoIntimal Thickness
NO	Nitric Oxyde
mRS	Modified Rankin Scale
OKM	O'Kelly-Marotta scale
PComA	Posterior Communicating Artery
PLGA	Poly(D,L)-Lactide-co-Glycolide
RIA	Ruptured Intracranial Aneurysm
ROS	Reactive Oxygen Species
Rosu	Rosuvastatin
SAC	Stent Assisted Coiling
SAH	Subarachnoid Hemorrhage
SC	Strut Coverage
SHG	Second-Harmonic Generation
SMCs	Smooth Muscle Cells
NF-κB	Transcription Factor Nuclear factor-Kappa B
UIA	Unruptured Intracranial Anerysm
VCAM-1	Vascular Cell Adhesion Molecule-1
VEGF-A	Vascular Endothelial Growth Factor A
WSS	Wall Shear Stress

License CC BY-NC-ND 4.0

Chapter I. Introduction to Intracranial Aneurysms

An intracranial aneurysm (IA) is defined as an abnormal dilatation of the arterial wall of intracranial blood vessels. These lesions most commonly occur at arterial bifurcations within the circle of Willis, such as the internal carotid artery (ICA), anterior (ACoA) and posterior communicating arteries (PComA), and middle cerebral artery (MCA). Saccular aneurysms account for approximately 90% of cases, while less common types include fusiform, mycotic, and dissecting aneurysms (Figure 1). The pathogenesis involves degeneration of the internal elastic lamina, endothelial dysfunction, hemodynamic stress, and inflammation, which collectively contribute to instability and potential rupture of the vascular wall.[1]

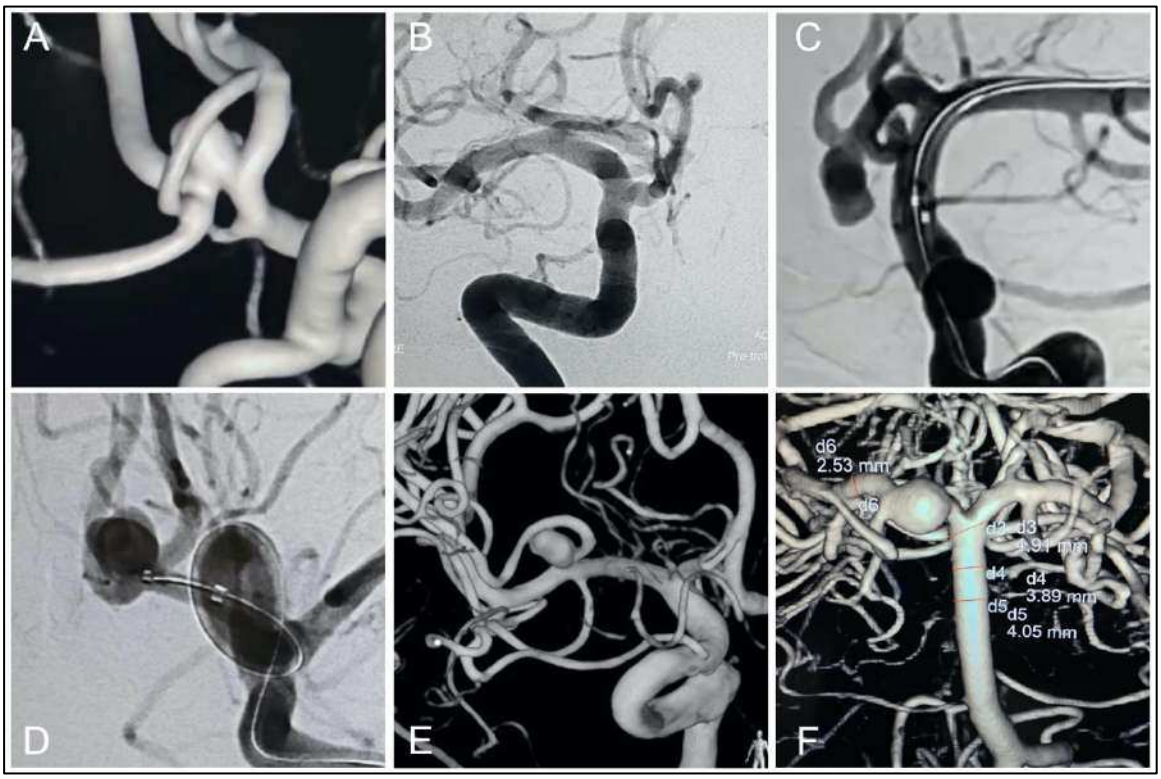


Figure 1. Examples of intracranial aneurysms. (A) Saccular aneurysm of the anterior communicating artery complex on a fenestration. (B) Saccular aneurysm of the superior hypophyseal segment of the right internal carotid artery. (C/D) Saccular aneurysm of the anterior communicating artery complex with dominance of the left A1 segment of the anterior cerebral artery and hypoplasia of the right one. (E)

License CC BY-NC-ND 4.0

Saccular aneurysm of the right middle cerebral artery on the origin of the fronto-opercular branch. (F) Fusiform aneurysm of the right posterior cerebral artery at the level of the P1 segment.

I.1. Epidemiology

The prevalence of unruptured IAs in the general adult population is consistently estimated at 2-3%, with detection rates increasing with age and advanced imaging use.[2–4] The risk of harboring multiple aneurysms is higher in women, older individuals, and those with a family history of aneurysms or subarachnoid hemorrhage (SAH); multiple aneurysms are present in approximately 20% of affected patients, and familial clustering is well established.[5–7]

Key risk factors include current smoking (hazard ratio up to 4.1), hypertension (odds ratio up to 2.2), and female sex (odds ratio up to 2.0), with these factors also influencing aneurysm size and multiplicity.[2–5,8,9] The American Heart Association/American Stroke Association guidelines highlight that modifiable risk factors such as hypertension, smoking, and alcohol abuse are strongly associated with both aneurysm formation and rupture, while certain genetic syndromes (e.g., autosomal dominant polycystic kidney disease, Ehlers-Danlos syndrome type IV) confer additional risk.[7]

Demographically, women over age 50 are at highest risk, and aneurysm prevalence increases with age.[2,4,5] Ethnic and geographic differences exist, with higher rates of multiple aneurysms reported in European and North American cohorts.[10] Heritable connective tissue disorders and a positive family history further elevate risk, and familial aneurysms tend to be larger, more often multiple, and more likely to occur at the middle cerebral artery.[6,7] These findings reinforce the interplay between genetic predisposition, vascular risk factors, and demographic patterns in the epidemiology of IAs.

License CC BY-NC-ND 4.0

I.2. Pathophysiology

The etiology of IAs involves a multifactorial process characterized by degeneration of the internal elastic lamina, endothelial dysfunction, hemodynamic stress, and inflammation, which collectively weaken the arterial wall and predispose to aneurysm formation.

Building on the multifactorial etiology described above, recent genetic studies have elucidated a polygenic architecture for IAs, identifying at least 17 risk loci that contribute to disease susceptibility, with notable overlap between genetic risk factors and clinical traits such as hypertension and smoking.[11] Familial clustering and heritable connective tissue disorders, including autosomal dominant polycystic kidney disease, Ehlers-Danlos syndrome, and Marfan syndrome, further underscore the importance of genetic predisposition, with specific gene variants (e.g., perlecan, elastin, collagen type 1 A2, endothelial nitric oxide synthase (eNOS), and interleukin-6) implicated in vascular wall integrity and inflammatory modulation.[6]

The pathophysiology of IAs formation is driven by endothelial dysfunction and abnormal wall shear stress, which initiate vascular inflammation and remodeling. This process involves apoptosis and migration of vascular smooth muscle cells, degradation of the extracellular matrix by matrix metalloproteinases, and infiltration of inflammatory cells, ultimately resulting in focal weakening of the arterial wall.[12–17] Inflammation is a central feature, with both cell-mediated and humoral responses contributing to aneurysm progression and rupture, as evidenced by differential gene expression and histopathological findings in aneurysmal tissue.[14,15,18]

Environmental factors such as chronic hypertension, cigarette smoking, and excessive alcohol consumption act synergistically with genetic susceptibility to accelerate vascular wall degeneration and aneurysm development.[11–13] The interplay between hemodynamic forces, genetic background, and inflammatory responses defines the current consensus on the underlying cause of IAs in the medical literature.[11–18]

License CC BY-NC-ND 4.0

I.3. Biological mechanisms

The biological mechanisms involved in the development and occurrence of IAs include degeneration of the internal elastic lamina, endothelial dysfunction, hemodynamic stress, and inflammation (Figure 2). Genetic predisposition plays a key role, with single-nucleotide polymorphisms in genes such as CDK2NB (cell-cycle regulation and vascular smooth-muscle proliferation), SOX17 (vascular endothelial maintenance), and EDNRA (vascular smooth-muscle response to hemodynamic stress) contributing to susceptibility.

Hemodynamic stress, particularly at the level of the arterial bifurcations, leads to focal injury and remodeling of the vessel wall. This process is exacerbated by modifiable risk factors such as hypertension and cigarette smoking, which independently and synergistically accelerate vascular wall degeneration and promote inflammatory cell infiltration. Inflammation is central for both aneurysm formation and rupture, causing vessel wall matrix degradation and smooth muscle cell apoptosis. Abnormal wall shear stress, particularly at the level of the arterial bifurcations, triggers the endothelial injury, with recruitment of inflammatory cells and upregulation of cytokines such as TNF-α, MCP-1, and matrix metalloproteinases (MMPs). This inflammatory cascade leads to the vascular smooth muscle cell apoptosis, migration, and phenotypic modulation, resulting in thinning and weakening of the vessel wall.[12,13,15] The imbalance between MMPs and their inhibitors increases the degradation of the internal elastic lamina and adventitia, further compromising the vascular wall integrity.[18]

Collectively, these mechanisms explain the epidemiological patterns observed: a higher prevalence in individuals with genetic predisposition, and underlying connective tissue abnormalities after the exposure to vascular risk factors. The central role of inflammation and vascular remodeling in aneurysm pathogenesis is supported by gene expression profiling and histopathological studies, which consistently demonstrate upregulation of immune and matrix-degrading pathways in aneurysmal tissue.[19]

License CC BY-NC-ND 4.0

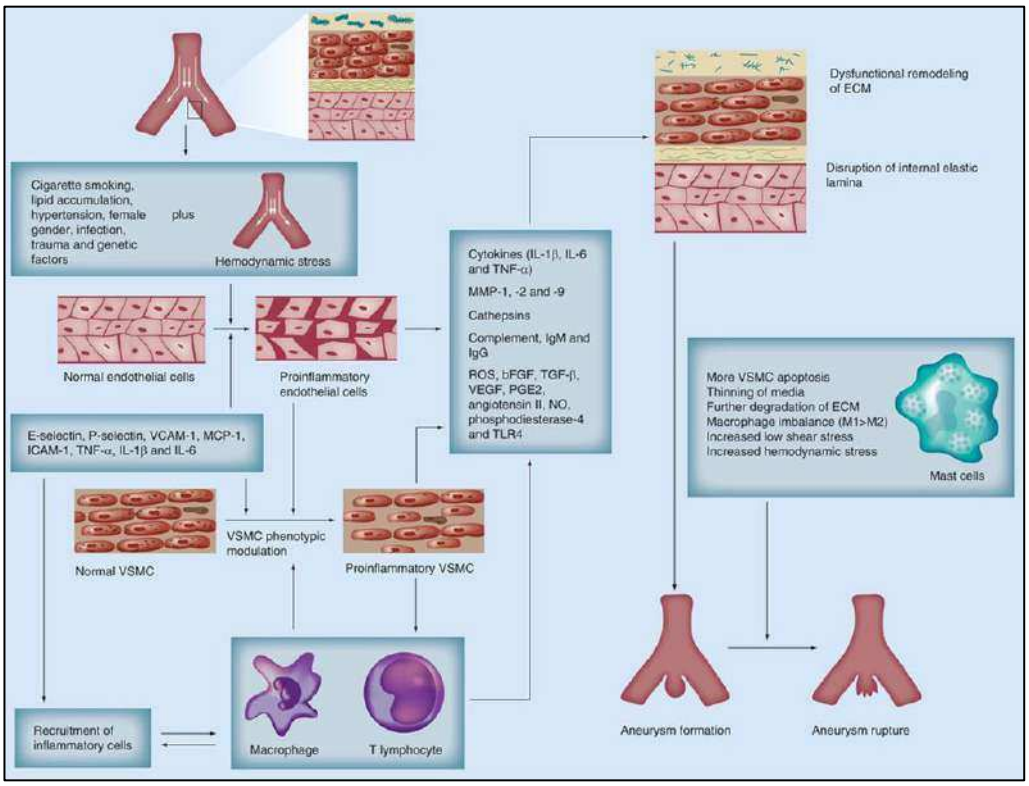


Figure 2. Schematic outlining the inflammatory mediators involved in aneurysm formation and progression to rupture. The hemodynamic stress predisposes the vascular endothelium to remodeling and degeneration process, mediated by macrophages, T lymphocytes, and other inflammatory cells. VSMCs undergo phenotypic modulation to a proinflammatory state, the IEL is disrupted, and the ECM is degraded, leading to aneurysm formation and eventual rupture. bFGF = basic fibroblast growth factor; ICAM = intercellular adhesion molecule; M1 = proinflammatory macrophage; M2 = antiinflammatory macrophage; NK = natural killer cell; PGE = prostaglandin E; ROS = reactive oxygen species; Rosu= Rosuvastatin; TGF = transforming growth factor; TLR = toll-like receptor; VEGF = vascular endothelial growth factor. Republished with permission of Hudson JS, Hoyne DS, Hasan DM: Inflammation and human cerebral aneurysms: current and future treatment prospects. Future Neurol 8:10.2217/fnl.13.40, 2013; permission conveyed through Copyright Clearance Center, Inc.[20]

Rupture occurs when the cumulative effects of genetic vulnerability, vascular wall degeneration, endothelial dysfunction, hemodynamic stress, and sustained inflammation, potentiated by hypertension and cigarette smoking, overwhelm the structural integrity of the aneurysm wall, resulting in catastrophic vessel failure and SAH.[11–18] The hemodynamic might

License CC BY-NC-ND 4.0

play a complex role in this process, particularly wall shear stress (WSS), in aneurysm pathophysiology (Figure 3). WSS is a vectorial force, defined as the tangential force per unit area exerted by flowing blood on the endothelial surface of the vessel wall.[21] Both high and low WSS can contribute to aneurysm progression and rupture, but through distinct biological pathways. High WSS and positive WSS gradient (WSSG= the spatial rate of change of WSS along the vessel wall), is associated with mural-cell-mediated pathways, potentially leading to the formation and rupture of small or secondary bleb-type aneurysms. In contrast, low WSS and high oscillatory shear index (OSI= hemodynamic parameter that quantifies the degree of oscillation or reversal in the direction of WSS, independent of its magnitude) are linked to inflammatory-cell-mediated pathways, which may drive the growth and rupture of larger, atherosclerotic aneurysm phenotypes. These evidences might suggest that aneurysm biology is shaped by a spectrum of hemodynamic environments rather than a single dominant factor (Figure 4).[21]

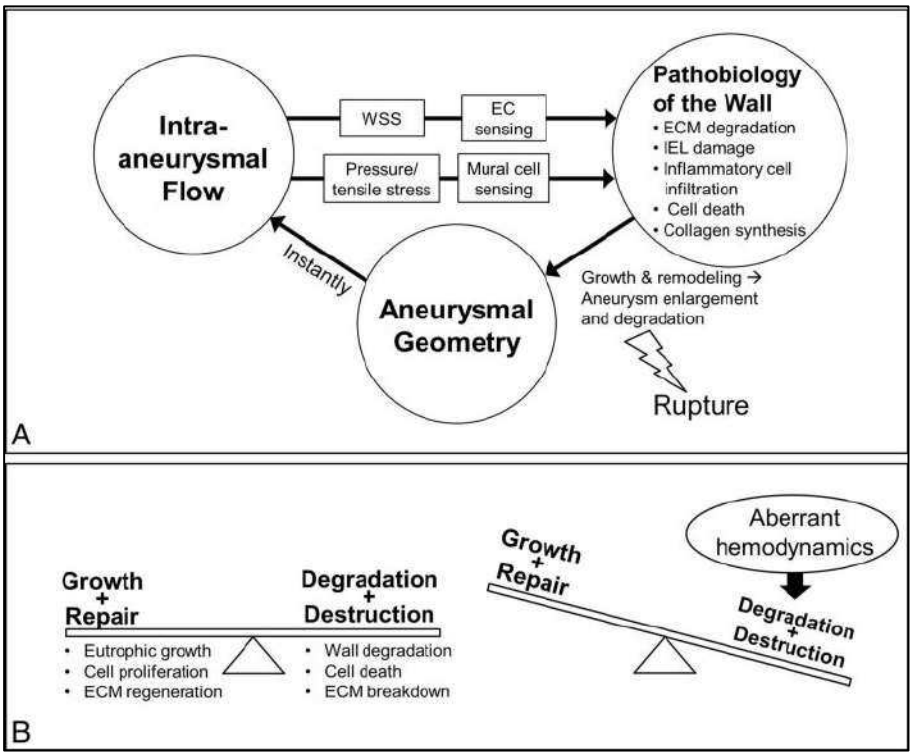


Figure 3. How hemodynamics plays into intracranial aneurysm dynamics. A, Three-way relationship of aneurysmal geometry, flow, and pathobiology. Flow exerts mechanical forces on the vessel wall, eliciting

License CC BY-NC-ND 4.0

cell-mediated biologic pathways. Sustained changes in flow (thus WSS and pressure) lead to remodeling of the wall, resulting in aneurysm geometry change. In turn, geometry determines the flow, which could drive further biologic processes. B, The balance between growth/repair and degradation/destruction results in aneurysm stability. Aberrant hemodynamics disrupts the balance and amplifies degradation and destruction mechanisms, leading to enlargement and rupture of aneurysm. Meng H. AJNR Am J Neuroradiol. 2014.[21]

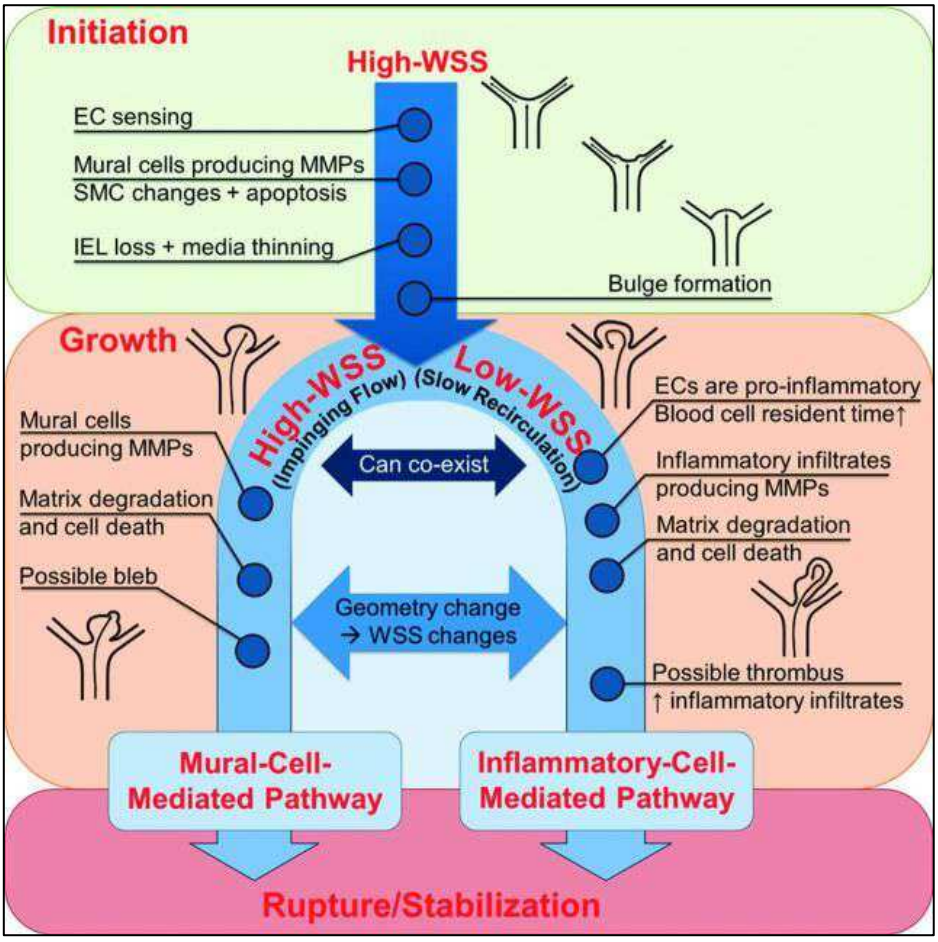


Figure 4. Role of high and low WSS in aneurysm initiation, growth, and rupture. Meng H. AJNR Am J Neuroradiol. 2014.[21]

I.4. Treatment

The aim of the treatment for IAs is to prevent aneurysm rupture[22] or second rupture by achieving durable exclusion of the aneurysm from the cerebral circulation, thereby reducing

License CC BY-NC-ND 4.0

the risk of SAH. Two treatments are actually used to treat IA: endovascular treatment (EVT), including minimally invasive strategies to exclude the sac from the circulation and to heal the parent vessel, and neurosurgical treatment (NT), based on an extravascular approach with the aim to position a metallic clip at the level of the aneurysmal neck to exclude it from the circulation.

I.4.1. Endovascular treatment

The aim of endovascular treatment (EVT) for IAs is to prevent aneurysm rupture or second rupture by achieving durable exclusion of the aneurysm from the cerebral circulation, thereby reducing the risk of SAH. This is accomplished by promoting thrombosis within the aneurysmal sac and reconstructing the parent vessel lumen, which directly addresses the consequences of the underlying biological mechanisms that lead to aneurysm formation and rupture.[1,22]

Endovascular techniques, such as coil embolization and flow diversion, are designed to disrupt intra-aneurysmal blood flow, reduce wall shear stress, and induce stable thrombus formation. By isolating the aneurysm from ongoing hemodynamic stress and blood-borne inflammatory mediators, these interventions mitigate further wall degeneration and inflammatory cell infiltration, which are central to aneurysm progression and rupture.[12,15,22] While EVT does not directly reverse genetic or molecular defects, it interrupts the final common pathway of mechanical and inflammatory injury that precipitates rupture (Figure 5).

License CC BY-NC-ND 4.0

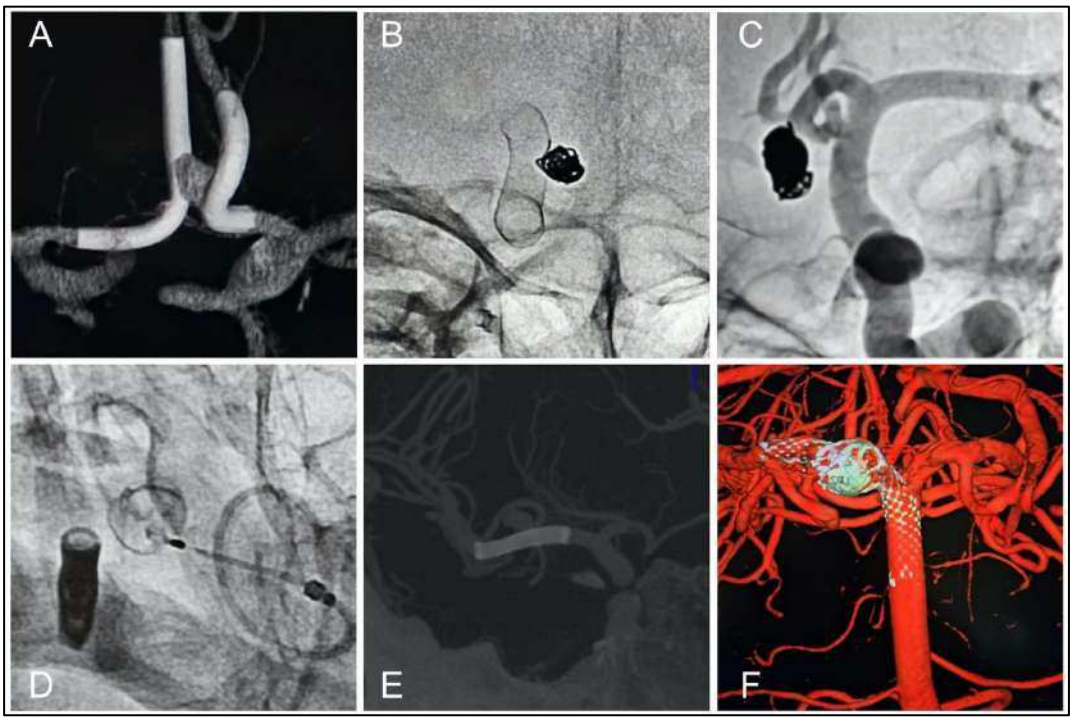


Figure 5. Treatments of the intracranial aneurysms previously described in Figure 1. (A) Double flow diverter. (B) Flow diverter and coils. (C) Coiling. (D) Intrasaccular device (Galaxy SEAL). (E) Flow diverter. (F) Stent assisted coiling.

I.4.1.1. Intrasaccular approach

Coil embolization, the most established intrasaccular technique, has demonstrated high rates of aneurysm occlusion and is associated with lower perioperative morbidity compared to surgical clipping, particularly in the setting of ruptured aneurysms.[1,23,24] The American Heart Association recommends coil occlusion as an appropriate treatment for both ruptured and unruptured aneurysms when technically feasible.[7,23] Adjunctive techniques (balloon- or stent-assisted coiling) have expanded the applicability of coiling to more complex aneurysms.[1,25]

Intrasaccular flow-disrupting devices (e.g., Woven EndoBridge [WEB], Contour, Artisse, Galaxy SEAL) have emerged as effective options for wide-neck and complex aneurysms, providing high rates of complete and satisfactory occlusion with acceptable complication profiles.[25–27] These devices disrupt intra-aneurysmal flow, promoting thrombosis and isolating the aneurysm from ongoing hemodynamic and inflammatory insults, which are central to the

License CC BY-NC-ND 4.0

biological mechanisms of aneurysm progression and rupture.[25–28] However, long-term data on recurrence and retreatment rates remain limited to the WEB device, that is the first one to be used in clinical practise.[25–29]

While these intrasaccular therapies (Figure 6) primarily address the mechanical exclusion of the aneurysm (lumen-oriented), they indirectly mitigate the underlying biological mechanisms (vascular wall degeneration, endothelial dysfunction, hemodynamic stress, and inflammation) by removing the aneurysm from the circulation and halting further wall injury.

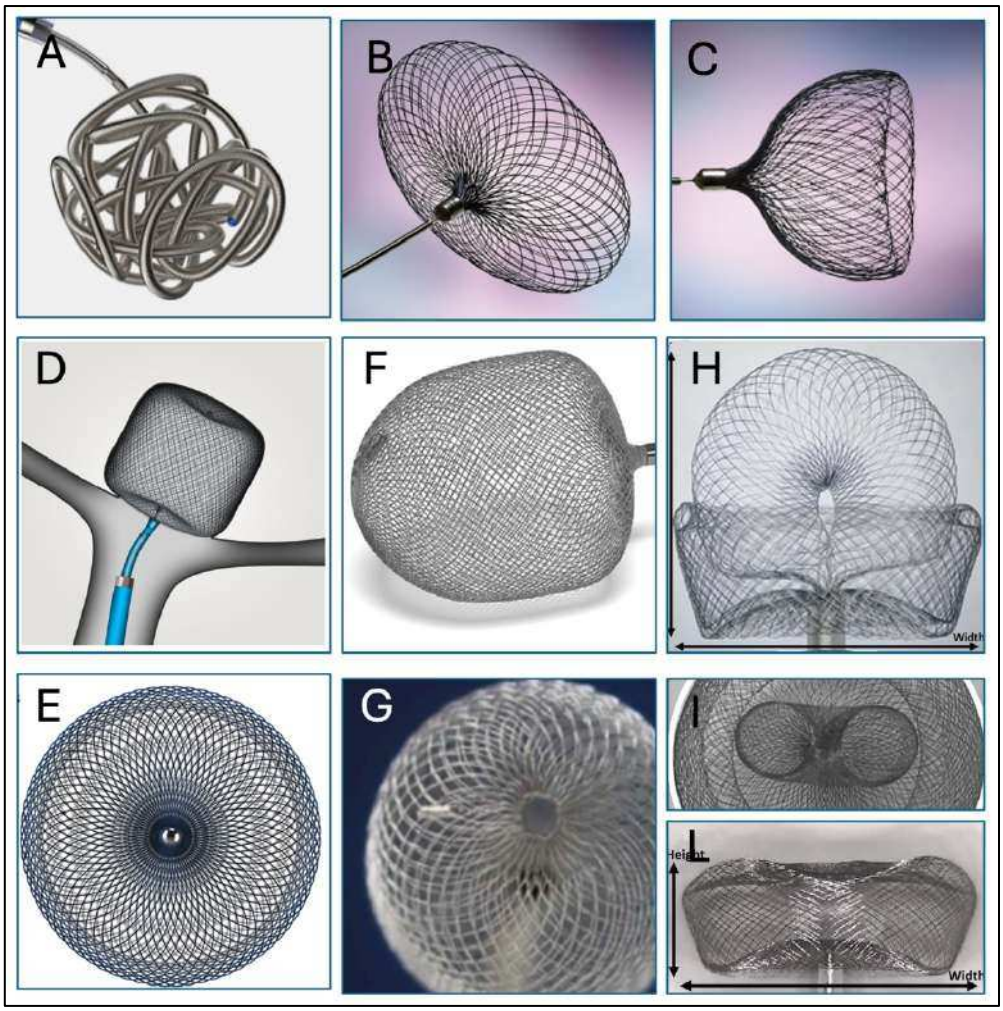


Figure 6. Intrasaccular devices actually available. (A) Coils. (B/C) Contour device. (D/E) Woven EndoBridge device. (F/G) Artisse device. (H/I/L) Galaxy SEAL device.

License CC BY-NC-ND 4.0

I.4.1.2. Extra-saccular approach

The extra-saccular approach for the treatment of IAs includes stent-assisted coiling (SAC) and flow diverter (FD) stents (Figure 7). Both have the aim to reconstruct the parent artery, bridging the aneurysm neck in order to enhance the intraluminal thrombus organization and, if used with other intrasaccular devices, to increase the intrasaccular packing. However, FD is the only one that reduces the intrasaccular flow sufficiently to induce the sac thrombosis without adjunctive intrasaccular devices.

SAC is widely used for wide-neck and complex aneurysms, providing stable anatomical results and expanding the treatable population. FD reconstruct the parent artery and are particularly effective for large, giant, or difficult-to-treat aneurysms, with high long-term occlusion rates and lower recurrence compared to SAC, but with a distinct risk profile including ischemic complications and the need for dual antiplatelet therapy.[23,30,31]

Comparative studies show that the SAC might be replaced by intrasaccular devices (even if the WEB device is the only one to be compared with the SAC). Both treatments achieve similar rates of adequate occlusion and clinical outcomes for wide-neck bifurcation aneurysms, but SAC is associated with higher periprocedural complication rates and often requires antiplatelet therapy.[32–34] The WEB device and other intrasaccular flow disruptors offer comparable efficacy, lower complication rates, and reduced need for adjunctive stenting, making them attractive for patients where antiplatelet therapy is contraindicated.[33–35]

Flow diverters are superior to SAC in long-term occlusion for wide-necked aneurysms, but carry higher risks in certain populations and are generally reserved for aneurysms not amenable to coiling or intrasaccular devices.[23–31] The American Heart Association highlights flow diversion as a major innovation, especially for large or recurrent aneurysms, but notes safety concerns in specific trials.[1]

License CC BY-NC-ND 4.0

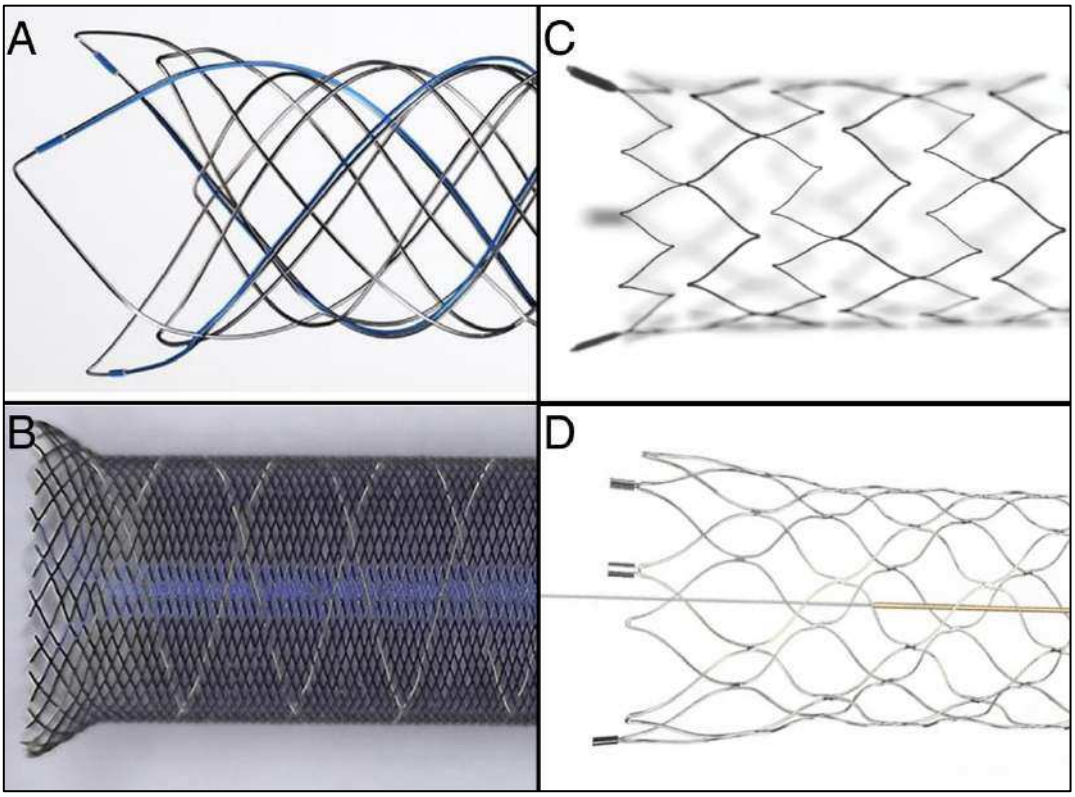


Figure 7. Stents most commonly used for the treatment of intracranial aneurysms. (A) Braided stent, generally with 16 braided wires, used for stent assisted coiling. (B) Flow diverter braided stent, with 48/64 wires. (C) Laser-cut open cells stent, used for stent assisted coiling. (D) Laser-cut closed cells stent, used for stent assisted coiling.

License CC BY-NC-ND 4.0

Summary

Intracranial aneurysms are abnormal dilatations of cerebral arteries, generally located at the level of arterial bifurcations and with saccular shape. Their prevalence is ~3% of the adult population. Risk factors are sex (women population), older age, smoking, hypertension, and genetic predisposition or connective tissue disorders. Their pathogenesis is multifactorial, involving genetic susceptibility, endothelial dysfunction, abnormal hemodynamics, and chronic inflammation, which together weaken the arterial wall and may lead to rupture. Wall shear stress plays a key role, with both high and low stress contributing to aneurysm growth and rupture through different biological pathways.

Endovascular treatments aim to exclude aneurysms from the circulation. Intrasaccular techniques (such as coiling and intrasaccular devices) fill the aneurysmal sac, without reconstructing the parent vessel. These approaches are associated with low complication rates, but carry a higher risk of aneurysm recanalization. Extra-saccular strategies (including stent-assisted coiling and flow diverters) reconstruct the parent vessel, achieving more stable occlusion, but they carry ischemic and hemorrhagic risks. Among extra-saccular strategies, flow diverters have been widely adopted because they promote the healing of the parent vessel, avoiding the risks associated with direct filling of the aneurysmal sac.

License CC BY-NC-ND 4.0

Chapter II. Improve the outcome of the treated IA

II.1. Definition of Complex IA

Scientific literature reports that complex IA (CIA) pose unique diagnostic and therapeutic challenges, but there is not a clear definition of CIA. This lack of a standardized definition leads to considerable heterogeneity in clinical decision-making.[36,37] Furthermore, the criteria used to classify an aneurysm as complex may differ between EVT and NT, and these differences may even influence the choice of treatment approach.

To address this challenge, we used a DELPHI approach to identify the variables that define a CIA according to a panel of experts in both EVT and NT fields (Appendix 1 for the article). An international panel of 50 physicians participated in the field participated in a three-round Delphi process. Panelists completed surveys containing Likert-scale items and open-ended questions. Predefined consensus thresholds were used to establish which variables should define a CIA, and statistical analyses assessed the degree and stability of consensus. For the EVT, the definition of CIA included giant size, very wide neck (dome/neck ratio ≤ 1:1), and collateral branch from the sac. For the NT, CIA were defined by fusiform or blister-like shape, dissecting aetiology, giant size (≥25 mm), broad neck encasing parent arteries, extensive neck surface, wall calcification, intraluminal thrombus, collateral branch from the sac, location (AICA, SCA, basilar), vasospasm context, and planned bypass (EC-IC or IC-IC).

By identifying the variables most strongly associated with aneurysm complexity, we were able to develop a morbidity-mortality risk score for both EVT and NT (presented in the following section). This score can be used in routine clinical practice, ideally in combination with existing scores that assess the risk of aneurysm rupture.

License CC BY-NC-ND 4.0

II.2. Creation of a morbidity and mortality risk score

For unruptured intracranial aneurysms (UIA), both EVT and NT carry a risk of serious complications,[24,38,39] around 4.96% for the EVT and 8.34% for the NT, with variability depending on patient and aneurysm characteristics.[40] For this reason, treatment risks must be weighed against rupture risk, life expectancy, and patient concerns. Nowadays rupture risk scores, like UIATS[41] and PHASES[42], are used to assess the cumulative risk of rupture, using accessible patient and aneurysm data. On the other side, treatment risk scores are less developed, often lack external validation, or are limited to specific treatments.[43–47] To address the need for an evidence-based assessment of the risk associated with treating UIA, we conducted a multicenter retrospective study. We included 1907 UIA receiving EVT (1460 in the development cohort and 447 in the testing cohort) and 740 receiving NT (602 in the development cohort and 138 in the testing cohort) consecutively treated at 15 international tertiary referral neurovascular centers within 2014 and August 2024 (Appendix 2 for the article). With this dataset, we developed and validated the Morbidity and Mortality Associated Risk in the Treatment of unruptured intracranial Aneurysms (MARTA) score, using routinely collected patient, aneurysm, and treatment data to predict complications for EVT and NT. Overall, both models had a good accuracy for predicting procedural complications (EVT c-statistic=0.78; 95%CI=0.75-0.84 and NT c-statistic=0.73; 95%CI=0.67-0.78). We then created a simplified score (Table 1) constructed by selecting a subset of variables based on consensus and statistical significance that demonstrated a moderate discrimination ability (EVT AUROC=0.68, 95%CI=0.57-0.78 and NT AUROC=0.65, 95%CI=0.54-0.77).

License CC BY-NC-ND 4.0

Table 1. MARTA score

MARTA score			
		EVT	**NT**
Age >45 years		1	1
Baseline mRS	>2	2	1
Location	ICA cavernous	1	NA
	ICA OphA	1	1
	ICA PCom / AChA	3	1
	ICA-T	5	1
	ACoA	3	1
	ACA	5	2
	MCA	5	1
	Basilar	5	5
	VA / PICA	5	5
	PCA / AICA / SCA	1	2
Dimensions	<5	1	1
	5-10	1	1
	>10	2	2
Morphology	Saccular regular	0	1
	Saccular multilobar	0	1
	Fusiform	0	1
	Shallow	0	2
Parent artery and collaterals	Focal stenosis	0	2
	Collaterals from the sac	2	0
EVT approach	Coiling (+ balloon assisted)	1	NA
	Intrasaccular device	0	
	Stent assisted coiling	1	
	Flow diverter	1	
Total			
Range		2 - 13	3 - 13

According to the score value, we defined 4 classes of risk (Figure 8). For the EVT, low-risk group (MARTA-EVT≤4=2.4%) to medium-risk (MARTA-EVT 5-6=5.1%), high-risk (MARTA-EVT 7-8=9.2%) and critical-risk groups (MARTA ≥9=18.3%). For the NT, low-risk group (MARTA-NT≤4= 4.2%) to medium (MARTA-NT 5-6= 13.7%), high (MARTA-NT 7-8= 29.6%) and critical-risk groups (MARTA-NT≥9= 75%). However, aneurysms represent a multifactorial and anatomically intricate disease, where variables such as location, morphology, and vessel geometry are not isolated predictors, but elements of a dynamic pathophysiological system,

License CC BY-NC-ND 4.0

and the creation of a simple scoring systems may fail to account for important non-linear interactions or correlated risks. For this reason, we also created an online tool based on the full predictive models (https://martascore.shinyapps.io/MARTA/) with the aim to update the model periodically with newer data.

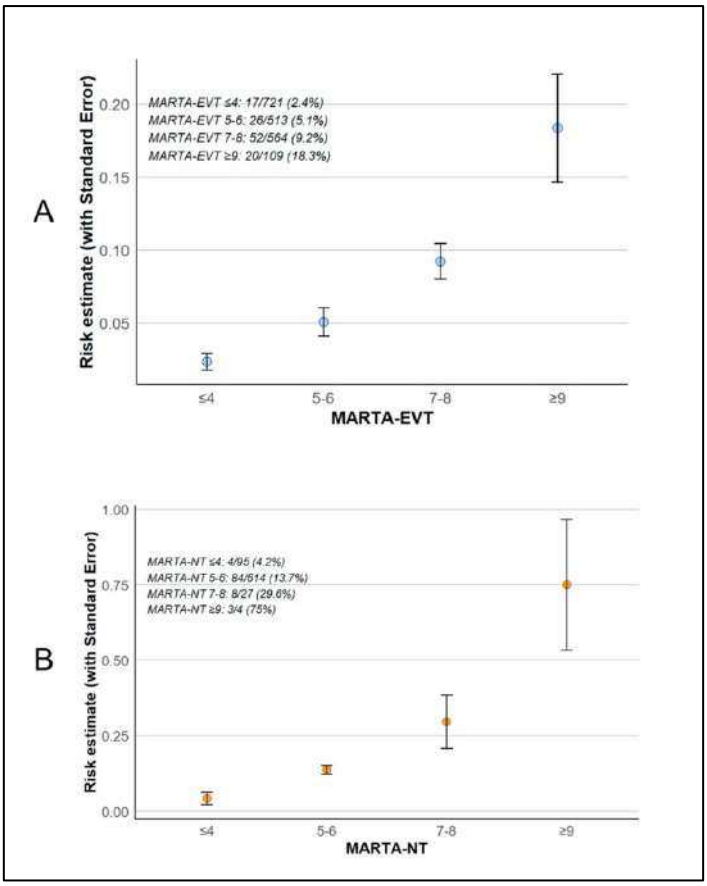


Figure 8. Pointplot for risk of combined primary outcome EVT (A) and NT (B).

II.3. Alternative technique for ruptured IA

For ruptured intracranial aneurysms (RIA), EVT is associated with lower rates of death, dependency, and seizures, but a slightly higher risk of rebleeding compared to surgical clipping.[48–50] However, with the EVT the recanalization rate is higher (20-22% at follow-up) regardless of the initial angiographic result, with higher risk if a body remnant is left after the initial procedure.

License CC BY-NC-ND 4.0

Intrasaccular flow disruptors (IFD) have been introduced in the treatment of intracranial aneurysms (IAs) to overcome the low aneurysm occlusion rate and the high recanalization rate of the coiling technique. Among them, the Contour Neurovascular System and the Neqstent were designed to reconstruct the aneurysmal neck and both can be used as assisting coiling devices. We conducted a study assessing efficacy and safety of the IFD-assisted coiling (Appendix 4 for the article). We performed a retrospective analysis of prospectively collected data of all patients with IAs treated with the IFD-assisted coiling between February 2021 and April 2022. In a cohort of 15 IAs, the IFD-assisted coiling was successfully performed in 13 cases, with a post-operative complete occlusion in 12 cases (92.3%) and neck remnant in 1 case (7.7%). There was one ischemic event (6.7%) and no hemorrhagic complications. At the mid-term radiologic follow-up, ten IAs (83.4%) presented an adequate occlusion, while 2 (16.7%) had a recurrence. We proved that the IFD-assisted coiling is promising and safe without antiplatelet therapy in ruptured cases.

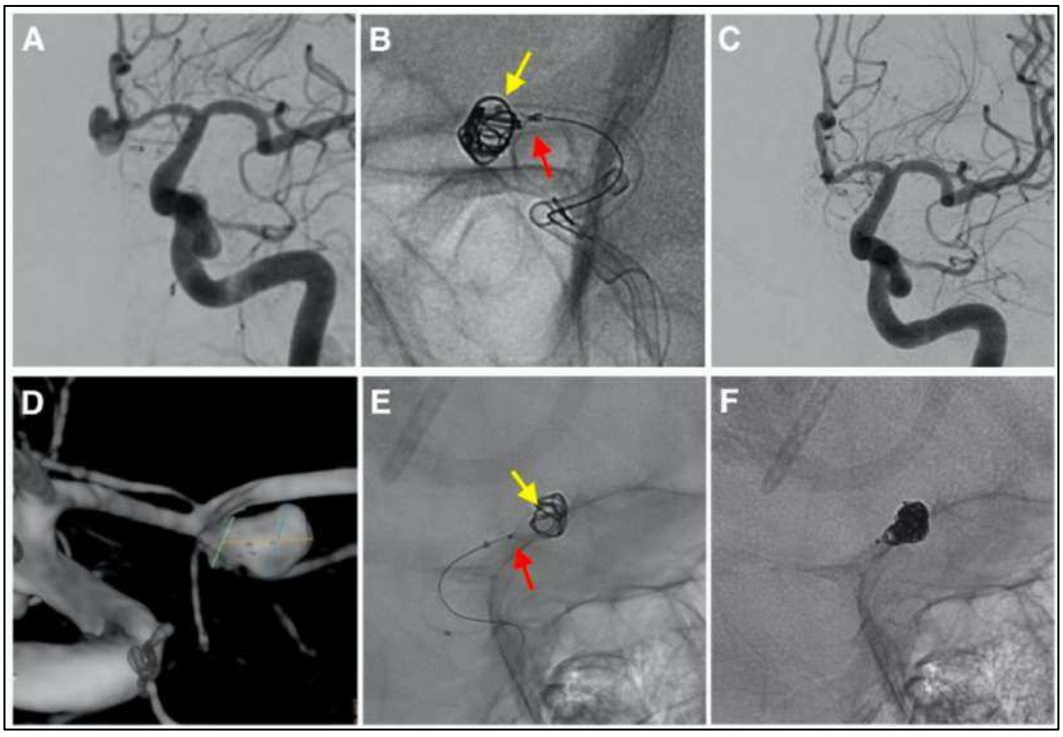


Figure 9. Cases of intrasaccular flow disruptor-assisted coiling (IFD-AC). (A–C) Case 15 performed with the CNS (red arrow) and a jailed coiling microcatheter (yellow arrow). (D–F). Case 12 performed with the NQS (red arrow), crossing its meshes with the coiling microcatheter (yellow arrow).

License CC BY-NC-ND 4.0

Summary

This chapter focuses on three articles published to improve treatment outcomes for both unruptured and ruptured intracranial aneurysms by refining patient selection and optimizing endovascular techniques.

For unruptured intracranial aneurysms (UIAs), treatment decisions require balancing procedural risks against rupture risk. We firstly identified the variables most strongly associated with aneurysm complexity, with a DELPHI consensus. To address the lack of validated treatment-specific treatment risk tools, we developed the MARTA (Morbidity and Mortality Associated Risk in the Treatment of unruptured intracranial Aneurysms) score using a large multicenter cohort of 1907 endovascular (EVT) and 740 neurosurgical (NT) treatments. The full predictive models showed good discrimination (EVT c-statistic 0.78; NT c-statistic 0.73), and a simplified point score stratified patients into four risk classes (low, medium, high, and critical), with complication rates ranging from 2.4-18.3% for EVT and 4.2-75% for NT. An online calculator based on the complete models (https://martascore.shinyapps.io/MARTA/) was deployed to provide individualized risk estimates and to allow future model updates.

For ruptured intracranial aneurysms (RIAs), where endovascular treatment offers favorable clinical outcomes but is limited by high recanalization rates, we evaluated intrasaccular flow disruptor-assisted coiling (IFD-AC) using the Contour Neurovascular System and Neqstent devices. In a series of 15 aneurysms (mostly ruptured), IFD-assisted coiling showed promising results and a safe profile.

The next chapter will focus on a specific endovascular strategy: flow diverters.

License CC BY-NC-ND 4.0

Chapter III. Flow Diverter

III.1.1. History of FD stent

Until the early 2010s, endovascular treatment of intracranial aneurysms primarily relied on intrasaccular coil embolization, often with balloon or stent assistance. However, achieving durable and complete occlusion was challenging, particularly for large, giant, fusiform, or blister aneurysms.[51] A 2011 meta-analysis revealed a 20% recurrence rate and 10% retreatment rate with coil embolization, with aneurysms larger than 10 mm being particularly prone to recurrence.[52]

To address these limitations, neurointerventionalists explored minimally invasive strategies to exclude complex aneurysms from circulation. Early experiments demonstrated that placing a stent across the aneurysm neck could promote blood stasis and thrombus formation, leading to aneurysm occlusion without intrasaccular manipulation. These studies introduced the concept of parent vessel remodeling, where a new intimal layer forms over the stent and aneurysm neck, effectively sealing it.[53,54]

Initial attempts using commercially available stents for dissecting or pseudoaneurysms showed promise but were not optimized for altering intra-aneurysmal hemodynamics across various aneurysm types.[55–57] Subsequent research focused on understanding aneurysm hemodynamics, parent artery configuration, and stent design. Studies revealed that stent effectiveness diminished in tortuous vessels or bifurcation aneurysms, prompting further design refinements.[58,59] Key parameters like stent strut thickness, porosity, and pore density were optimized to balance aneurysm neck coverage with sufficient radial force for vessel wall apposition.[60]

In 2004, Lieber et al. coined the term "flow diverter" (FD) in an NIH grant,[61] marking a shift toward devices designed to disrupt blood flow into the aneurysm sac. These devices, typically braided cobalt-chromium or nickel-titanium constructs, act as "speed bumps" to reduce flow inertia, promoting thrombosis over days to weeks. Optimal porosity (70-75%) and pore density

License CC BY-NC-ND 4.0

were established through in vitro studies, ensuring aneurysm occlusion while maintaining patency of adjacent perforator branches.[58,62,63]

By 2007, FDs were introduced as "flow-diverting" devices, becoming widely known as flow diverters by 2008.[64] This technology marked a paradigm shift, moving away from intrasaccular occlusion to parent artery reconstruction. FDs redirect blood flow away from the aneurysm, inducing stasis, thrombosis, and eventual endothelialization across the aneurysm neck, permanently excluding it from circulation (Figure 8). Early clinical studies on large, giant, and complex aneurysms demonstrated high occlusion rates and parent vessel healing, revolutionizing endovascular treatment.[65–68]

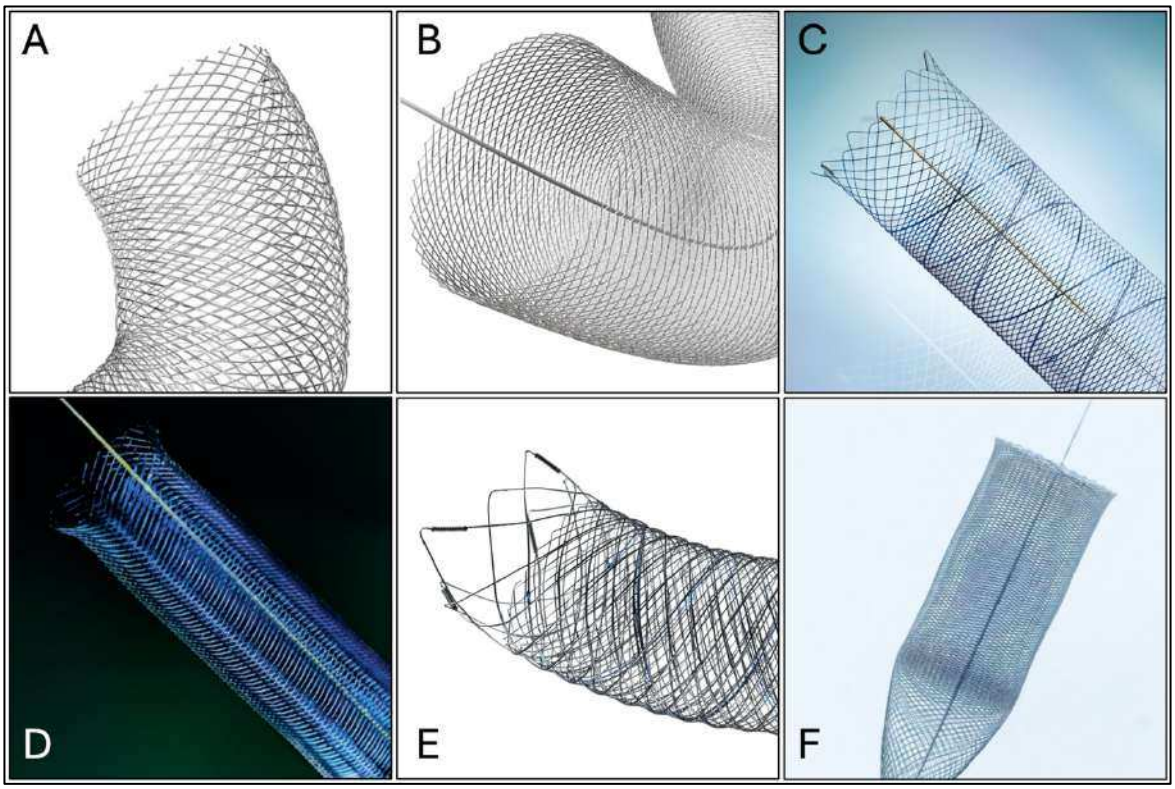


Figure 10. Some flow diverters commercialized. (A) Pipeline, Medtronic. (B) Surpass, Stryker. (C) Derivo, Acandis. (D) Silk Vista, Balt. (E) FRED, Microvention. (F) P64, Phenox.

License CC BY-NC-ND 4.0

III.1.2. Mechanism of action and biology of flow diversion

FD therapeutic effect is achieved through intrinsic modifications of hemodynamic parameters in both the parent artery and the aneurysmal sac. In addition, the device struts serve as a scaffold for endothelial cell proliferation across the aneurysm neck, ultimately resulting in the exclusion of the aneurysm from the circulation (Figure 9).

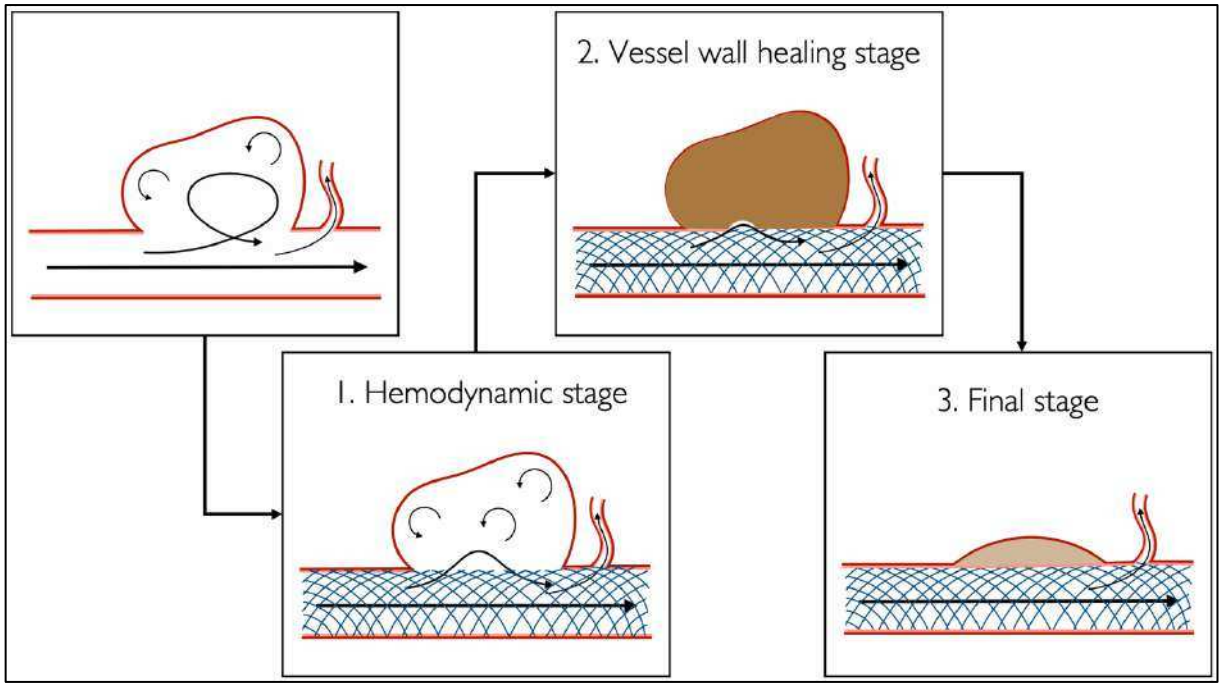


Figure 11. Mechanism of flow diversion. The flow diverter deployment induces hemodynamic changes in the parent artery and aneurysmal sac. This hemodynamic alteration activates biological processes leading to the thrombus formation within the sac and the endothelialization of the stent.

III.1.2.1. Thrombus formation after flow diversion

Following deployment of a FD, the primary mechanism leading to aneurysm occlusion involves disruption of intra-aneurysmal flow and the subsequent formation of a thrombus within the sac. This flow-modifying effect depends predominantly on device porosity, defined as the proportion

License CC BY-NC-ND 4.0

of metal-free surface area relative to the total stent surface area, and pore density, the number of pores per unit area at the device-neck interface (Figure 10). Both parameters directly influence resistance to blood flow into the aneurysmal sac: lower porosity increases resistance, promotes stagnation of inflow, and facilitates intra-aneurysmal stasis, thereby favoring thrombosis.[69]

While the temporal sequence of biological healing following coil embolization of cerebral aneurysms has been well described, there is a lack of data regarding the FD treatment. After coiling, histopathological studies demonstrated that within seven days of coiling, the aneurysmal sac contains a fibrin-rich thrombus, followed by macrophage and fibroblast infiltration, with the coils becoming covered by a fibrin layer within approximately one month after treatment.[70,71] By comparison, histopathological data on thrombus formation after flow diversion remain limited, primarily derived from preclinical studies or postmortem case reports. Autopsy examinations of aneurysms treated with the PED have revealed intra-aneurysmal thrombus formation.[72] Both early (as soon as seven days post-treatment) and delayed (up to 12 months) findings of unorganized thrombus have been reported, even in cases where angiography demonstrated complete aneurysm occlusion.[73–75]

License CC BY-NC-ND 4.0

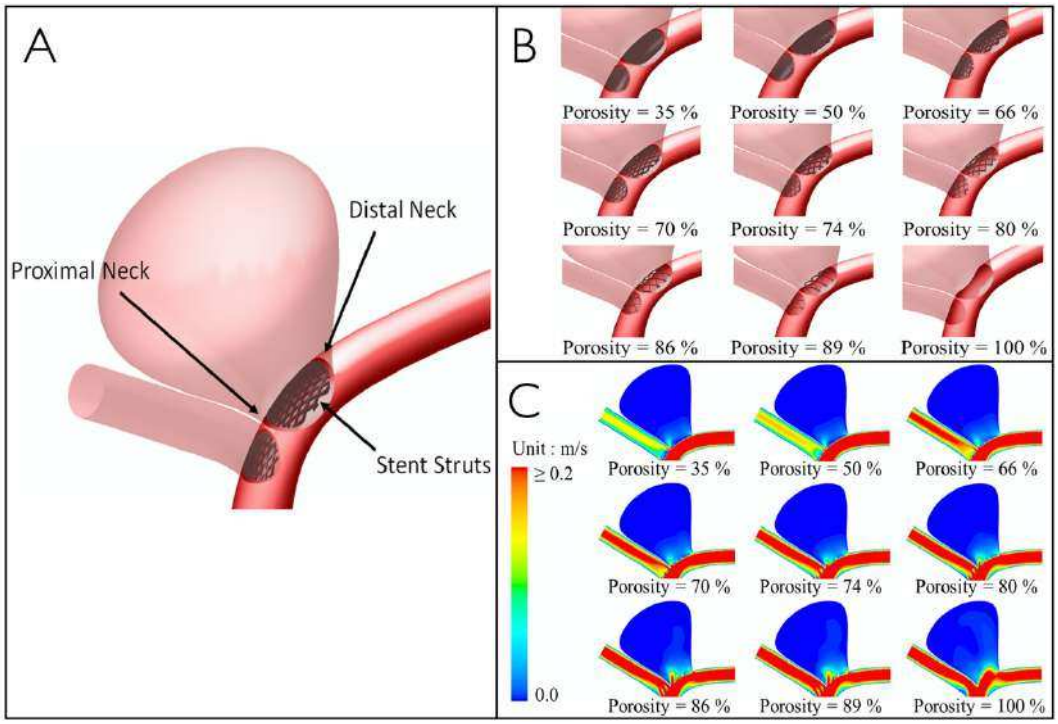


Figure 12. Relation between porosity and hemodynamic changes. (A) A flow diverter covering both the aneurysmal sac and a collateral branch. (B) Examples of stents with different porosities (defined as the proportion of metal-free surface area relative to the total stent surface area), determined by the number of struts covering the aneurysmal neck and the ostium of the collateral branch. (C) Contour maps of flow velocity at peak systole (t/T = 0.25), showing the progressive reduction of blood flow within the aneurysmal sac and collateral branch as stent porosity decreases. Abraham Yik-Sau Tang et al., Journal of Biomedical Science and Engineering, 2013[76]

III.1.2.2. Cellular and molecular processes activated in flow diversion

Previous investigations using RNA sequencing have demonstrated marked differences in gene expression profiles between coiled and FD treated aneurysms.[77] In FD treated aneurysms, when compared with untreated controls, key genes related to endothelial function, such as apelin and CXCL-8, were significantly upregulated. Many of the upregulated genes were associated with mitogenic activity and cell cycle progression, including cyclin B2 and cyclin-dependent kinase 1 (cyclin B1). Notably, expression of ICAM2, a molecule central to angiogenesis and leukocyte transmigration,[78] was observed exclusively in the FD group. This

License CC BY-NC-ND 4.0

pattern supports the hypothesis that FD technology inherently promotes endothelialization. Moreover, another study revealed higher expression of tumor necrosis factor alpha (TNF-α) and monocyte chemoattractant protein-1 (MCP-1) in FD treated aneurysms compared with those treated by coil embolization.[79] These findings suggest that inflammatory cell infiltration, particularly by macrophages, plays an important role in healing after FD. During aneurysm healing, invading fibroblasts and myofibroblasts produce matrix metalloproteinases (MMPs) and transforming growth factor beta (TGF-β), creating an inflammatory substratum that activates local vascular endothelium.[80] A notable difference in gene expression between treatments is the presence of local inflammatory cells in FD treated aneurysms, likely recruited from the circulation. Direct contact between the device and the parent vessel intima may induces remodeling of the vessel and explain this phenomenon. At the FD-artery interface, localized inflammation is initially triggered, and the healing process progresses through the activation of endothelial cells (ECs), producing chemoattractants. The deployment of the FD across the aneurysm neck specifically facilitates paracrine signaling between vascular ECs and smooth muscle cells (SMCs), potentially driving the fibroblastic response observed both in the parent vessel wall and in the aneurysmal dome. In the dome itself, where endothelium is scarce, this activation does not occur with intrasaccular coil placement, limiting the recruitment of circulating monocytes and local macrophages. Among the molecules involved, Angiopoietin-1 (Ang-1), a SMC-derived growth factor, acts on the TIE-2 receptor expressed by ECs. Formation of the Ang1-TIE-2 complex regulates matrix adhesion and cellular interactions (Figure 11), with leukocyte adhesion potentially representing an early step in the cascade of aneurysm healing. Interestingly, analogous molecular interactions have been described in coronary stent restenosis, where neointimal growth occurs under substantially different hemodynamic conditions.[81,82]

License CC BY-NC-ND 4.0

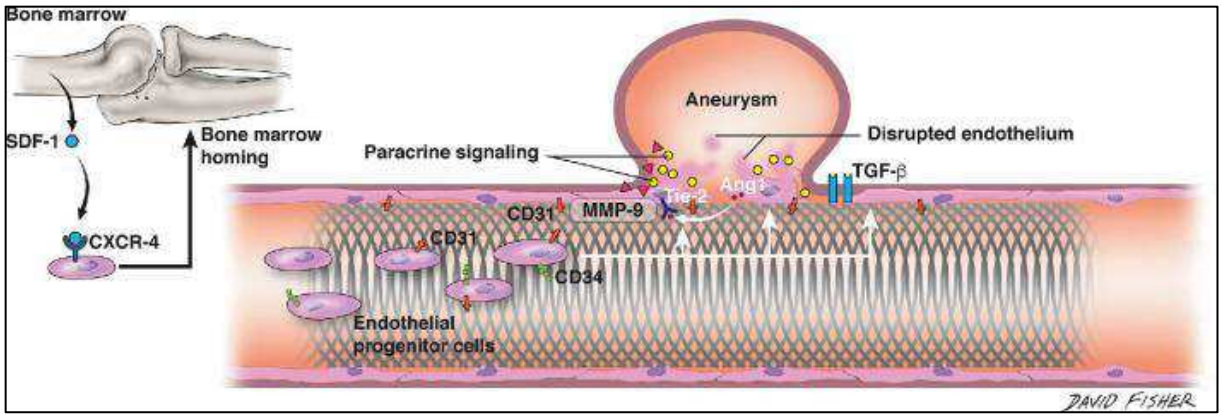


Figure 13. Cellular and molecular mechanisms underpinning device endothelialization follow flow diversion treatment of cerebral aneurysms. Depicted are the contributing roles of local endothelial cells, activated by paracrine factors at site of flow diverter deployment, and circulating endothelial progenitor cells origination from the bone marrow. Artist: David Fisher, Department of Neurosurgery, University of Alabama-Birmingham.[83]

III.1.2.3. Endothelialization process in flow diversion

While initial thrombus formation represents the first step in aneurysm healing after flow diversion, the development of a nonpermeable, continuous endothelial layer covering the stent struts is essential for the definitive aneurysm cure. Endothelialization begins immediately after FD implantation, with undifferentiated scattered clusters of inflammatory cells adhering at random points along the device surface as early as day 1.[84–86] The process initiates at the FD-arterial wall interface and gradually progresses toward the aneurysmal neck. This is accompanied by progressive adhesion of differentiated SMCs, forming an initial neointimal layer that is histologically visible by day 7. By approximately eight weeks, this neointima typically comprises CD31+ ECs overlaying smooth muscle actin (SMA)-positive SMCs.[84–86] These observations suggest a two-phase pattern of the endothelialization process after FD deployment: a rapid phase along the parent artery, and a slower phase across the aneurysmal neck, the latter requiring a supporting scaffold of the stent struts, of the matrix cells related to the aneurysm thrombosis, and SMCs. The intravascular optical coherence tomography (OCT)

License CC BY-NC-ND 4.0

imaging has demonstrated complete intimal formation as early as day 21.[85] The precise origin of the ECs involved in this process remains uncertain: while some evidence supports recruitment from circulating bone marrow-derived progenitors, the EPCs,[87] other studies support the migration of ECs from the adjacent arterial tissue.[84–88]

III.2. Clinical evidences on FD efficacy and safety

Efficacy and safety of FD have been assessed in several pivotal studies demonstrating the high performance of the FD treatment. Performance of the PED (Medtronic) has been assessed in different trials. Firstly, the PITA trial (Pipeline Embolization Device for the Intracranial Treatment of Aneurysms),[89] enrolling patients with unruptured, wide-necked aneurysms (>4 mm), unfavorable dome/neck ratios (<1.5), or those who had failed previous therapy. Thirty-one patients, with 31 aneurysms predominantly located in the ICA, were treated. Technical success for PED placement was achieved in 96.8% of cases. Most aneurysms were treated with one or two PEDs, and nearly half received adjunctive coil embolization. At 6-month follow-up, complete angiographic occlusion was achieved in 93.3% of patients. The safety profile was comparable to SAC, with two major periprocedural ischemic complications and no significant in-stent stenosis (≥50%) at follow-up. The second one was the PUFS trial (Pipeline for Uncoilable or Failed Aneurysms Study) for the treatment of large and giant, wide-neck, ICA aneurysms that were either uncoilable or had failed previous therapy.[90] The trial enrolled 107 patients with 109 aneurysms, with a mean maximum aneurysm sac diameter of 18.2 mm and 20% classified as giant (≥25 mm). Successfully PED placement was 99.1%. At 180 days, complete aneurysm occlusion was achieved in 73.6% of cases, with increasing occlusion rates over time: 86.8% at 1 year, 93.4% at 3 years, and 95.2% at 5 years. No recanalization of previously occluded aneurysms was observed at long-term follow-up.[90,91] The rate of major ipsilateral stroke or death at 180 days was 5.6%, and the rate of serious device-related complications at late time point was 2.6%. Rate of favorable

License CC BY-NC-ND 4.0

functional outcomes was high, with 96.3% of patients having a modified Rankin Scale (mRS) ≤2 at 5 years.[90]

Regarding the performance of the Suprass (Stryker), the most robust data come from the SCENT trial,[92] a multicenter, prospective, single-arm pivotal study enrolling 180 patients with large or giant wide-neck IAs, primarily located on the ICA. The SCENT trial demonstrated successful device implantation in 97.8% of cases, with the 62.8% of complete occlusion rate after 12-month and the 8.3% of major ipsilateral stroke or death at 12 months.[92] Long-term follow-up at 3 and 5 years showed increased aneurysm occlusion rates (77.8% at 3 years, 90.2% at 5 years) and no late aneurysm rupture, supporting durable efficacy and safety.[93–95] Additional prospective multicenter studies and single-center series have reported similar findings, with high rates of complete occlusion and acceptable safety profiles in both anterior and posterior circulation aneurysms.[96,97] Surpass has been later changed with other generations, the Surpass Evolve and actually the Surpass Elite, that need further controlled trials.

Regarding the performance of the Silk (Balt) FD there are both prospective and retrospective multicenter cohorts, as well as systematic reviews. Initial experience with the Silk, found notable procedural difficulties in deploying the FD (21%) and high rate of thromboembolic events (11%), causing permanent morbidity in 4% of cases and death in 8% of cases.[98] Other prospective and retrospective series, as well as systematic reviews, showed that the Silk achieves high rates of aneurysm occlusion (between 70-85% at 6-12 months), with a complication profile comparable to the Pipeline device.[99,100] Balt started to produce also the Silk Vista Baby (SVB) for the treatment of aneurysms located in the distal circulation. The SVB was the first FD to be compatible with 0.017-inch microcatheters, allowing the delivery of the FD in vessels that are not accessible with conventional FD. Retrospective studies showed complete occlusion rates between 65% and 75% of cases, with low complication rates (2-4%), including in-stent thrombosis, side branch occlusion, and intracerebral hemorrhage.[101–103]

License CC BY-NC-ND 4.0

The efficacy and safety of the FRED (Flow Re-direction Endoluminal Device; Microvention) FD, the only double-layered, self-expanding nitinol device, for the treatment of IA are supported by multicenter prospective and retrospective studies, as well as several comparative meta-analyses. Most studies report complete occlusion rates of 70-80% at 12 months and up to 85% at 24 months,[104–106] with acceptable safety profile (permanent neurological deficits in 3-8% of cases and mortality in 2-4% of cases). Complication rates are similar to other devices, though some series report a slightly higher rate of in-stent stenosis with FRED compared to PED.[104–108]

The Derivo is another FD (Acandis) designed for the treatment of IAs. It was developed with a nitinol structure and an oxide surface finish, with the aim to improve deliverability, reduce thrombogenicity, and enhance endothelialization compared to first-generation devices.[109–111] Clinical evaluation of the Derivo has included multicenter retrospective and prospective studies. In these studies, the technical succes is consistently high (near 100%), the safety profile is high (with major complication rates ranging from 4 to 6% and procedure-related mortality <2%),[109–113] the complete occlusion rates are between 75 and 83% after 6-12 months, and including the near-complete occlusions they reach the 97%.[109–113] Recent innovations include the Derivo 2Heal, which incorporates fibrin and heparin coatings to further reduce thrombogenicity and potentially allow for single antiplatelet therapy.[109]

The p64 FD (Phenox) was initially designed with a mechanical detachment allowing a complete retrieving of the FD.[114] Several prospective and retrospective studies, including large multicenter cohorts, have demonstrated high rates of complete aneurysm occlusion (typically 77-88% at mid- to long-term follow-up) and low rates of permanent morbidity and mortality (generally <2.5%) in the treatment of both anterior and posterior circulation aneurysms, including complex and wide-necked lesions.[115–117] the company also produced the p48 FD for small-caliber distal vessels, showing complete occlusion rates ranging from 58-88%, with favorable clinical outcomes in 96% of cases and morbidity rates around 1%.[115]

License CC BY-NC-ND 4.0

A meta-analysis analyzing the overall efficacy and safety of all flow diverters,[118] showed that the overall aneurysmal complete occlusion rate was 76% (95%CI, 70-81%), and procedure-related morbidity and mortality were 5% (95%CI, 4-7%) and 4% (95%CI, 3-6%). Moreover, a pragmatic randomized clinical trial showed that for patients with unruptured, large, anterior circulation aneurysms (the majority located in the ICA) flow diversion is more effective than other endovascular approaches in terms of angiographic outcome,[119] but still with 30.9% of incomplete occlusion after 12 months (vs. 45.6% with other endovascular strategies).

III.3. Limits of the treatment

As previously seen, the hemodynamic changes induced by the FD are central for the activation of the biological processes leading to the neointima formation. Hence, an effective endothelialization requires a preserved vessel wall integrity, a direct contact of the FD struts with the parent artery, but also a reduced WSS.[120,121] The WSS modulates ECs biology by triggering intracellular signaling cascades that can promote a proinflammatory phenotype. In vitro, has been shown that an elevated WSS inhibits endothelial proliferation by inducing cell-cycle arrest, and in vivo, that reduced WSS promotes endothelial proliferation.[122,123] Consequently, the low WSS within the reconstructed parent artery and across the aneurysmal neck following the FD implantation promotes endothelial proliferation,[124] but if the FD treatment fails to reduce the WSS and the residual flow across the neck is still high the neointimal formation is delayed.[120] The predictability of the hemodynamic alterations induced by the FD represents a limitation, as they depend on both intrinsic (device-related) and extrinsic (anatomy-related) factors.

III.3.1.1. Intrinsic limitations

Computational fluid dynamics (CFD) studies using patient-specific aneurysm morphologies have shown that FD struts reduce systolic blood flow velocity within the aneurysm, with a more

License CC BY-NC-ND 4.0

pronounced effect in smaller arteries likely due to higher vascular resistance, and the higher anatomical modification induced by the FD in the distal circulation, while flow in the parent artery remains generally unaffected. The effect of the FD porosity has been studied in silico models, showing the relation between the lower porosity and the reduction of intra-aneurysmal flow, but it is difficult to correlate the hemodynamic alterations with the biological processes involved in the arterial wall healing with FD. Moreover, even reaching a sort of predictability, the porosity may change after FD implantation, due to parent artery remodeling and further device expansion.[125] Although a linear correlation between porosity and occlusion rates has not been established, evidence suggests that achieving low intra-aneurysmal velocities (<0.025 m/s) provides optimal conditions for thrombosis.[126] In numerical simulations conducted by Zhang et al.,[127] effective velocity reduction occurred at 65% FD porosity, whereas efficacy declined in larger aneurysms once porosity exceeded 75%. Therefore, intrinsic limitations of the FD are determined by the small effective porosity range, and the need to balance porosity with technical and anatomical considerations. Lower porosity improves flow disruption but reduces stent flexibility, complicating deployment in tortuous arterial segments and increasing the risk of side-branch occlusion. Conversely, higher porosity preserves flexibility and conformability but allows higher residual flow velocities, which have been associated with treatment failure.[127]

Other engineering parameters are critical determinant of FD efficacy. Strut thickness plays a role in FD wall apposition (Table 1), that is mandatory to obtain a compete endothelial coverage.[84] Increased strut thickness improves wall contact, but increases FD rigidity, changes the struts angle and count.[128] However, it is certain that arterial healing and stent endothelialization start on the FD-arterial interface. Given this mechanism, in case of incomplete wall apposition, the malapposed portion of the device will fail to endothelialize due to a lack of direct contact with the parent artery. Even microscopical malappositions can reduce the FD efficacy, so much that the evaluation of wall apposition with bidimensional angiography is poorly predictive of the final aneurysm exclusion,[129] suggesting that alternative methods

License CC BY-NC-ND 4.0

should be developed to assess wall apposition. Two-dimensional angiography cannot provide cross-sectional views, limiting assessment of the relationship between the FD and the arterial wall. New tools are currently being used in the context of IA treatment with flow-diverters to measure wall apposition, such as the high-resolution cone-beam CT (HR-CBCT),[130] and the Optical Coherence Tomography (OCT).[131] HR-CBCT can detect FD malapposition in a timely manner during the surgery, but the OCT might be even better in detecting FD malappositions.[131] However, whether or how to deal with it is controversial. Long et al.[130] showed a reduction of FD malapposition (from 18.7% to 2.5%) by active intervention with balloon angioplasty, but this could led to problems, such as stent migration, vessel puncture caused by stent microfilaments, and thrombosis. This mechanism has also been discussed in the literature in the context of coronary stents, which similarly fail to endothelialize in cases of malapposition.[132,133]

Table 2. Parameters related to the stent design.

Various parameters related to the stent design	
Pore size Cell size Mesh size	The small spaces in a mesh made of stent filaments are called pores or cells. These are terms referring to their size.
Pore density Cell density Mesh density	Terms referring to the number of pores per unit area.
Cell angle	The angle of woven filaments constituting an FD is called the cell angle. It reflects the shape of the pores (cells) after FD placement.
Porosity	The percentage of the area of stent deployment not covered by metal is called the porosity. The porosity of a neck bridging stent for coil embolization is about 90%, and that of an FD is about 70%. The porosity of a covered stent is 0%.
Metal coverage ratio	The percentage of the area covered by metal, i.e., the stent struts, is called the metal coverage ratio. The relationship between the porosity and metal coverage ratio is expressed as [Porosity(%)+Metal coverage ratio (%) = 100 (%)].
Filament diameter	Current FDs are prepared by weaving metal filaments into a mesh. The thickness of the metal filaments is the filament diameter.
Biocompatibility	Biocompatibility may affect inflammation due to foreign-body reaction, stent stenosis, in-stent thrombosis, etc
Radial force	The term referring to the force that supports the blood vessel from inside toward the outside or the force of stent expansion. It may affect the prevention of restenosis or wall apposition of the stent.

License CC BY-NC-ND 4.0

Surface change	Since the surface of erythrocytes is negatively charged, the charge state of the stent surface may affect in-stent thrombosis.

III.3.1.2. Extrinsic limitations

The effectiveness of flow diverters (FDs) in treating intracranial aneurysms depends on parent artery characteristics, aneurysm morphology, and patient-specific factors such as aneurysm size, location, neck geometry, baseline hemodynamics, and platelet function. These factors influence stable thrombus formation and treatment outcomes.[134] Aneurysms are traditionally classified as side-wall (typically on the internal carotid artery) or terminal (at bifurcations), with side-wall aneurysms assumed to have lower intrasaccular flow. However, this classification oversimplifies flow dynamics, which are better categorized as shear-driven or inertia-driven (Figure 12).[62] Shear-driven flow occurs when the aneurysm neck aligns parallel to the parent vessel, causing intrasaccular flow to follow the main vessel flow. Inertia-driven flow occurs when the neck is perpendicular to the parent flow, allowing high inflow due to momentum. Side-wall aneurysms may exhibit inertia-driven flow depending on vascular curvature and neck orientation, while most aneurysms show a mix of both flow types. Understanding these dynamics is crucial, as FD efficacy varies by flow type.[62]

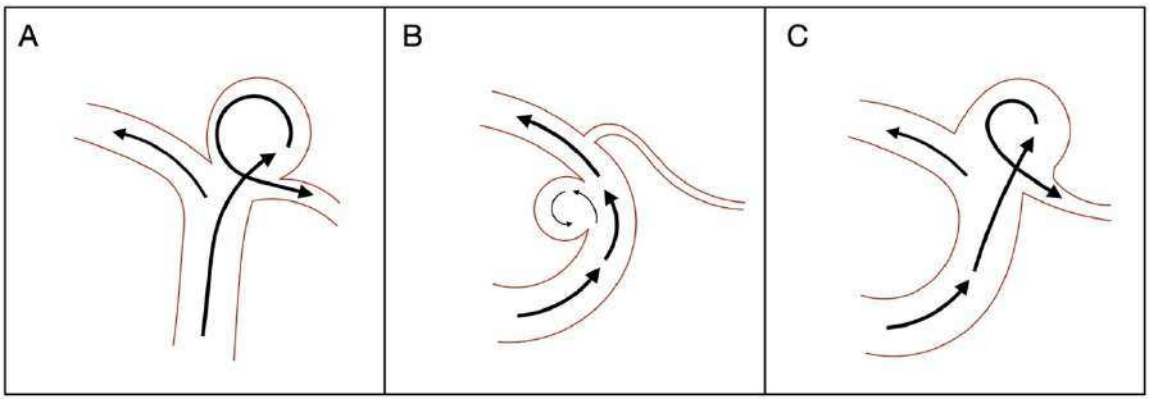


Figure 14. Examples of shear-driven and inertia-driven types. (A) Bifurcation terminal type aneurysm, with inertia-driven flow. (B) Side-wall aneurysm located in the inner curve of the ICA, with shear-driven flow. (C) Side-wall aneurysm located in the outer curve of the ICA, with inertia-driven flow.

License CC BY-NC-ND 4.0

In vitro studies using 10 mm aneurysms on straight (shear-driven) and curved (inertia-driven) 4 mm parent vessels showed that FD deployment reduced intra-aneurysmal flow by 85% in shear-driven aneurysms but only 54% in inertia-driven ones, resulting in an eight-fold difference in residual inflow (Figure 13). This indicates that FD-induced flow reduction is less effective in inertia-driven aneurysms, potentially explaining some treatment failures where hemodynamic changes are insufficient for arterial wall healing.[62]

Aneurysm location also impacts FD outcomes. Anterior circulation aneurysms experience 30–50% higher peak systolic flow velocities than posterior circulation ones.[135] Consequently, FDs may reduce aneurysmal inflow more effectively in the posterior circulation, even for inertia-driven aneurysms, though the impact on WSS remains unclear.

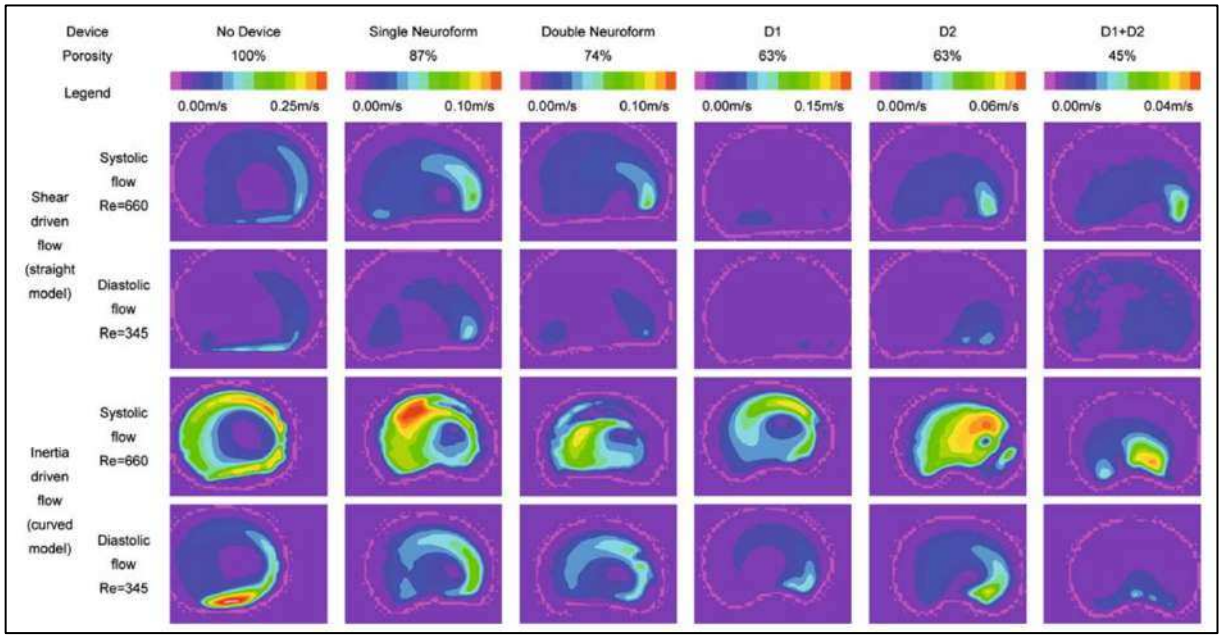


Figure 15. Intrasaccular flow alteration induced by different stents. Scalar map of the velocity field at peak systole and diastole under shear-driven and inertia-driven flow. Augsburger L et al., Klin Neuroradiol. 2009.[62]

License CC BY-NC-ND 4.0

III.4. Risks of FD treatment

III.4.1. Aneurysm patency

Complete occlusion rate of IAs treated with FD is approximately 77-83% at 1 year, 87-90% at 2 years and up to 96% at 5 years based on pooled meta-analyses and large cohort studies.[136,137] These rates are consistent across various device types and can be associated with several variables:

- Large aneurysm size and wide neck: larger aneurysms and those with wider necks are consistently associated with incomplete occlusion after flow diversion, likely due to persistent inflow and difficulty in achieving complete endothelialization.[138–142]
- Incorporation of branch vessels: aneurysms that incorporate branch vessels (e.g., side branches or perforators) are less likely to occlude, as persistent flow is required to maintain these branches patent.[139,140,143]
- Hypertension: Both pre-existing hypertension and high baseline blood pressure are independent predictors of incomplete occlusion, possibly due to adverse effects on vessel healing and neointimal formation.[141,144,145]
- Complex morphology (fusiform, blister, or branch-involving aneurysms): Fusiform and morphologically complex aneurysms have higher rates of treatment failure, as shown in multivariate analyses.[140,143]
- Older age: Increasing patient age is associated with lower rates of complete occlusion, potentially reflecting impaired vascular healing.[140,146]
- Absence of adjunctive coiling: Use of adjunctive coiling with flow diverters increases the likelihood of complete occlusion, especially in large or wide-necked aneurysms.[139,140,146]

License CC BY-NC-ND 4.0

- Strong ostium inflow and unfavorable hemodynamics: High preprocedural inflow rates and complex flow patterns at the aneurysm ostium are associated with delayed or incomplete occlusion.[142,147,148]
- Lower size ratio (aneurysm size relative to parent vessel diameter): A lower size ratio is independently associated with incomplete occlusion in small aneurysms.[141]

These factors should be considered to optimize outcomes with FD therapy, particularly in large and giant aneurysms. We conducted a systematic review and meta-analysis, searching the scientific literature up to December 2022,[149] to evaluate rates of adequate occlusion and complications in large and giant IAs. Among 146 articles identified, 10 were included in the meta-analysis. In this studies, 541 large and giant IAs were treated with or without adjunctive coiling (Appendix 3 for the article). The aim was to address the question of which treatment is safer and more effective, given the complexity of such aneurysms. We found that the adjunctive coiling was not associated with a statistically significant higher adequate occlusion rate (RR 1.06 [0.96, 1.17]; p=0.280), but it decreased significantly the complication rates (RR 0.56 [0.33, 0.95]; I2=0%; p=0.03), especially device-related ischemic complications, with a trend toward reduction of mortality (RR 0.86 [0.34, 2.18]; I2=0%; p=0.75). Our results suggest that in this complex scenario the adjunctive coiling is not mandatory to increase FD efficacy, but it could increase and stabilize the intrasaccular thrombosis, reducing treatment-related complications.

III.4.2. Risk of delayed rupture

Aneurysm patency after FD treatment carries a risk of spontaneous rupture.[72,150,151] The underlying mechanism remains unclear and is not necessarily associated with persistent high intrasaccular inflow, since spontaneous rupture has also been reported in nearly completely occluded aneurysms at the time of rupture. In giant or fusiform aneurysms, FD treatment may even increase the risk of delayed hemorrhage. Although the specific triggering factor remains

License CC BY-NC-ND 4.0

uncertain, until complete healing of the parent vessel is achieved through neointimal coverage of the FD across the neck, the intrasaccular thrombus may act as an inflammatory substrate, releasing proteases that contribute to wall degradation and subsequent rupture.[152,153]

The overall incidence of this complication is unknown, although it is thought to be low and critically related to the complexity of the treated aneurysm. A meta-analysis reported a delayed aneurysm rupture in ≈4% of patients treated with FD, with significantly higher rates among patients with large and giant aneurysms (OR for small aneurysms, 0.10; 95% CI, 0.02–0.42; p<0.0001) and no association with location (OR, 1.89; 95% CI, 0.43–8.21; p=0.55). Delayed rupture occurred mainly within 1 month after treatment (≈3%) while after 1 month was rare (<2% of cases).[118] Nonetheless, concerns regarding delayed rupture are serious due to the mortality risk associated with this event and some studies suggest to use FD with coils.[149] Therefore, strategies that promote faster FD endothelialization could enhance the healing process of the parent vessel, facilitating more rapid neointimal coverage across the aneurysm neck. This accelerated healing may reduce the duration of exposure to inflammatory processes driven by the intrasaccular thrombus, thereby potentially lowering the risk of delayed aneurysm rupture.

III.4.3. Distal intracerebral hemorrhage

FD treatment carries a risk of periprocedural thromboembolic (overall 7.5%) and hemorrhagic events (overall 4.7%),[154] however the distal intracerebral hemorrhage is another rare, but possible complication. It is specifically associated with FD treatment, or other extrasaccular approaches, that has not been encountered with intrasaccular approaches. Its incidence is not precisely known, with the largest study reporting a rate of 2.5%.[155] In almost 20% of cases, this hemorrhage occurs distal to the aneurysm, often contralateral to the treated side.[156] The 2 leading explanations for intracerebral hemorrhage (ICH) include (1) deranged downstream hemodynamics resulting from FD implantation and (2) hemorrhagic transformation of small

License CC BY-NC-ND 4.0

ischemic infarcts associated with the procedure.[155,156] The hemodynamic hypothesis involves a reduction in the “Windkessel effect,” which refers to a decrease in blood vessel elasticity that leads to an increase in distal pulse pressure, subsequently leading to ICH.[157] Interesting insights have been obtained from in vivo blood flow measurements using MRI.[158] In these studies, the blood flow velocity and waveform of the parent vessels were recorded distally and proximally to the ICA aneurysm. In large aneurysms (>20 mm), distal blood flow velocity was reduced during systole and increased during diastole, resulting in decreased pulsatility, while such changes were not observed in smaller aneurysms (around 10 mm). FD treatment significantly altered the blood flow dynamics in large aneurysms: systolic velocity increased, diastolic velocity decreased, and pulsatility was restored, while the overall blood flow volume remained unchanged. A study conducted in rabbit models, showed also that FD implantation increased the pulse wave velocity and the vascular contractility.[159]

The ischemic hypothesis suggests that small thromboembolic infarcts, especially in the setting of dual antiplatelet therapy, subsequently undergo hemorrhagic transformation. As with any device placed inside a blood vessel, FD carry a relatively high risk of thromboembolism compared with intrasaccular devices.[160] Reported rates are greater than 5%, even among patients receiving appropriate dual antiplatelet therapy.[161] This risk is thought to result from injury to the endothelium, as well as the inherently thrombogenic surface of the devices or the poor wall apposition that may create small areas of blood stagnation and abnormal flow.

III.4.4. Covered branches and risk of occlusion

Although angiographic evidence of branch narrowing or occlusion is common (e.g., anterior cerebral artery [ACA] 66.6%, PComA 44.3%, MCA-M2 39.2%), the risk of clinically significant thromboembolic events related to the collateral branch coverage is <5%. The collateral circulation seems to mitigate the clinical impact of branch occlusion, while the risk of symptomatic ischemia increases when perforators or branches without robust collateral supply

License CC BY-NC-ND 4.0

are involved.[162] Blood flow analyses suggest that the direct effect of the FD struts on side branch hemodynamics is relatively minor. For example, a CFD simulation using 3D CT images of the basilar artery in 31 patients showed that FD placement altered blood flow in the AICA by only 3.6%.[163] Similarly, in rabbit models the CFD analysis of lumbar arteries covered by the FD placed in aorta demonstrated a modest reduction in blood flow volume (9-20%) and maximum flow velocity (15-36%).[138] Based on current CFD data, thrombus formation associated with neointima and stent coverage is thought to play a larger role in covered branch infarction associated to FD treatment than the direct flow-blocking effect of the struts themselves.

Summary

Flow diverters are an innovative treatment for intracranial aneurysms. They induce hemodynamic alterations of the blood flow within the aneurysmal sac and trigger biological processes leading to the healing of the parent vessel for stable aneurysm occlusion. They demonstrate high long-term occlusion rates, even though efficacy and safety of the FD treatment are influenced by device design, vessel anatomy, and patient factors. Complications like thromboembolism, hemorrhage, and branch occlusion, are important limitations. The ongoing technological innovation aims to optimize the deployment, reduce thrombogenicity, improving the safety, especially in challenging anatomies. However, drugs such as Rosuvastatin, influencing the healing process of flow diverters, might further enhance its efficacy and safety.

License CC BY-NC-ND 4.0

Chapter IV. Antiplatelet therapy and FD coatings

IV.1. Double antiplatelet therapy

Antiplatelet therapy is essential to prevent thromboembolic complications in endovascular procedures, including simple coiling.[164] The use of antiplatelet agents has increased in recent years due to the elevated risk of thromboembolic events associated with intracranial stents.[118] Consequently, dual antiplatelet therapy (DAPT) has become the standard for flow diversion and SAC.[165]

DAPT, typically combining aspirin (75–325 mg daily) with clopidogrel (75 mg daily), remains the standard regimen for most patients undergoing flow diverter placement.[165] However, the high prevalence of Clopidogrel hyporesponsiveness has prompted the consideration of alternative P2Y12 inhibitors, such as Prasugrel (10 mg daily) or Ticagrelor (90 mg twice daily), to optimize therapeutic outcomes. A recent meta-analysis by Jang et al.[166] demonstrated that platelet reactivity test (PRT)-guided tailored DAPT using Prasugrel or Ticagrelor in Clopidogrel hyporesponders significantly reduces thromboembolic complications (RR 0.40, 95% CI 0.22-0.74, p=0.004) compared to conventional clopidogrel-based DAPT in endovascular treatment of intracranial aneurysms, without increasing hemorrhagic risks (Figure 14). The study suggests that Prasugrel or Ticagrelor may serve as first-line P2Y12 inhibitors for DAPT in these procedures.

A large multicenter cohort study evaluated the relationship between duration of DAPT and long-term outcome in FD and SAC treatments, showing that thromboembolic events most frequently occurred within 30 days after the procedure and rarely thereafter.[167] The cumulative event-free survival rate was not different between the long-DAPT (>91 days) and short-DAPT (<90 days) groups in a population limited to patients who completed any DAPT period without major clinical events.[167] This result suggests that a DAPT duration of less than 90 days after FD treatment may be sufficient, although the study lacks multivariate analysis to assess

License CC BY-NC-ND 4.0

variables associated with a higher risk of thromboembolic complications that might benefit from longer DAPT.

As previously analyzed the FD treatment is associated with a 2-5% risk of hemorrhagic events, some of them related to the DAPT. For this reason, evidence regarding the single antiplatelet therapy (SAPT) in FD treatment is increasing. Moreover, strategies that accelerate FD endothelialization could promote faster neointimal coverage across the aneurysm neck, enabling a shorter duration of DAPT. The faster FD healing might reduce the risk of hemorrhagic complications associated with prolonged DAPT while maintaining protection against thromboembolic events, thereby improving the safety profile of FD treatment.

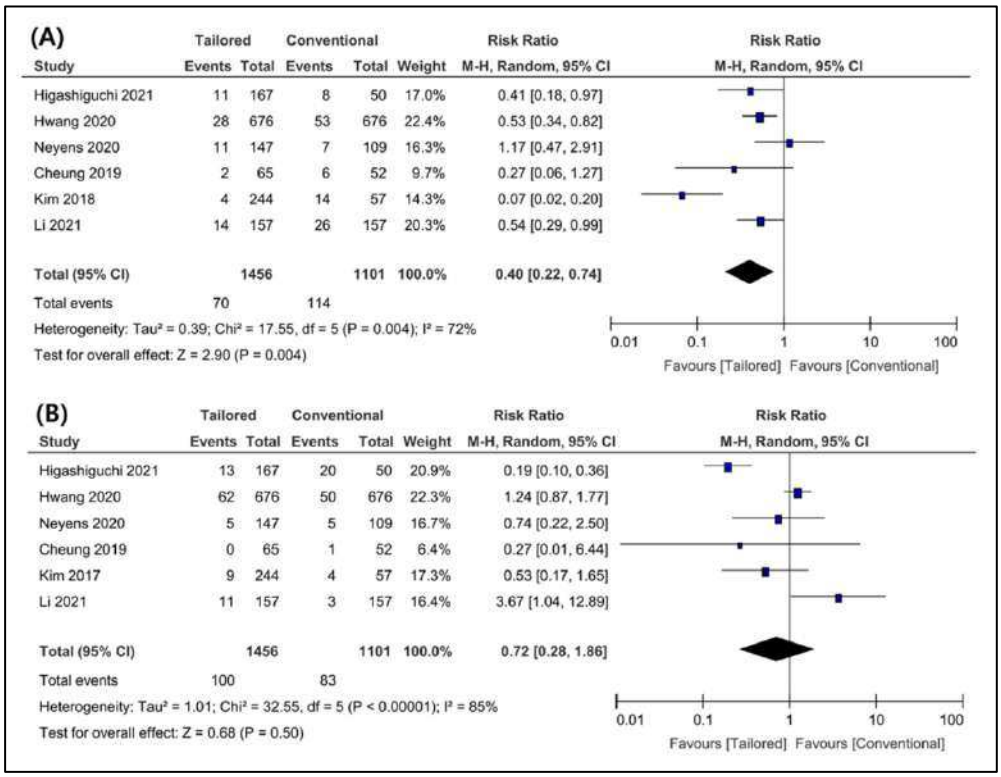


Figure 16. Forest plots presenting association of tailored dual antiplatelet therapy (DAPT) compared with conventional DAPT for (A) thromboembolic and (B) hemorrhagic complications. Tests for heterogeneity are described using I2 and P value. Min Jang et al. JNIS, 2023[166]

License CC BY-NC-ND 4.0

IV.2. Single antiplatelet therapy

SAPT is increasingly considered for FD treatment of cerebral aneurysms, particularly with newer FDs featuring antithrombogenic surface coatings designed to minimize thrombus formation and potentially reduce the need for DAPT. A recent meta-analysis[168] evaluated the safety profile of SAPT in FD treatment, reporting a pooled ischemic complication rate of 9.8% (95% CI: 4.87–18.95%; p=0.09) across all SAPT regimens. The analysis compared aspirin (ASA) with P2Y12 inhibitors (Prasugrel or Ticagrelor), revealing significantly higher ischemic complication rates in the ASA group (20.8%) compared to the non-ASA group (6.3%; p=0.02). The hemorrhagic complications (3.5% [95% CI: 1.38–8.81%]; p>0.99), and the in-stent stenosis (2.3% [95% CI: 1.06–5.14%]; p>0.99) were uncommon. Subgroup analyses showed no significant differences in ischemic complication rates between coated and non-coated FDs (10.7% vs. 5.5%; p=0.39) or between ruptured and unruptured aneurysms (17.6% vs. 7.1%; p=0.24), although the hemorrhagic complications tended to be higher in ruptured cases (9.8% vs. 1.1%; p=0.08). These findings suggest that SAPT with Prasugrel or Ticagrelor is relatively safe and effective for specific applications, such as coated FDs or ruptured aneurysms, but ASA monotherapy warrants cautious consideration due to elevated ischemic risks. These results are also endorsed by the recently presented COATING trial,[169,170] showing the non-inferiority of the treatment with the p64 HPC-coated FD under SAPT with P2Y12, compared with the p64 bare meal FD under DAPT, in terms of thromboembolic complications evaluated with the Diffusion-weighted Imaging within 48 hours (+/- 24 hours) of the index procedure by 3T-MRI.

IV.3. Antiplatelet therapy and FD healing

Antiplatelet therapy plays a pivotal role to prevent ischemic complications in FD treatment, but its implication in neointimal formation and FD integration is unknown. A preclinical study comparing the in vivo endothelial coverage and arterial wall integration of three different FDs,

License CC BY-NC-ND 4.0

coated and uncoated, implanted in the aortas of rabbits, also assessed the impact of varying antiplatelet regimens (no antiplatelets-NAPT, SAPT with Aspirin alone and DAPT with Aspirin and Ticagrelor) on device integration, patency, and neointimal formation.[171] They showed that both SAPT and DAPT did not increase the FD wall integration compared to NAPT, but rabbits premedicated with SAPT and DAPT presented a lower neointimal thickness compared to rabbits without premedication. These results suggest that antiplatelet therapy is not directly implicated with the FD wall integration, but that can reduce hyperplasia.

Summary

Dual antiplatelet therapy (DAPT), typically combining Aspirin and Clopidogrel, is the standard regimen for preventing thromboembolic complications in flow diverter (FD) and stent-assisted coiling treatments for intracranial aneurysms. Due to clopidogrel hyporesponsiveness, alternative P2Y12 inhibitors like Prasugrel or Ticagrelor are increasingly used, with studies showing that tailored DAPT reduces thromboembolic risks without increasing hemorrhagic complications. A large cohort study indicated that a DAPT duration of less than 90 days might be sufficient after FD treatment, as most thromboembolic events occur within 30 days. Single antiplatelet therapy (SAPT) is gaining attention, particularly with antithrombogenic FD coatings, showing a pooled ischemic complication rate of 9.8% and lower hemorrhagic risks, though Aspirin monotherapy has higher ischemic risks compared to P2Y12 inhibitors. Preclinical studies suggest that the antiplatelet therapy prevents ischemic complications, probably reducing the neointimal hyperplasia, but does not enhance FD wall integration, indicating a complex role in FD healing. For this reason, wall-oriented strategies have been recently investigated to enhance FD healing, modulate the biological response, and potentially shorten or eliminate the need for DAPT.

License CC BY-NC-ND 4.0

Chapter V. Wall-oriented treatment strategies

The development of new treatment strategies for IAs has long been, and remains, a major focus of neurovascular research. Early therapeutic concepts were primarily rooted in a physical-mechanistic view of aneurysm occlusion, commonly referred to as lumen-oriented therapies. Lumen-oriented strategies include enhancement of intraluminal thrombus organization, increased intraluminal packing, and bridging the aneurysmal neck. These strategies, however, underscores the crucial role of the aneurysmal wall biology in achieving durable obliteration. However, in recent years the importance the pathobiology in the aneurysmal healing after EVT has become increasingly recognized, giving rise to wall-oriented therapeutic approaches. Wall-oriented strategies focus on stimulating the proliferative response, preventing aneurysm wall cell injury, inhibiting inflammation and oxidative stress, and reducing extracellular matrix degradation.[22] Consequently, novel treatment strategies aim not only to mechanically treat the visible disease, but also to modulate the molecular pathways underlying aneurysmal wall pathology. A deeper understanding of the interplay between blood flow, intraluminal thrombosis, and aneurysmal wall remodeling has spurred the development of therapies designed to achieve a curative treatment, through systemic pharmacological interventions or local drug delivery, such as drug-eluting coils and stents, progressively connecting lumen-oriented and wall-oriented concepts.

V.1. Biological optimization of FDs

Surface modifications of FDs is a new strategy with the aim to reduce thromboembolic complications and the need for DAPT by either decreasing device thrombogenicity or accelerating endothelialization (Figure 15).

License CC BY-NC-ND 4.0

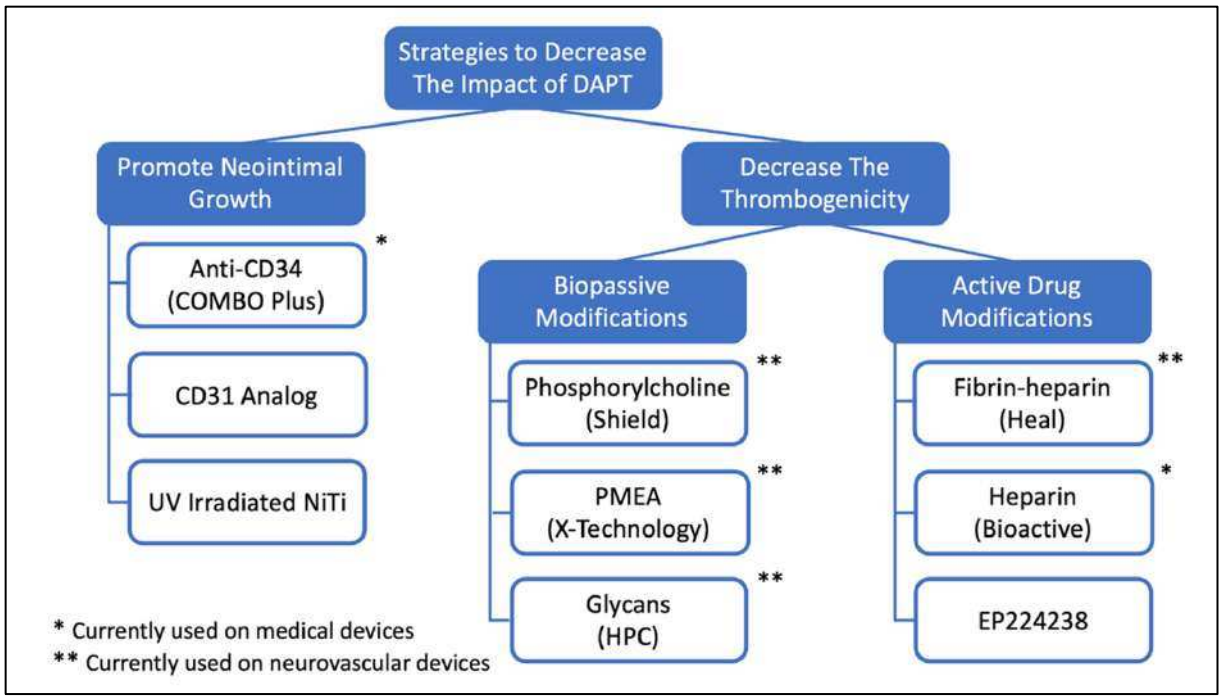


Figure 17. Chart showing the approaches taken by various surface modifications to reduce or eliminate the need for dual antiplatelet therapy (DAPT). NiTi, nitinol; PMEA, poly(2-methoxyethyl acrylate)

Biopassive coatings, such as phosphorylcholine (e.g., Shield technology), glycans (e.g., HPC on p48/p64 devices), and PMEA (e.g., FRED-X), create hydrophilic barriers that reduce platelet adhesion and intrinsic coagulation pathway activation.[172] Biopassive coatings are actually used in the clinical practice and their efficacy is controversial. Preclinical studies showed significantly less thrombus formation with biopassive coatings.[173–178] Clinical studies on FDs with biopassive surface modifications (FDSM) confirmed their safety profile regarding thromboembolic complications.[179] Authors reported an overall rate of 1.2% for major ischemic stroke and 1.5% for minor stroke or transient ischemic attack (TIA) when using DAPT. SAPT with Prasugrel was primarily used with the p64-HPC, showing an overall ischemic complication rate of 2% with prasugrel compared to 1.1% with DAPT. However, the complete aneurysm occlusion rate at 6-24 months post-implantation remained low, with an overall rate of 72.3% (even lower with the FRED-X; 66.2%). Additionally, a non-negligible rate of in-stent thrombosis and stenosis was observed, higher in Phenox-HPC (3.4%) and FRED-X (4.3%) devices

License CC BY-NC-ND 4.0

compared to the PED-Shield (0.8%, p <0.05). Consequently, in the clinical practice, the use of SAPT with FDSM remains controversial, particularly in ruptured cases where SAPT could be beneficial, as its safety profile is still uncertain and appears comparable the ASA use with bare metal FDs. A meta-analysis of bare metal FDs for ruptured aneurysms reported an 8% ischemic stroke rate, a 7% hemorrhagic event rate, and a 4% acute in-stent thrombosis rate. Among 12 studies of FDSM in ruptured aneurysms, 3 focused exclusively on these cases, with 2 using SAPT with ASA alone. However, these studies indicated a high ischemic stroke risk (7.1-10%) and a 7.1% stent thrombosis occlusion rate. Consequently, the feasibility of using FDSM with SAPT for acute aneurysmal subarachnoid hemorrhage remains uncertain due to these heightened risks.[179]

Drug-bound coatings, are alternative strategies for creating antithrombotic devices eliminating the need for systemic drug therapy. Drug-bound coatings like immobilized heparin and fibrin-heparin nanocoatings,[180–184] leverage anticoagulant properties to minimize thrombosis, with early evidence suggesting safety with aspirin monotherapy in coronary applications and promise in neurovascular models.[185]

Coating promoting endothelialization, such as anti-CD34 antibodies[186,187] and CD31 analogs,[188] enhance vessel wall integration, potentially reducing DAPT duration, with in vitro and animal studies demonstrating improved endothelial growth and reduced platelet activation (Figure 16). It has been shown that the P8RI peptide, an analog of the extramembrane portion of CD31, can be linked to the surface of Silk Vista Baby devices, showing improved endothelial adhesion, reduced reaction with blood components.[188] Importantly, being surface modification with a CD31 analog a promising approach to promote rapid endothelial coverage, it might reduce the duration of the antiplatelet therapy in FD treatment.

License CC BY-NC-ND 4.0

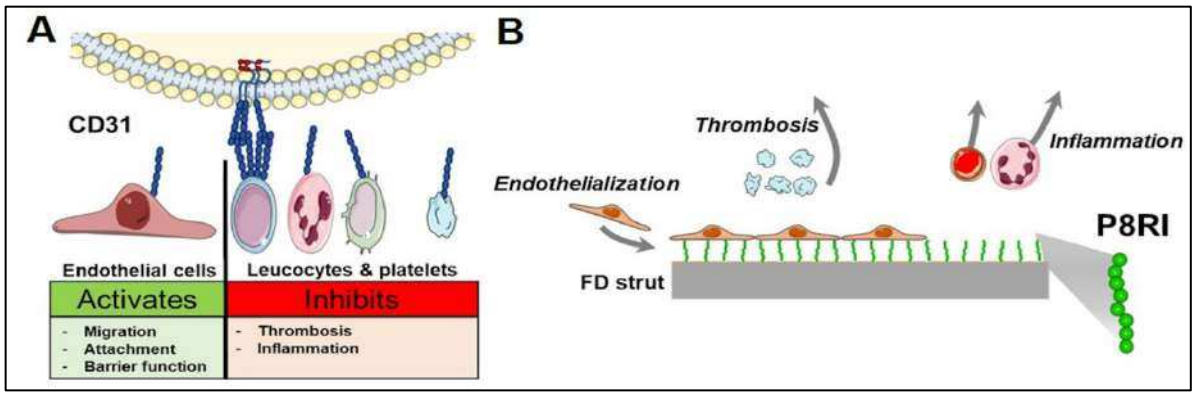


Figure 18. Principal functions of CD31. (A) CD31 is highly expressed at the surface of endothelial cells, platelets, and leukocytes. It plays key regulatory functions for circulation homeostasis on intercellular trans-homophilic binding. (B) Schematic of the P8RI peptide grafted onto the flow diverter strut. P8RI acts as a CD31 agonist by binding to a juxtamembrane CD31 domain. It aims at favoring endothelialization over the flow diverter while preventing thrombosis and inflammation. (Figure courtesy of Professors Aymeric Rouchaud and Jonathan Cortese).

V.2. Stimulation of proliferative response

Some molecules showed to be linked with the aneurysmal wall proliferative response. Blood coagulation factor XIII, also known as the fibrin-stabilizing factor, is a transglutaminase enzyme of the coagulation system that crosslinks fibrin. Beyond its role in hemostasis, factor XIII contributes to wound healing by modulating fibroblast adhesion, migration, and proliferation. In a rodent aneurysm model, exogenous administration of factor XIII induced intimal proliferation in sites predisposed to aneurysm formation.[189] Similarly, in another rodent aneurysm model, high-dose intravenous basic Fibroblast Growth Factor (bFGF) administered three months after aneurysm creation showed to induce some degrees of intimal thickening within aneurysmal walls. Immunohistochemical analysis demonstrated that this effect was mediated by proliferating SMCs.[190]

Modulation of the ECs and SMCs has emerged as promising therapeutic strategy to limit aneurysm initiation and progression. Inducible nitric oxide synthase (iNOS), implicated in ECs and SMCs injury, was found to be upregulated during early aneurysmal changes.

License CC BY-NC-ND 4.0

Pharmacological inhibition of iNOS attenuated aneurysmal alterations and reduced the incidence of aneurysm formation. In a rodent model, has been shown that genetic ablation of iNOS ($iNOS^{-}/^{-}$ mice) did not lower the incidence of induced aneurysms, but significantly reduced aneurysm size and SMCs apoptosis compared with $iNOS^{+}/^{+}$ mice.[191] Consistent with the detrimental role of iNOS, defective interleukin-1β (IL-1β), a potent activator of iNOS-signaling was found to protect SMCs from inflammation-associated cell death.[192] Collectively, these findings suggest that targeting iNOS signaling and NO-mediated SMCs apoptosis may represent a therapeutic avenue for aneurysm prevention and treatment.

Similarly to FDSM, have been developed coted coils to stimulate the proliferative response of the arterial wall after aneurysm coiling.[193] Fucoidans are marine sulfated polysaccharide candidates with complex and heterogeneous chemical structures derived from the cell walls of brown seaweeds, with a range of medical applications related to their antiviral, antithrombotic, anticoagulant, antitumor, antioxidant, immunoregulatory, and anti-inflammatory effects. Fucoidans bind platelets and thrombi, interact with numerous growth factors, and are involved in stromal cell proliferation, spreading, adhesion, and promotion of extracellular matrix synthesis and secretion. Low molecular weight fucoidan (LMWF) also mobilizes bone marrow and hematopoietic stem cells that are recruited to IAs and may participate in the healing process.[193] In rabbit elastase-induced aneurysm model, fucoidan-coated coils showed an improved histological aneurysm healing (according to the presence of more collagen in the neck) compared to bare platinum and dextran-coated groups ($p=0.011$).[193]

V.3. Prevention of aneurysm wall cell injury

Estrogen receptors are expressed on both ECs and SMCs, and estrogen is thought to exert protective effects by enhancing EC function and growth. Experimental studies have shown that estrogen prevents the induction and progression of aneurysms,[194] and estrogen deficiency

License CC BY-NC-ND 4.0

leads to endothelial dysfunction and excessive reactive oxygen species (ROS) generation, triggering EC injury and promoting aneurysm formation.[195]

Pharmacological control of the WSS, seemed another strategy to modulate ECs and SMCs injury. In a rat aneurysm model, batroxobin, a thrombin-like serine protease, lowered fibrinogen concentration and blood viscosity, thereby reducing WSS and limiting ECs and SMCs damage.[196] Similar effects have been shown with inhibition of endothelin B receptors (ETBR), reducing SMCs apoptosis and preventing the development of IAs.[197] Statins, beyond their lipid-lowering effects, exert pleiotropic vascular protective actions. These include improvement of ECs and SMCs function through inhibition of IL-1β and iNOS-induced apoptosis, reduction of free radical formation, and attenuation of endothelial inflammatory responses via suppression of macrophage recruitment and adhesion. Despite these potentially beneficial mechanisms, the role of statins in aneurysm treatment and prevention remains uncertain, with both experimental[198–200] and clinical[201,202] studies yielding contradictory findings.

V.4. Inhibition of inflammation and oxidative stress

A growing body of evidence implicates chronic inflammation as a key driver of IA pathogenesis. The transcription factor nuclear factor-kappa B (NF-κB) has been identified as a central inflammatory mediator in IA formation (Figure 17).[15,203] NF-κB transactivates genes involved in endothelial dysfunction, including vascular cell adhesion molecule-1 (VCAM-1) and monocyte chemoattractant protein-1 (MCP-1), both of which promote macrophage recruitment into the aneurysmal wall. NF-κB also regulates transcription of iNOS, which mediates SMCs death, of the IL-1β, which activates iNOS and suppresses extracellular matrix [ECM] biosynthesis), and of matrix metalloproteinases (MMPs), which exacerbate ECM degradation in addition to MMP-2 and MMP-9 secretion by macrophages.

Targeting NF-κB and its downstream pathways has therefore emerged as a promising therapeutic approach. Inhibition of NF-κB DNA binding by decoy oligodeoxynucleotides

License CC BY-NC-ND 4.0

prevented IA formation by suppressing proinflammatory gene expression.[204,205] Nifedipine reduced NF-κB transcriptional activity, downregulated MCP-1 expression in aneurysmal wall, decreased macrophage infiltration, and lowered MMP-2 expression and activity.[206] Similarly, inhibition of the transcription factor Ets-1 suppressed MCP-1 expression and macrophage accumulation.[207] Anti-MCP-1 gene therapy inhibited IA progression in rats.[208] Ibudilast, a phosphodiesterase-4 inhibitor, decreased endothelial adhesion molecule expression and reduced macrophage migration into aneurysmal walls.[209] Additional anti-inflammatory strategies, such as inhibition of mast cell degranulation or monocyte depletion, have likewise been shown to attenuate IA-related inflammation.[210,211] Anti-inflammatory drugs have also been explored in this context. Aspirin has been hypothesized to reduce IA incidence through inhibition of NF-κB activity, leading to downregulation of MMP-2, MMP-9, and TNF-α in SMCs, as well as decreased endothelial adhesion molecule expression.[212] However, a causal relationship remains unproven.[213] Tetracycline derivatives have shown anti-inflammatory activity via MMP inhibition and reduced aneurysmal rupture rates in mice.[214]

Oxidative stress represents another critical mediator of inflammation in IA pathogenesis. Edaravone, a free radical scavenger, decreased ROS production, inhibited macrophage invasion, and reduced expression of NF-κB, MCP-1, VCAM-1, and MMP-2, showing a potential role in reduction the oxidative stress.[214] ROS is generated primarily through enzymatic activity of nicotinamide adenine dinucleotide phosphate (NADPH) oxidase, heme oxygenase-1 (HO-1), and iNOS. Rosuvastatin also showed a vasoprotective effect, attributed to inhibition of ROS production with consequent increase in NO bioavailability. In a rodent model, Rosuvastatin showed to modulate the endothelial function, reversing the impaired acetylcholine-induced endothelium-dependent dilatations in both renal arteries and aorta and preventing the exaggerated contractions to angiotensin II and phenylephrine renal arteries and aortae.[215]

License CC BY-NC-ND 4.0

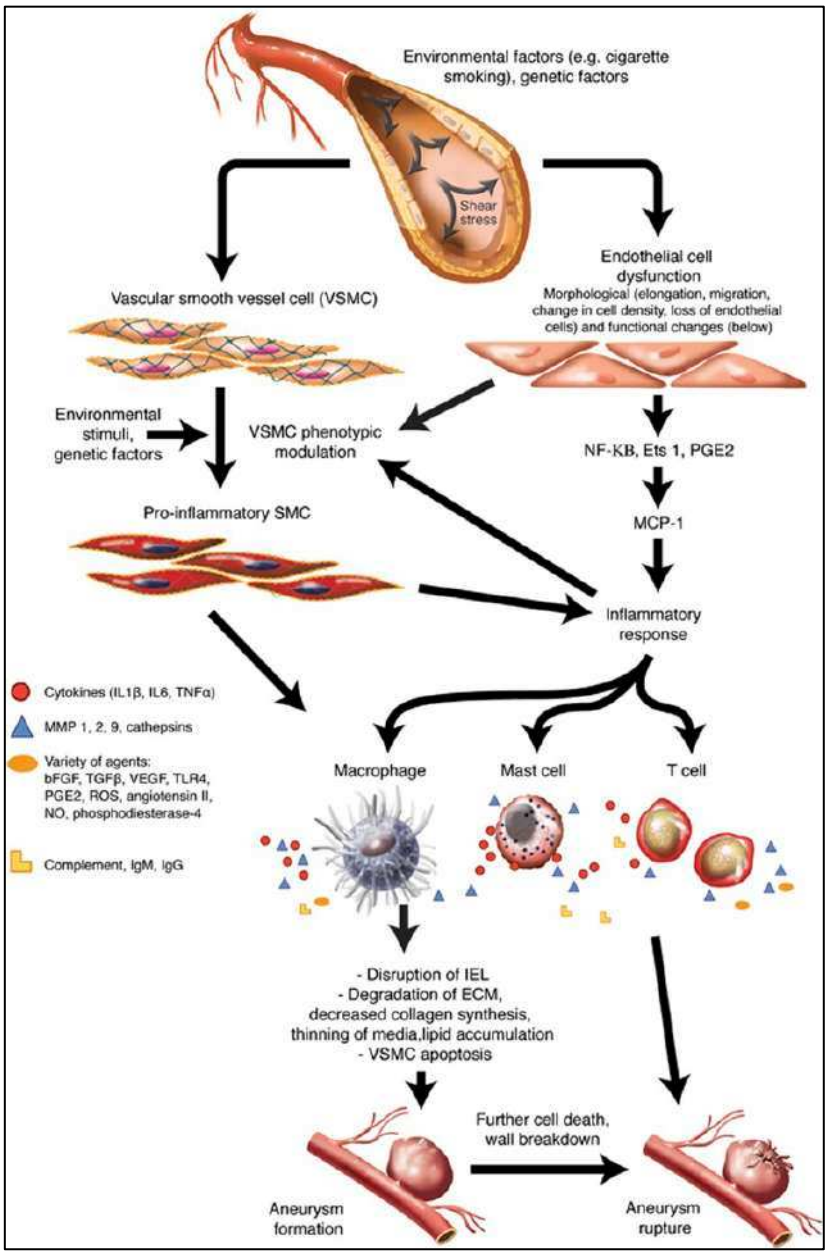


Figure 19. Inflammatory reaction associated with intracranial aneurysm (IA) formation. Aneurysm formation begins with a hemodynamically triggered endothelial dysfunction, followed by a mounting inflammatory response (implicating several inflammatory cells and mediators) and phenotypic modulation of VSMC from a contractile to pro-inflammatory/pro-matrix remodeling phenotype. The inflammatory response in vessel wall leads to disruption of IEL, extracellular matrix remodeling, and subsequent aneurysm formation. Further cell death and vessel wall degeneration ultimately culminate in IA rupture. VSMC, vascular smooth muscle cell; NF-κB, nuclear factor-κB; MCP1, monocyte chemoattractant protein 1; ECM, extracellular matrix; IEL, internal elastic lamina; IL, interleukin; TNFα, tumor necrosis factor-α; MMPs, matrix metalloproteinases; PGE2, prostaglandin E2; bFGF, basic

License CC BY-NC-ND 4.0

fibroblast growth factor; TGF, transforming growth factor; VEGF, vascular endothelial growth factor; TLR4, Toll like receptor-4; ROS, reactive oxygen species; Ig, immunoglobulin; SMC, smooth muscle cell; NO, nitric oxide. Chalouhi et al. Biology of intracranial aneurysms: role of inflammation. J Cereb Blood Flow Metab. 2012[15]

V.5. Inhibition of extracellular matrix degradation

Inhibition of ECM degradation has been obtained in animal models with selective inhibition of MMPs, specifically MMP-2, MMP-9, and MMP-12,[216] of cysteine cathepsins, which possess elastolytic and collagenolytic activity, preventing IA progression.[217] Similar to MMP-mediated damage, these findings suggest that macrophages actively contribute to cathepsin-mediated ECM degradation. Importantly, MMP inhibition may be relevant not only for slowing the natural progression of untreated IAs but also for influencing aneurysm remodeling after EVT. In support of this, MMP-9 knockout mice exhibited a significant reduction in recanalization and recurrence following carotid artery coiling compared with controls.[218]

License CC BY-NC-ND 4.0

Summary

This chapter explores the evolution of treatment strategies for intracranial aneurysms, shifting from lumen-oriented therapies, which focus on physical occlusion through thrombus organization and neck bridging, to wall-oriented approaches that target aneurysmal wall biology for durable healing. Wall-oriented strategies focus on stimulating proliferative responses, preventing wall cells injury, inhibiting inflammation and oxidative stress, and reducing extracellular matrix degradation, through systemic pharmacological interventions or local drug delivery systems such as drug-eluting coils and stents. Surface modified flow diverters (FDSM) are an example of the local delivered wall-oriented strategies. FDSM used in the clinical practice have mainly biopassive coatings (e.g., phosphorylcholine, PMEA, HPC), aiming to reduce thrombogenicity, though clinical outcomes show mixed results, with low complete occlusion rates and persistent risks of thrombosis. Drug-bound coatings (e.g., heparin) have been also studied, but still in preclinical phase. Coatings promoting endothelialization, like anti-CD34 antibodies and CD31 analogs, show promising results in enhancing vessel wall integration and potentially reducing the need for dual antiplatelet therapy. Several systemic pharmacological interventions have been tested, such as (1) factor XIII and basic fibroblast growth factor, enhancing proliferative responses in animal models, (2) target induction of nitric oxide synthase (iNOS) and inhibition of inflammatory mediators (like NF-κB), reducing aneurysm progression by mitigating smooth muscle cell apoptosis and inflammation, (3) Estrogen and Statins, offering protective effects on endothelial and smooth muscle cells, (4) target inhibition of matrix metalloproteinases (MMPs) and cysteine cathepsins, showing potential role in preventing IA progression and improving outcomes post-endovascular treatment.

License CC BY-NC-ND 4.0

Chapter VI. Statins as wall-oriented treatment

Statins are a class of drugs used to reduce the risk of atherosclerotic cardiovascular disease (ASCVD) by lowering low-density lipoprotein cholesterol (LDL-C). They inhibit HMG-CoA reductase, a key enzyme in cholesterol production, increasing LDL-C clearance from the blood.[219,220] Statins are the primary treatment for preventing heart attacks, strokes, and cardiovascular death, with strong evidence supporting their use across diverse patients.[221,222] Statins are classified by intensity: high-intensity (e.g., Atorvastatin 40-80 mg, Rosuvastatin 20-40 mg) reduces LDL-C by ≥50%, moderate-intensity by 30-49%, and low-intensity by <30%.[223] The choice of statin and dose should be tailored to a patient's ASCVD risk, age, comorbidities, and tolerance. Generally well-tolerated, statins may cause muscle pain, rarely severe muscle damage (rhabdomyolysis), and a slight increase in diabetes risk, but their cardiovascular benefits outweigh these risks.[224]

VI.1. Pleiotropic effect of statins

Statins provide benefits beyond cholesterol reduction through pleiotropic effects, independent of LDL-C lowering. These effects include improved endothelial function via increased nitric oxide, reduced inflammation by lowering proinflammatory cytokines, antioxidant effects by decreasing reactive oxygen species, stabilization of atherosclerotic plaques, reduced vascular smooth muscle proliferation, and less vascular and myocardial remodeling. Statins also decrease platelet reactivity and exhibit antithrombotic properties, enhancing cardiovascular protection (Figure 18).[225–228]

License CC BY-NC-ND 4.0

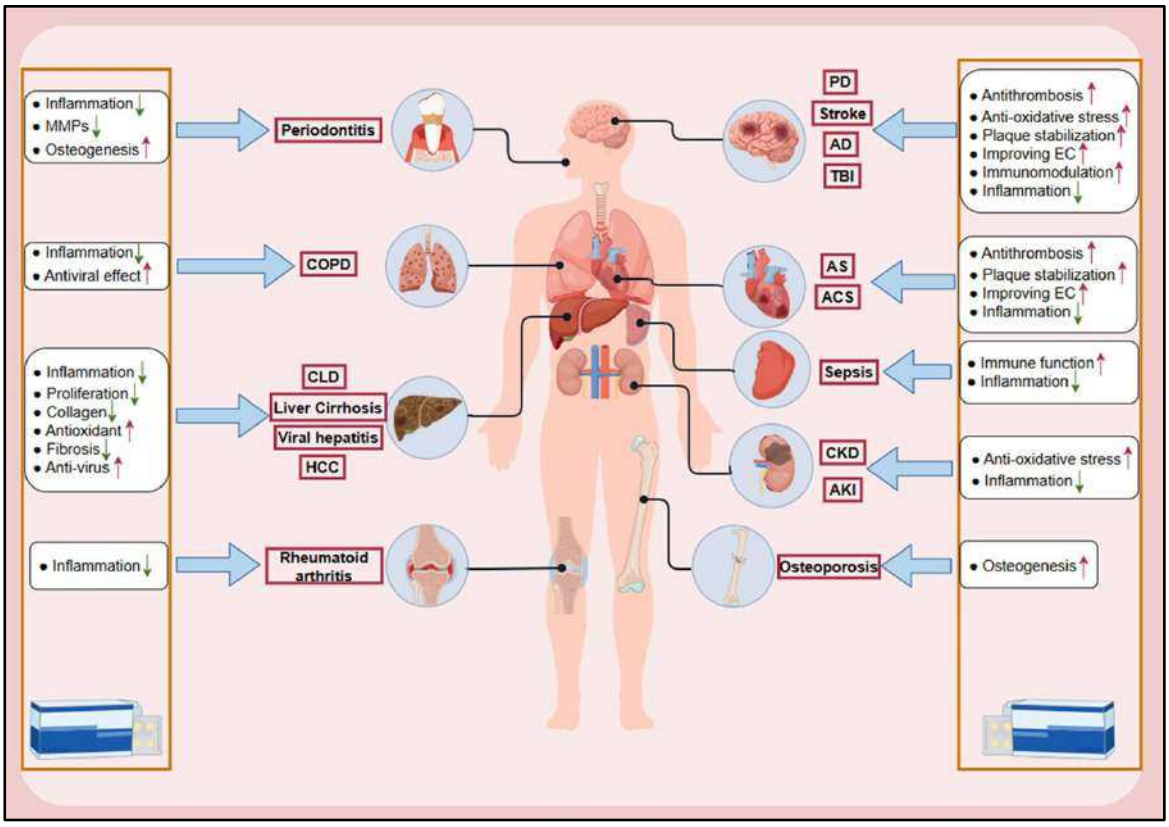


Figure 20. Pleiotropic effects and mechanisms of statins in various organs or systems. COPD, chronic obstructive pulmonary disease; CLD, chronic liver disease; HCC, hepatocellular carcinoma; PD, Parkinson's disease; AD, Alzheimer's disease; TBI, Traumatic brain injury; AS, atherosclerosis; ACS, acute coronary syndrome; CKD, chronic kidney disease; AKI, acute kidney injury; EC, endothelial cell.[228]

Mechanistically, these effects stem from inhibiting isoprenoid synthesis in the mevalonate pathway, which blocks prenylation of small GTP-binding proteins like Rho, Rac, and Cdc42, thereby reducing Rho kinase and NADPH oxidase activity, which modulates vascular tone, inflammation, and oxidative stress (Figure 19).[225,226,229–231] Emerging evidence suggests epigenetic modifications, such as histone acetylation and DNA methylation, also contribute to statin pleiotropy.[232]

Statins are classified into two groups differing in their pharmacological properties, mechanisms of action, and clinical implications: lipophilic statins (e.g., Atorvastatin, Simvastatin, Pitavastatin, and Cerivastatin) and hydrophilic statins (e.g., Rosuvastatin and Pravastatin).[233]

License CC BY-NC-ND 4.0

Overall, lipophilic statins easily cross cell membranes, distributing widely into extrahepatic tissues like vascular smooth muscle and skeletal muscle, while hydrophilic statins present less penetration into non-hepatic tissues,[234] even if the mechanism of action is the same. Due to greater interaction with cell membranes and non-hepatic tissues, lipophilic statins exhibit stronger pleiotropic effects,[225,228,234] but higher risk of muscle-related side effects due to greater skeletal muscle exposure. Hence, hydrophilic statins are preferred for patients under multiple pharmacological therapies or with higher myopathy risk.[235]

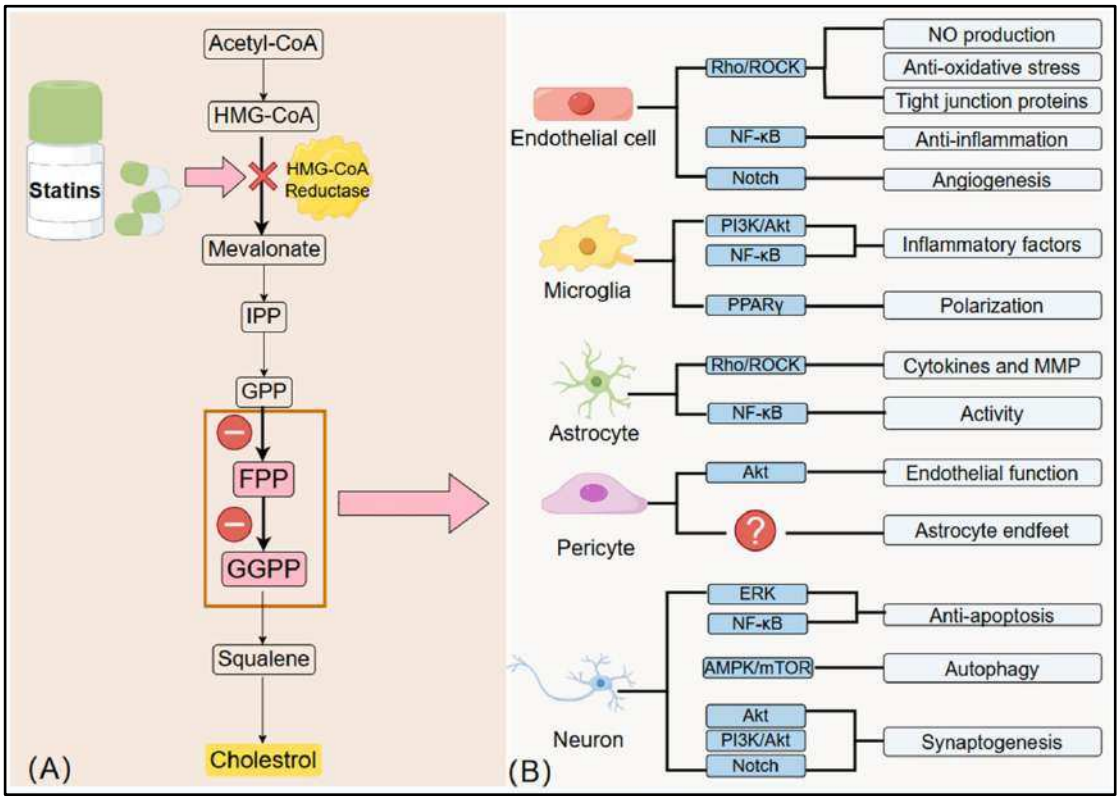


Figure 21. Mechanism of the pleiotropic effects of statins: statins exert pleiotropic effects by inhibiting HMG-CoA reductase to reduce the production of FPP and GGPP, affecting multiple signaling pathways. B Pleiotropic effects of statins on individual NVU cells. Acetyl-CoA: Acetoacetyl coenzyme A; HMG-CoA: 3-hydroxy-methylglutaryl coenzyme A; IPP: isopentenyl pyrophosphate; GPP: geranyl pyrophosphate; FPP: farnesyl pyrophosphate; GGPP: geranylgeranyl pyrophosphate; ROCK: Rho-associated protein kinase; AMPK, adenosine monophosphate-activated protein kinase; ERK: extracellular regulated protein kinases; NF-κB: nuclear factor kappa-B; NVU: neurovascular unit.[228]

License CC BY-NC-ND 4.0

VI.1.1. Statin and endothelium

Endothelial dysfunction, is marked by reduced availability of NO, a molecule essential for vasodilation, inhibition of platelet aggregation, control of smooth muscle proliferation, and regulation of leukocyte-endothelial interactions.[236] Statins improve endothelial function by increasing NO production, mainly through upregulation of endothelial NO synthase (eNOS).[237,238]

Several pathways contribute to eNOS activation (Figure 20):

- Rho/ROCK signaling: Statins inhibit RhoA and ROCK, both of which suppress eNOS. Blocking this pathway also activates PI3K/Akt, which further enhances eNOS activity and provides cardioprotection.[239,240]
- Caveolin-1 regulation: Caveolin-1 normally inhibits eNOS activity. Statins reduce caveolin-1 expression, thereby promoting NO production.[241]
- Kruppel-like factor-2 (KLF2): Statins induce KLF2, a transcription factor that supports eNOS expression and may mediate some of the immunomodulatory effects of statins.[242,243]
- EPCs: Statins enhance EPC mobilization, improving endothelial repair and NO availability.[244–247]

License CC BY-NC-ND 4.0

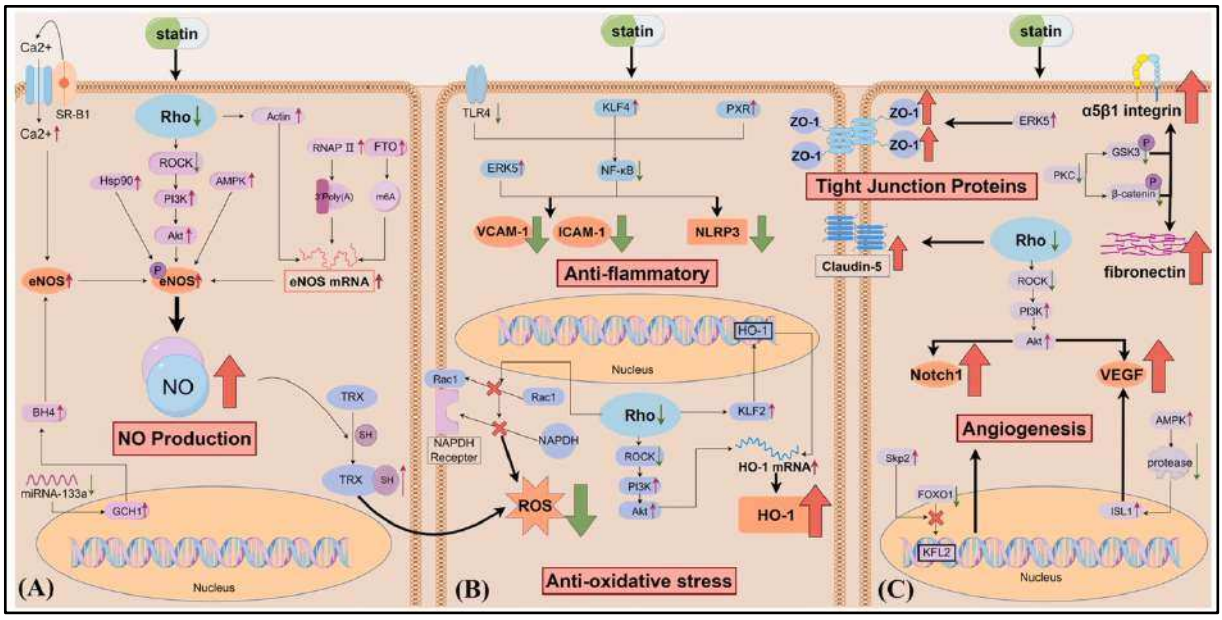


Figure 22. Pleiotropic effects and mechanisms of statins in cerebrovascular ECs. A Mechanisms by which statins improve ECs function. B Antioxidative stress and anti-inflammatory effects of statins in ECs. C Mechanisms by which statins promote angiogenesis and increase TJPs in ECs. SR-B1, scavenger receptor-B1; RNAP II, RNA polymerase II; FTO, Fat Mass and Obesity-Associated Protein; TRX, thioredoxin-1; GCH1, GTP cyclohydrolase 1; BH4, tetrahydrobiopterin; ISL1, insulin gene enhancer protein 1; HO-1, Heme oxygenase 1.[228]

VI.1.2. Statin and smooth muscle cells

The proliferation and migration of vascular SMCs are central to the development of vascular lesions.[248] Statins inhibit these processes through pleiotropic mechanisms, independent of cholesterol lowering. In transplant arteriosclerosis, an immune-mediated reaction against donor ECs and SMCs, statins attenuate disease progression despite the absence of hypercholesterolemia.[249] The inhibition of Rho GTPase activity leads to increased expression of the cell-cycle regulator p27^Kip1 and reduced platelet-derived growth factor (PDGF)-induced SMC proliferation. In experimental models, statins reduced intimal thickening, cellular proliferation, leukocyte accumulation, and PDGF receptor phosphorylation.[250]

License CC BY-NC-ND 4.0

Statins also counteract pro-inflammatory signaling in SMCs. Atorvastatin inhibited IL-18 induced migration, NF-κB activation, and MMP-9 expression in vitro.[251] Similarly, in bovine pulmonary artery SMCs, atorvastatin blocked SMC migration, an effect reversed by geranylgeranyl pyrophosphate (GGPP) and mevalonate, again highlighting the role of Rho/ROCK signaling in SMC proliferation and migration.[252]

VI.1.3. Statin and platelets

Statin therapy reduces the prothrombotic activity, through both cholesterol-dependent and cholesterol-independent mechanisms (Figure 21).

Pravastatin has been shown to decrease platelet reactivity and thrombin generation, effects only partly explained by LDL-C lowering.[253] In mice, Atorvastatin increased platelet eNOS activity and downregulated platelet factor 4 and β-thromboglobulin, effects absent in eNOS knockout animals.[254] Fluvastatin reduced platelet aggregation via activation of PPAR-α and PPAR-γ, and proved more effective than colestimide in this respect.[255,256] Atorvastatin has also been reported to acutely inhibit platelet recruitment, suppressing Nox2, Rac1, protein kinase C, phospholipase A2, and thromboxane A2, while simultaneously increasing NO levels.[257]

The clinical relevance of these antiplatelet effects was supported by the JUPITER trial, in which Rosuvastatin therapy was associated with a reduced risk of venous thromboembolism.[258] This finding is particularly noteworthy because hypercholesterolemia itself is not a strong risk factor for venous thrombosis, suggesting cholesterol-independent, pleiotropic mechanisms underlie this benefit.

License CC BY-NC-ND 4.0

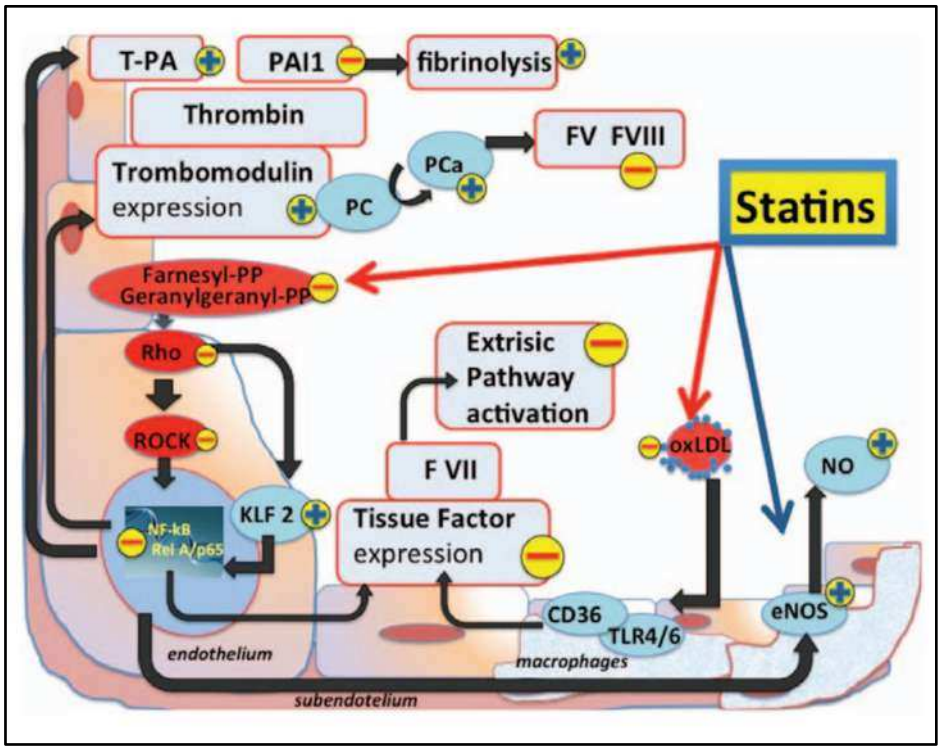


Figure 23. Statins as antithrombotic drug. Statins act by (1) inhibiting tissue factor synthesis and increasing thrombomodulin formation via inhibition of geranylgeranylation of the Rho/Rho kinase pathway and, in turn, nuclear factor-κB (NF-kB) activity; (2) increasing Kruppel-like factor 2 (KLF2) expression and endothelial nitric oxide synthase (eNOS) activity; (3) inhibiting oxidized low-density lipoprotein (oxLDL)–mediated CD36 and Toll-like receptor 4/6 (TLR4/6) activation; and (4) enhancing fibrinolysis. FV indicates factor V; FVIII, factor VIII; NO, nitric oxide; PAI1, plasminogen activator inhibitor 1; PC, protein C; PCa, activated protein C; PP, pyrophosphate; Rho, Rho/ Rho kinase; and T-PA, tissue-type plasminogen activator.[259]

VI.2. Rosuvastatin as wall-oriented strategy

Even if Rosuvastatin is a hydrophilic statin, it has demonstrated strong pleiotropic effects, including anti-inflammatory, antioxidant, and endothelial-protective actions, which may help to stabilize IAs and reduce rupture risk.[215,260,261] Its high affinity for HMG-CoA reductase strongly inhibits the mevalonate pathway, reducing isoprenoid intermediates (e.g., farnesyl pyrophosphate and geranylgeranyl pyrophosphate), which impairs prenylation of small GTP-binding proteins like Rho, Rac, and Cdc42, thereby decreasing vascular inflammation,

License CC BY-NC-ND 4.0

oxidative stress, and endothelial dysfunction.[225,229,260,261,261] Clinical and translational studies showed that Rosuvastatin promotes endothelialization at the aneurysm neck post-coil embolization by enhancing EPCs mobilization, upregulating vascular endothelial growth factor (VEGF)-A, and increasing CD31 expression, supporting vascular repair and integrity.[262–265] Compared to lipophilic statins like atorvastatin, rosuvastatin more effectively downregulates pro-inflammatory markers (e.g., IL-1β, IL-18, IL-23) and upregulates anti-inflammatory cytokines (e.g., IL-10, IL-37) in endothelial cells, attributed to its unique molecular structure and high tissue selectivity.[260,261] Epidemiological data and meta-analyses indicate statin therapy, particularly Rosuvastatin, is associated with lower aneurysm rupture and recurrence rates after EVT, with a dose-response relationship and no significant increase in adverse events like ischemic stroke or intracerebral hemorrhage.[266,267] In rat models of vascular injury, Rosuvastatin (10 mg/kg/day) significantly increased CD31 and other angiogenic marker expression, enhancing endothelial regeneration, reducing neointimal hyperplasia, and improving arterial wall integration compared to controls.[262–265] While other statins (e.g., Atorvastatin, Pravastatin, Simvastatin) also promote endothelialization, Rosuvastatin showed superior efficacy in improving endothelial function and reducing inflammation in endothelial cells, making it a promising adjunctive therapy for IA management, and might be investigated in the treatment with FDs.[260,268–276]

Evidence regarding the administration of Rosuvastatin in rabbit models exists, but it is not specific to IAs or their vascular repair. Multiple studies have investigated the pleiotropic effects of Rosuvastatin in rabbit models of atherosclerosis, vascular inflammation, and endothelial dysfunction. These studies demonstrated that Rosuvastatin reduces aortic stiffness, improves endothelial function, decreases inflammatory and oxidative stress biomarkers, and stabilizes atherosclerotic plaques in rabbits fed a high-cholesterol diet.[277–282] However, none of the identified studies directly addressed the use of Rosuvastatin in rabbit models of IAs or its effects on aneurysm healing, endothelialization, or recurrence in this specific vascular territory and neither after EVT. Nevertheless, the pleiotropic vascular benefits of Rosuvastatin have

License CC BY-NC-ND 4.0

been described in a rodent model, suggesting potential for further investigation in IA-specific contexts.[264]

Summary

This chapter focus on statins, primarily used to lower LDL cholesterol and reduce atherosclerotic cardiovascular disease risk, as a wall-oriented treatment for intracranial aneurysms (IAs) due to their pleiotropic effects. Statins improve endothelial function, reduce inflammation, provide antioxidant effects, stabilize atherosclerotic plaques, inhibit vascular smooth muscle cell (SMC) proliferation, and decrease platelet reactivity. These effects are induced by the inhibition of isoprenoid synthesis in the mevalonate pathway, affecting signaling pathways like Rho/ROCK and NF-κB, by the increase of nitric oxide (NO) production in the endothelial cells, and the mobilization and recruitment of endothelial progenitor cell (EPC) in the vascular wall injury site. Rosuvastatin, a hydrophilic statin, exhibits strong pleiotropic effects, including anti-inflammatory and endothelial-protective actions, by downregulating proinflammatory cytokines (e.g., IL-1β, IL-18) and upregulating anti-inflammatory markers (e.g., IL-10), potentially stabilizing IAs and reducing rupture risk. In preclinical studies, Rosuvastatin enhances endothelialization at the aneurysm neck post-coil embolization by upregulating VEGF-A and CD31, reducing neointimal hyperplasia, and improving arterial wall integration. Epidemiological data suggest that statins, particularly Rosuvastatin, are associated with lower IA rupture and recurrence rates after endovascular treatment, with a dose-response relationship and minimal adverse events. The chapter poses key research questions about Rosuvastatin's role in improving aneurysm occlusion that has been addressed in the next one.

License CC BY-NC-ND 4.0

Chapter VII. Rationale for Rosuvastatin therapy to enhance FD healing

FDs represent a paradigm shift in the endovascular treatment of IAs, promoting parent artery reconstruction and aneurysm exclusion through hemodynamic redirection and progressive endothelialization. However, FD therapy is limited by incomplete aneurysm occlusion in up to 20-30% of cases, delayed healing, and risks such as side branch occlusion or thromboembolic events.[23,118,119] These limitations underscore the need for adjunctive therapies to accelerate and optimize FD healing. Here I outline the rationale of the statin therapy, particularly Rosuvastatin, in the FD treatment, formulating the key research questions addressed in this thesis.

First of all, statin therapy has been shown to inhibit platelet recruitment,[257] reduce platelet reactivity, decrease thrombin generation,[253] and, when combined with aspirin, enhance its antithrombotic effect,[283] and reduce aspirin resistance.[284] Incomplete or late aneurysm occlusion is often caused by insufficient reduction of intrasaccular flow, leading to delayed or absent thrombosis of the sac, which is further inhibited by DAPT. Thus, in these cases, DAPT reduces platelet aggregation on FD struts, but may also hinder the sac thrombosis that is essential for aneurysm occlusion. Statin therapy could reduce the duration[285] or even the need for DAPT thanks to faster endothelialization. SAPT combined with high-dose statin therapy might be sufficient to prevent platelet aggregation and may be more effective than DAPT in accelerating sac thrombosis, particularly when using FDSMs.

Second, FD healing requires sac thrombosis followed by the development of stable fibrous tissue, as well as endothelialization of FD struts, which occurs more slowly across the aneurysm neck.[84–86] 69-71 A pharmacological approach to enhance endogenous endothelial repair could accelerate this healing process. Statins stimulate mechanisms that directly support neointimal growth and vascular remodeling (Figure 11).[80,87,124]

License CC BY-NC-ND 4.0

Third, FDs cover perforators and side branches, risking occlusion in 5-15% of cases, particularly for smaller vessels.[154] Low porosity of FDs reduces the inflow within side branches leading to thrombosis without adequate neointimal remodeling of the ostia (Figure 10).[69] Enhancing endothelialization induced by statin therapy could preserve branch patency by accelerating EC migration and reducing inflammatory thrombus formation.

Fourth, statins offer a compelling adjunctive strategy to promote endothelialization while mitigating inflammation and thrombosis, but Rosuvastatin, a hydrophilic statin, exhibits superior vascular benefits compared to other statins, as shown by comparative studies on endothelial function and plaque stabilization.[274–276,278] Rosuvastatin oral administration with Aspirin might offer a non-invasive, cost-effective approach to enhance FD healing.

VII.1. Main thesis questions

This thesis aimed to investigate Rosuvastatin to enhance FD healing in a preclinical model, using elastase-induced aneurysms in rabbits, that were randomly assigned to Rosuvastatin plus Aspirin (Rosu+ASA) versus Aspirin alone (ASA) to address the following key questions:

1. **Does Rosuvastatin, when combined with aspirin, improve aneurysm occlusion rates compared to the antiplatelet therapy alone?**

Hypothesis: Rosu+ASA increase and accelerate complete aneurysm occlusion by enhancing vascular wall healing.

2. **Does Rosuvastatin, when combined with aspirin, increase the patency of side branches covered by the FD compared to the antiplatelet therapy alone?**

License CC BY-NC-ND 4.0

Hypothesis: The pleiotropic effects of Rosuvastatin preserve patency of side branches covered by the FD.

3. **What is the overall impact of Rosuvastatin therapy on complete occlusion and full patency of covered branches (composite outcome)?**

Hypothesis: Rosu+ASA yields superior efficacy and safety outcomes.

4. **Is there a correlation between Rosuvastatin serum levels and vessel wall components (endothelial cells and collagen fibers) covering the FD struts?**

Hypothesis: Higher Rosuvastatin serum levels correlate with increased FD struts colonization.

These questions were tested in 22 rabbits, with assessments conducted 2 weeks post-implantation, providing evidence for Rosuvastatin as an adjunctive therapy in FD treatment.

License CC BY-NC-ND 4.0

Summary

This chapter focus on the rationale of the hypothesis: add Rosuvastatin to the standard antiplatelet therapy to increase safety and efficacy of the FD treatment of intracranial aneurysms (IAs). Despite FDs' ability to redirect blood flow and induce endothelialization, limitations such as incomplete occlusion in 20-30% of cases and risks of side branch occlusion or thromboembolism necessitate improved strategies. Rosuvastatin, a hydrophilic statin, is investigated for its ability to reduce platelet reactivity, enhance endothelial repair, and mitigate inflammation, potentially reducing the need for dual antiplatelet therapy (DAPT) and accelerating sac thrombosis and neointimal growth. Using a preclinical rabbit model with elastase-induced aneurysms, the study tests whether Rosuvastatin combined with Aspirin improves aneurysm occlusion rates, preserves side branch patency, and correlates with increased endothelial and collagen coverage of FD struts compared to Aspirin alone. The research has the aim to assess if Rosuvastatin can be a cost-effective and non-invasive approach to optimize FD healing and increase efficacy and safety of FD treatment. The protocol is presented in the following chapter.

License CC BY-NC-ND 4.0

Chapter VIII. Preparation of the rabbit model

VIII.1. Rabbit model creation and FD deployment

To better understand the biological mechanisms involved in EVT of IA, it is necessary to use experimental animal models. Each model carries its own advantages and limitations. Various IA models have been developed in animals such as rabbits, mice, rats, pigs, dogs, and sheep.[286–288] Rodent models offer the advantage of producing aneurysms in an intracranial location without requiring direct surgical manipulation of intracranial arteries.[288–293] However, their main limitation lies in the small size of the aneurysms and vessels, which makes them unsuitable for testing endovascular devices. A systematic review published in 2010 by a consortium of research groups working on animal models for the evaluation of endovascular procedures summarized the strengths and weaknesses of each available model.[288] It concluded that the two most appropriate were the surgically created bifurcation aneurysm model in dogs and the elastase-induced aneurysm model in rabbits. The advantages and limitations of the rabbit elastase model have been extensively described by Brinjikji et al.[287]

All experimental procedures in this work used the elastase-induced aneurysm model in rabbits (Figure 22).[294–296] This saccular aneurysm model was derived from the fusiform aneurysm model originally developed in rat aortas by Michel et al.[297] Its advantages include similarities between the rabbit and human coagulation systems, low inflammation, sparse cellularity (mainly SMCs, fibroblasts, and rare mononuclear cells), and intra-saccular thrombus formation[298], features that closely resemble the human pathophysiology. As a result, the histological and morphological characteristics of aneurysms generated with this model are comparable to human IAs.[299] Moreover, the vessel size in rabbits is compatible with clinical endovascular devices, making the model particularly suitable for device testing.

Aneurysms were created in New Zealand White rabbits (3.5–4 kg) under general anesthesia with intramuscular ketamine (20 mg/kg), xylazine (4.5 mg/kg), and acepromazine 1% (1 mg/kg). After shaving the cervical region, local anesthesia with 2% lidocaine (Xylocaine®,

License CC BY-NC-ND 4.0

AstraZeneca) was administered subcutaneously, followed by a midline incision to expose the right common carotid artery (CCA). After dissection, an arteriotomy was performed, and a 5-Fr introducer sheath (Radiofocus® Introducer II, Terumo Europe) was inserted retrogradely about 1 cm from the CCA origin. Intravenous heparin (2000 IU; Héparine Choay®, 25,000 IU/5 mL) was administered to prevent intraprocedural thrombosis. Under fluoroscopic guidance (Artis Icono, Siemens Healthineers), a 4-Fr arterial embolectomy catheter (EMB 40, Fogarty®, Edwards Lifesciences, Germany) was advanced retrogradely to the CCA origin. The balloon was inflated with a contrast solution (Hexabrix® 320 mg/mL, Guerbet, Roissy CdG, France) to create a filling chamber (Figure 17). A solution containing 45 IU of porcine pancreatic elastase (type I, E1250-50 MG, Sigma®, France) was then injected into this chamber and left in place for 20 minutes. The catheter and introducer were subsequently removed, and the distal CCA ligated.

After closure of the deep muscle layers and skin with 4-0 Vicryl sutures, the rabbit was returned to its cage. Three weeks after surgery, aneurysms histologically and morphologically comparable to human IAs, with a maximum diameter of 5-10 mm and a neck of approximately 4 mm, were obtained on the right subclavian artery.

License CC BY-NC-ND 4.0

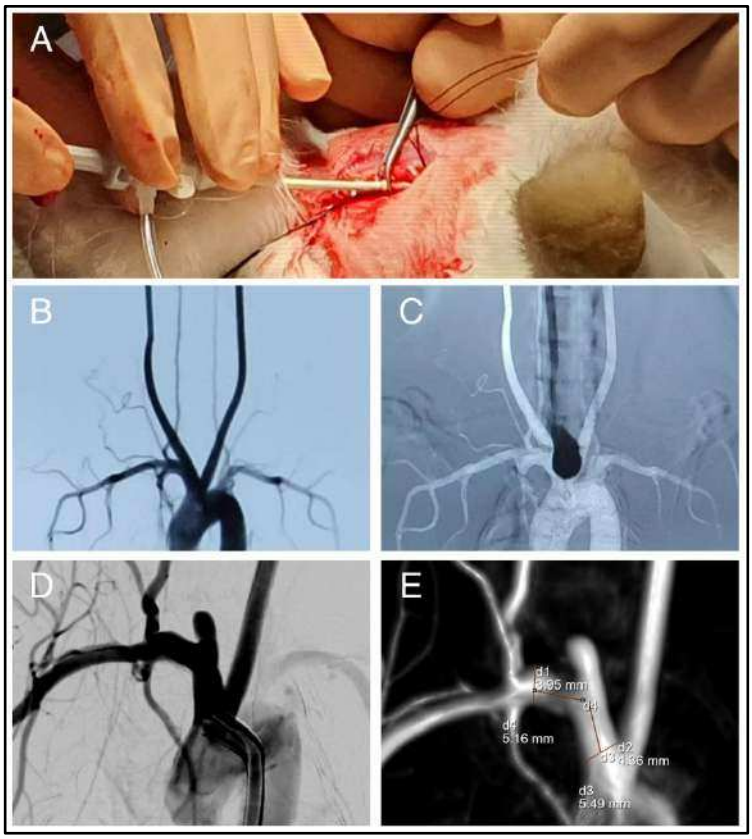


Figure 24. Elastase-induced aneurysm model in the rabbit. (A) A sheath is inserted retrogradely into the right common carotid artery (RCC), and a balloon catheter is advanced through the sheath and inflated at the RCC origin (B/C). After 20 minutes of elastase incubation and ligation of the RCC, an aneurysmal lesion develops at the RCC origin (D/E).

VIII.2. FD deployment

For the purpose of the study, one month after model creation FDs were deployed. After shaving the right femoral region, local anesthesia with 2% lidocaine (Xylocaine®, AstraZeneca) were administered subcutaneously, followed by an incision to expose the right common femoral artery (CFA). After dissection, an arteriotomy was performed, and a 6F introducer sheath (Radiofocus® Introducer II, Terumo Europe) was inserted retrogradely about 3 cm reaching the right iliac artery origin. Intravenous heparin (2000 IU; Héparine Choay®, 25,000 IU/5 mL) was administered to prevent intraprocedural thrombosis. Under fluoroscopic guidance a 6F guide catheter (Envoy 6F) was advanced over a 0.35-inch guidewire in the right subclavian

License CC BY-NC-ND 4.0

artery. A run and a 3D acquisition were acquired to confirm the aneurysm and to select the FD according to subclavian artery diameters. With a 0.21-inch microcatheter (Headway21, MicroVention) a bare metal FD (Silk Vista, Balt) was deployed. Subsequently, pulling back the Envoy 6F, a run of the infrarenal descending aorta was acquired to select an arterial segment with lumbar branches to be covered with a second FD (Figure 23). After FD implantation OCT imaging was acquired with the Spryte® HF-OCT, with a 100 mm/s pull-back speed, generating 540 frames/pull-back with simultaneous intra-arterial iodine contrast injection at a rate of 3–6 ml/s for a total volume of 16– 24 ml to clear the blood from the vessel (Figure 24).

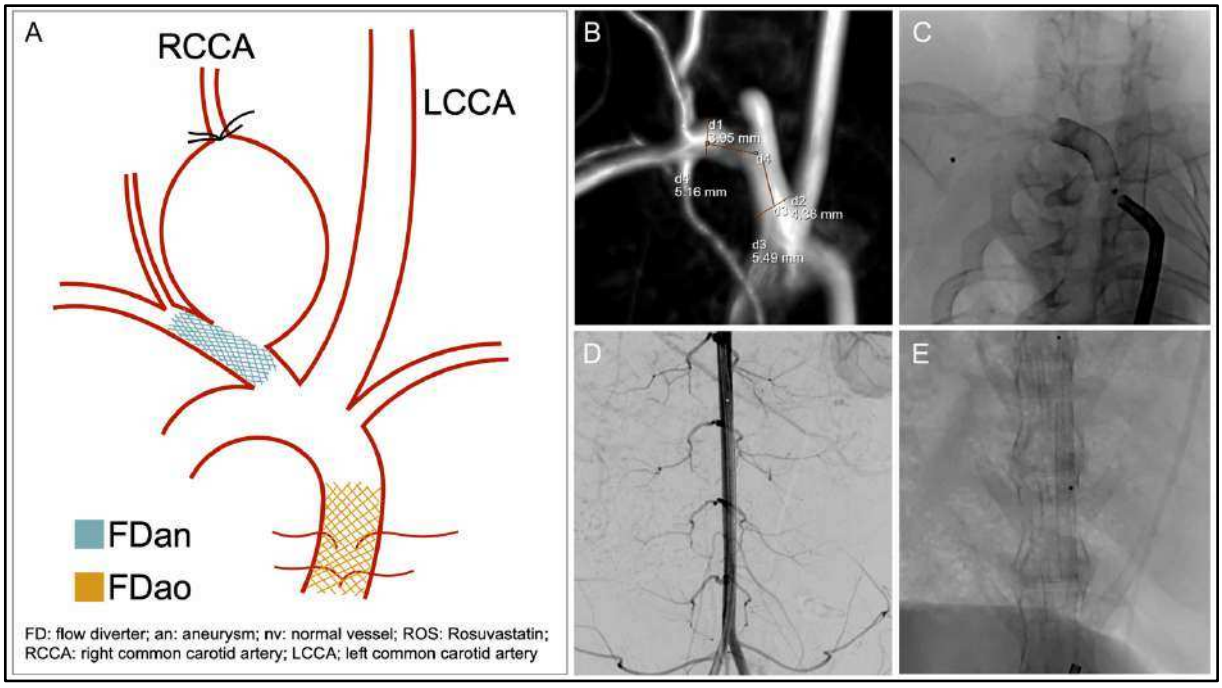


Figure 25. Protocol of FD implantation. We implanted two bare metal FD: the first one at the level of the right subclavian artery (A/B/C); the second one in the descending aorta (A/D/E).

The catheter and introducer were subsequently removed, and the CFA ligated. After closure of the deep muscle layers and skin with 4-0 Vicryl sutures, the rabbit returned to its cage.

Two weeks after FDs implantations, we did the final controls. We exposed and introduced a vascular sheath in the left CFA, following the same process described before. Under

License CC BY-NC-ND 4.0

fluoroscopic guidance a 6F Envoy was advanced over a 0.35-inch guidewire proximally to the FD deployed in the descending aorta. An OCT imaging was acquired for the assessment of the covered branches. Then, the Envoy 6F was advanced in the ostium of the right subclavia. A run and a 3D imaging were done to assess the aneurysm occlusion. Finally, under general anesthesia, animals were euthanized using a lethal injection of pentobarbital (60 mg/kg). Through a bilateral thoracotomy, the right subclavian artery containing the FD and aneurysm was carefully dissected and transected both proximally and distally to the FD to obtain the sample. Through a midline abdominal incision, the retroperitoneal space was exposed. The infrarenal aorta containing the FD was then carefully dissected and transected proximally and distally to the FD to obtain the sample.

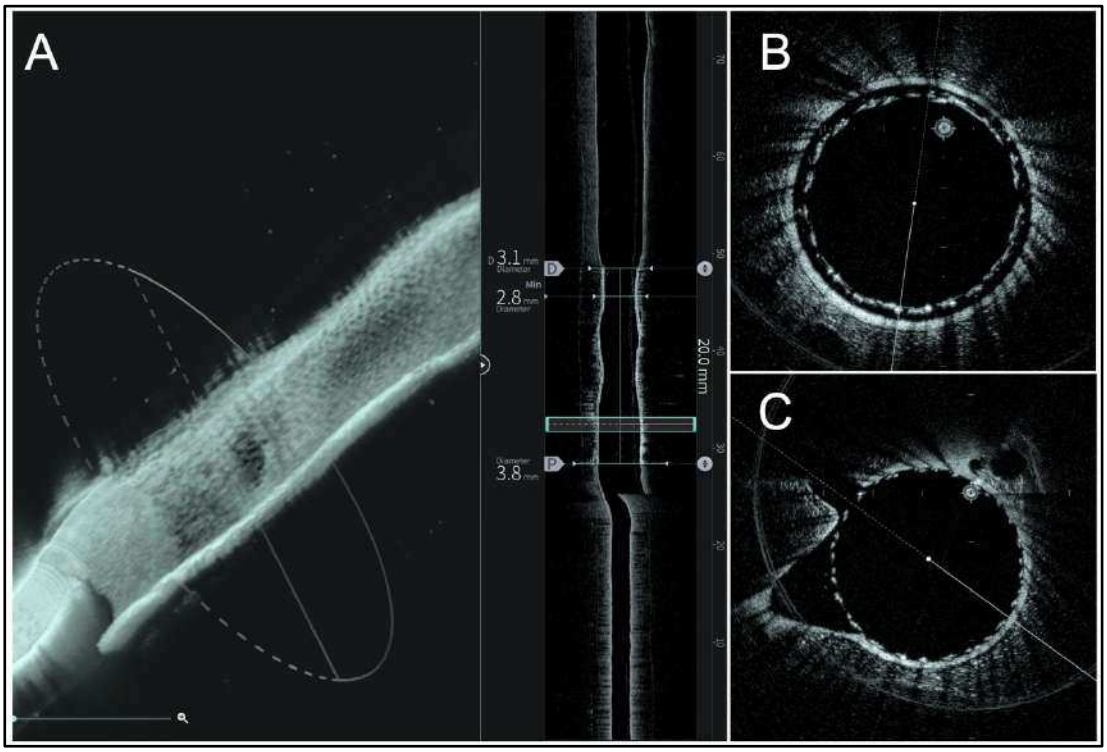


Figure 26. High-Frequency Optic Coherence Tomography. (A) Superficial 3D reconstruction of the flow diverter implanted in the descending aorta. (B) Axial view showing the distal gap between the flow diverter and the arterial wall. (C) Axial view showing the ostia of two branches covered by the flow diverter.

License CC BY-NC-ND 4.0

VIII.3. Rosuvastatin and Aspirin administration

The study conducted by Liu P et al. provided direct evidence that Rosuvastatin enhances vascular repair and endothelialization of IAs after coil embolization.[264] In this model, Rosuvastatin was administered at the dosage of 20 mg/kg by gavage, significantly increased the repair score at the aneurysm neck, promoted integration of the endothelial layer, and elevated the number of kinase insert domain receptor-positive cells, indicating improved endothelialization. Rosuvastatin also increased the total amount of circulating EPCs. Available animal studies indicate that higher or standard experimental doses of Rosuvastatin (e.g., 10–20 mg/kg) are required to achieve significant EPC mobilization, endothelialization, and vascular repair in models of carotid artery injury and IA repair.[263,264] In mouse models of hindlimb ischemia, low-dose Rosuvastatin (0.1 mg/kg) increased EPC mobilization and angiogenesis, whereas higher doses (5 mg/kg) did not further enhance these effects, suggesting a non-linear, context-dependent dose-response that may not generalize to all vascular beds or injury models.[300] Overall, the consensus from animal models is that effective EPC mobilization and endothelialization typically require standard or higher experimental doses of Rosuvastatin, although the dose-response may vary depending on the model and endpoint. For our study, we chose to use a standard dose of Rosuvastatin (10 mg/kg).

Regarding Aspirin administration, the typical dosage used in animal models of vascular repair, endothelialization, or IA stabilization is 10 mg/kg/day (oral or via gavage).[301–305] We did not use dual antiplatelet therapy, based on the results of the CICAFLOW study.[171] In this study on rabbit models, Forestier et al. compared arterial wall integration and endothelial coverage of different coated and uncoated FDs (Silk Vista, Pipeline Shield, and Surpass Evolve) under different antiplatelet regimens (no therapy, Aspirin alone, or Aspirin plus Ticagrelor). They found no differences between Aspirin alone and Aspirin plus Ticagrelor in terms of stent patency or neointimal thickness, and the type of stent (coated vs. uncoated) did not affect the results. Notably, the study observed a higher rate of neointimal coverage in the group without

License CC BY-NC-ND 4.0

antiplatelet therapy compared with those receiving Aspirin or dual therapy, suggesting a modulatory effect of pharmacological treatment on the endothelialization process.

In our study, Rosuvastatin was prepared from powdered ROS Arrow® 20 mg tablets. Aspirin was prepared from ASPIRINE Bayer® 500 mg. Both drugs were administered as an aqueous solution. The tablets were pulverized using a RM 200 RETSCH® mortar grinder for 3 minutes with a crushing force setting of 3. The resulting powder was dissolved in 3 mL of water and administered orally via gavage at approximately 14:30 daily. Five days before FD implantation, subjects were premedicated with Aspirin and Rosuvastatin or Aspirin alone according to the randomization group, and this medication regimen was continued until the final procedure.

VIII.4. Timeline of the follow-up

The follow-up timeline of this study, set at two weeks after FD implantation, was designed to assess the early effects of Rosuvastatin on FD healing and aneurysm occlusion. This early time window was chosen based on preclinical evidence indicating that thrombus formation, endothelialization, and neointimal growth initiate rapidly after FD deployment, typically within 7-14 days. Histopathological studies support this, demonstrating undifferentiated inflammatory cells adhesion as early as day 1 and visible neointimal layers by day 7.[84–86] A longer follow-up period (e.g., 4-8 weeks or beyond) could allow more complete occlusion in both groups (Rosu+ASA vs. ASA alone) due to natural healing progression, potentially masking subtle differences in early healing dynamics attributable to Rosuvastatin. Rosuvastatin's pleiotropic effects, including enhanced NO bioavailability, EPCs mobilization, and reduced inflammation, likely influence intermediate and late healing stages throughout therapy. However, extending the analysis to multiple time windows while maintaining the same sample size could reduce statistical power and introduce bias. Further studies are needed to evaluate the long-term (3-6 months) effects of statin therapy on FD efficacy and aneurysm occlusion.

License CC BY-NC-ND 4.0

VIII.5. Aneurysm occlusion assessment

For the efficacy outcome of our study a DSA of the subclavian FD was done. Aneurysm occlusion was evaluated with the O'Kelly-Marotta (OKM) scale (Figure 25), an angiographic grading system specifically designed to evaluate aneurysm occlusion following treatment with FD. Unlike traditional scales, the OKM scale accounts for the unique hemodynamic changes induced by flow diversion, which often result in gradual aneurysm thrombosis rather than immediate occlusion.

The OKM scale is a two-axis system:

• Aneurysm Filling (A-D):

A: Total filling

B: Subtotal filling

C: Entry remnant

D: No filling (complete occlusion)

• Contrast Stasis (1-3):

1: No stasis

2: Stasis in the venous phase

3: Stasis persisting into the next arterial phase

Each angiogram is graded by combining the filling and stasis scores (e.g., B2, C3). This allows for a nuanced assessment of both the degree of residual aneurysm filling and the dynamics of contrast washout, which are critical for predicting long-term occlusion after flow diversion.

The OKM scale has demonstrated substantial inter-observer reliability (κ=0.74) and near-perfect intra-observer reliability (κ=0.99), making it suitable for use by clinicians with varying backgrounds and levels of training.[306] It is widely used in clinical studies to report angiographic

License CC BY-NC-ND 4.0

outcomes after flow diverter treatment and is considered a reliable tool for standardized assessment.

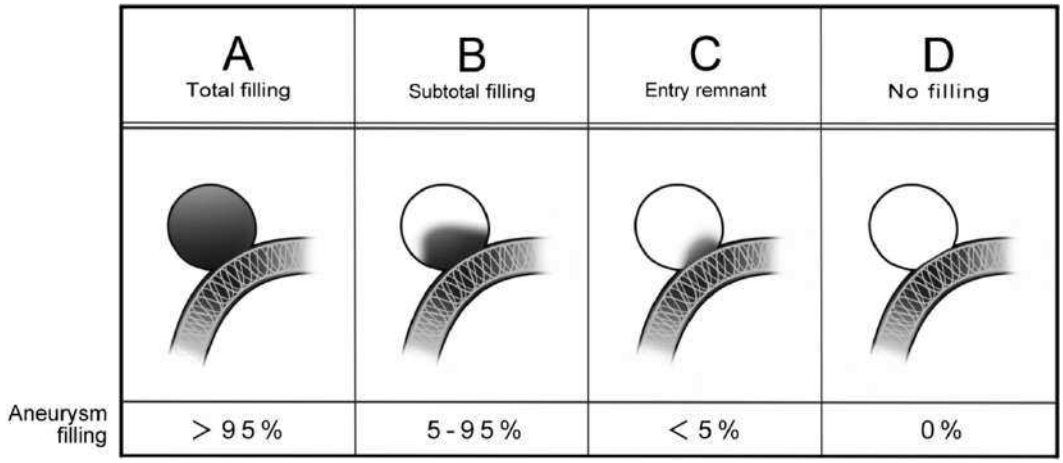


Figure 27. Schematic illustration of modified O'Kelly-Marotta scale.[307]

VIII.6. Patency of covered branches assessment

For the safety control of our study a High Frequency-Optical Coherence Tomography (HF-OCT) was done at the level of the aortic FD, immediately after deployment and after two weeks. Covered branches (lumbar arteries) were defined patent when no neo-tissue was observed over the FD at the level of the ostium, stenotic when ≥50% of the neo-tissue covered the FD over the ostium or occluded when neo-tissue completely occluded the ostium (Figure 26). We assessed the effect on different size branches, analyzing the patency of covered arteries smaller or bigger than 1 mm. OCT imaging was acquired with the Spryte® HF-OCT, with a 100 mm/s pull-back speed, generating 540 frames/pull-back with simultaneous intra-arterial iodine contrast injection at a rate of 3-6 ml/s for a total volume of 16-24 ml to clear the blood from the vessel. While HF-OCT is not yet standard in clinical practice, its feasibility and utility for in situ cerebrovascular volumetric microscopy and prediction of aneurysm healing have been demonstrated in both animal models and early human experience.[308–310]

License CC BY-NC-ND 4.0

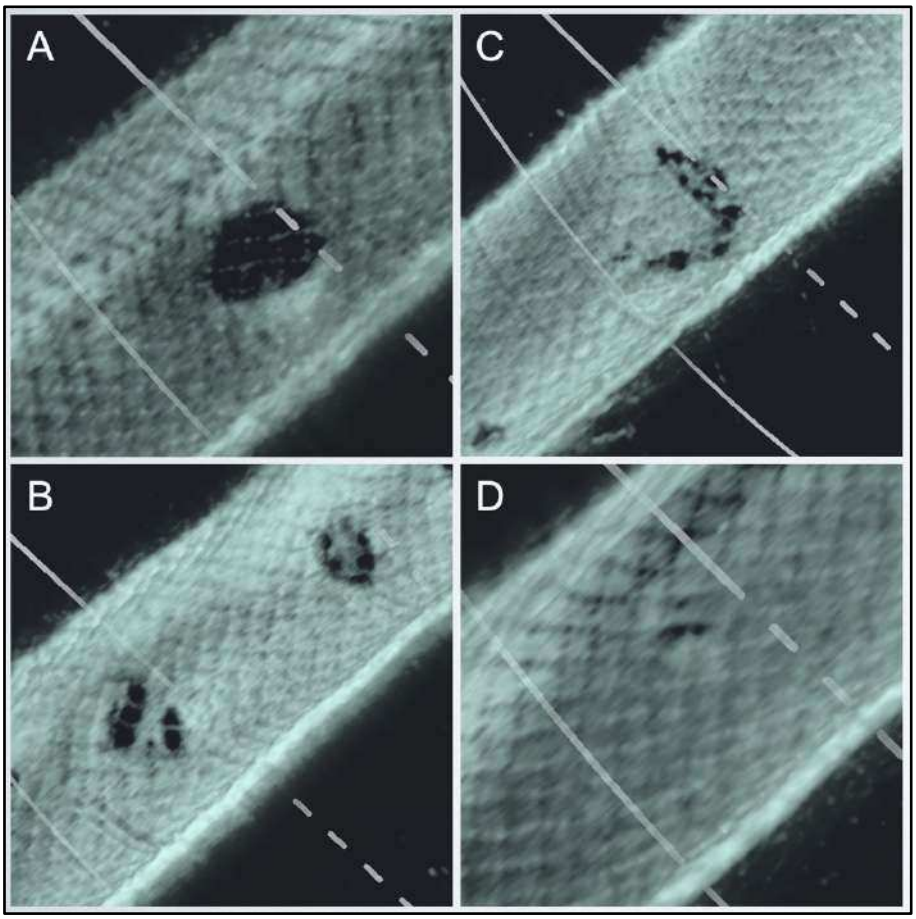


Figure 28. Covered branch patency. (A/B) Patent branches with a neointimal tissue covering the ostium <50%. (C) Suboccluded branch with neointimal tissue covering the ostium ≥50%. (D) Occluded branch with the ostium completely occluded.

VIII.7. Histological analysis

Qualitative and quantitative analysis of the neo-tissue covering the aortic FD was done with the histomorphological and Multiphoton Microscopy (MPM) analyses.[188,311,312]

For the histomorphological analysis (Figure 27), fixed specimens were dehydrated in a graded series of ethanol and then embedded in methyl methacrylate. Transversal (in the case of stented-descending aorta branch) or longitudinal (FD-treated aneurysm; across the neck) tissue sections (10 µm) across the aneurysm neck were performed with diamond wire swa or

License CC BY-NC-ND 4.0

with a laser microtome (TissueSurgeon, LLS ROWIAK GmbH, Hannover, Germany). Tissue sections were stained with H&E (hematein and eosin). Stained tissue sections were digitized using the Hamamatsu NanoZoomer 2.0-RS digital slide scanner (Hamamatsu Photonics, Hamamatsu City, Shizuoka, Japan) at a 40x magnification (i.e. 227 nm/pixel). For quantitative tissue strut coverage, we used QuPath software (v0.5.1). Several parameters were determined including, the percentage of strut cover (SC), the mean NeoIntimal Thickness (NIT, µm), neointimal coverage ratio, neointima-to-media ratio in the regions outside the neck. To assess the overall quality of stent coverage, we determined the percentage of struts covered (SC) by neotissue, regardless of the morphology of the tissue or the neointimal thickness. We then analyzed the extent of quantitative stent coverage by measuring the exact values (µm) of NIT. Table 2 for histological analysis protocol.

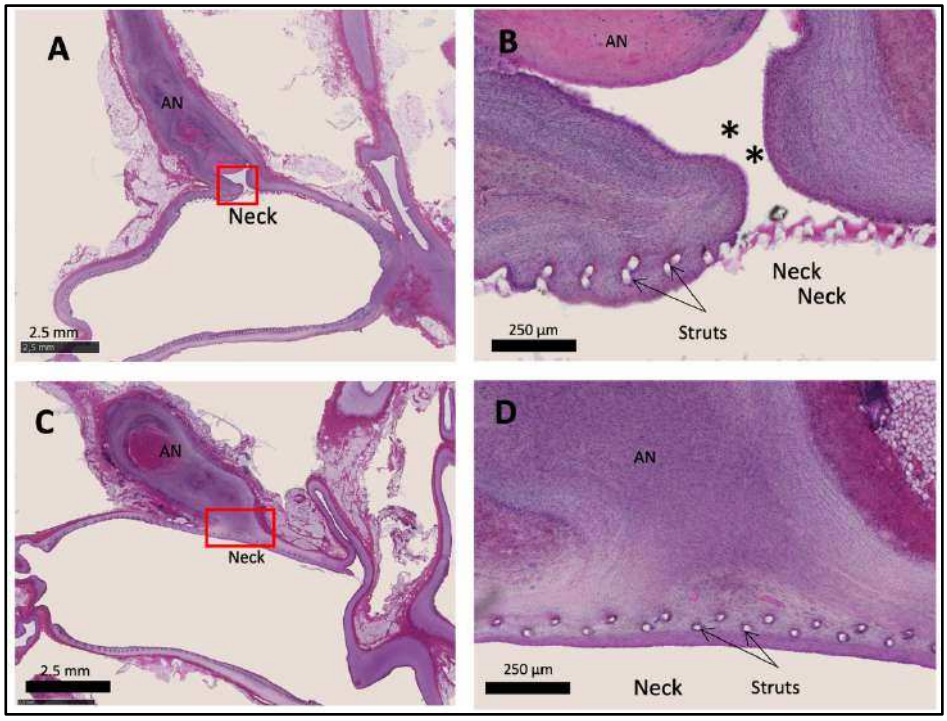


Figure 29. Histology of the aneurysmal neck. H&E staining of longitudinal sections across the neck showing an aneurysm with a residual neck where endothelialization (struts coverage) was absent (A/B), and an aneurysm completely embolized with tissue material, showing excellent strut coverage/endothelialization, especially at the neck site (C/D).

License CC BY-NC-ND 4.0

Table 3. Histomorphological analysis protocol.

For quantitative of tissue strut coverage, we used QuPath software (v0.5.1). A threshold-S)based script was developed to enable automatic detection of the struts. Each strut was examined individually, and the percentage of covered struts (SC) was determined. The Artery Lumen (AL) and the area encompassing the neointima, AL, and struts, were manually delineated. The areas of these regions were measured. The mean Neointima Thickness (NIT) was calculated as follow:

- AAL (µm2 , red line) = Area of the stented Artery Lumen
- AL (µm), the mean lumen Diameter was calculated as :
  - AAL (μm^2)=π(AL/2)2
  - AL (µm)= 2x√(AAL/π)
- NSAL (μm^2, blue line) = area of zone including Neointima (NI), Struts (AS, green lines) and AAL
  - NI (μm^2)= NSLA-NI-AAL
  - NLA (μm^2)= NSAL-AS
  - DNLA =Mean diameter of NLA: DNLA (µm)= 2x$\sqrt{\frac{NLA}{\pi}}$
- NIT (µm)= mean NeoIntimal Thickness = (DNLA-AAL)/2

Aneurysm embolization analysis was performed similarly to the angiographic evaluation, (based on OKM scale), by assessing the degree of filling of the aneurysmal sac with embolic material (complete, partial, or <5%).

For histological analysis of strut coverage proximal to (Z2), across (Neck), and distal to the aneurysm neck (Z1), we defined three zones: two outside the neck, Z1 (distal) and Z2 (proximal) and one encompassing the entire neck (Neck). Using QuPath software, we quantified:

- The area of struts in each zone : AS1 for Z1, AS2 for Z2, and AS_{neck} for the neck

- The distance (in µm) from the edge of each strut to the arterial lumen (D1, D2, Dneck), reflecting the extent of strut coverage by tissue and the recruitment of cells at the strut surface;

- The neointimal area in each zone – AN1 for Z1, AN2 for Z2, and AN_{neck} for the neck;

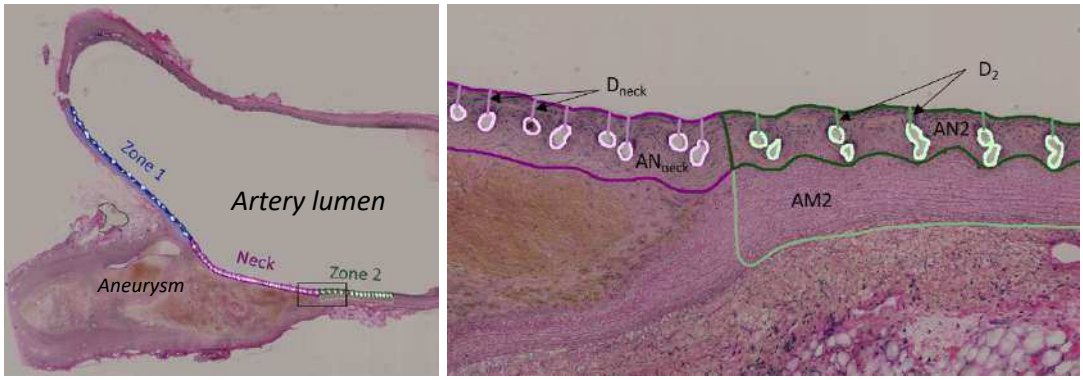
- The area of the media in Z1 and Z2 – AM1 for Z1 and AM2 for Z2 ;

We then calculated:

- The neointimal coverage ratio for each zone = AN/AS

- The neointima-to-media ratio in the regions outside the neck = AN/AM

License CC BY-NC-ND 4.0



Supplementary image for the protocol.

For MPM, the samples were stained with 4′,6-diamidino-2-fenilindolo (DAPI) and imaged using a custom-built multiphoton microscope (Olympus BX61WI/FV1200MPE) equipped with a Ti:sapphire femtosecond laser (810 nm excitation). A 25× water immersion objective (NA 1.05, 2 mm WD) was used for deep tissue imaging (up to 400 μm). Images (512 × 512 pixels) were acquired at 4-μm z-steps, covering a 500 × 500 μm field of view in 4-8 different zones. SHG (collagen), red autofluorescence (elastin or mesenchymal-like cells), and DAPI (nuclei) were detected on dedicated PMTs. All images were corrected for background and processed identically. Collagen quantification and directionality was based on second-harmonic generation (SHG) signal z-projections in 5 zones and analyzed with FIJI using the “Analyze Particles” and “Directionality” (scored from 0 – no direction to 3 – unique and homogeneous direction) plugins, as previously described.[312] Utility of the MPM to assess FD struts wall integration has been already proved.[171,188,312] MPM enables high-resolution, three-dimensional imaging of tissue morphology, including collagen, elastin, and cells, without sample preparation, providing detailed insights into microstructural changes involved in the FD healing.

License CC BY-NC-ND 4.0

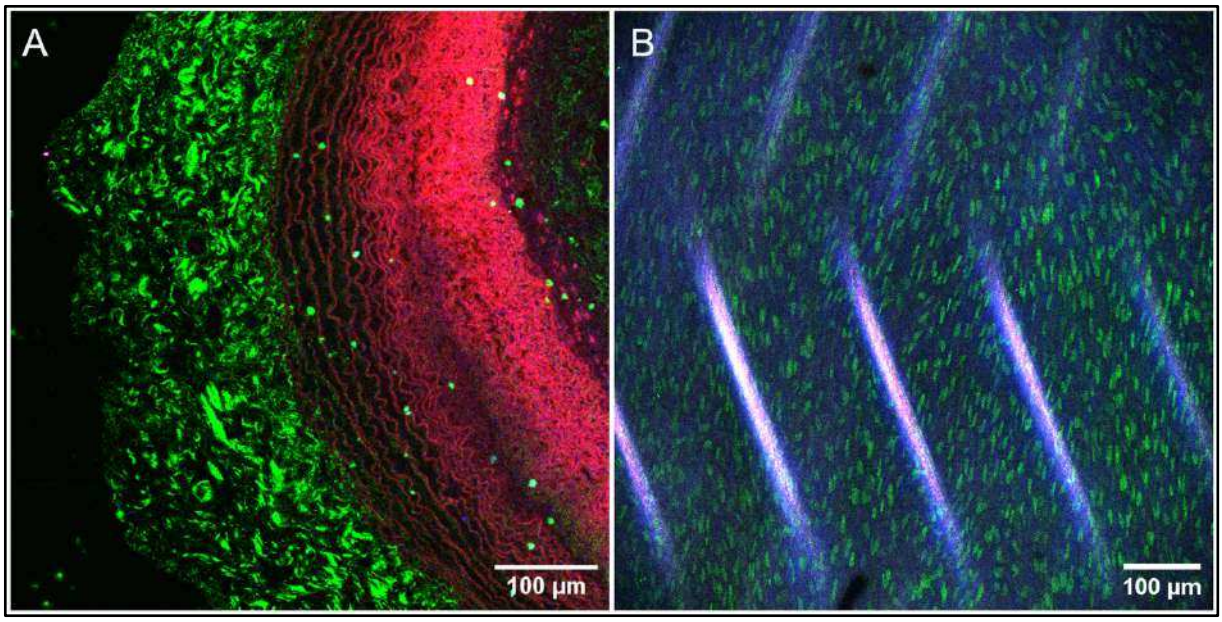


Figure 30. Multiphoton microscopy. (A) Second Harmonic Generation (SHG) green for collagen, and autofluorescence (red for elastin) in a normal vessel wall, highlighting tissue structure. (B) Third Harmonic Generation (THG violet) at the metal stent-tissue interface representing the FD struts and green fluo for DAPI+ nucleus (endothelial cells).

VIII.8. Rosuvastatin serum concentration measurement

Before implanting the FD, a blood sample was collected in dry tubes using the marginal ear vein of the rabbit. Upon arrival at the Pharmacology-Toxicology laboratory, the samples were centrifuged at 13,000 rpm for 10 minutes. The supernatant (150 µL) was then transferred into vials for analysis. Samples were immediately frozen at -20°C until further analysis.

The sample analysis was performed using the LC-MS/MS Sciex Qtrap 5500® system. The quantification of the rosuvastatin serum concentration was performed with injection of 5 µL of the supernatant. The method used was validated following the QuEChERS protocol (Quick Easy Cheap Effective Rugged Safe), ensuring effective extraction and precise analysis.

The liquid chromatography-tandem mass spectrometry (LC-MS/MS) is the gold standard for quantifying Rosuvastatin and its metabolites in human plasma due to its high sensitivity, specificity, and ability to simultaneously measure parent drug and metabolites such as N-

License CC BY-NC-ND 4.0

desmethyl Rosuvastatin and Rosuvastatin-5S-lactone.[313–316] Sample preparation typically involves protein precipitation or liquid-liquid extraction from plasma, followed by chromatographic separation using a C18 or HILIC column. Detection is performed via electrospray ionization (ESI), most commonly in the positive ion mode, although negative ion mode is also validated. Calibration curves for Rosuvastatin are linear over a wide range (e.g., 0.1–50 ng/mL or up to 2000 ng/mL), with lower limits of quantification as low as 0.02 ng/mL depending on the method.

VIII.9. Correlation between Rosuvastatin serum concentration and FD struts coverage

There are no studies in the medical literature that directly compare the serum concentration of Rosuvastatin, as measured in blood using LC-MS/MS, with the concentration of the endothelial cells covering a stent. Preclinical studies have investigated local delivery of Rosuvastatin from drug-eluting stents and have demonstrated high local tissue concentrations and biological effects in the vessel wall or endothelium, but they do not address the correlation between systemic Rosuvastatin levels and endothelial cell coverage of a stent.[262]

We assessed the correlation between the Rosuvastatin serum concentration, and the percentage of collagen (Collagen SHG+) and endothelial surface (Nucleus DAPI+ surface) covering the aortic FD after 2 weeks, obtained with the MPM.

VIII.10. Budget and resources

The study required substantial resources, including rental of the EMIS platform, creation and longitudinal follow-up of the rabbit aneurysm model, daily individual preparation and administration of Aspirin and Rosuvastatin, specific consumables (including OCT probes), multimodal imaging (DSA, HF-OCT, and MPM), and comprehensive histological processing

License CC BY-NC-ND 4.0

and analysis. The global budget amounted to approximately €320000, in addition to 44 flow-diverter stents (~€10,000 each) generously provided by Balt.

Summary

This chapter outlines the preparation of a rabbit elastase-induced aneurysm model to study flow diverters and administration of Aspirin and Rosuvastatin. New Zealand White rabbits underwent surgical elastase incubation in the right common carotid artery, producing saccular aneurysms that histologically resemble human intracranial aneurysms. One month later, bare metal flow diverters were deployed in the subclavian artery (at the neck of the elastase aneurysm) and descending aorta (to evaluate side branch coverage). High-frequency Optical Coherence Tomography (HF-OCT) and angiographical images were acquired immediately and two weeks post-implantation, followed by histological analysis. Rabbits were randomized to receive Aspirin alone (10 mg/kg/day) or Aspirin plus Rosuvastatin (10 mg/kg/day each drug). Drugs were administered by gavage, starting five days before flow diverter implantation, and were maintained until sacrifice. Efficacy was evaluated with the O'Kelly-Marotta angiographic scale, safety through HF-OCT-based branch patency analysis, and healing via histology and multiphoton microscopy (quantifying collagen and endothelial coverage). Rosuvastatin serum concentrations were measured by LC-MS/MS, and their correlation with FD strut coverage was explored.

License CC BY-NC-ND 4.0

Chapter IX. Effect of Rosuvastatin on FD treatment

In this paper our objective was to assess the effect of Rosuvastatin on bare metal FD treatment, using the model previously described.

Appendix 5 for the article.

IX.1. Summary of the study design

This study includes an efficacy and a security analysis in a rabbit model with elastase-induced aneurysms.

For the efficacy study, aneurysms have been induced with the elastase model at the origin of the right CCA and FD have been implanted 4 weeks after in the right subclavian artery, covering the neck of the aneurysm.

In the same rabbits, a security study has been conducted with implantation of a FD in the sub-renal descending aorta covering lumbar arteries, to assess the follow-up patency of these small arteries considered to have collateral branches and perform histological analysis of strut coverage.

A total of twenty-two rabbits (with 44 implanted FDs) were included in the study and randomly assigned to one of two groups. Thirteen rabbits were allocated to the test group, receiving Rosuvastatin plus Aspirin (Rosu+ASA, both at a dosage of 10 mg/kg/day), and nine to the control group, receiving Aspirin alone (ASA at a dosage of 10 mg/kg/day). The initial aim was to include fifteen rabbits in each group; however, eight rabbits were euthanized: four due to brain ischemia following right CCA ligation for the aneurysm creation, three due to vascular access complications, and one due to occlusion of the aortic FD.

Rabbits have been sacrificed two weeks after stent implantations.

License CC BY-NC-ND 4.0

The outcomes assessed were: (I) the 2-weeks aneurysm occlusion rate with the O`Kelly-Marotta scale[317], (II) the 2-weeks patency of branches covered by FD with the high frequency optical coherence tomography (HF-OCT), (III) FD coverage with the histological staining, including Hematoxylin and Eosin stain for endothelial cells and Multiphoton Microscopy (MPM) for endothelial cells and collagen fibers, (IV) the correlation between Rosuvastatin serum concentration and endothelial cells covering the FD (Figure 29).

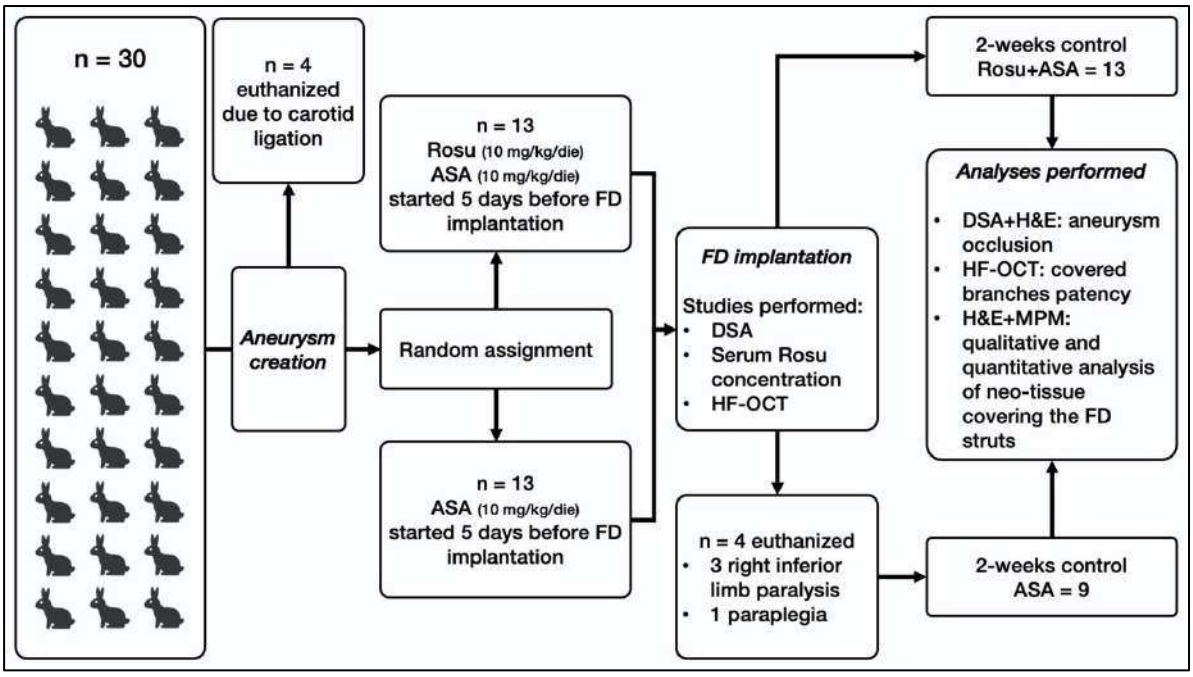


Figure 31. Study protocol. DSA: digital subtracted angiography; FD: flow divert; H&E: hematoxilin-eosin; HF-OCT: high frequency optical coherence tomography: MPM: multiphoton microscopy; Rosu: Rosuvastatin; ASA: Aspirin.

IX.2. Main results of the study

In all rabbits included in the analysis, FD were successfully implanted. All FD were patent immediately after implantation. Thirteen rabbits were included in the Rosu+ASA group and nine in the ASA group.

License CC BY-NC-ND 4.0

IX.2.1. Aneurysm occlusion

The 2-weeks DSA control showed a higher not statistically significant complete aneurysm occlusion rate in the Rosu+ASA group compared with the ASA group (OKM D 11/13 [84.6%] vs 6/9 [66.6%], p=0.323; Table 4). An OKM C was observed in two cases in both groups (15.4% vs 22.2%), and in one case of the control groups there was a sac remnant (OKM B). An adequate occlusion was higher in the Rosu+ASA group (OKM C-D 13/13 [100%] vs 8/9 [88.8%]; Table 4). Examples of the DSA control in Figure 30.

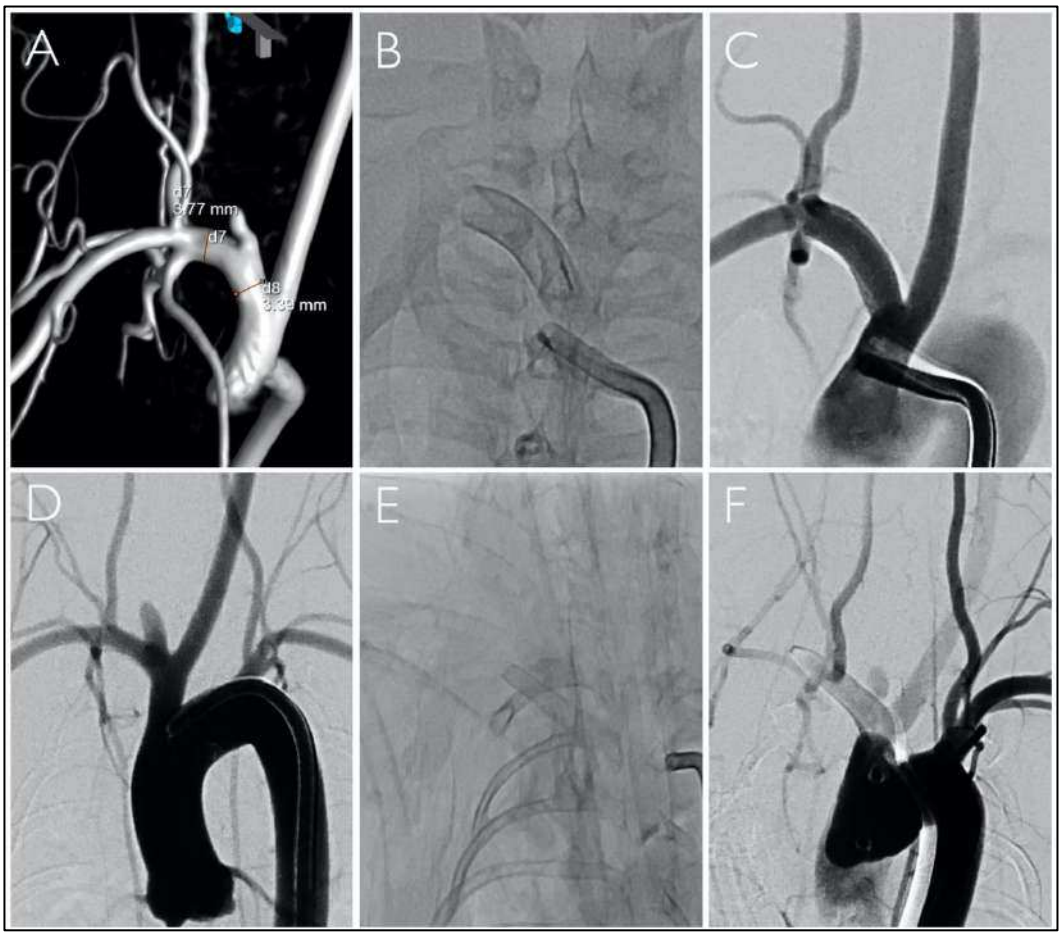


Figure 32. DSA controls. (A/B/C) A complete aneurysm occlusion; (D/E/F) with a sac remnant.

License CC BY-NC-ND 4.0

IX.2.2. Branches covered by the FD

With the HF-OCT done immediately after the FD implantation at the level of the descending aorta we identified 40 covered branches in the Rosu+ASA group and 28 in the ASA group (Table 4). Examples of the HF-OCT control in Figure 31.

Thirty-seven covered branches had an ostium diameter smaller than 1 mm (22 in the Rosu+ASA group and 15 in the ASA group). The 2-weeks HF-OCT control showed a significantly higher patency rate in the Rosu+ASA group compared with the ASA group (21/22 [95.4%] vs 11/15 [73.4%]; p=0.036). Stenosis and occlusion were also lower in the Rosu+ASA group compared with ASA group (0/22 vs 2/15 [13.3%] and 1/22 [4.6%] vs 2/15 [13.3%]).

Thirty-one covered branches had an ostium diameter ≥1 mm (18 in the Rosu+ASA group and 13 in the ASA group). The 2-weeks HF-OCT control showed a significantly higher patency rate in the Rosu+ASA group compared with the ASA group (17/18 [94.4%] vs 6/13 [46.1%]; p=0.007). Stenosis and occlusion were also lower in the Rosu+ASA group (0/18 vs 4/13 [30.8%] and 1/18 [5.6%] vs 3/13 [23.1%]).

License CC BY-NC-ND 4.0

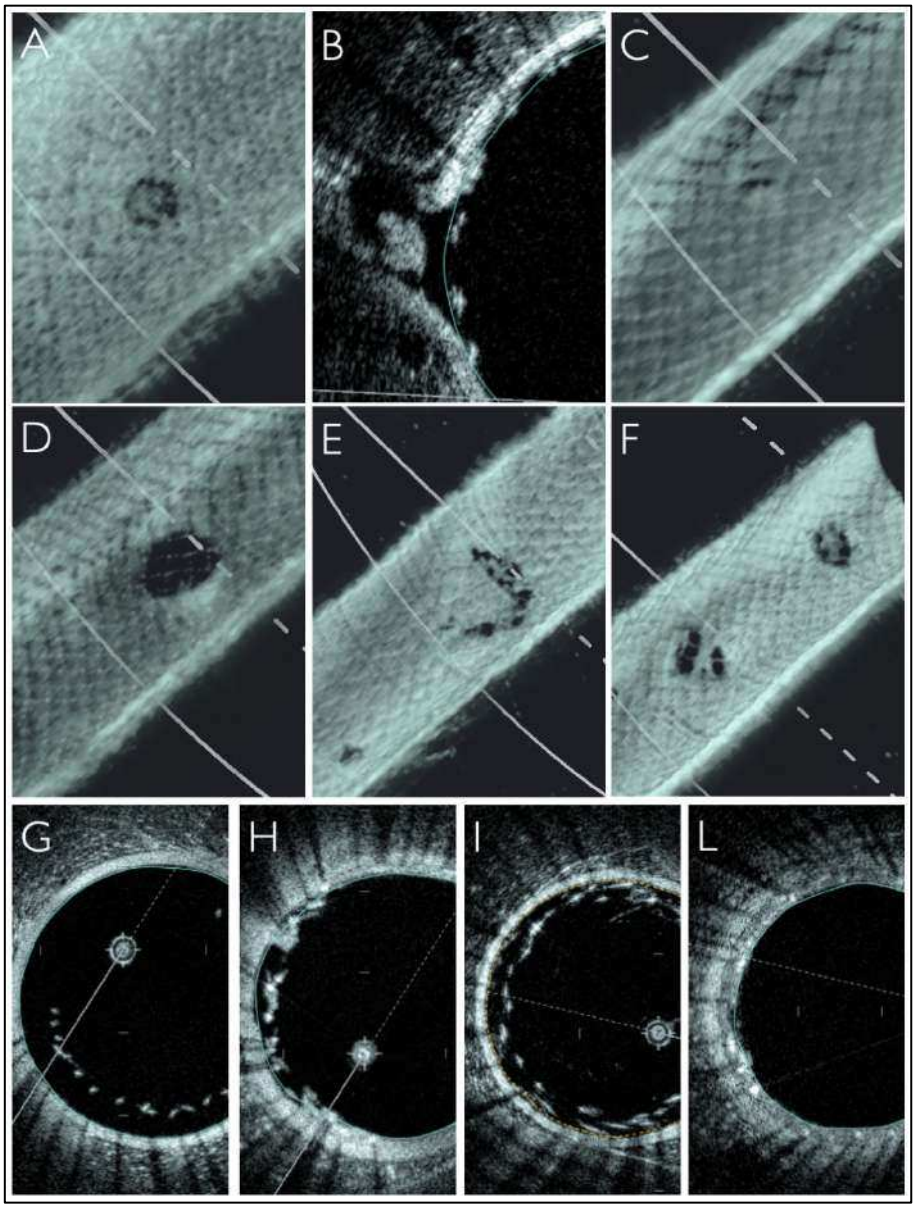


Figure 33. HF-OCT controls. (A/B/C) Collateral branch occluded at the follow up; there was already a thrombus in the ostium (A/B), with a complete occlusion after 2 weeks (C). (D/E/F) Patent and suboccluded covered branches: the same covered branch of the image D was suboccluded in the image E, while in the image F two covered branches patent. (G/H) the malapposed distal end of a flow diverter no endothelialized in the HF-OCT control, while (I/L) the malapposed distal end of a flow diverter endothelialized in the HF-OCT control.

License CC BY-NC-ND 4.0

IX.2.3. Composite outcome

The composite outcome, including all rabbit models with the aneurysm completely occluded and all covered branches patent, was significantly higher with Rosuvastatin therapy (10/13 [76.9%] vs 2/9 [22.2%], p=0.011; Table 4).

Table 4. DSA and HF-OCT outcomes.

		Rosu+ASA	**ASA**	**p-value**
DSA – aneurysm occlusion				
Aneurysms number, n		**13**	**9**	
Aneurysm status, n (%)	OKM D	11 (84.6%)	6 (66.6%)	0.323
	OKM C	2 (15.4%)	2 (22.2%)	
	OKM B	0	1 (11.1%)	
	OKM A	0	0	
HF-OCT – side branches and distal end of the FD				
Basal HF-OCT - covered branches <1 mm, n		**22**	**15**	
Control HF-OCT, n (%)	Patent	21 (95.4%)	11 (73.4%)	0.036
	Stenotic	0	2 (13.3%)	
	Occluded	1 (4.6%)	2 (13.3%)	
Basal HF-OCT - covered branches ≥ 1 mm, n		**18**	**13**	
Control HF-OCT, n (%)	Patent	17 (94.4%)	6 (46.1%)	0.007
	Stenotic	0	4 (30.8%)	
	Occluded	1 (5.6%)	3 (23.1%)	
Basal HF-OCT - FD distal end malapposed, n		**14**	**9**	
Control HF-OCT	Endothelialized	9 (64.3%)	7 (77.8%)	0.421
	No endothelialized	5 (35.7%)	2 (22.2%)	
Composite outcome		**13**	**9**	
Aneurysm occlusion and patent covered branches	Yes	10 (76.9%)	2 (22.2%)	0.011
	No	3 (23.1%)	7 (77.8%)	

License CC BY-NC-ND 4.0

IX.2.4. Histomorphological analysis FD/stent coverage by neotissue

In stented aortas, examination of H&E-stained sections showed that in both the ASA group and the Rosu+ASA group, the stent struts were generally covered with well-organized tissue, with no evidence of persistent inflammatory cells, residual fibrin, or red blood cells, indicating advanced healing (Figure 32). All samples exhibited good stent apposition (Figure 32A/B). Both groups demonstrated excellent coverage rates, with a trend toward improved strut coverage in the Rosu+ASA group compared to the ASA group, in both SC (97.9-100% in the Rosu+ASA group vs. 83.3-100% in the ASA group; Figure 32C) and NIT (55.9-145 µm [median: 107 µm] in the Rosu+ASA group vs. 35.7-138 µm [median: 95.4 µm] in the ASA group; Figure 32D).

In FD-treated aneurysms (Figure 32E), histology confirmed the data obtained by DSA, indicating that the Rosu+ASA group showed a better rate of successful aneurysm occlusion compared to the ASA group. Assessment of the percentage of strut coverage (SC) in FD-treated aneurysms, both in zones adjacent to the neck (proximal and distal) and at the neck itself (Figure 32F), confirmed the data obtained in aortas and indicated that at the neck, as well as in adjacent zones, NIT tended to be higher (Figure 32G) in the Rosu+ASA group compared with the ASA group (Figure 32B). In the zones adjacent to the neck, this tendency was confirmed when analyzing the neointima-to-media ratio (Figure 32H).

License CC BY-NC-ND 4.0

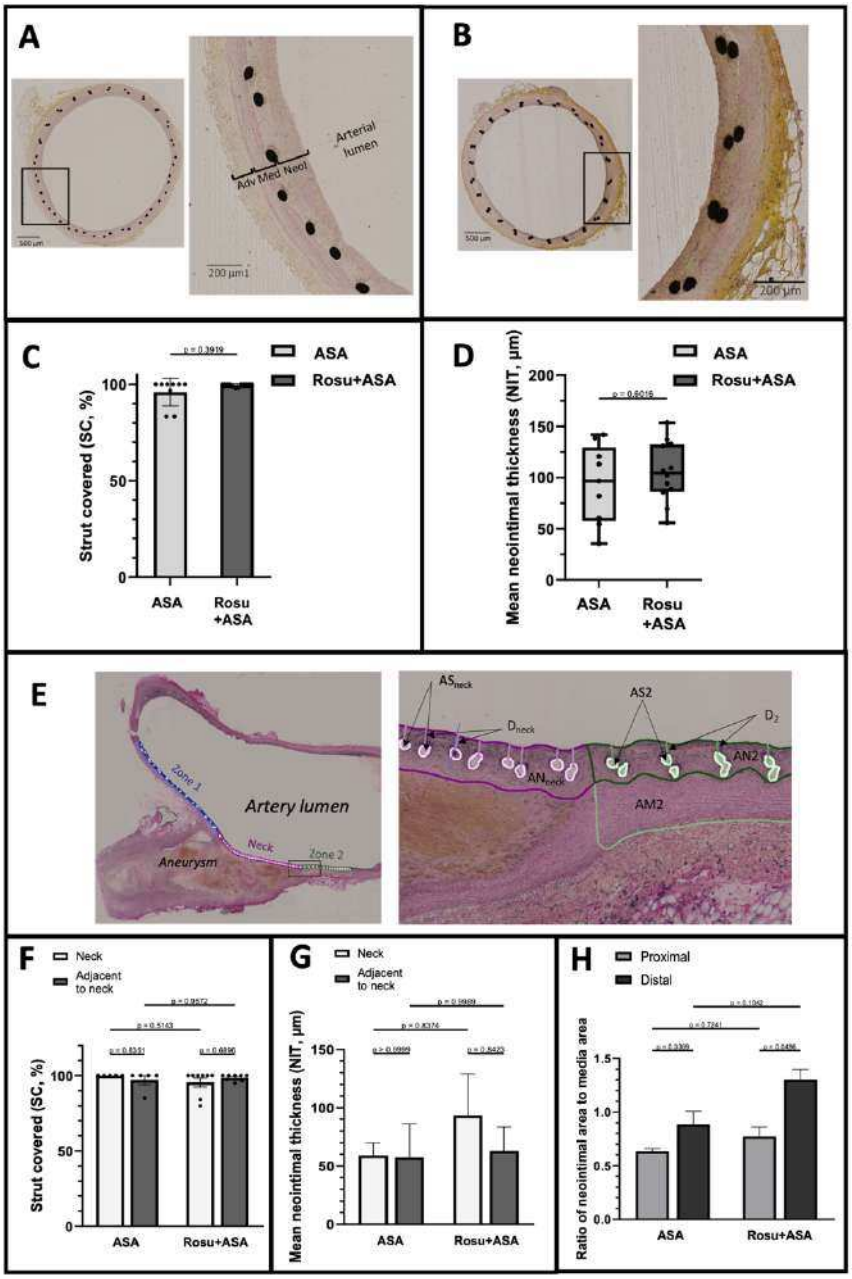


Figure 34. Effects of Rosuvastatin on strut coverage by neotissue. (A/B), Representative images of H&E-stained transverse sections (diamond wire saw) of stented aortas from the ASA group (A) and the Rosu+ASA group (B). Both groups show comparable and uniform strut coverage (SC). (C) Histogram representation of the mean percentage of struts covered in each group. Data are expressed as mean ± SD. (D) Box-and-whisker plots (median; 25th and 75th percentiles) showing the mean neointimal thickness (NIT) in the ASA and Rosu+ASA groups. (E) Illustrations of the zones delineated for the quantitative analysis of flow diverter (FD) coverage in the subrenal aorta (A, H&E-stained transverse section) and in FD-treated aneurysms (B, H&E-stained longitudinal section), using QuPath software (v0.5.1). NeoI: neointima; Med: media; Adv : adventitia. Zone 2 is proximal to the aneurysm neck; Zone

License CC BY-NC-ND 4.0

1 is distal. Dneck: distance from the device strut to the arterial lumen at the neck. D2: distance from the strut to the arterial lumen in Zone 2 (proximal to the neck). ASneck: area of the strut at the neck site. AS2: area of the strut in Zone 2. AM2: area of the media in Zone 2. See text for details. For FD-treated samples, (F) Percentage of SC, (G) mean of NIT both, in zones adjacent to the neck and at the neck itself, and the ratio of neointima-to-media in zones adjacent to the neck (p values are indicated, ANOVA test).

IX.2.5. MPM in stented aorta: endothelial cells and collagen

The percentage of the luminal surface covered by DAPI+ nuclei, assessed by MPM (Figure 33A), was not statistical different between groups (ASA 30.62% vs. Rosu+ASA 32.90%, p=0.149), suggesting comparable cellular colonization. Collagen coverage, quantified via SHG signal (Figure 33E), did not show statistical difference between groups (ASA 44.98% vs. Rosu+ASA 41.99%, p=0.286), indicating that both treatments led to similar levels of extracellular matrix (ECM) deposition. Collagen fiber alignment (Figure 33G) was not statistical different between groups (ASA 1.978 vs. Rosu+ASA 1.677, p=0.132), suggesting that overall collagen organization remained largely unaffected by Rosuvastatin co-treatment.

License CC BY-NC-ND 4.0

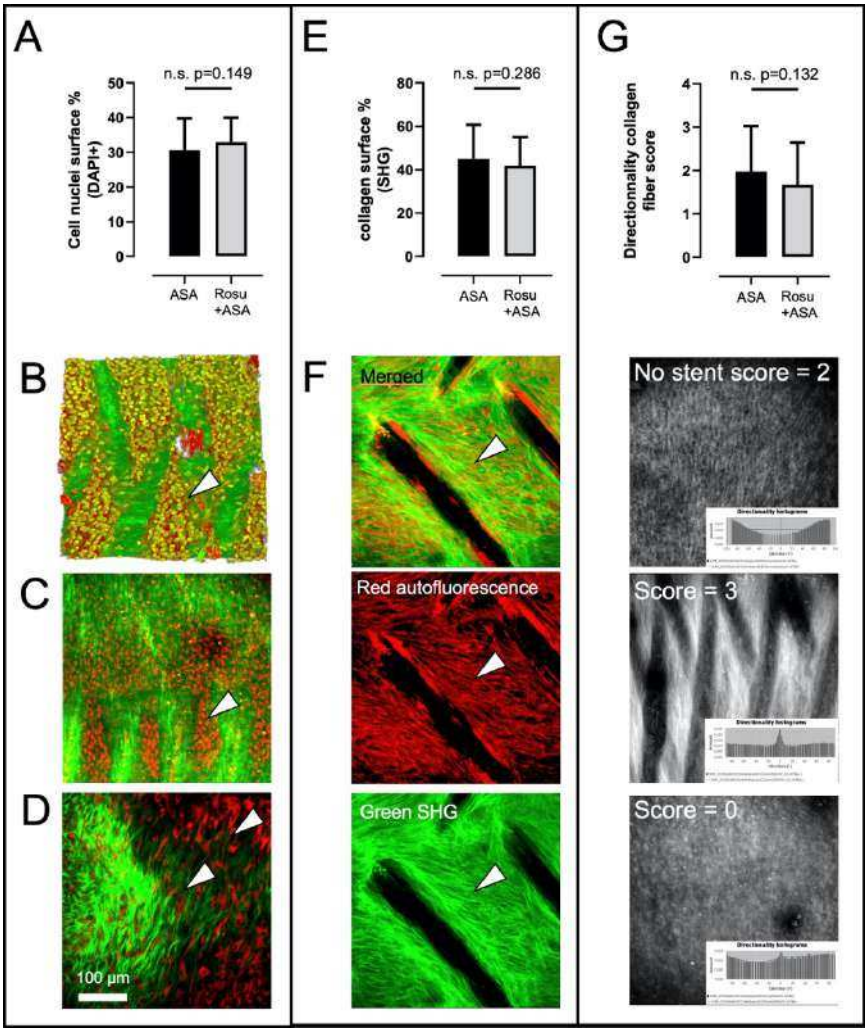


Figure 35. Multiscale analysis of neotissue formation and extracellular matrix remodeling following flow-diverter stent (FD) implantation in rabbit arteries. (A) Quantification of endothelial cell coverage by Multiphoton Microscopy (MPM), based on the surface area occupied by DAPI- nuclei. No significant difference between treatment groups (p= 0.149). (B/D) MPM images showing 3D reconstructions of the vascular wall at distinct depths. DAPI-stained nuclei are pseudo-colored yellow (arrowheads indicate endothelial cells in B and C), SHG-positive collagen appears green, and red autofluorescence highlights endothelial cells in C and mesenchymal-like cells in D. (E) Collagen surface area (%) assessed from SHG signal in MPM images; no significant difference was observed between groups (p= 0.286). (F) Multichannel MPM views showing neotissue bridging between stent struts. Top: merged image (SHG green + red autofluorescence); middle: red channel only; bottom: SHG signal only. Arrowheads highlight aligned collagen bundles and adjacent smooth muscle-like cells. (G) Collagen fiber directionality scores derived from SHG image analysis showed no significant difference (p= 0.132). The right column presents representative images ranging from score 0 (disorganized fibers) to score 3 (highly aligned),

License CC BY-NC-ND 4.0

including a "no stent" control with minimal orientation. Data are presented as mean ± SD or individual values. Statistical comparisons were performed using appropriate nonparametric tests. Scale bar: 100 µm.

IX.2.6. Rosuvastatin concentration and endothelialization

Rosuvastatin serum concentration was successfully measured in each rabbit of the Rosu+ASA group (µg/L). The Pearson correlation coefficient between Rosuvastatin serum concentration and endothelial cells coverage (Nucleus DAPI+ surface) of FD was r=0.92, indicating a strong statistical positive relationship (p=0.02). The Pearson correlation coefficient between Rosuvastatin serum concentration and collagen surface (Collagen SHG+) on FD was r=-0.51, indicating no relationship. Finally, the Pearson correlation coefficient between Rosuvastatin serum concentration and collagen directionality (Collagen dir Score) was r=-0.53, indicating no relationship (Figure 34).

License CC BY-NC-ND 4.0

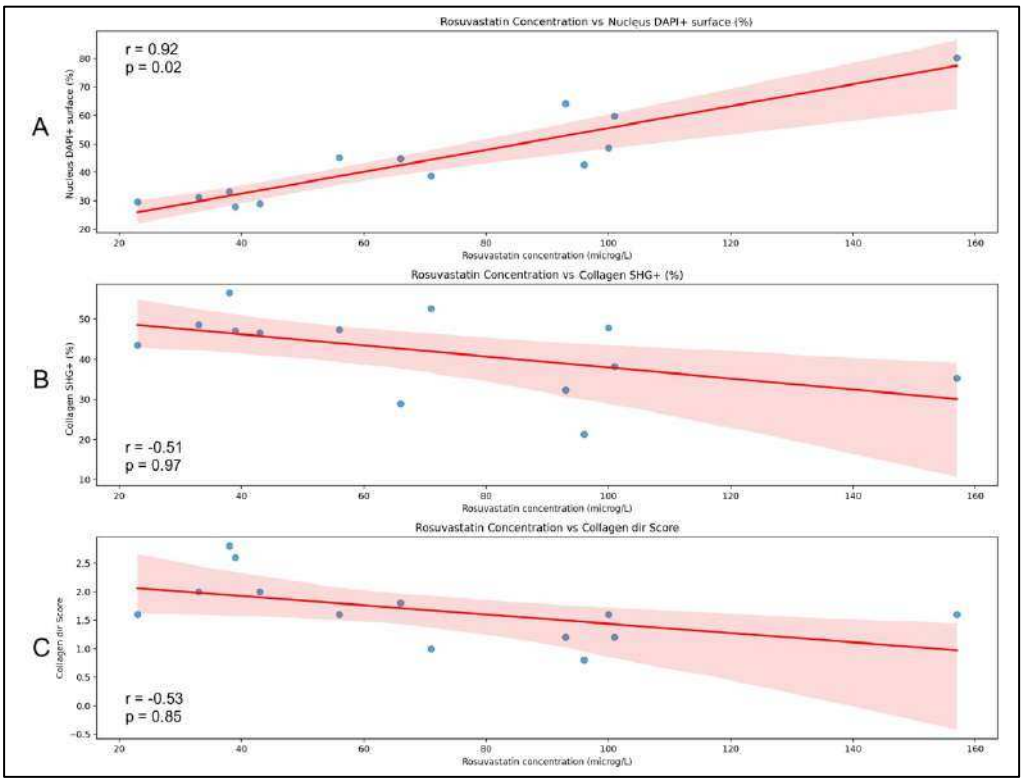


Figure 36. Pearson's correlation between Rosuvastatin concentration and DAPI-positive nuclei endothelial cells (A), Collagen SHG-positive fibers (B), and collagen directionality score (C).

IX.3. Discussion

This preclinical study in a rabbit model of elastase-induced aneurysms investigated the safety and efficacy of Rosuvastatin as an adjunctive therapy to bare metal FD treatment. The rabbit model closely replicates the histopathological and hemodynamic features of human IAs, including endothelial dysfunction, inflammation, and thrombus formation.[159,318] Our findings provide four key insights into Rosuvastatin's effects on FD therapy: (1) a trend toward higher aneurysm occlusion rates, (2) significantly reduced occlusion of side branches covered by FDs, (3) a trend toward improved neotissue coverage of FD struts, and (4) a strong positive correlation between Rosuvastatin serum concentration and endothelial cell coverage, without excessive neointimal hyperplasia. **These results suggest that Rosuvastatin enhances FD outcomes by promoting endothelialization and reducing thromboembolic**

License CC BY-NC-ND 4.0

complications, addressing critical limitations of FD therapy and supporting its potential as a wall-oriented strategy.

The observed trend toward higher complete occlusion rates in the Rosuvastatin plus Aspirin group (84.6% vs. 66.6%, p=0.323) aligns with prior studies suggesting statins enhance aneurysm healing. For example, Salih et al.[319], reported a non-significant increase in occlusion rates with statin use (79.6% vs. 67.4%) in patients treated with the PED. Our results, while not statistically significant, are consistent with this trend and may reflect the short 2-week follow-up period in our study, as FD occlusion rates typically increase over time (77-83% at 1 year, 87-96% at 2-5 years).[137] Rosuvastatin's ability to enhance endothelialization, as evidenced by the strong correlation between serum concentration and endothelial cell coverage (r=0.92, p=0.02), likely contributes to this effect. Rosuvastatin upregulates eNOS and VEGF-A, promoting EPCs mobilization and vascular repair.[264,276,300,320–322] These mechanisms address FD limitations, such as incomplete occlusion due to persistent inflow or poor wall apposition.[120,129] However, the lack of statistical significance may be due to our small sample size (n=22), highlighting the need for larger studies to confirm these findings.

The significantly higher patency rates of covered branches in the Rosuvastatin plus Aspirin group (94.4% vs. 46.1% for ≥1 mm arteries, p=0.007; 95.4% vs. 73.4% for <1 mm arteries, p=0.036) suggest that Rosuvastatin reduces thromboembolic complications associated with FD branch coverage.[162] This is a critical finding, as branch occlusion remains a concern in FD therapy, particularly for perforators or branches with limited collateral supply.[162] Rosuvastatin's antiplatelet effects, mediated by eNOS activation and reduced platelet reactivity,[254,257] likely contribute to maintaining branch patency. Additionally, its anti-inflammatory properties, such as inhibition of NF-κB and MMPs[215,260] may stabilize neotissue formation, preventing excessive thrombus or neointimal hyperplasia that could occlude branches. The composite outcome (aneurysm occlusion and branch patency) further underscores Rosuvastatin's dual benefit in enhancing efficacy and safety (76.9% vs. 22.2%, p=0.011), supporting its potential to improve FD outcomes in complex aneurysms.[138–142]

License CC BY-NC-ND 4.0

Histomorphological and MPM analyses revealed trends toward improved SC and NIT in the Rosu+ASA group, both in stented aortas and FD-treated aneurysms. These findings align with Rosuvastatin's role in promoting endothelialization and vascular repair, as seen in prior studies of vascular injury and aneurysm models.[263,264] However, the lack of significant differences in collagen deposition or fiber alignment suggests that Rosuvastatin primarily enhances endothelial coverage rather than ECM remodeling. This may be due to the short 2-week follow-up, as collagen remodeling typically occurs over longer periods.[312] Alternatively, Rosuvastatin's anti-inflammatory effects may suppress excessive fibroblast activity, preventing pathological ECM deposition.[216–218] The layered neotissue structure observed in MPM (endothelial monolayer over mesenchymal scaffolding) highlights the interplay between endothelial and mesenchymal cells in FD healing,[84–86] with Rosuvastatin selectively enhancing the endothelial component.

Our findings highlight areas of discrepancy with previous studies. Unlike Salih et al.,[319] which found no significant statin effect on FD occlusion rates, our study suggests a promising trend, possibly due to our controlled preclinical design versus their retrospective clinical approach. Conflicting evidence on statins in IA treatment[198–202] may depend on differences in patient populations, statin types, or dosing regimens. For example, patients with hyperlipidemia have an altered inflammatory profile and may respond differently to the statin therapy.

Our study has several limitations. First, the rabbit model, while histologically similar to human IAs,[299] differs in arterial wall composition and hemodynamics, potentially limiting translation to human intracranial circulation.[11–13,15–18] Second, the small cohort size (n=22) and loss of eight rabbits due to complications (e.g., brain ischemia, vascular access issues) reduced statistical power, particularly for aneurysm occlusion outcomes. Third, the use of single antiplatelet therapy (Aspirin) rather than dual antiplatelet therapy (DAPT), standard in human FD treatment, may have influenced endothelialization and branch patency results. While the CICAFLOW study[171] found no difference between Aspirin and DAPT in rabbit FD models, in the clinical practice DAPT is still largely used, potentially affecting Rosuvastatin's efficacy.[161]

License CC BY-NC-ND 4.0

Finally, the 2-week follow-up may not capture long-term effects, such as sustained occlusion or late complications like delayed rupture.[150–152] These limitations highlight the need for larger, longer-term studies and clinical trials to validate Rosuvastatin's role in FD therapy.

IX.4. Future scenarios

The findings of this study, demonstrating Rosuvastatin's potential to enhance FD efficacy and safety in a rabbit elastase-induced aneurysm model, open several avenues for future research, clinical practice, and technological development. Building on the pathophysiology of IAs, FD mechanisms and limitations, Rosuvastatin's pleiotropic effects, and our experimental results, we can speculate different future scenarios:

1. Rosuvastatin-Eluting FDs: The strong correlation between Rosuvastatin serum concentration and endothelial cell coverage suggests that local delivery of Rosuvastatin via drug-eluting FDs could enhance endothelialization and reduce complications like delayed rupture.[150–152] Rosuvastatin-eluting FDs could deliver the drug directly to the aneurysm neck, minimizing systemic side effects. Preclinical studies should evaluate the feasibility of coating FDs with Rosuvastatin, optimizing release kinetics to align with the endothelialization timeline.[84–86]
2. Biomarker-Guided Therapy: Our finding that Rosuvastatin enhances endothelialization suggests that biomarkers like CD31, VEGF-A, or eNOS levels[262–265] could predict treatment response in FD-treated patients. Future studies could develop biomarker panels to identify patients likely to benefit from Rosuvastatin, tailoring therapy based on genetic, inflammatory, or hemodynamic profiles (e.g., WSS).[21,62] For example, patients with high NF-κB or MMP-9 expression[15,203,216] may require higher Rosuvastatin doses to suppress inflammation.
3. Personalized Dosing Regimens: The strong correlation between Rosuvastatin serum concentration and endothelial coverage (r=0.92, p=0.02) highlights the importance of

License CC BY-NC-ND 4.0

optimizing dosing. Future clinical trials could use pharmacokinetic modeling to determine human-equivalent doses based on our rabbit model (10 mg/kg),[263,264] adjusting for factors like hyperlipidemia or baseline inflammation.

4. Clinical Implementation: Our findings of improved occlusion rates and branch patency support the integration of Rosuvastatin into clinical FD protocols, particularly for complex aneurysms with high rupture or complication risks.[138–142] This medication present the advantages of being safe with already CE and FDA approval and present also a low cost. Randomized controlled trials (RCTs) should evaluate Rosuvastatin's efficacy in humans, comparing outcomes with and without statin therapy in FD-treated patients, to confirm our preclinical results. They should also assess the effective time window of the statin therapy.
5. Combination with other wall-oriented therapies: Rosuvastatin's anti-inflammatory and pro-endothelial effects could be combined with other wall-oriented therapies, such as MMP inhibitors or anti-inflammatory agents,[204–212,216–218] to further enhance FD outcomes. For example, combining Rosuvastatin with nifedipine or tetracycline derivatives could synergistically reduce inflammation and ECM degradation, stabilizing aneurysm walls and preventing delayed rupture.[150–152]
6. Revised Antiplatelet Protocols: Our finding of reduced side branch occlusion with Rosuvastatin support the preclinical[253–258] and clinical[258] evidence regarding the enhanced antiplatelet effect of the adjunctive statin therapy. Our use of single antiplatelet therapy (Aspirin) was based on the preclinical CICAFLOW study,[171] and there is increased clinical evidence showing the safety profile of single antiplatelet therapy for FD treatment, even if there is still a concern regarding thromboembolic complications.[323] Future studies should investigate Rosuvastatin's interaction with antiplatelets to determine whether it can reduce the duration or intensity of antiplatelet therapy with FD, minimizing bleeding risks while maintaining branch patency.
7. Larger Cohort Studies: The small cohort size (n=22) reduced the statistical power. Larger preclinical studies in rabbits or other models[300] are needed to confirm our

License CC BY-NC-ND 4.0

findings, particularly the trend toward higher occlusion rates. Moreover, human cohort studies should stratify patients by aneurysm characteristics (e.g., size, morphology) and lipid profiles to address variability in statin response.

8. Exploration of Collagen Dynamics: The lack of significant differences in collagen deposition or alignment warrants further investigation. Future studies could examine longer time points to assess whether Rosuvastatin influences ECM remodeling, given its role in suppressing MMPs.[216–218] Additionally, combining Rosuvastatin with therapies targeting fibroblast activity (e.g., TGF-β modulators)[83] could optimize neotissue structure.

IX.5. Translation of these results in a RCT

Built on the preclinical evidence of this thesis, exploring the potential of Rosuvastatin in modulating the arterial wall biological response in FD treatment, and given the need of a clinical evidence, I designed the protocol of a RCT.

Title	**RosuvaStatin plus anti-platelet therapy use in patients treated with Flow Diverters for Intracranial Aneurysms.**
Study name	**STATIN-FDIA**
Study Objective(s)	Our purpose is to assess effects of Rosuvastatin on technical and functional outcomes in patients treated with FD for IAs taking the antiplatelet therapy.
Study Design	The STATIN-FDIA is designed as a randomised, controlled, unblinded multicenter trial with two parallel groups and a primary composite outcome, including complete occlusion of the aneurysm without minor or major post-procedural ischemic complications, at 3 months. Randomization will be performed with a 1:1 allocation.
Intervention(s)	*Cases*: Patients premedicated with Rosuvastatin and antiplatelets for treatment of IA with FDs. Dosage: - Rosuvastatin 40 mg / daily (reducing the dosage to 20 mg / daily in case of side effects related to the statin therapy)

License CC BY-NC-ND 4.0

	- Dosage and timeline of the antiplatelet treatments will be determined by each participating center in accordance to their protocol. Timeline of the treatment with Rosuvastatin: - Aneurysm excluded at the 3 months follow-up: stop Rosuvastatin. - Aneurysm not excluded at the 3 months follow-up: continue Rosuvastatin until the 6 months control. - Aneurysm not occluded at the 6 months control: stop Rosuvastatin. *Controls*: Patients premedicated with antiplatelets for treatment of IA with FDs. Dosage: - Dosage and timeline of the antiplatelet treatments will be determined by each participating center in accordance to their protocol.
Eligibility criteria	Patients with unruptured IAs eligible for treatment with FD. **Inclusion criteria** - Age ≥18 years. - Unruptured or recanalized IAs (saccular and fusiform will be assessed separately). - Only one target aneurysm with FD. - Subjects with a pre-treatment mRS≤2. - Informed consent form signed as per local requirement. **Exclusion criteria** - Subjects under any long lasting antiplatelet and/or anticoagulation therapy. - Subjects who had endovascular procedures/intracranial hemorrhage and/or subarachnoid hemorrhage in the last 30 days prior to the procedure or is expected to be treated for another aneurysm during the 30 days post procedure. - Subjects with the target aneurysm previously treated with a stent or FD. - Any known contraindication to FD treatment and premedication with stains and/or antiplatelets. - Subjects already enrolled in other clinical trials that would interfere with study endpoints or with comorbidities that would confound the neurological and functional evaluation. - Known renal failure or coagulation disorders. - Pregnant woman or breast feeding.
Outcomes	**Primary outcome**

License CC BY-NC-ND 4.0

	Composite outcome, including complete aneurysm occlusion and absence of ischemic complications (minor or major) determining a worsening of the basal mRS at the 3 months follow-up. Evaluation of the aneurysm occlusion: O'Kelly-Marotta scale. Evaluation the clinical outcome: modified Rankin Scale. **Secondary efficacy outcomes** - Complete and adequate occlusion rates at 3, 6 and 12 months. - Retreatment rates. **Safety outcomes** - Absence of ischemic lesions (silent and/or symptomatic) after treatment, at 3, 6 and 12 months. - mRS at 3, 6, and 12 months. - Rates of statin treatment failure due to side effects. Evaluation of ischemic lesions: MR with (T2, T1, DWI, ADC, FLAIR 3D)
Follow-up methods	*Imaging follow-up* The imaging follow up will be done with the DSA (alternatively an angioCT if also done before the treatment) to assess aneurysm exclusion, and with the MR to assess ischemic lesions.
Sample size	Based on prior reports, we considered a 55% rate of complete aneurysm occlusion without ischemic complications at 3 months in the control (antiplatelet-only) group. We hypothesize that the addition of rosuvastatin will increase this rate by 15% (to 70%). Assuming a two-sided α of 0.05 and 80% power to detect this difference, and using equal allocation (1:1) between groups, we calculated 162 patients required per arm. To account for potential attrition of up to 2%, the trial will enrol 330 patients (165 per group).
Statistical methods	The primary analysis will follow the intention-to-treat principle. The primary composite endpoint (complete occlusion without ischemic complications at 3 months) will be compared between groups using a chi-squared test. Absolute risk differences with 95% confidence intervals and odds ratios from logistic regression (adjusted for centers and aneurysm morphology) will also be reported. Secondary outcomes (occlusion rates at 6 and 12 months, mRS scores, retreatment rate, and statin treatment failure due to side effects) will be analysed using mixed-effects logistic regression for categorical outcomes and ordinal regression (for mRS). Time-to-event outcomes, where applicable, will be analysed with Kaplan–Meier curves and Cox proportional hazards models. Sensitivity analyses will be performed per protocol and with multiple imputation for missing data. Statistical significance will be set at $p<0.05$ (two-sided). Analyses will be performed using R.

License CC BY-NC-ND 4.0

Several questions may arise regarding the protocol. First, the choice of Rosuvastatin over another statin or the entire statin class. Rosuvastatin appears to have a higher pleiotropic effect compared to other statins, and as a hydrophilic statin, it is associated with lower rates of side effects.[260,268–276] If we plan to add a drug to the current pharmacological protocol FD treatment to enhance the healing process, we should prioritize a fast and safe therapy. Additionally, selecting a single statin agent aims to avoid potential bias related to the variable effects of different drugs. Second, regarding the concentration, although it is controversial whether Rosuvastatin's pleiotropic effect is dose-dependent, we argue that if this is true, we are already achieving the maximum therapeutic effect. Moreover, in our study, we observed varying serum concentrations of Rosuvastatin, suggesting inter-subject differences in the drug's pharmacokinetics. Third, the timeline of the therapy: although there is no consensus on the duration of DAPT in FD treatment, the decision to stop it is generally associated with a follow-up imaging. We should plan a DSA control (or a CT angiogram if performed pre-treatment), because MR Angiography may produce artifacts that reduce the ability to detect aneurysm remnants, that is the primary outcome of the trial. At the three-month follow-up, if the aneurysm is occluded, we can consider our objective achieved and discontinue the statin therapy. In some centers, this may also coincide with the cessation of the DAPT. For cases where the aneurysm remains patent or exhibits a neck remnant, we should continue the statin therapy until the next follow-up at six months. At that point, if the aneurysm is still patent, we may conclude that Rosuvastatin has failed to enhance healing and can be discontinued.

IX.6. Statin therapy and FDSM

The preclinical findings from our study suggest that Rosuvastatin, through its pleiotropic effects on EPC mobilization, NO bioavailability, and anti-inflammatory actions, may enhance the biological healing processes induced by bare metal FDs. However, the development of FDSMs, introduces a new layer of complexity to adjunctive pharmacological strategies, because FDSMs are designed to optimize device integration by reducing thrombogenicity,

License CC BY-NC-ND 4.0

promoting endothelialization, and minimizing inflammatory responses at the device-vessel interface.[173–178]

Statins and FDSMs share complementary mechanisms that could enhance FD efficacy and safety when combined. For example, phosphorylcholine (e.g., Pipeline Shield), glycocalyx (e.g., HPC), and PMEA (X technology) coatings reduce platelet deposition on FD struts, minimizing thrombogenicity.[172] Rosuvastatin may amplify this effect by increasing endogenous t-PA,[259] further inhibiting thrombus formation. Similarly, bioactive fibrin-heparin nanocoatings (e.g., Derivo 2Heal) create a surface highly conducive to endothelial growth while inactivating thrombin, reducing clot formation.[172] Rosuvastatin could further enhance endothelialization by EPCs mobilization and upregulating CD31 receptors, acting synergistically to promote vessel healing. This synergistic effect may be further enhanced with coatings designed to promote neointimal growth, such as the P8RI peptide (Balt), which actively stimulates endothelial cell adhesion and proliferation (Appendix 6 for the article).[172,324] The higher serum concentration of EPCs induced by Rosuvastatin could further amplify endothelial adhesion on such coatings, accelerating the formation of a stable neointimal layer across the aneurysm neck and improving long-term occlusion outcomes.

IX.7. Rosuvastatin coated FD

An alternative approach to oral administration, which can result in suboptimal local concentrations and potential side effects, is the development of Rosuvastatin-eluting coatings for targeting the delivery on the affected vessel. An example, has been already presented by Lee et al.[265] who developed poly(D,L)-lactide-co-glycolide (PLGA) nanofiber-loaded stents, that were able to deliver different doses of Rosuvastatin (Figure 35). The in vitro and in vivo studies demonstrated that the Rosuvastatin coated stents accelerated the re-endothelialization, improved the endothelial function, reduced the platelet adhesion and the inflammatory responses, and significant inhibited the neointimal hyperplasia. Adapting such

License CC BY-NC-ND 4.0

PLGA-based, Rosuvastatin-loaded nanofibers to FDs could similarly foster a favorable vascular healing environment, potentially improving long-term outcomes in aneurysm management by offering an effective alternative to existing coatings while maintaining comparable antithrombotic effects. Same results have been also highlighted in other studies with similar design.[262,277,325,326]

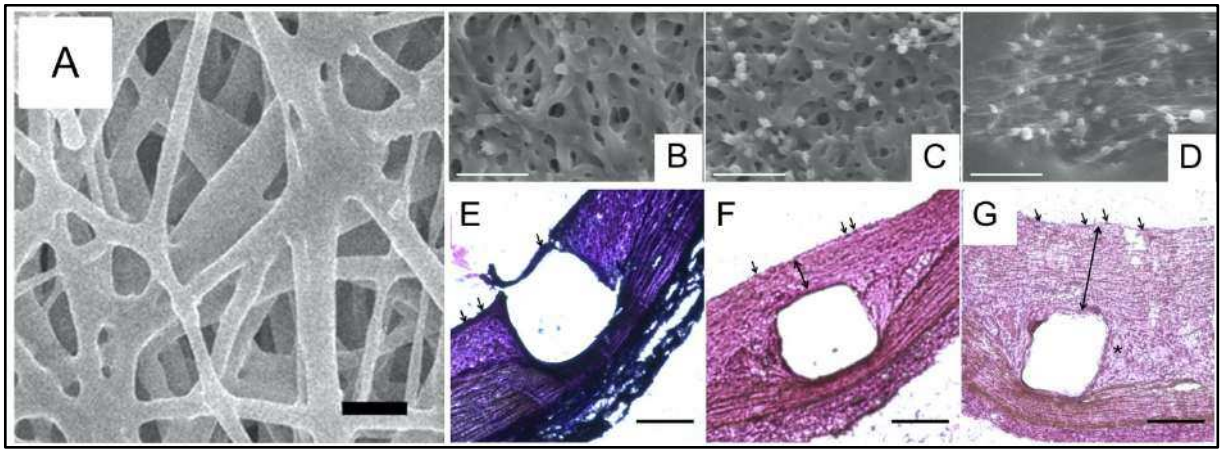


Figure 37. PLGA-Rosuvastatin-loaded stent. (A) swollen sponge-like structures. (B/C/D) Platelet adhesion test in vitro. Immersion of nanofibrous membranes with or without rosuvastatin in platelet rich plasma for three hours. (A) No platelet adhered to the nanofibers in group A with Rosuvastatin loadings of 5 mg/mm^2; (B) few platelets adhered to group B nanofibers with rosuvastatin loading of 2 mg/mm^2; (C) larger platelet aggregates and more extensive platelet pseudopod formation were observed on nanofibers without Rosuvastatin loading. (E/F/G) Photomicrographs of representative rabbit vessel sections 28 days after intervention. Inflammation response was low in drug-loaded groups. (A) Almost no intimal hyperplasia; (B/C) consistent intimal hyperplasia with a thickness of approximately 50 mm and 150 mm, respectively. Single arrow=ECs; double arrow= neointimal hyperplasia; asterisk= inflammatory cells surrounding the stent struts.[327]

IX.8. Oral Rosuvastatin vs Rosuvastatin coated FD

While FDSMs with Rosuvastatin represents a feasible approach to enhance local endothelialization and reduce complications such as in-stent stenosis and thrombosis, as

License CC BY-NC-ND 4.0

demonstrated in a preclinical study,[265] this strategy may be unnecessary given the pharmacokinetic profile of orally administered Rosuvastatin. Despite its relatively low absolute oral bioavailability of approximately 20%,[327] Rosuvastatin achieves high serum concentrations (~88% of the total absorbed dose) and therapeutically effective peak plasma concentrations (Cmax) of around 6 µg/L within 3-5 hours post-dosing,[328] enabling sufficient systemic exposure. We can assume that this is sufficient to support FD healing in IAs treatment without the need for device-specific coatings. Notably, our study in rabbits demonstrated serum Rosuvastatin concentrations comparable to the typical human therapeutic range of 5-10 µg/L, confirming the reliability of our findings for clinical translation. This systemic efficacy, combined with the simplicity and established safety of oral administration, suggests that pursuing FD surface modifications with Rosuvastatin could add complexity to the therapeutic regimen. Moreover, oral administration achieves target concentrations with easily manageable treatment durations, whereas coated FDs face challenges, including unknown local pharmacokinetics, uncertain dosage to determine sufficient serum concentrations for pleiotropic effects (e.g., EPCs mobilization) critical for endothelialization, and a limited drug release duration (typically ~4 weeks), which may be insufficient for complete IA healing.[262,277,325,326] However, this conclusion warrants caution, as Rosuvastatin's therapeutic range is primarily optimized for lipid-lowering effects rather than its pleiotropic effects on vascular healing, and direct comparisons between oral and local delivery approaches are lacking.

License CC BY-NC-ND 4.0

Summary

This chapter focus on the results of the project, comparing the effects of the Rosuvastatin combined with Aspirin (Rosu+ASA) versus Aspirin alone (ASA) on flow diverter (FD) treatment. The research included efficacy and safety analyses, assessing aneurysm occlusion rates, patency of FD-covered branches, and histological strut coverage in 22 rabbits: 13 in the Rosu+ASA group and 9 in the ASA group. The Rosu+ASA group showed a higher, though not statistically significant, aneurysm occlusion rate (84.6% vs. 66.6%, p=0.323) and significantly improved patency of covered branches, especially for larger arteries (94.4% vs. 46.1%, p=0.007). Histological analysis indicated a trend toward better neo-tissue coverage in the Rosu+ASA group, with a strong correlation between Rosuvastatin serum concentration and endothelial cell coverage (r=0.92, p=0.02). The composite outcome of complete aneurysm occlusion and patent branches was significantly higher in the Rosu+ASA group (76.9% vs. 22.2%, p=0.011). These findings suggest Rosuvastatin enhances FD outcomes by promoting endothelialization and reducing thromboembolic complications. Finally, are proposed future scenarios, including a randomized controlled trial (STATIN-FDIA), to validate these results in human patients with intracranial aneurysms.

License CC BY-NC-ND 4.0

Conclusion

In this thesis, we have explored the pivotal role of biological optimization in the EVT of IAs, with a particular focus on integrating novel therapeutic strategies to enhance occlusion rates and reduce complications. Our first four articles aimed to improve treatment outcomes for both unruptured and ruptured intracranial aneurysms by refining patient selection and optimizing endovascular techniques. In the first one we identified variables most strongly associated with aneurysm complexity, through a DELPHI study. In the second one we developed a morbidity-mortality risk score for both EVT and NT, the MARTA score, and we identified four risk classes (low, medium, high, and critical), with complication rates ranging from 2.4-18.3% for EVT and 4.2-75% for NT. This score can be used in routine clinical practice, ideally in combination with existing scores that assess the risk of aneurysm rupture. In the third one we showed that IFD-AC using the Contour Neurovascular System and Neqstent devices is promising and safe. The fourth one showed that adding coils during FD treatment reduces the complication rate in large and giant aneurysms.

Our preclinical study, conducted on rabbit elastase-induced aneurysm models, revealed that oral Rosuvastatin therapy, when combined with Aspirin, enhances the therapeutic effect of FD treatment, increasing aneurysm occlusion rates and promoting occlusion of collateral branches. The main hypothesis of this thesis is that the oral administration of Rosuvastatin offers a promising strategy to optimize FD healing. As demonstrated in our model, oral Rosuvastatin provides systemic benefits that support neointimal formation and branch preservation within a short timeframe. We propose a clinical trial to assess its role in clinical practice and validate our findings. Additionally, extending this concept, integrating Rosuvastatin into dedicated FD coatings could enable localized drug release, enhancing endothelialization directly at the stent-vessel interface while potentially minimizing systemic exposure and side effects. This dual approach aligns with emerging trends in bioengineered devices, where coatings such as phosphorylcholine or heparin have already demonstrated reduced thrombogenicity. Incorporating Rosuvastatin could further amplify these effects by

License CC BY-NC-ND 4.0

leveraging its anti-inflammatory and pro-endothelial properties, ultimately bridging the gap between hemodynamic flow diversion and biological vessel remodeling. Finally, in the last study we also showed that the P8RI peptide linked to the surface of an FD promotes rapid endothelial coverage.

On a personal level, undertaking this research has been an immensely enriching journey, blending my passion for interventional neuroradiology with my fascination for biotechnological innovations. I have been deeply inspired by the precision and creativity required to develop these experimental models, as well as by the invaluable guidance from mentors such as Professor Aymeric Rouchaud, whose support has been a cornerstone of this work, and the team at the EMIS Lab, whose enthusiasm has infused this project with unique vitality. While the rabbit models used here provide a valuable approximation of human conditions, I am keenly aware of their limitations, such as short follow-up durations and physiological differences, which necessitate further clinical studies to validate these findings. This thesis has reinforced my belief in the power of interdisciplinary collaboration, and I am eager to continue this research with international partners to translate these approaches into clinical practice. These efforts open new horizons for personalized medicine in IA treatment, and I am excited to contribute to their evolution, continually learning and innovating within this captivating field, with the hope of making a tangible difference in patient care.

License CC BY-NC-ND 4.0

Bibliography

1. Ogilvy CS. Unruptured Intracranial Aneurysms. *N Engl J Med*. 2025;392(23):2357-2366. doi:10.1056/NEJMcp2409371

2. Kang HG, Kim BJ, Lee J, et al. Risk Factors Associated With the Presence of Unruptured Intracranial Aneurysms. *Stroke*. 2015;46(11):3093-3098. doi:10.1161/STROKEAHA.115.011351

3. Tromp G, Weinsheimer S, Ronkainen A, Kuivaniemi H. Molecular basis and genetic predisposition to intracranial aneurysm. *Ann Med*. 2014;46(8):597-606. doi:10.3109/07853890.2014.949299

4. Cras TY, Bos D, Ikram MA, et al. Determinants of the Presence and Size of Intracranial Aneurysms in the General Population: The Rotterdam Study. *Stroke*. 2020;51(7):2103-2110. doi:10.1161/STROKEAHA.120.029296

5. Jabbarli R, Dinger TF, Darkwah Oppong M, et al. Risk Factors for and Clinical Consequences of Multiple Intracranial Aneurysms: A Systematic Review and Meta-Analysis. *Stroke*. 2018;49(4):848-855. doi:10.1161/STROKEAHA.117.020342

6. Caranci F, Briganti F, Cirillo L, Leonardi M, Muto M. Epidemiology and genetics of intracranial aneurysms. *Eur J Radiol*. 2013;82(10):1598-1605. doi:10.1016/j.ejrad.2012.12.026

7. Thompson BG, Brown RD, Amin-Hanjani S, et al. Guidelines for the Management of Patients With Unruptured Intracranial Aneurysms: A Guideline for Healthcare Professionals From the American Heart Association/American Stroke Association. *Stroke*. 2015;46(8):2368-2400. doi:10.1161/STR.0000000000000070

8. Müller TB, Vik A, Romundstad PR, Sandvei MS. Risk Factors for Unruptured Intracranial Aneurysms and Subarachnoid Hemorrhage in a Prospective Population-Based Study. *Stroke*. 2019;50(10):2952-2955. doi:10.1161/STROKEAHA.119.025951

9. Sun X, Liu B, Chen Y, Lv L, Ye D, Mao Y. Modifiable risk factors for intracranial aneurysms: Evidence from genetic studies. *Int J Stroke*. 2022;17(10):1107-1113. doi:10.1177/17474930211065640

10. Jabbarli R, Pierscianek D, Wrede K, et al. Aneurysm remnant after clipping: the risks and consequences. *J Neurosurg*. 2016;125(5):1249-1255. doi:10.3171/2015.10.JNS151536

11. Bakker MK, van der Spek RAA, van Rheenen W, et al. Genome-wide association study of intracranial aneurysms identifies 17 risk loci and genetic overlap with clinical risk factors. *Nat Genet*. 2020;52(12):1303-1313. doi:10.1038/s41588-020-00725-7

12. Liu Z, Ajimu K, Yalikun N, Zheng Y, Xu F. Potential Therapeutic Strategies for Intracranial Aneurysms Targeting Aneurysm Pathogenesis. *Front Neurosci*. 2019;13:1238. doi:10.3389/fnins.2019.01238

13. Penn DL, Witte SR, Komotar RJ, Sander Connolly E. The role of vascular remodeling and inflammation in the pathogenesis of intracranial aneurysms. *J Clin Neurosci*. 2014;21(1):28-32. doi:10.1016/j.jocn.2013.07.004

License CC BY-NC-ND 4.0

14. Frösen J, Tulamo R, Paetau A, et al. Saccular intracranial aneurysm: pathology and mechanisms. *Acta Neuropathol*. 2012;123(6):773-786. doi:10.1007/s00401-011-0939-3

15. Chalouhi N, Ali MS, Jabbour PM, et al. Biology of intracranial aneurysms: role of inflammation. *J Cereb Blood Flow Metab*. 2012;32(9):1659-1676. doi:10.1038/jcbfm.2012.84

16. Texakalidis P, Sweid A, Mouchtouris N, et al. Aneurysm Formation, Growth, and Rupture: The Biology and Physics of Cerebral Aneurysms. *World Neurosurg*. 2019;130:277-284. doi:10.1016/j.wneu.2019.07.093

17. Huang Z, Ling C. Pathophysiological Mechanisms for Intracranial Aneurysms. *World Neurosurg*. 2025;201:124273. doi:10.1016/j.wneu.2025.124273

18. Xu Z, Rui YN, Hagan JP, Kim DH. Intracranial Aneurysms: Pathology, Genetics, and Molecular Mechanisms. *Neuromolecular Med*. 2019;21(4):325-343. doi:10.1007/s12017-019-08537-7

19. Wang J, Wei L, Lu H, Zhu Y. Roles of inflammation in the natural history of intracranial saccular aneurysms. *J Neurol Sci*. 2021;424:117294. doi:10.1016/j.jns.2020.117294

20. Hudson JS, Hoyne DS, Hasan DM. Inflammation and human cerebral aneurysms: current and future treatment prospects. *Future Neurol*. 2013;8(6). doi:10.2217/fnl.13.40

21. Meng H, Tutino VM, Xiang J, Siddiqui A. High WSS or low WSS? Complex interactions of hemodynamics with intracranial aneurysm initiation, growth, and rupture: toward a unifying hypothesis. *AJNR Am J Neuroradiol*. 2014;35(7):1254-1262. doi:10.3174/ajnr.A3558

22. Grüter BE, von Faber-Castell F, Marbacher S. Lumen-oriented versus wall-oriented treatment strategies for intracranial aneurysms - A systematic review of suggested therapeutic concepts. *J Cereb Blood Flow Metab*. 2022;42(9):1568-1578. doi:10.1177/0271678X211057498

23. Eskey CJ, Meyers PM, Nguyen TN, et al. Indications for the Performance of Intracranial Endovascular Neurointerventional Procedures: A Scientific Statement From the American Heart Association. *Circulation*. 2018;137(21):e661-e689. doi:10.1161/CIR.0000000000000567

24. Algra AM, Lindgren A, Vergouwen MDI, et al. Procedural Clinical Complications, Case-Fatality Risks, and Risk Factors in Endovascular and Neurosurgical Treatment of Unruptured Intracranial Aneurysms: A Systematic Review and Meta-analysis. *JAMA Neurol*. 2019;76(3):282-293. doi:10.1001/jamaneurol.2018.4165

25. Fatania K, Patankar DT. Comprehensive review of the recent advances in devices for endovascular treatment of complex brain aneurysms. *Br J Radiol*. 2022;95(1129):20210538. doi:10.1259/bjr.20210538

26. Zhuo K, Wu H, Gou Z, Zhang C. Intrasaccular therapy in wide-neck intracranial aneurysms: a narrative review. *Front Neurol*. 2025;16:1552848. doi:10.3389/fneur.2025.1552848

27. Shao MM, White TG, Bassett JB, et al. Intrasaccular Treatment of Intracranial Aneurysms: A Comprehensive Review. *J Clin Med*. 2024;13(20):6162. doi:10.3390/jcm13206162

License CC BY-NC-ND 4.0

28. Rostamian A, Fallah K, Rostamiyan Y, Alinejad J. Computational study of the blood hemodynamic inside the cerebral double dome aneurysm filling with endovascular coiling. *Sci Rep*. 2023;13(1):2909. doi:10.1038/s41598-023-29988-w

29. Palmisano V, Ganimede MP, Diana F, et al. Long-term outcomes of the Woven EndoBridge device for intracranial aneurysms: systematic review and meta-analysis. *J Neurointerv Surg*. Published online August 5, 2025:jnis-2025-023799. doi:10.1136/jnis-2025-023799

30. Mine B, Bonnet T, Vazquez-Suarez JC, Iosif C, Lubicz B. Comparison of stents used for endovascular treatment of intracranial aneurysms. *Expert Rev Med Devices*. 2018;15(11):793-805. doi:10.1080/17434440.2018.1538779

31. Guo H, Liu JF, Li CH, Wang JW, Li H, Gao BL. Effects of stent-assisted coiling in comparison with flow diversion on intracranial aneurysms. *Front Neurol*. 2022;13:937536. doi:10.3389/fneur.2022.937536

32. Kashkoush A, El-Abtah ME, Srivatsa S, et al. Comparative effectiveness of stent-assisted coiling and Woven EndoBridge embolization for the treatment of unruptured wide-neck bifurcation intracranial aneurysms. *J Neurosurg*. 2023;138(6):1487-1493. doi:10.3171/2022.10.JNS221138

33. Naamani KE, Chen CJ, Abbas R, et al. Woven EndoBridge versus stent-assisted coil embolization of cerebral bifurcation aneurysms. *J Neurosurg*. 2022;137(6):1786-1793. doi:10.3171/2022.3.JNS2217

34. Kabbasch C, Goertz L, Siebert E, et al. WEB embolization versus stent-assisted coiling: comparison of complication rates and angiographic outcomes. *J Neurointerv Surg*. 2019;11(8):812-816. doi:10.1136/neurintsurg-2018-014555

35. Mouchtouris N, Hasan D, Samaniego EA, et al. The Woven EndoBridge (WEB) device: feasibility, techniques, and outcomes after FDA approval. *J Neurosurg*. 2022;136(5):1266-1272. doi:10.3171/2021.5.JNS21889

36. Diana F, Pesce A, Toccaceli G, et al. Microsurgical clipping versus newer endovascular techniques in treatment of unruptured anterior communicating artery-complex aneurysms: a meta-analysis and systematic review. *Neurosurg Rev*. 2022;45(2):1089-1100. doi:10.1007/s10143-021-01647-6

37. Togashi S, Shimizu H. Complex Intracranial Aneurysms. *Adv Tech Stand Neurosurg*. 2022;44:225-238. doi:10.1007/978-3-030-87649-4_12

38. Kotowski M, Naggara O, Darsaut TE, et al. Safety and occlusion rates of surgical treatment of unruptured intracranial aneurysms: a systematic review and meta-analysis of the literature from 1990 to 2011. *J Neurol Neurosurg Psychiatry*. 2013;84(1):42-48. doi:10.1136/jnnp-2011-302068

39. Naggara ON, Lecler A, Oppenheim C, Meder JF, Raymond J. Endovascular treatment of intracranial unruptured aneurysms: a systematic review of the literature on safety with emphasis on subgroup analyses. *Radiology*. 2012;263(3):828-835. doi:10.1148/radiol.12112114

40. Thompson BG, Brown RD, Amin-Hanjani S, et al. Guidelines for the Management of Patients With Unruptured Intracranial Aneurysms: A Guideline for Healthcare Professionals

License CC BY-NC-ND 4.0

From the American Heart Association/American Stroke Association. *Stroke*. 2015;46(8):2368-2400. doi:10.1161/STR.0000000000000070

41. Etminan N, Brown RD, Beseoglu K, et al. The unruptured intracranial aneurysm treatment score: a multidisciplinary consensus. *Neurology*. 2015;85(10):881-889. doi:10.1212/WNL.0000000000001891

42. Greving JP, Wermer MJH, Brown RD, et al. Development of the PHASES score for prediction of risk of rupture of intracranial aneurysms: a pooled analysis of six prospective cohort studies. *Lancet Neurol*. 2014;13(1):59-66. doi:10.1016/S1474-4422(13)70263-1

43. Algra AM, Greving JP, de Winkel J, et al. Development of the SAFETEA Scores for Predicting Risks of Complications of Preventive Endovascular or Microneurosurgical Intracranial Aneurysm Occlusion. *Neurology*. 2022;99(16):e1725-e1737. doi:10.1212/WNL.0000000000200978

44. Ji W, Liu A, Lv X, et al. Risk Score for Neurological Complications After Endovascular Treatment of Unruptured Intracranial Aneurysms. *Stroke*. 2016;47(4):971-978. doi:10.1161/STROKEAHA.115.012097

45. Ogilvy CS, Carter BS. A proposed comprehensive grading system to predict outcome for surgical management of intracranial aneurysms. *Neurosurgery*. 1998;42(5):959-968; discussion 968-970. doi:10.1097/00006123-199805000-00001

46. Newman WC, Neal DW, Hoh BL. A new comorbidities index for risk stratification for treatment of unruptured cerebral aneurysms. *J Neurosurg*. 2016;125(3):713-719. doi:10.3171/2015.8.JNS14553

47. Sweid A, Starke RM, Herial N, et al. Predictors of Complications, Functional Outcome, and Morbidity in a Large Cohort Treated With Flow Diversion. *Neurosurgery*. 2020;87(4):730-743. doi:10.1093/neuros/nyz508

48. Willinsky RA, Peltz J, da Costa L, Agid R, Farb RI, terBrugge KG. Clinical and angiographic follow-up of ruptured intracranial aneurysms treated with endovascular embolization. *AJNR Am J Neuroradiol*. 2009;30(5):1035-1040. doi:10.3174/ajnr.A1488

49. Grunwald IQ, Papanagiotou P, Struffert T, et al. Recanalization after endovascular treatment of intracerebral aneurysms. *Neuroradiology*. 2007;49(1):41-47. doi:10.1007/s00234-006-0153-5

50. Yarahmadi P, Kabiri A, Bavandipour A, Jabbour P, Yousefi O. Intra-procedural complications, success rate, and need for retreatment of endovascular treatments in anterior communicating artery aneurysms: a systematic review and meta-analysis. *Neurosurg Rev*. 2022;45(5):3157-3170. doi:10.1007/s10143-022-01853-w

51. Raymond J, Guilbert F, Weill A, et al. Long-term angiographic recurrences after selective endovascular treatment of aneurysms with detachable coils. *Stroke*. 2003;34(6):1398-1403. doi:10.1161/01.STR.0000073841.88563.E9

52. Ferns SP, Sprengers MES, van Rooij WJ, et al. Late reopening of adequately coiled intracranial aneurysms: frequency and risk factors in 400 patients with 440 aneurysms. *Stroke*. 2011;42(5):1331-1337. doi:10.1161/STROKEAHA.110.605790

License CC BY-NC-ND 4.0

53. Wakhloo AK, Schellhammer F, de Vries J, Haberstroh J, Schumacher M. Self-expanding and balloon-expandable stents in the treatment of carotid aneurysms: an experimental study in a canine model. *AJNR Am J Neuroradiol*. 1994;15(3):493-502.

54. Turjman F, Acevedo G, Moll T, Duquesnel J, Eloy R, Sindou M. Treatment of experimental carotid aneurysms by endoprosthesis implantation: preliminary report. *Neurol Res*. 1993;15(3):181-184. doi:10.1080/01616412.1993.11740132

55. Lanzino G, Wakhloo AK, Fessler RD, Hartney ML, Guterman LR, Hopkins LN. Efficacy and current limitations of intravascular stents for intracranial internal carotid, vertebral, and basilar artery aneurysms. *J Neurosurg*. 1999;91(4):538-546. doi:10.3171/jns.1999.91.4.0538

56. Mehta V, Harward SC, Sankey EW, Nayar G, Codd PJ. Evidence based diagnosis and management of chronic subdural hematoma: A review of the literature. *J Clin Neurosci*. 2018;50:7-15. doi:10.1016/j.jocn.2018.01.050

57. Vanninen R, Manninen H, Ronkainen A. Broad-based intracranial aneurysms: thrombosis induced by stent placement. *AJNR Am J Neuroradiol*. 2003;24(2):263-266.

58. Lieber BB, Stancampiano AP, Wakhloo AK. Alteration of hemodynamics in aneurysm models by stenting: influence of stent porosity. *Ann Biomed Eng*. 1997;25(3):460-469. doi:10.1007/BF02684187

59. Aenis M, Stancampiano AP, Wakhloo AK, Lieber BB. Modeling of flow in a straight stented and nonstented side wall aneurysm model. *J Biomech Eng*. 1997;119(2):206-212. doi:10.1115/1.2796081

60. Lieber BB, Sadasivan C. Endoluminal scaffolds for vascular reconstruction and exclusion of aneurysms from the cerebral circulation. *Stroke*. 2010;41(10 Suppl):S21-25. doi:10.1161/STROKEAHA.110.595066

61. Lieber BB, Livescu V, Hopkins LN, Wakhloo AK. Particle image velocimetry assessment of stent design influence on intra-aneurysmal flow. *Ann Biomed Eng*. 2002;30(6):768-777. doi:10.1114/1.1495867

62. Augsburger L, Farhat M, Reymond P, et al. Effect of flow diverter porosity on intraaneurysmal blood flow. *Klin Neuroradiol*. 2009;19(3):204-214. doi:10.1007/s00062-009-9005-0

63. Sadasivan C, Cesar L, Seong J, et al. An original flow diversion device for the treatment of intracranial aneurysms: evaluation in the rabbit elastase-induced model. *Stroke*. 2009;40(3):952-958. doi:10.1161/STROKEAHA.108.533760

64. Kallmes DF, Ding YH, Dai D, Kadirvel R, Lewis DA, Cloft HJ. A new endoluminal, flow-disrupting device for treatment of saccular aneurysms. *Stroke*. 2007;38(8):2346-2352. doi:10.1161/STROKEAHA.106.479576

65. D'Urso PI, Lanzino G, Cloft HJ, Kallmes DF. Flow diversion for intracranial aneurysms: a review. *Stroke*. 2011;42(8):2363-2368. doi:10.1161/STROKEAHA.111.620328

66. Fiorella D, Woo HH, Albuquerque FC, Nelson PK. Definitive reconstruction of circumferential, fusiform intracranial aneurysms with the pipeline embolization device. *Neurosurgery*. 2008;62(5):1115-1120; discussion 1120-1121. doi:10.1227/01.neu.0000325873.44881.6e

License CC BY-NC-ND 4.0

67. Fiorella D, Kelly ME, Albuquerque FC, Nelson PK. Curative reconstruction of a giant midbasilar trunk aneurysm with the pipeline embolization device. *Neurosurgery*. 2009;64(2):212-217; discussion 217. doi:10.1227/01.NEU.0000337576.98984.E4

68. Lylyk P, Miranda C, Ceratto R, et al. Curative endovascular reconstruction of cerebral aneurysms with the pipeline embolization device: the Buenos Aires experience. *Neurosurgery*. 2009;64(4):632-642; discussion 642-643; quiz N6. doi:10.1227/01.NEU.0000339109.98070.65

69. Roszelle BN, Babiker MH, Hafner W, Gonzalez LF, Albuquerque FC, Frakes DH. In vitro and in silico study of intracranial stent treatments for cerebral aneurysms: effects on perforating vessel flows. *J Neurointerv Surg*. 2013;5(4):354-360. doi:10.1136/neurintsurg-2012-010322

70. Szikora I, Seifert P, Hanzely Z, et al. Histopathologic evaluation of aneurysms treated with Guglielmi detachable coils or matrix detachable microcoils. *AJNR Am J Neuroradiol*. 2006;27(2):283-288.

71. Brinjikji W, Kallmes DF, Kadirvel R. Mechanisms of Healing in Coiled Intracranial Aneurysms: A Review of the Literature. *AJNR Am J Neuroradiol*. 2015;36(7):1216-1222. doi:10.3174/ajnr.A4175

72. Kulcsár Z, Houdart E, Bonafé A, et al. Intra-aneurysmal thrombosis as a possible cause of delayed aneurysm rupture after flow-diversion treatment. *AJNR Am J Neuroradiol*. 2011;32(1):20-25. doi:10.3174/ajnr.A2370

73. Ikeda H, Ishii A, Kikuchi T, et al. Delayed aneurysm rupture due to residual blood flow at the inflow zone of the intracranial paraclinoid internal carotid aneurysm treated with the Pipeline embolization device: Histopathological investigation. *Interv Neuroradiol*. 2015;21(6):674-683. doi:10.1177/1591019915609121

74. Dai D, Ding YH, Kelly M, Kadirvel R, Kallmes D. Histopathological findings following pipeline embolization in a human cerebral aneurysm at the basilar tip. *Interv Neuroradiol*. 2016;22(2):153-157. doi:10.1177/1591019915622165

75. Szikora I, Turányi E, Marosfoi M. Evolution of Flow-Diverter Endothelialization and Thrombus Organization in Giant Fusiform Aneurysms after Flow Diversion: A Histopathologic Study. *AJNR Am J Neuroradiol*. 2015;36(9):1716-1720. doi:10.3174/ajnr.A4336

76. Tang AYS, Chan HN, Tsang ACO, et al. The effects of stent porosity on the endovascular treatment of intracranial aneurysms located near a bifurcation. *Journal of Biomedical Science and Engineering*. 2013;6(8):812-822. doi:10.4236/jbise.2013.68099

77. Rouchaud A, Johnson C, Thielen E, et al. Differential Gene Expression in Coiled versus Flow-Diverter-Treated Aneurysms: RNA Sequencing Analysis in a Rabbit Aneurysm Model. *AJNR Am J Neuroradiol*. 2016;37(6):1114-1121. doi:10.3174/ajnr.A4648

78. Huang MT, Mason JC, Birdsey GM, et al. Endothelial intercellular adhesion molecule (ICAM)-2 regulates angiogenesis. *Blood*. 2005;106(5):1636-1643. doi:10.1182/blood-2004-12-4716

79. Puffer C, Dai D, Ding YH, Cebral J, Kallmes D, Kadirvel R. Gene expression comparison of flow diversion and coiling in an experimental aneurysm model. *J Neurointerv Surg*. 2015;7(12):926-930. doi:10.1136/neurintsurg-2014-011452

License CC BY-NC-ND 4.0

80. Ravindran K, Salem MM, Alturki AY, Thomas AJ, Ogilvy CS, Moore JM. Endothelialization following Flow Diversion for Intracranial Aneurysms: A Systematic Review. *AJNR Am J Neuroradiol*. 2019;40(2):295-301. doi:10.3174/ajnr.A5955

81. Welt FGP, Rogers C. Inflammation and restenosis in the stent era. *Arterioscler Thromb Vasc Biol*. 2002;22(11):1769-1776. doi:10.1161/01.atv.0000037100.44766.5b

82. Inoue T, Croce K, Morooka T, Sakuma M, Node K, Simon DI. Vascular inflammation and repair: implications for re-endothelialization, restenosis, and stent thrombosis. *JACC Cardiovasc Interv*. 2011;4(10):1057-1066. doi:10.1016/j.jcin.2011.05.025

83. Ravindran K, Casabella AM, Cebral J, Brinjikji W, Kallmes DF, Kadirvel R. Mechanism of Action and Biology of Flow Diverters in the Treatment of Intracranial Aneurysms. *Neurosurgery*. 2020;86(Suppl 1):S13-S19. doi:10.1093/neuros/nyz324

84. Kadirvel R, Ding YH, Dai D, Rezek I, Lewis DA, Kallmes DF. Cellular mechanisms of aneurysm occlusion after treatment with a flow diverter. *Radiology*. 2014;270(2):394-399. doi:10.1148/radiol.13130796

85. Matsuda Y, Chung J, Lopes DK. Analysis of neointima development in flow diverters using optical coherence tomography imaging. *J Neurointerv Surg*. 2018;10(2):162-167. doi:10.1136/neurintsurg-2016-012969

86. Ramirez-Velandia F, Mensah E, Salih M, et al. Endothelial Progenitor Cells: A Review of Molecular Mechanisms in the Pathogenesis and Endovascular Treatment of Intracranial Aneurysms. *Neuromolecular Med*. 2024;26(1):25. doi:10.1007/s12017-024-08791-4

87. Li ZF, Fang XG, Yang PF, et al. Endothelial progenitor cells contribute to neointima formation in rabbit elastase-induced aneurysm after flow diverter treatment. *CNS Neurosci Ther*. 2013;19(5):352-357. doi:10.1111/cns.12086

88. Frösen J, Marjamaa J, Myllärniemi M, et al. Contribution of mural and bone marrow-derived neointimal cells to thrombus organization and wall remodeling in a microsurgical murine saccular aneurysm model. *Neurosurgery*. 2006;58(5):936-944; discussion 936-944. doi:10.1227/01.NEU.0000210260.55124.A4

89. Nelson PK, Lylyk P, Szikora I, Wetzel SG, Wanke I, Fiorella D. The pipeline embolization device for the intracranial treatment of aneurysms trial. *AJNR Am J Neuroradiol*. 2011;32(1):34-40. doi:10.3174/ajnr.A2421

90. Becske T, Brinjikji W, Potts MB, et al. Long-Term Clinical and Angiographic Outcomes Following Pipeline Embolization Device Treatment of Complex Internal Carotid Artery Aneurysms: Five-Year Results of the Pipeline for Uncoilable or Failed Aneurysms Trial. *Neurosurgery*. 2017;80(1):40-48. doi:10.1093/neuros/nyw014

91. Becske T, Potts MB, Shapiro M, et al. Pipeline for uncoilable or failed aneurysms: 3-year follow-up results. *J Neurosurg*. 2017;127(1):81-88. doi:10.3171/2015.6.JNS15311

92. Meyers PM, Coon AL, Kan PT, Wakhloo AK, Hanel RA. SCENT Trial. *Stroke*. 2019;50(6):1473-1479. doi:10.1161/STROKEAHA.118.024135

93. Hanel RA, Cortez GM, Coon AL, et al. Surpass Intracranial Aneurysm Embolization System Pivotal Trial to Treat Large or Giant Wide-Neck Aneurysms - SCENT: 3-year outcomes. *J Neurointerv Surg*. 2023;15(11):1084-1089. doi:10.1136/jnis-2022-019512

License CC BY-NC-ND 4.0

94. Meyers PM, Coon AL, Kan P, et al. Five-year results of the SCENT trial with Surpass flow diverters to treat large or giant wide-neck aneurysms. *J Neurointerv Surg*. Published online May 14, 2025:jnis-2024-022977. doi:10.1136/jnis-2024-022977

95. Kan P, Mohanty A, Meyers PM, et al. Treatment of large and giant posterior communicating artery aneurysms with the Surpass streamline flow diverter: results from the SCENT trial. *J Neurointerv Surg*. 2023;15(7):679-683. doi:10.1136/neurintsurg-2021-018189

96. Wakhloo AK, Lylyk P, de Vries J, et al. Surpass flow diverter in the treatment of intracranial aneurysms: a prospective multicenter study. *AJNR Am J Neuroradiol*. 2015;36(1):98-107. doi:10.3174/ajnr.A4078

97. De Vries J, Boogaarts J, Van Norden A, Wakhloo AK. New generation of Flow Diverter (surpass) for unruptured intracranial aneurysms: a prospective single-center study in 37 patients. *Stroke*. 2013;44(6):1567-1577. doi:10.1161/STROKEAHA.111.000434

98. Byrne JV, Beltechi R, Yarnold JA, Birks J, Kamran M. Early experience in the treatment of intra-cranial aneurysms by endovascular flow diversion: a multicentre prospective study. *PLoS One*. 2010;5(9):e12492. doi:10.1371/journal.pone.0012492

99. Pumar JM, Banguero A, Cuellar H, et al. Treatment of Intracranial Aneurysms With the SILK Embolization Device in a Multicenter Study. A Retrospective Data Analysis. *Neurosurgery*. 2017;81(4):595-601. doi:10.1093/neuros/nyw123

100. Murthy SB, Shah S, Shastri A, Venkatasubba Rao CP, Bershad EM, Suarez JI. The SILK flow diverter in the treatment of intracranial aneurysms. *J Clin Neurosci*. 2014;21(2):203-206. doi:10.1016/j.jocn.2013.07.006

101. Hajikarimloo B, Mohammadzadeh I, Tos SM, et al. Endovascular treatment of intracranial aneurysms with silk vista baby flow diverter: A systematic review and meta-analysis. *Neuroradiol J*. Published online February 27, 2025:19714009251324324. doi:10.1177/19714009251324324

102. Scarcia L, Clarençon F, Dmytriw AA, et al. Silk Vista Baby for the treatment of distal anterior cerebral artery aneurysms. *Neuroradiology*. Published online July 2, 2025. doi:10.1007/s00234-025-03678-y

103. Hanel RA, de Toledo OF, De Oliveira Souza NV, et al. The Silk Vista Baby Study: A Multicenter Aneurysm Report From North America and Europe. *Neurosurgery*. Published online July 10, 2025. doi:10.1227/neu.0000000000003611

104. Jaworski M, Krysiak R, Żyłkowski J, et al. The evaluation of the flow re-direction endoluminal device (FRED) for the treatment of selected intracranial aneurysms: a Polish multicenter study. *Sci Rep*. 2025;15(1):6386. doi:10.1038/s41598-025-90463-9

105. Piano M, Valvassori L, Lozupone E, et al. FRED Italian Registry: a multicenter experience with the flow re-direction endoluminal device for intracranial aneurysms. *J Neurosurg*. 2020;133(1):174-181. doi:10.3171/2019.1.JNS183005

106. Manzato LB, Santos RB, Filho PMM, Miotto G, Bastos AM, Vanzin JR. Brazilian FRED Registry: A Prospective Multicenter Study for Brain Aneurysm Treatment-The BRED Study. *AJNR Am J Neuroradiol*. 2021;42(10):1822-1826. doi:10.3174/ajnr.A7258

License CC BY-NC-ND 4.0

107. Khorasanizadeh M, Shutran M, Schirmer CM, et al. North American multicenter experience with the Flow Redirection Endoluminal Device in the treatment of intracranial aneurysms. *J Neurosurg*. 2023;138(4):933-943. doi:10.3171/2022.7.JNS221371

108. Salem MM, Kvint S, Hendrix P, et al. The Pennsylvania Postmarket Multicenter Experience With Flow Redirection Endoluminal Device. *Neurosurgery*. 2022;91(2):280-285. doi:10.1227/neu.0000000000001970

109. Uysal A, Cay F, Balcı S, Arat A. Initial Experience with the Derivo 2Heal Flow Diverter under Standard or Reduced-Dose Single Antiplatelet Therapy. *AJNR Am J Neuroradiol*. 2024;45(8):1038-1043. doi:10.3174/ajnr.A8292

110. Li YL, Roalfe A, Chu EYL, Lee R, Tsang ACO. Outcome of Flow Diverters with Surface Modifications in Treatment of Cerebral Aneurysms: Systematic Review and Meta-analysis. *AJNR Am J Neuroradiol*. 2021;42(2):327-333. doi:10.3174/ajnr.A6919

111. Piñana C, Remollo S, Zamarro J, et al. Derivo embolization device for intracranial aneurysms: a Spanish multicenter retrospective study. *J Neurointerv Surg*. 2023;15(9):871-875. doi:10.1136/jnis-2022-019220

112. Trivelato FP, Abud DG, Ulhôa AC, et al. Derivo Embolization Device for the Treatment of Intracranial Aneurysms. *Stroke*. 2019;50(9):2351-2358. doi:10.1161/STROKEAHA.119.025407

113. Chagas Lourenço G, Dantas F, Silva E Carvalho T, et al. Endovascular treatment of intracranial aneurysms using the Derivo Embolization Device: a multicenter experience. *J Neurointerv Surg*. 2023;15(8):776-780. doi:10.1136/neurintsurg-2022-018648

114. Briganti F, Leone G, Marseglia M, Cicala D, Caranci F, Maiuri F. p64 Flow Modulation Device in the treatment of intracranial aneurysms: initial experience and technical aspects. *J Neurointerv Surg*. 2016;8(2):173-180. doi:10.1136/neurintsurg-2015-011743

115. Vivanco-Suarez J, Salem MM, Sioutas GS, et al. Safety and efficacy of the p48 MW and p64 flow modulation devices: a systematic review and meta-analysis. *Neurosurg Focus*. 2023;54(5):E7. doi:10.3171/2023.2.FOCUS22648

116. Bonafe A, Perez MA, Henkes H, et al. Diversion-p64: results from an international, prospective, multicenter, single-arm post-market study to assess the safety and effectiveness of the p64 flow modulation device. *J Neurointerv Surg*. 2022;14(9):898-903. doi:10.1136/neurintsurg-2021-017809

117. Hellstern V, Aguilar-Pérez M, Henkes E, et al. Endovascular Treatment of Posterior Circulation Saccular Aneurysms With the p64 Flow Modulation Device: Mid-and Long-Term Results in 54 Aneurysms From a Single Center. *Front Neurol*. 2021;12:711863. doi:10.3389/fneur.2021.711863

118. Brinjikji W, Murad MH, Lanzino G, Cloft HJ, Kallmes DF. Endovascular treatment of intracranial aneurysms with flow diverters: a meta-analysis. *Stroke*. 2013;44(2):442-447. doi:10.1161/STROKEAHA.112.678151

119. Darsaut TE, Findlay JM, Bojanowski MW, et al. A Pragmatic Randomized Trial Comparing Surgical Clipping and Endovascular Treatment of Unruptured Intracranial Aneurysms. *American Journal of Neuroradiology*. 2023;44(6):634-640. doi:10.3174/ajnr.A7865

License CC BY-NC-ND 4.0

120. Cha KS, Balaras E, Lieber BB, Sadasivan C, Wakhloo AK. Modeling the interaction of coils with the local blood flow after coil embolization of intracranial aneurysms. *J Biomech Eng*. 2007;129(6):873-879. doi:10.1115/1.2800773

121. Wentzel JJ, Gijsen FJH, Stergiopulos N, Serruys PW, Slager CJ, Krams R. Shear stress, vascular remodeling and neointimal formation. *J Biomech*. 2003;36(5):681-688. doi:10.1016/s0021-9290(02)00446-3

122. Akimoto S, Mitsumata M, Sasaguri T, Yoshida Y. Laminar shear stress inhibits vascular endothelial cell proliferation by inducing cyclin-dependent kinase inhibitor p21(Sdi1/Cip1/Waf1). *Circ Res*. 2000;86(2):185-190. doi:10.1161/01.res.86.2.185

123. Malek AM, Alper SL, Izumo S. Hemodynamic shear stress and its role in atherosclerosis. *JAMA*. 1999;282(21):2035-2042. doi:10.1001/jama.282.21.2035

124. Berg P, Iosif C, Ponsonnard S, Yardin C, Janiga G, Mounayer C. Endothelialization of over- and undersized flow-diverter stents at covered vessel side branches: An in vivo and in silico study. *J Biomech*. 2016;49(1):4-12. doi:10.1016/j.jbiomech.2015.10.047

125. Jou LD, Mitchell BD, Shaltoni HM, Mawad ME. Effect of structural remodeling (retraction and recoil) of the pipeline embolization device on aneurysm occlusion rate. *AJNR Am J Neuroradiol*. 2014;35(9):1772-1778. doi:10.3174/ajnr.A3920

126. Zhang Y, Wang Y, Kao E, Flórez-Valencia L, Courbebaisse G. Towards optimal flow diverter porosity for the treatment of intracranial aneurysm. *J Biomech*. 2019;82:20-27. doi:10.1016/j.jbiomech.2018.10.002

127. Chong W, Zhang Y, Qian Y, Lai L, Parker G, Mitchell K. Computational hemodynamics analysis of intracranial aneurysms treated with flow diverters: correlation with clinical outcomes. *AJNR Am J Neuroradiol*. 2014;35(1):136-142. doi:10.3174/ajnr.A3790

128. Seong J, Wakhloo AK, Lieber BB. In vitro evaluation of flow divertors in an elastase-induced saccular aneurysm model in rabbit. *J Biomech Eng*. 2007;129(6):863-872. doi:10.1115/1.2800787

129. Rouchaud A, Ramana C, Brinjikji W, et al. Wall Apposition Is a Key Factor for Aneurysm Occlusion after Flow Diversion: A Histologic Evaluation in 41 Rabbits. *AJNR Am J Neuroradiol*. 2016;37(11):2087-2091. doi:10.3174/ajnr.A4848

130. Long S, Shi S, Tian Q, et al. Correlation of Flow Diverter Malapposition at the Aneurysm Neck with Incomplete Aneurysm Occlusion in Patients with Small Intracranial Aneurysms: A Single-Center Experience. *AJNR Am J Neuroradiol*. 2023;45(1):16-21. doi:10.3174/ajnr.A8079

131. Li J, Gong W, Li D, et al. Evaluation of the apposition in unruptured aneurysms treated with flow diverters by optical coherence tomography: Preliminary clinical experience. *Front Neurol*. 2022;13:1029699. doi:10.3389/fneur.2022.1029699

132. Foin N, Gutiérrez-Chico JL, Nakatani S, et al. Incomplete stent apposition causes high shear flow disturbances and delay in neointimal coverage as a function of strut to wall detachment distance: implications for the management of incomplete stent apposition. *Circ Cardiovasc Interv*. 2014;7(2):180-189. doi:10.1161/CIRCINTERVENTIONS.113.000931

133. Attizzani GF, Capodanno D, Ohno Y, Tamburino C. Mechanisms, pathophysiology, and clinical aspects of incomplete stent apposition. *J Am Coll Cardiol*. 2014;63(14):1355-1367. doi:10.1016/j.jacc.2014.01.019

License CC BY-NC-ND 4.0

134. Shojima M. Basic Fluid Dynamics and Tribia Related to Flow Diverter. *Journal of Neuroendovascular Therapy*. 2017;11(3):109-116. doi:10.5797/jnet.ra-diverter.2016-0012

135. Wallace AN, Grossberg JA, Almandoz JED, et al. Endovascular Treatment of Posterior Cerebral Artery Aneurysms With Flow Diversion: Case Series and Systematic Review. *Neurosurgery*. 2018;83(4):790-799. doi:10.1093/neuros/nyx561

136. Griessenauer CJ, Ogilvy CS, Adeeb N, et al. Pipeline embolization of posterior circulation aneurysms: a multicenter study of 131 aneurysms. *J Neurosurg*. 2019;130(3):923-935. doi:10.3171/2017.9.JNS171376

137. Shehata MA, Ibrahim MK, Ghozy S, et al. Long-term outcomes of flow diversion for unruptured intracranial aneurysms: a systematic review and meta-analysis. *J Neurointerv Surg*. 2023;15(9):898-902. doi:10.1136/jnis-2022-019240

138. Cebral JR, Chung BJ, Mut F, et al. Analysis of Flow Dynamics and Outcomes of Cerebral Aneurysms Treated with Intrasaccular Flow-Diverting Devices. *AJNR Am J Neuroradiol*. 2019;40(9):1511-1516. doi:10.3174/ajnr.A6169

139. Bender MT, Colby GP, Lin LM, et al. Predictors of cerebral aneurysm persistence and occlusion after flow diversion: a single-institution series of 445 cases with angiographic follow-up. *J Neurosurg*. 2019;130(1):259-267. doi:10.3171/2017.11.JNS171738

140. Meyer L, Stracke CP, Bester M, et al. Predictors of aneurysm occlusion after treatment with flow diverters: a systematic literature review. *J Neurointerv Surg*. 2024;16(5):482-490. doi:10.1136/jnis-2022-019993

141. Huang C, Lei X, Feng X, et al. Risk Factors for Incomplete Occlusion in Patients with Small Intracranial Aneurysms (<7 mm) after Flow-Diversion Treatment: A Multicenter Experience. *Cerebrovasc Dis*. Published online March 3, 2025:1-8. doi:10.1159/000544991

142. Su T, Reymond P, Brina O, et al. Large Neck and Strong Ostium Inflow as the Potential Causes for Delayed Occlusion of Unruptured Sidewall Intracranial Aneurysms Treated by Flow Diverter. *AJNR Am J Neuroradiol*. 2020;41(3):488-494. doi:10.3174/ajnr.A6413

143. Salem MM, Sweid A, Kuhn AL, et al. Repeat Flow Diversion for Cerebral Aneurysms Failing Prior Flow Diversion: Safety and Feasibility From Multicenter Experience. *Stroke*. 2022;53(4):1178-1189. doi:10.1161/STROKEAHA.120.033555

144. Gory B, Berge J, Bonafé A, et al. Flow Diverters for Intracranial Aneurysms: The DIVERSION National Prospective Cohort Study. *Stroke*. 2019;50(12):3471-3480. doi:10.1161/STROKEAHA.119.024722

145. Weinberg JH, Gruber M, Ritchey N, et al. Evolving treatment paradigms of cerebral aneurysm stasis in flow diversion. *J Clin Neurosci*. 2025;132:110996. doi:10.1016/j.jocn.2024.110996

146. Kaiser DPO, Boulouis G, Soize S, et al. Flow Diversion for ICA Aneurysms with Compressive Neuro-Ophthalmologic Symptoms: Predictors of Morbidity, Mortality, and Incomplete Aneurysm Occlusion. *AJNR Am J Neuroradiol*. 2022;43(7):998-1003. doi:10.3174/ajnr.A7550

147. Cebral J, Ollikainen E, Chung BJ, et al. Flow Conditions in the Intracranial Aneurysm Lumen Are Associated with Inflammation and Degenerative Changes of the Aneurysm Wall. *AJNR Am J Neuroradiol*. 2017;38(1):119-126. doi:10.3174/ajnr.A4951

License CC BY-NC-ND 4.0

148. Paliwal N, Damiano RJ, Davies JM, Siddiqui AH, Meng H. Association between hemodynamic modifications and clinical outcome of intracranial aneurysms treated using flow diverters. *Proc SPIE Int Soc Opt Eng*. 2017;10135:101352F. doi:10.1117/12.2254584

149. Sein ME, Ceciliano A, Navarro F, et al. Flow diverter with or without adjunctive coils in the treatment of large and giant intracranial aneurysms: a meta-analysis. *Neurosurg Rev*. 2025;48(1):519. doi:10.1007/s10143-025-03675-y

150. Turowski B, Macht S, Kulcsár Z, Hänggi D, Stummer W. Early fatal hemorrhage after endovascular cerebral aneurysm treatment with a flow diverter (SILK-Stent): do we need to rethink our concepts? *Neuroradiology*. 2011;53(1):37-41. doi:10.1007/s00234-010-0676-7

151. Cruz JP, Chow M, O'Kelly C, et al. Delayed ipsilateral parenchymal hemorrhage following flow diversion for the treatment of anterior circulation aneurysms. *AJNR Am J Neuroradiol*. 2012;33(4):603-608. doi:10.3174/ajnr.A3065

152. Adolph R, Vorp DA, Steed DL, Webster MW, Kameneva MV, Watkins SC. Cellular content and permeability of intraluminal thrombus in abdominal aortic aneurysm. *J Vasc Surg*. 1997;25(5):916-926. doi:10.1016/s0741-5214(97)70223-4

153. Carrell TWG, Burnand KG, Booth NA, Humphries J, Smith A. Intraluminal thrombus enhances proteolysis in abdominal aortic aneurysms. *Vascular*. 2006;14(1):9-16. doi:10.2310/6670.2006.00008

154. Zhou G, Su M, Yin YL, Li MH. Complications associated with the use of flow-diverting devices for cerebral aneurysms: a systematic review and meta-analysis. *Neurosurg Focus*. 2017;42(6):E17. doi:10.3171/2017.3.FOCUS16450

155. Benaissa A, Tomas C, Clarençon F, et al. Retrospective Analysis of Delayed Intraparenchymal Hemorrhage after Flow-Diverter Treatment: Presentation of a Retrospective Multicenter Trial. *AJNR Am J Neuroradiol*. 2016;37(3):475-480. doi:10.3174/ajnr.A4561

156. Rouchaud A, Brinjikji W, Lanzino G, Cloft HJ, Kadirvel R, Kallmes DF. Delayed hemorrhagic complications after flow diversion for intracranial aneurysms: a literature overview. *Neuroradiology*. 2016;58(2):171-177. doi:10.1007/s00234-015-1615-4

157. Fiorella D, Sadasivan C, Woo HH, Lieber B. Regarding "Aneurysm rupture following treatment with flow-diverting stents: computational hemodynamics analysis of treatment." *AJNR Am J Neuroradiol*. 2011;32(5):E95-97; author reply E98-100. doi:10.3174/ajnr.A2534

158. Eker OF, Boudjeltia KZ, Jerez RAC, et al. MR derived volumetric flow rate waveforms of internal carotid artery in patients treated for unruptured intracranial aneurysms by flow diversion technique. *J Cereb Blood Flow Metab*. 2015;35(12):2070-2079. doi:10.1038/jcbfm.2015.176

159. Kolumam Parameswaran P, Dai D, Ding YH, et al. Downstream vascular changes after flow-diverting device deployment in a rabbit model. *J Neurointerv Surg*. 2019;11(5):523-527. doi:10.1136/neurintsurg-2018-014123

160. Tomas C, Benaissa A, Herbreteau D, Kadziolka K, Pierot L. Delayed ipsilateral parenchymal hemorrhage following treatment of intracranial aneurysms with flow diverter. *Neuroradiology*. 2014;56(2):155-161. doi:10.1007/s00234-013-1302-2

161. Hu YC, Deshmukh VR, Albuquerque FC, et al. Histopathological assessment of fatal ipsilateral intraparenchymal hemorrhages after the treatment of supraclinoid aneurysms with

License CC BY-NC-ND 4.0

the Pipeline Embolization Device. *J Neurosurg*. 2014;120(2):365-374. doi:10.3171/2013.11.JNS131599

162. Liu J, Cao F, Zhenmei N, et al. Flow-diverter stents in intracranial aneurysm treatment: impact on covered cerebral artery branches. *Int J Surg*. 2024;110(1):53-65. doi:10.1097/JS9.0000000000000762

163. Hu P, Qian Y, Zhang Y, et al. Blood flow reduction of covered small side branches after flow diverter treatment: a computational fluid hemodynamic quantitative analysis. *J Biomech*. 2015;48(6):895-898. doi:10.1016/j.jbiomech.2015.02.015

164. Yamada NK, Cross DT, Pilgram TK, Moran CJ, Derdeyn CP, Dacey RG. Effect of antiplatelet therapy on thromboembolic complications of elective coil embolization of cerebral aneurysms. *AJNR Am J Neuroradiol*. 2007;28(9):1778-1782. doi:10.3174/ajnr.A0641

165. Hohenstatt S, Vollherbst DF, Nguyen TN, et al. The SAFEST Study: Survey on Antiplatelets in Flow Diversion for Aneurysm Endovascular Treatment. *Stroke: Vascular and Interventional Neurology*. 2024;4(6):e001464. doi:10.1161/SVIN.124.001464

166. Jang KM, Jang JS, Choi H, Cho YD. Safety and efficacy of tailored antiplatelet therapy using prasugrel or ticagrelor based on clopidogrel responsiveness in endovascular treatment for intracranial aneurysms: a meta-analysis. *J Neurointerv Surg*. 2024;16(10):1013-1020. doi:10.1136/jnis-2023-020548

167. Enomoto Y, Matsubara H, Ishihara T, et al. Optimal duration of dual antiplatelet therapy for stent-assisted coiling or flow diverter placement. *Journal of NeuroInterventional Surgery*. 2024;16(5):491-498. doi:10.1136/jnis-2023-020285

168. Senol YC, Orscelik A, Ghozy S, et al. The safety profile of single antiplatelet therapy with flow diverters: Systematic review and meta-analysis. *Interv Neuroradiol*. Published online April 18, 2023:15910199231168669. doi:10.1177/15910199231168669

169. Pierot L, Lamin S, Cognard C, Spelle L. E-118 COATING study: a RCT evaluating the coated flow diverter P64-MW-HPC. *Journal of NeuroInterventional Surgery*. 2022;14(Suppl 1):A140-A140. doi:10.1136/neurintsurg-2022-SNIS.229

170. Pierot L, Lamin S, Barreau X, et al. Coating (Coating to Optimize Aneurysm Treatment in the New Flow Diverter Generation) study. The first randomized controlled trial evaluating a coated flow diverter (p64 MW HPC): study design. *Journal of NeuroInterventional Surgery*. 2023;15(7):684-688. doi:10.1136/neurintsurg-2022-018969

171. Forestier G, Cortese J, Bardet SM, et al. Comparison of arterial wall integration of different flow diverters in rabbits: The CICAFLOW study. *Journal of Neuroradiology*. 2024;51(3):236-241. doi:10.1016/j.neurad.2023.08.005

172. Zoppo CT, Mocco J, Manning NW, Bogdanov AA, Gounis MJ. Surface modification of neurovascular stents: from bench to patient. *Journal of NeuroInterventional Surgery*. 2024;16(9):908-913. doi:10.1136/jnis-2023-020620

173. Marosfoi M, Clarencon F, Langan ET, et al. Acute thrombus formation on phosphorilcholine surface modified flow diverters. *J Neurointerv Surg*. 2018;10(4):406-411. doi:10.1136/neurintsurg-2017-013175

License CC BY-NC-ND 4.0

174. Starke RM, Thompson J, Pagani A, et al. Preclinical safety and efficacy evaluation of the Pipeline Vantage Embolization Device with Shield Technology. *J Neurointerv Surg*. 2020;12(10):981-986. doi:10.1136/neurintsurg-2020-016043

175. Caroff J, Tamura T, King RM, et al. Phosphorylcholine surface modified flow diverter associated with reduced intimal hyperplasia. *J Neurointerv Surg*. 2018;10(11):1097-1101. doi:10.1136/neurintsurg-2018-013776

176. Yoshizawa K, Kobayashi H, Kaneki A, et al. Poly(2-methoxyethyl acrylate) (PMEA) improves the thromboresistance of FRED flow diverters: a thrombogenic evaluation of flow diverters with human blood under flow conditions. *J Neurointerv Surg*. 2023;15(10):1001-1006. doi:10.1136/jnis-2022-019248

177. Lenz-Habijan T, Bhogal P, Peters M, et al. Hydrophilic Stent Coating Inhibits Platelet Adhesion on Stent Surfaces: Initial Results In Vitro. *Cardiovasc Intervent Radiol*. 2018;41(11):1779-1785. doi:10.1007/s00270-018-2036-7

178. Lenz-Habijan T, Brodde M, Kehrel BE, et al. Comparison of the Thrombogenicity of a Bare and Antithrombogenic Coated Flow Diverter in an In Vitro Flow Model. *Cardiovasc Intervent Radiol*. 2020;43(1):140-146. doi:10.1007/s00270-019-02307-5

179. Ma L, Hoz SS, Al-Bayati AR, Nogueira RG, Lang MJ, Gross BA. Flow Diverters with Surface Modification in Patients with Intracranial Aneurysms: A Systematic Review and Meta-Analysis. *World Neurosurgery*. 2024;185:320-326.e17. doi:10.1016/j.wneu.2023.12.132

180. Gott VL, Whiffen JD, Dutton RC. HEPARIN BONDING ON COLLOIDAL GRAPHITE SURFACES. *Science*. 1963;142(3597):1297-1298. doi:10.1126/science.142.3597.1297

181. Biran R, Pond D. Heparin coatings for improving blood compatibility of medical devices. *Adv Drug Deliv Rev*. 2017;112:12-23. doi:10.1016/j.addr.2016.12.002

182. Stenach N, Korn RL, Fisher CA, Jeevanandam V, Addonizio VP. The effects of heparin bound surface modification (Carmeda Bioactive Surface) on human platelet alterations during simulated extracorporeal circulation. *J Extra Corpor Technol*. 1992;24(3):97-102.

183. Weber N, Wendel HP, Ziemer G. Hemocompatibility of heparin-coated surfaces and the role of selective plasma protein adsorption. *Biomaterials*. 2002;23(2):429-439. doi:10.1016/s0142-9612(01)00122-3

184. Mehran R, Nikolsky E, Camenzind E, et al. An Internet-based registry examining the efficacy of heparin coating in patients undergoing coronary stent implantation. *Am Heart J*. 2005;150(6):1171-1176. doi:10.1016/j.ahj.2005.01.027

185. Gupta V, Aravamuthan BR, Baskerville S, et al. Reduction of subacute stent thrombosis (SAT) using heparin-coated stents in a large-scale, real world registry. *J Invasive Cardiol*. 2004;16(6):304-310.

186. Marosfoi M, Langan ET, Strittmatter L, et al. In situ tissue engineering: endothelial growth patterns as a function of flow diverter design. *J Neurointerv Surg*. 2017;9(10):994-998. doi:10.1136/neurintsurg-2016-012669

187. Granada JF, Inami S, Aboodi MS, et al. Development of a novel prohealing stent designed to deliver sirolimus from a biodegradable abluminal matrix. *Circ Cardiovasc Interv*. 2010;3(3):257-266. doi:10.1161/CIRCINTERVENTIONS.109.919936

License CC BY-NC-ND 4.0

188. Cortese J, Rasser C, Even G, et al. CD31 Mimetic Coating Enhances Flow Diverting Stent Integration into the Arterial Wall Promoting Aneurysm Healing. *Stroke*. 2021;52(2):677-686. doi:10.1161/STROKEAHA.120.030624

189. Kang Y, Hashimoto N, Kikuchi H, Yamazoe N, Hazama F. Effects of blood coagulation factor XIII on the development of experimental cerebral aneurysms in rats. *J Neurosurg*. 1990;73(2):242-247. doi:10.3171/jns.1990.73.2.0242

190. Futami K, Yamashita J, Tachibana O, et al. Basic fibroblast growth factor may repair experimental cerebral aneurysms in rats. *Stroke*. 1995;26(9):1649-1654. doi:10.1161/01.str.26.9.1649

191. Sadamasa N, Nozaki K, Hashimoto N. Disruption of gene for inducible nitric oxide synthase reduces progression of cerebral aneurysms. *Stroke*. 2003;34(12):2980-2984. doi:10.1161/01.STR.0000102556.55600.3B

192. Moriwaki T, Takagi Y, Sadamasa N, Aoki T, Nozaki K, Hashimoto N. Impaired progression of cerebral aneurysms in interleukin-1beta-deficient mice. *Stroke*. 2006;37(3):900-905. doi:10.1161/01.STR.0000204028.39783.d9

193. Szatmáry Z, Bardet SM, Mounier J, et al. Fucoidan-coated coils improve healing in a rabbit elastase aneurysm model. *J Neurointerv Surg*. 2024;16(8):824-829. doi:10.1136/jnis-2023-020596

194. Jamous MA, Nagahiro S, Kitazato KT, Tamura T, Kuwayama K, Satoh K. Role of estrogen deficiency in the formation and progression of cerebral aneurysms. Part II: experimental study of the effects of hormone replacement therapy in rats. *J Neurosurg*. 2005;103(6):1052-1057. doi:10.3171/jns.2005.103.6.1052

195. Tamura T, Jamous MA, Kitazato KT, et al. Endothelial damage due to impaired nitric oxide bioavailability triggers cerebral aneurysm formation in female rats. *J Hypertens*. 2009;27(6):1284-1292. doi:10.1097/HJH.0b013e328329d1a7

196. Fukuda S, Hashimoto N, Naritomi H, et al. Prevention of rat cerebral aneurysm formation by inhibition of nitric oxide synthase. *Circulation*. 2000;101(21):2532-2538. doi:10.1161/01.cir.101.21.2532

197. Sadamasa N, Nozaki K, Takagi Y, et al. Cerebral aneurysm progression suppressed by blockage of endothelin B receptor. *J Neurosurg*. 2007;106(2):330-336. doi:10.3171/jns.2007.106.2.330

198. Aoki T, Kataoka H, Ishibashi R, Nozaki K, Hashimoto N. Simvastatin suppresses the progression of experimentally induced cerebral aneurysms in rats. *Stroke*. 2008;39(4):1276-1285. doi:10.1161/STROKEAHA.107.503086

199. Tada Y, Kitazato KT, Yagi K, et al. Statins promote the growth of experimentally induced cerebral aneurysms in estrogen-deficient rats. *Stroke*. 2011;42(8):2286-2293. doi:10.1161/STROKEAHA.110.608034

200. Kimura N, Shimizu H, Eldawoody H, et al. Effect of olmesartan and pravastatin on experimental cerebral aneurysms in rats. *Brain Res*. 2010;1322:144-152. doi:10.1016/j.brainres.2010.01.044

License CC BY-NC-ND 4.0

201. Marbacher S, Schläppi JA, Fung C, Hüsler J, Beck J, Raabe A. Do statins reduce the risk of aneurysm development? A case-control study. *J Neurosurg*. 2012;116(3):638-642. doi:10.3171/2011.10.JNS11153

202. Yoshimura Y, Murakami Y, Saitoh M, et al. Statin use and risk of cerebral aneurysm rupture: a hospital-based case-control study in Japan. *J Stroke Cerebrovasc Dis*. 2014;23(2):343-348. doi:10.1016/j.jstrokecerebrovasdis.2013.04.022

203. Chalouhi N, Hoh BL, Hasan D. Review of cerebral aneurysm formation, growth, and rupture. *Stroke*. 2013;44(12):3613-3622. doi:10.1161/STROKEAHA.113.002390

204. Aoki T, Kataoka H, Shimamura M, et al. NF-kappaB is a key mediator of cerebral aneurysm formation. *Circulation*. 2007;116(24):2830-2840. doi:10.1161/CIRCULATIONAHA.107.728303

205. Aoki T, Kataoka H, Ishibashi R, Nozaki K, Morishita R, Hashimoto N. Reduced collagen biosynthesis is the hallmark of cerebral aneurysm: contribution of interleukin-1beta and nuclear factor-kappaB. *Arterioscler Thromb Vasc Biol*. 2009;29(7):1080-1086. doi:10.1161/ATVBAHA.108.180760

206. Aoki T, Kataoka H, Ishibashi R, Nozaki K, Hashimoto N. Nifedipine inhibits the progression of an experimentally induced cerebral aneurysm in rats with associated down-regulation of NF-kappa B transcriptional activity. *Curr Neurovasc Res*. 2008;5(1):37-45. doi:10.2174/156720208783565663

207. Aoki T, Kataoka H, Nishimura M, Ishibashi R, Morishita R, Miyamoto S. Ets-1 promotes the progression of cerebral aneurysm by inducing the expression of MCP-1 in vascular smooth muscle cells. *Gene Ther*. 2010;17(9):1117-1123. doi:10.1038/gt.2010.60

208. Aoki T, Kataoka H, Ishibashi R, Nozaki K, Egashira K, Hashimoto N. Impact of monocyte chemoattractant protein-1 deficiency on cerebral aneurysm formation. *Stroke*. 2009;40(3):942-951. doi:10.1161/STROKEAHA.108.532556

209. Yagi K, Tada Y, Kitazato KT, Tamura T, Satomi J, Nagahiro S. Ibudilast inhibits cerebral aneurysms by down-regulating inflammation-related molecules in the vascular wall of rats. *Neurosurgery*. 2010;66(3):551-559; discussion 559. doi:10.1227/01.NEU.0000365771.89576.77

210. Ishibashi R, Aoki T, Nishimura M, Hashimoto N, Miyamoto S. Contribution of mast cells to cerebral aneurysm formation. *Curr Neurovasc Res*. 2010;7(2):113-124. doi:10.2174/156720210791184916

211. Kanematsu Y, Kanematsu M, Kurihara C, et al. Critical roles of macrophages in the formation of intracranial aneurysm. *Stroke*. 2011;42(1):173-178. doi:10.1161/STROKEAHA.110.590976

212. Hasan DM, Mahaney KB, Brown RD, et al. Aspirin as a promising agent for decreasing incidence of cerebral aneurysm rupture. *Stroke*. 2011;42(11):3156-3162. doi:10.1161/STROKEAHA.111.619411

213. Tymianski M. Aspirin as a promising agent for decreasing incidence of cerebral aneurysm rupture. *Stroke*. 2011;42(11):3003-3004. doi:10.1161/STROKEAHA.111.626762

214. Aoki T, Nishimura M, Kataoka H, Ishibashi R, Nozaki K, Hashimoto N. Reactive oxygen species modulate growth of cerebral aneurysms: a study using the free radical scavenger

License CC BY-NC-ND 4.0

edaravone and p47phox(-/-) mice. *Lab Invest*. 2009;89(7):730-741. doi:10.1038/labinvest.2009.36

215. Tian XY, Wong WT, Xu A, et al. Rosuvastatin improves endothelial function in db/db mice: role of angiotensin II type 1 receptors and oxidative stress. *Br J Pharmacol*. 2011;164(2b):598-606. doi:10.1111/j.1476-5381.2011.01416.x

216. Aoki T, Kataoka H, Morimoto M, Nozaki K, Hashimoto N. Macrophage-derived matrix metalloproteinase-2 and -9 promote the progression of cerebral aneurysms in rats. *Stroke*. 2007;38(1):162-169. doi:10.1161/01.STR.0000252129.18605.c8

217. Aoki T, Kataoka H, Ishibashi R, Nozaki K, Hashimoto N. Cathepsin B, K, and S are expressed in cerebral aneurysms and promote the progression of cerebral aneurysms. *Stroke*. 2008;39(9):2603-2610. doi:10.1161/STROKEAHA.107.513648

218. Bouzeghrane F, Darsaut T, Salazkin I, Ogoudikpe C, Gevry G, Raymond J. Matrix metalloproteinase-9 may play a role in recanalization and recurrence after therapeutic embolization of aneurysms or arteries. *J Vasc Interv Radiol*. 2007;18(10):1271-1279. doi:10.1016/j.jvir.2007.06.034

219. Michos ED, McEvoy JW, Blumenthal RS. Lipid Management for the Prevention of Atherosclerotic Cardiovascular Disease. *New England Journal of Medicine*. 2019;381(16):1557-1567. doi:10.1056/NEJMra1806939

220. Maron DJ, Fazio S, Linton MF. Current perspectives on statins. *Circulation*. 2000;101(2):207-213. doi:10.1161/01.cir.101.2.207

221. Paparodis RD, Bantouna D, Livadas S, Angelopoulos N. Statin therapy in primary and secondary cardiovascular disease prevention. *Curr Atheroscler Rep*. 2024;27(1):21. doi:10.1007/s11883-024-01265-9

222. Chou R, Cantor A, Dana T, et al. Statin Use for the Primary Prevention of Cardiovascular Disease in Adults: Updated Evidence Report and Systematic Review for the US Preventive Services Task Force. *JAMA*. 2022;328(8):754-771. doi:10.1001/jama.2022.12138

223. Grundy SM, Stone NJ, Bailey AL, et al. 2018 AHA/ACC/AACVPR/AAPA/ABC/ACPM/ADA/AGS/APhA/ASPC/NLA/PCNA Guideline on the Management of Blood Cholesterol. *JACC*. 2019;73(24):e285-e350. doi:10.1016/j.jacc.2018.11.003

224. Azemawah V, Movahed MR, Centuori P, et al. State of the Art Comprehensive Review of Individual Statins, Their Differences, Pharmacology, and Clinical Implications. *Cardiovasc Drugs Ther*. 2019;33(5):625-639. doi:10.1007/s10557-019-06904-x

225. Oesterle A, Laufs U, Liao JK. Pleiotropic Effects of Statins on the Cardiovascular System. *Circ Res*. 2017;120(1):229-243. doi:10.1161/CIRCRESAHA.116.308537

226. Wasim R, Ansari TM, Ahsan F, et al. Pleiotropic Benefits of Statins in Cardiovascular Diseases. *Drug Res (Stuttg)*. 2022;72(9):477-486. doi:10.1055/a-1873-1978

227. Davignon J. Beneficial cardiovascular pleiotropic effects of statins. *Circulation*. 2004;109(23 Suppl 1):III39-43. doi:10.1161/01.CIR.0000131517.20177.5a

License CC BY-NC-ND 4.0

228. Liu JC, Lei SY, Zhang DH, et al. The pleiotropic effects of statins: a comprehensive exploration of neurovascular unit modulation and blood–brain barrier protection. *Molecular Medicine*. 2024;30(1):256. doi:10.1186/s10020-024-01025-0

229. Zhou Q, Liao JK. Statins and cardiovascular diseases: from cholesterol lowering to pleiotropy. *Curr Pharm Des*. 2009;15(5):467-478. doi:10.2174/138161209787315684

230. Zhou Q, Liao JK. Pleiotropic effects of statins. - Basic research and clinical perspectives -. *Circ J*. 2010;74(5):818-826. doi:10.1253/circj.cj-10-0110

231. Takemoto M, Liao JK. Pleiotropic effects of 3-hydroxy-3-methylglutaryl coenzyme a reductase inhibitors. *Arterioscler Thromb Vasc Biol*. 2001;21(11):1712-1719. doi:10.1161/hq1101.098486

232. Kayzuka C, Rondon-Pereira VC, Nogueira Tavares C, et al. Epigenetics is involved in the pleiotropic effects of statins. *Expert Opin Drug Metab Toxicol*. 2025;21(6):689-701. doi:10.1080/17425255.2025.2491732

233. Wood WG, Műller WE, Eckert GP. Statins and neuroprotection: basic pharmacology needed. *Mol Neurobiol*. 2014;50(1):214-220. doi:10.1007/s12035-014-8647-3

234. Ricci G, Ciccone MM, Giordano P, Cortese F. Statins: Pharmacokinetics, Pharmacodynamics and Cost-Effectiveness Analysis. *Curr Vasc Pharmacol*. 2019;17(3):213-221. doi:10.2174/1570161116666180706144824

235. Arnaboldi L, Corsini A. Do structural differences in statins correlate with clinical efficacy? *Curr Opin Lipidol*. 2010;21(4):298-304. doi:10.1097/MOL.0b013e32833b776c

236. Gauthier TW, Scalia R, Murohara T, Guo JP, Lefer AM. Nitric oxide protects against leukocyte-endothelium interactions in the early stages of hypercholesterolemia. *Arterioscler Thromb Vasc Biol*. 1995;15(10):1652-1659. doi:10.1161/01.atv.15.10.1652

237. Wei H, Fang L, Song J, Chatterjee S. Statin-inhibited endothelial permeability could be associated with its effect on PECAM-1 in endothelial cells. *FEBS Lett*. 2005;579(5):1272-1278. doi:10.1016/j.febslet.2005.01.020

238. Wójciak-Stothard B, Williams L, Ridley AJ. Monocyte adhesion and spreading on human endothelial cells is dependent on Rho-regulated receptor clustering. *J Cell Biol*. 1999;145(6):1293-1307. doi:10.1083/jcb.145.6.1293

239. Takemoto M, Sun J, Hiroki J, Shimokawa H, Liao JK. Rho-kinase mediates hypoxia-induced downregulation of endothelial nitric oxide synthase. *Circulation*. 2002;106(1):57-62. doi:10.1161/01.cir.0000020682.73694.ab

240. van der Heijden M, Versteilen AMG, Sipkema P, van Nieuw Amerongen GP, Musters RJP, Groeneveld ABJ. Rho-kinase-dependent F-actin rearrangement is involved in the inhibition of PI3-kinase/Akt during ischemia-reperfusion-induced endothelial cell apoptosis. *Apoptosis*. 2008;13(3):404-412. doi:10.1007/s10495-007-0173-6

241. Pelat M, Dessy C, Massion P, Desager JP, Feron O, Balligand JL. Rosuvastatin decreases caveolin-1 and improves nitric oxide-dependent heart rate and blood pressure variability in apolipoprotein E-/- mice in vivo. *Circulation*. 2003;107(19):2480-2486. doi:10.1161/01.CIR.0000065601.83526.3E

License CC BY-NC-ND 4.0

242. Sen-Banerjee S, Mir S, Lin Z, et al. Kruppel-like factor 2 as a novel mediator of statin effects in endothelial cells. *Circulation*. 2005;112(5):720-726. doi:10.1161/CIRCULATIONAHA.104.525774

243. Bu D xiu, Tarrio M, Grabie N, et al. Statin-induced Krüppel-like factor 2 expression in human and mouse T cells reduces inflammatory and pathogenic responses. *J Clin Invest*. 2010;120(6):1961-1970. doi:10.1172/JCI41384

244. Giannotti G, Doerries C, Mocharla PS, et al. Impaired endothelial repair capacity of early endothelial progenitor cells in prehypertension: relation to endothelial dysfunction. *Hypertension*. 2010;55(6):1389-1397. doi:10.1161/HYPERTENSIONAHA.109.141614

245. Vasa M, Fichtlscherer S, Adler K, et al. Increase in circulating endothelial progenitor cells by statin therapy in patients with stable coronary artery disease. *Circulation*. 2001;103(24):2885-2890. doi:10.1161/hc2401.092816

246. Weis M, Heeschen C, Glassford AJ, Cooke JP. Statins have biphasic effects on angiogenesis. *Circulation*. 2002;105(6):739-745. doi:10.1161/hc0602.103393

247. Koutouzis M, Nomikos A, Nikolidakis S, et al. Statin treated patients have reduced intraplaque angiogenesis in carotid endarterectomy specimens. *Atherosclerosis*. 2007;192(2):457-463. doi:10.1016/j.atherosclerosis.2007.01.035

248. Braun-Dullaeus RC, Mann MJ, Dzau VJ. Cell cycle progression: new therapeutic target for vascular proliferative disease. *Circulation*. 1998;98(1):82-89. doi:10.1161/01.cir.98.1.82

249. Kobashigawa JA, Katznelson S, Laks H, et al. Effect of pravastatin on outcomes after cardiac transplantation. *N Engl J Med*. 1995;333(10):621-627. doi:10.1056/NEJM199509073331003

250. Chen Z, Fukutomi T, Zago AC, et al. Simvastatin reduces neointimal thickening in low-density lipoprotein receptor-deficient mice after experimental angioplasty without changing plasma lipids. *Circulation*. 2002;106(1):20-23. doi:10.1161/01.cir.0000022843.76104.01

251. Chandrasekar B, Mummidi S, Mahimainathan L, et al. Interleukin-18-induced human coronary artery smooth muscle cell migration is dependent on NF-kappaB- and AP-1-mediated matrix metalloproteinase-9 expression and is inhibited by atorvastatin. *J Biol Chem*. 2006;281(22):15099-15109. doi:10.1074/jbc.M600200200

252. Li M, Liu Y, Dutt P, Fanburg BL, Toksoz D. Inhibition of serotonin-induced mitogenesis, migration, and ERK MAPK nuclear translocation in vascular smooth muscle cells by atorvastatin. *Am J Physiol Lung Cell Mol Physiol*. 2007;293(2):L463-471. doi:10.1152/ajplung.00133.2007

253. Aoki I, Aoki N, Kawano K, et al. Platelet-dependent thrombin generation in patients with hyperlipidemia. *J Am Coll Cardiol*. 1997;30(1):91-96. doi:10.1016/s0735-1097(97)00129-0

254. Laufs U, Gertz K, Huang P, et al. Atorvastatin upregulates type III nitric oxide synthase in thrombocytes, decreases platelet activation, and protects from cerebral ischemia in normocholesterolemic mice. *Stroke*. 2000;31(10):2442-2449. doi:10.1161/01.str.31.10.2442

255. Haramaki N, Ikeda H, Takenaka K, et al. Fluvastatin alters platelet aggregability in patients with hypercholesterolemia: possible improvement of intraplatelet redox imbalance via HMG-CoA reductase. *Arterioscler Thromb Vasc Biol*. 2007;27(6):1471-1477. doi:10.1161/ATVBAHA.106.128793

License CC BY-NC-ND 4.0

256. Ali FY, Armstrong PCJ, Dhanji ARA, et al. Antiplatelet actions of statins and fibrates are mediated by PPARs. *Arterioscler Thromb Vasc Biol*. 2009;29(5):706-711. doi:10.1161/ATVBAHA.108.183160

257. Pignatelli P, Carnevale R, Pastori D, et al. Immediate antioxidant and antiplatelet effect of atorvastatin via inhibition of Nox2. *Circulation*. 2012;126(1):92-103. doi:10.1161/CIRCULATIONAHA.112.095554

258. Glynn RJ, Danielson E, Fonseca FAH, et al. A randomized trial of rosuvastatin in the prevention of venous thromboembolism. *N Engl J Med*. 2009;360(18):1851-1861. doi:10.1056/NEJMoa0900241

259. Violi F, Calvieri C, Ferro D, Pignatelli P. Statins as Antithrombotic Drugs. *Circulation*. 2013;127(2):251-257. doi:10.1161/CIRCULATIONAHA.112.145334

260. Woźniak E, Broncel M, Niedzielski M, Woźniak A, Gorzelak-Pabiś P. The effect of lipid-lowering therapies on the pro-inflammatory and anti-inflammatory properties of vascular endothelial cells. *PLoS One*. 2023;18(2):e0280741. doi:10.1371/journal.pone.0280741

261. Mahalwar R, Khanna D. Pleiotropic antioxidant potential of rosuvastatin in preventing cardiovascular disorders. *Eur J Pharmacol*. 2013;711(1-3):57-62. doi:10.1016/j.ejphar.2013.04.025

262. Liu P, Liu Y, Li P, et al. Rosuvastatin- and Heparin-Loaded Poly(l-lactide- co-caprolactone) Nanofiber Aneurysm Stent Promotes Endothelialization via Vascular Endothelial Growth Factor Type A Modulation. *ACS Appl Mater Interfaces*. 2018;10(48):41012-41018. doi:10.1021/acsami.8b11714

263. Sheu JJ, Hsiao HY, Chung SY, et al. Endothelial progenitor cells, rosuvastatin and valsartan have a comparable effect on repair of balloon-denudated carotid artery injury. *Am J Transl Res*. 2019;11(3):1282-1298.

264. Liu P, An Q, Chen X, Huang J, Yang GY, Zhu W. Rosuvastatin for enhancement of aneurysm neck endothelialization after coil embolization: promotion of endothelial progenitor cells in a rodent model. *J Neurosurg*. 2016;124(5):1265-1274. doi:10.3171/2015.3.JNS142841

265. Lee CH, Chang SH, Lin YH, et al. Acceleration of re-endothelialization and inhibition of neointimal formation using hybrid biodegradable nanofibrous rosuvastatin-loaded stents. *Biomaterials*. 2014;35(15):4417-4427. doi:10.1016/j.biomaterials.2014.02.017

266. Shimizu K, Imamura H, Tani S, et al. Candidate drugs for preventive treatment of unruptured intracranial aneurysms: A cross-sectional study. *PLoS One*. 2021;16(2):e0246865. doi:10.1371/journal.pone.0246865

267. Li M, Yao Y, Liu J, Pang Y, Wu Q, Liu C. Effect of Statin Therapy Following Endovascular Treatment of Intracranial Aneurysms: A Meta-analysis. *Cerebrovasc Dis*. Published online July 24, 2025:1-20. doi:10.1159/000547504

268. Wolfrum S, Jensen KS, Liao JK. Endothelium-dependent effects of statins. *Arterioscler Thromb Vasc Biol*. 2003;23(5):729-736. doi:10.1161/01.ATV.0000063385.12476.A7

269. Martínez-González J, Badimon L. Influence of statin use on endothelial function: from bench to clinics. *Curr Pharm Des*. 2007;13(17):1771-1786. doi:10.2174/138161207780831220

270. Ii M, Losordo DW. Statins and the endothelium. *Vascul Pharmacol*. 2007;46(1):1-9. doi:10.1016/j.vph.2006.06.012

License CC BY-NC-ND 4.0

271. Khaidakov M, Wang W, Khan JA, Kang BY, Hermonat PL, Mehta JL. Statins and angiogenesis: is it about connections? *Biochem Biophys Res Commun*. 2009;387(3):543-547. doi:10.1016/j.bbrc.2009.07.057

272. Meyer N, Brodowski L, Richter K, von Kaisenberg CS, Schröder-Heurich B, von Versen-Höynck F. Pravastatin Promotes Endothelial Colony-Forming Cell Function, Angiogenic Signaling and Protein Expression In Vitro. *J Clin Med*. 2021;10(2):183. doi:10.3390/jcm10020183

273. Margaritis M, Channon KM, Antoniades C. Statins as regulators of redox state in the vascular endothelium: beyond lipid lowering. *Antioxid Redox Signal*. 2014;20(8):1198-1215. doi:10.1089/ars.2013.5430

274. Rawlings R, Nohria A, Liu PY, et al. Comparison of effects of rosuvastatin (10 mg) versus atorvastatin (40 mg) on rho kinase activity in caucasian men with a previous atherosclerotic event. *Am J Cardiol*. 2009;103(4):437-441. doi:10.1016/j.amjcard.2008.10.008

275. Thondapu V, Kurihara O, Yonetsu T, et al. Comparison of Rosuvastatin Versus Atorvastatin for Coronary Plaque Stabilization. *Am J Cardiol*. 2019;123(10):1565-1571. doi:10.1016/j.amjcard.2019.02.019

276. Schroeter MR, Humboldt T, Schäfer K, Konstantinides S. Rosuvastatin reduces atherosclerotic lesions and promotes progenitor cell mobilisation and recruitment in apolipoprotein E knockout mice. *Atherosclerosis*. 2009;205(1):63-73. doi:10.1016/j.atherosclerosis.2008.11.013

277. Lin PY, Lee FY, Wallace CG, et al. The therapeutic effect of rosuvastatin and propylthiouracil on ameliorating high-cholesterol diet-induced rabbit aortic atherosclerosis and stiffness. *Int J Cardiol*. 2017;227:938-949. doi:10.1016/j.ijcard.2016.09.040

278. Li Z, Wang L, Hu X, et al. Effect of rosuvastatin on atherosclerotic plaque stability: An intravascular ultrasound elastography study. *Atherosclerosis*. 2016;248:27-35. doi:10.1016/j.atherosclerosis.2016.02.028

279. Li Z, Lian H, Liang Q, Zeng F, Zheng D. Effects of rosuvastatin combined with fasudil therapy on rabbits with dyslipidemia. *Lipids Health Dis*. 2015;14:52. doi:10.1186/s12944-015-0050-1

280. Chen L, Wang C, Wu Y. Cholesterol (Blood lipid) lowering potential of Rosuvastatin chitosan nanoparticles for atherosclerosis: Preclinical study in rabbit model. *Acta Biochim Pol*. 2020;67(4):495-499. doi:10.18388/abp.2020_5186

281. Tziakas D, Chalikias G, Kapelouzou A, et al. Erythrocyte membrane cholesterol and lipid core growth in a rabbit model of atherosclerosis: modulatory effects of rosuvastatin. *Int J Cardiol*. 2013;170(2):173-181. doi:10.1016/j.ijcard.2013.10.070

282. D'Annunzio V, Donato M, Erni L, et al. Rosuvastatin given during reperfusion decreases infarct size and inhibits matrix metalloproteinase-2 activity in normocholesterolemic and hypercholesterolemic rabbits. *J Cardiovasc Pharmacol*. 2009;53(2):137-144. doi:10.1097/FJC.0b013e318197c5e9

283. Khan SU, Lone AN, Kleiman NS, et al. Aspirin With or Without Statin in Individuals Without Atherosclerotic Cardiovascular Disease Across Risk Categories. *JACC: Advances*. 2023;2(2):100197. doi:10.1016/j.jacadv.2022.100197

License CC BY-NC-ND 4.0

284. Tirnaksiz E, Pamukcu B, Oflaz H, Nisanci Y. Effect of high dose statin therapy on platelet function; statins reduce aspirin-resistant platelet aggregation in patients with coronary heart disease. *J Thromb Thrombolysis*. 2009;27(1):24-28. doi:10.1007/s11239-007-0154-1

285. Deng T, He W, Yao X, et al. Safety and efficacy of short-term dual antiplatelet therapy combined with intensive rosuvastatin in acute ischemic stroke. *Clinics (Sao Paulo)*. 2023;78. doi:10.1016/j.clinsp.2023.100171

286. Osborne-Pellegrin MJ, Coutard M, Poitevin P, Michel JB, Levy BI. Induction of aneurysms in the rat by a stenosing cotton ligature around the inter-renal aorta. *Int J Exp Pathol*. 1994;75(3):179-190.

287. Brinjikji W, Ding YH, Kallmes DF, Kadirvel R. From bench to bedside: utility of the rabbit elastase aneurysm model in preclinical studies of intracranial aneurysm treatment. *J Neurointerv Surg*. 2016;8(5):521-525. doi:10.1136/neurintsurg-2015-011704

288. Bouzeghrane F, Naggara O, Kallmes DF, Berenstein A, Raymond J, International Consortium of Neuroendovascular Centres. In vivo experimental intracranial aneurysm models: a systematic review. *AJNR Am J Neuroradiol*. 2010;31(3):418-423. doi:10.3174/ajnr.A1853

289. Nagata I, Handa H, Hashimoto N, Hazama F. Experimentally induced cerebral aneurysms in rats: Part VI. Hypertension. *Surg Neurol*. 1980;14(6):477-479.

290. Hashimoto N, Handa H, Nagata I, Hazama F. Animal model of cerebral aneurysms: pathology and pathogenesis of induced cerebral aneurysms in rats. *Neurol Res*. 1984;6(1-2):33-40. doi:10.1080/01616412.1984.11739661

291. Morimoto M, Miyamoto S, Mizoguchi A, Kume N, Kita T, Hashimoto N. Mouse model of cerebral aneurysm: experimental induction by renal hypertension and local hemodynamic changes. *Stroke*. 2002;33(7):1911-1915. doi:10.1161/01.str.0000021000.19637.3d

292. Zhu YQ, Dai DY, Xing HX, Ding YH, Kadirvel R, Kallmes DF. Concomitant aneurysm detection in an intracranial dolichoectasia mouse model using a MicroFil polymer perfusion technique. *J Neurointerv Surg*. 2017;9(8):783-786. doi:10.1136/neurintsurg-2016-012469

293. Chu Y, Wilson K, Gu H, et al. Myeloperoxidase is increased in human cerebral aneurysms and increases formation and rupture of cerebral aneurysms in mice. *Stroke*. 2015;46(6):1651-1656. doi:10.1161/STROKEAHA.114.008589

294. Rouchaud A, Journé C, Louedec L, et al. Autologous mesenchymal stem cell endografting in experimental cerebrovascular aneurysms. *Neuroradiology*. 2013;55(6):741-749. doi:10.1007/s00234-013-1167-4

295. Altes TA, Cloft HJ, Short JG, et al. 1999 ARRS Executive Council Award. Creation of saccular aneurysms in the rabbit: a model suitable for testing endovascular devices. American Roentgen Ray Society. *AJR Am J Roentgenol*. 2000;174(2):349-354. doi:10.2214/ajr.174.2.1740349

296. Krings T, Möller-Hartmann W, Hans FJ, et al. A refined method for creating saccular aneurysms in the rabbit. *Neuroradiology*. 2003;45(7):423-429. doi:10.1007/s00234-003-0976-2

License CC BY-NC-ND 4.0

297. Anidjar S, Salzmann JL, Gentric D, Lagneau P, Camilleri JP, Michel JB. Elastase-induced experimental aneurysms in rats. *Circulation*. 1990;82(3):973-981. doi:10.1161/01.cir.82.3.973

298. Sarda-Mantel L, Coutard M, Rouzet F, et al. 99mTc-annexin-V functional imaging of luminal thrombus activity in abdominal aortic aneurysms. *Arterioscler Thromb Vasc Biol*. 2006;26(9):2153-2159. doi:10.1161/01.ATV.0000237605.25666.13

299. Abruzzo T, Shengelaia GG, Dawson RC, Owens DS, Cawley CM, Gravanis MB. Histologic and morphologic comparison of experimental aneurysms with human intracranial aneurysms. *AJNR Am J Neuroradiol*. 1998;19(7):1309-1314.

300. Zhou J, Cheng M, Liao YH, et al. Rosuvastatin enhances angiogenesis via eNOS-dependent mobilization of endothelial progenitor cells. *PLoS One*. 2013;8(5):e63126. doi:10.1371/journal.pone.0063126

301. Li S, Wang D, Tian Y, et al. Aspirin Inhibits Degenerative Changes of Aneurysmal Wall in a Rat Model. *Neurochem Res*. 2015;40(7):1537-1545. doi:10.1007/s11064-015-1603-4

302. Suzuki T, Kamio Y, Makino H, et al. Prevention Effect of Antiplatelets on Aneurysm Rupture in a Mouse Intracranial Aneurysm Model. *Cerebrovasc Dis*. 2018;45(3-4):180-186. doi:10.1159/000487812

303. Khan SI, Shihata WA, Andrews KL, et al. Effects of high- and low-dose aspirin on adaptive immunity and hypertension in the stroke-prone spontaneously hypertensive rat. *FASEB J*. 2019;33(1):1510-1521. doi:10.1096/fj.201701498RR

304. Liu Q, Dong S, Zhou X, et al. Effects of Long-Term Intervention with Losartan, Aspirin and Atorvastatin on Vascular Remodeling in Juvenile Spontaneously Hypertensive Rats. *Molecules*. 2023;28(4):1844. doi:10.3390/molecules28041844

305. Wanderer S, Grüter BE, Strange F, et al. Aspirin treatment prevents inflammation in experimental bifurcation aneurysms in New Zealand White rabbits. *J Neurointerv Surg*. 2022;14(2):189-195. doi:10.1136/neurintsurg-2020-017261

306. Joshi MD, O'Kelly CJ, Krings T, Fiorella D, Marotta TR. Observer variability of an angiographic grading scale used for the assessment of intracranial aneurysms treated with flow-diverting stents. *AJNR Am J Neuroradiol*. 2013;34(8):1589-1592. doi:10.3174/ajnr.A3431

307. Miyazaki A, Nishio M, Fujita A, et al. Predicting the O'Kelly-Marotta scale score after flow-diverter stent placement using silent MRA. *Jpn J Radiol*. 2024;42(12):1403-1412. doi:10.1007/s11604-024-01632-1

308. Ughi GJ, Marosfoi MG, King RM, et al. A neurovascular high-frequency optical coherence tomography system enables in situ cerebrovascular volumetric microscopy. *Nat Commun*. 2020;11(1):3851. doi:10.1038/s41467-020-17702-7

309. King RM, Peker A, Anagnostakou V, et al. High-frequency optical coherence tomography predictors of aneurysm occlusion following flow diverter treatment in a preclinical model. *J Neurointerv Surg*. 2023;15(9):919-923. doi:10.1136/jnis-2022-019275

310. Gutiérrez-Baños J de J, Castillo-Rangel C, Rodriguez-Pereira MI, et al. Early experience using optical coherence tomography for intraluminal evaluation of vascular healing associated with endovascular treatment of intracranial aneurysms. *J Neurosurg*. 2025;143(3):668-677. doi:10.3171/2025.1.JNS242458

License CC BY-NC-ND 4.0

311. Verhaegen C, Kautbally S, Zapareto DC, et al. Early thrombogenicity of coronary stents: comparison of bioresorbable polymer sirolimus-eluting and bare metal stents in an aortic rat model. *Am J Cardiovasc Dis*. 2020;10(2):72-83.

312. Bardet SM, Cortese J, Blanc R, Mounayer C, Rouchaud A. Multiphoton microscopy for pre-clinical evaluation of flow-diverter stents for treating aneurysms. *J Neuroradiol*. 2021;48(3):200-206. doi:10.1016/j.neurad.2020.03.005

313. Bai X, Wang XP, He GD, et al. Simultaneous Determination of Rosuvastatin, Rosuvastatin-5 S-lactone, and N-desmethyl Rosuvastatin in Human Plasma by UPLC-MS/MS and Its Application to Clinical Study. *Drug Res (Stuttg)*. 2018;68(6):328-334. doi:10.1055/s-0043-123576

314. Macwan JS, Ionita IA, Akhlaghi F. A simple assay for the simultaneous determination of rosuvastatin acid, rosuvastatin-5S-lactone, and N-desmethyl rosuvastatin in human plasma using liquid chromatography-tandem mass spectrometry (LC-MS/MS). *Anal Bioanal Chem*. 2012;402(3):1217-1227. doi:10.1007/s00216-011-5548-4

315. Lee HK, Ho CS, Hu M, Tomlinson B, Wong CK. Development and validation of a sensitive method for simultaneous determination of rosuvastatin and N-desmethyl rosuvastatin in human plasma using liquid chromatography/negative electrospray ionization/tandem mass spectrometry. *Biomed Chromatogr*. 2013;27(11):1369-1374. doi:10.1002/bmc.2944

316. Lan K, Jiang X, Li Y, et al. Quantitative determination of rosuvastatin in human plasma by ion pair liquid-liquid extraction using liquid chromatography with electrospray ionization tandem mass spectrometry. *J Pharm Biomed Anal*. 2007;44(2):540-546. doi:10.1016/j.jpba.2006.12.022

317. O'kelly CJ, Krings T, Fiorella D, Marotta TR. A novel grading scale for the angiographic assessment of intracranial aneurysms treated using flow diverting stents. *Interv Neuroradiol*. 2010;16(2):133-137. doi:10.1177/159101991001600204

318. Chiang KH, Cheng WL, Shih CM, et al. Statins, HMG-CoA Reductase Inhibitors, Improve Neovascularization by Increasing the Expression Density of CXCR4 in Endothelial Progenitor Cells. *PLoS One*. 2015;10(8):e0136405. doi:10.1371/journal.pone.0136405

319. Salih M, Young M, Filo J, Shutran M, Taussky P, Ogilvy CS. Effect of Statin on Radiographic and Clinical Outcomes of Intracranial Aneurysms Treated With Pipeline Embolization: A Propensity Score-Matched Analysis. *Neurosurgery*. 2023;93(5):1000-1006. doi:10.1227/neu.0000000000002522

320. Zeng Z, Kallmes DF, Durka MJ, et al. Hemodynamics and anatomy of elastase-induced rabbit aneurysm models: similarity to human cerebral aneurysms? *AJNR Am J Neuroradiol*. 2011;32(3):595-601. doi:10.3174/ajnr.A2324

321. Enomoto S, Sata M, Fukuda D, Nakamura K, Nagai R. Rosuvastatin prevents endothelial cell death and reduces atherosclerotic lesion formation in ApoE-deficient mice. *Biomed Pharmacother*. 2009;63(1):19-26. doi:10.1016/j.biopha.2007.11.002

322. Landsberger M, Jantzen F, Könemann S, Felix SB. Blockade of geranylgeranylation by rosuvastatin upregulates eNOS expression in human venous endothelial cells. *Biochem Biophys Res Commun*. 2005;336(4):1005-1009. doi:10.1016/j.bbrc.2005.08.225

323. Ma Y, Madjidyar J, Schubert T, Thurner P, Barnaure I, Kulcsar Z. Single antiplatelet regimen in flow diverter treatment of cerebral aneurysms: The drug matters. A systematic

License CC BY-NC-ND 4.0

review and meta-analysis. *Interv Neuroradiol*. Published online May 23, 2023:15910199231177745. doi:10.1177/15910199231177745

324. Cortese J, Forestier G, Bardet SM, et al. Comparative assessment of early neointimal formation: P8RI-coated Silk Vista versus Pipeline Vantage (Shield) in a rabbit model using optical coherence tomography. *J Neurointerv Surg*. Published online October 23, 2025:jnis-2025-024213. doi:10.1136/jnis-2025-024213

325. Liu Y, Liu P, Song Y, et al. A heparin–rosuvastatin-loaded P(LLA-CL) nanofiber-covered stent inhibits inflammatory smooth-muscle cell viability to reduce in-stent stenosis and thrombosis. *J Nanobiotechnology*. 2021;19:123. doi:10.1186/s12951-021-00867-8

326. Janjic M, Pappa F, Karagkiozaki V, Gitas C, Ktenidis K, Logothetidis S. Surface modification of endovascular stents with rosuvastatin and heparin-loaded biodegradable nanofibers by electrospinning. *IJN*. 2017;12:6343-6355. doi:10.2147/IJN.S138261

327. Martin PD, Warwick MJ, Dane AL, Brindley C, Short T. Absolute oral bioavailability of rosuvastatin in healthy white adult male volunteers. *Clin Ther*. 2003;25(10):2553-2563. doi:10.1016/s0149-2918(03)80316-8

328. Chapman MJ, McTaggart F. Optimizing the pharmacology of statins: characteristics of rosuvastatin. *Atherosclerosis Supplements*. 2002;2(4):33-37. doi:10.1016/S1567-5688(01)00016-2

License CC BY-NC-ND 4.0

Appendices

Appendix 1. DELPHI consensus on CIA 151
Appendix 2. MARTA score 160
Appendix 3. IFD-assisted coiling 175
Appendix 4. FD with or without coils 185
Appendix 5. Article Rosuvastatin 194
Appendix 6. Article P8RI-coated Silk Vista versus Pipeline Vantage (Shield) 204

License CC BY-NC-ND 4.0

Appendix 1. DELPHI consensus on CIA

DELPHI

Acta Neurochirurgica (2024) 166:294
https://doi.org/10.1007/s00701-024-06182-z

ORIGINAL ARTICLE

Complex intracranial aneurysms: a DELPHI study to define associated characteristics

Francesco Diana[1,2,43] · Michele Romoli[3] · Eytan Raz[4] · Ronit Agid[5] · Felipe C. Albuquerque[6] · Adam S. Arthur[7] · Jürgen Beck[8] · Jerome Berge[9] · Hieronymus D. Boogaarts[10] · Jan-Karl Burkhardt[11] · Marco Cenzato[12] · René Chapot[13] · Fady T. Charbel[14] · Hubert Desal[15] · Giuseppe Esposito[16] · Johanna T. Fifi[17] · Stefan Florian[18] · Andreas Gruber[19] · Ameer E. Hassan[20] · Pascal Jabbour[21] · Ashutosh P. Jadhav[6] · Miikka Korja[22] · Timo Krings[23] · Giuseppe Lanzino[24] · Torstein R. Meling[25] · Jaques Morcos[26] · Pascal J. Mosimann[23] · Erez Nossek[27] · Vitor Mendes Pereira[28] · Andreas Raabe[29] · Luca Regli[16] · Veit Rohde[30] · Adnan H. Siddiqui[31] · Rokuya Tanikawa[32] · Stavropoula I. Tjoumakaris[33] · Alejandro Tomasello[1,2] · Peter Vajkoczy[34] · Luca Valvassori[35] · Nikolay Velinov[36] · Daniel Walsh[37] · Henry Woo[38] · Bin Xu[39] · Shinichi Yoshimura[40] · Wim H. van Zwam[41] · Simone Peschillo[42]

Received: 15 April 2024 / Accepted: 2 July 2024
© The Author(s), under exclusive licence to Springer-Verlag GmbH Austria, part of Springer Nature 2024

Abstract

Purpose Intracranial aneurysms present significant health risks, as their rupture leads to subarachnoid haemorrhage, which in turn has high morbidity and mortality rates. There are several elements affecting the complexity of an intracranial aneurysm. However, criteria for defining a complex intracranial aneurysm (CIA) in open surgery and endovascular treatment could differ, and actually there is no consensus on the definition of a "complex" aneurysm. This DELPHI study aims to assess consensus on variables defining a CIA.

Methods An international panel of 50 members, representing various specialties, was recruited to define CIAs through a three-round Delphi process. The panelists participated in surveys with Likert scale responses and open-ended questions. Consensus criteria were established to determine CIA variables, and statistical analysis evaluated consensus and stability.

Results In open surgery, CIAs were defined by fusiform or blister-like shape, dissecting aetiology, giant size (≥ 25 mm), broad neck encasing parent arteries, extensive neck surface, wall calcification, intraluminal thrombus, collateral branch from the sac, location (AICA, SCA, basilar), vasospasm context, and planned bypass (EC-IC or IC-IC). For endovascular treatment, CIAs included giant size, very wide neck (dome/neck ratio ≤ 1:1), and collateral branch from the sac.

Conclusions The definition of aneurysm complexity varies by treatment modality. Since elements related to complexity differ between open surgery and endovascular treatment, these consensus criteria of CIAs could even guide in selecting the best treatment approach.

Keywords Brain aneurysm · SAH · Clipping · Coiling · DELPHI

Abbreviations

AICA	Anterior-inferior cerebellar artery
CIA	Complex intracranial aneurysm
EC	External carotid
IC	Internal carotid
MCA	Middle cerebral artery
SCA	Superior cerebellar artery

Introduction

Intracranial aneurysms are the main cause of subarachnoid hemorrhage and, when ruptured, are associated with high rates of morbidity and mortality. Following the advancements in the endovascular techniques in recent years, most intracranial aneurysms can nowadays be treated endovascularly, while open surgical cases have followingly been limited to ever more complex cases. [17]. Scientific literature reports that complex intracranial aneurysms (CIA) pose unique diagnostic and therapeutic challenges, [28] but there is not a clear definition of CIA. This ambiguity in defining the complexity of intracranial aneurysms results in a

Extended author information available on the last page of the article

Published online: 11 July 2024

License CC BY-NC-ND 4.0

heterogeneous decision-making process.[2, 7, 9, 12, 13, 20, 23, 27, 29–31]. Moreover, criteria for defining a CIA in open surgery and endovascular treatment could differ, and the difference could even guide treatment approaches.

To address this challenge, we used a DELPHI approach to assess consensus on variables to define a CIA among a panel of experienced experts in both neurosurgical and neuroendovascular fields. Specifically, we utilized a modified Delphi process to identify areas of existing consensus rather than to achieve new consensus.

Materials and methods

Expert panel selection

An international panel of 54 operators, operating in high-volume centers (treating over 100 aneurysms per year), were identified from among some of the most experienced neurosurgeons and neurointerventionalists in Europe, North and South America, and Asia (Supplement Table 1). The protocol was approved by the local internal regulatory board (IRB), and all procedures were followed in accordance with the ethical standards of the IRB and the Helsinki Declaration of 1975. An email invitation and information sheet were sent to all potential participants, who then had the option to assent to participation or decline. Fifty participants consented prior to answering the survey questions. Each panelist answered questions related to his own field.

Delphi study design

We conducted a three-round Delphi process, with all rounds based on surveys (Table 1). All surveys were completed anonymously. In Round 1, we presented a binary closed-ended question (Yes or No), which included clinical and neuroradiological considerations. The aim was to select variables useful in defining a CIA. Structured statements were constructed using a Likert scale based on the Grading of Recommendations Assessment, Development, and Evaluation paradigm [16] and the recommended Delphi approach. [4] Open-ended questions were also included to generate ideas and variables for Round 2.

All statements were developed and agreed upon by three authors (SP, FD, MR). Results of round 1 were summarized and feedback to the participants before Round 2. This feedback allowed the panelists to reconsider their positions considering the collective opinions, as is standard in Delphi studies. Round 2 incorporated the collective results from Round 1 and a structured survey comprising statements that required Likert scale responses (19 items). It excluded variables that did not achieve an agreement in Round 1. In this phase, participants were asked to provide their viewpoints on the definition of a CIA from both surgical and endovascular perspectives. Experts could only participate in Rounds 2 and 3 if they had completed the previous round.

Participants could indicate disagreement (scores 1–2), remain neutral (score 3), or express agreement (scores 4–5) with the statements. Round 3 included statements that did not meet the consensus criteria or did not exhibit stability between rounds. These were re-evaluated for final consensus using a 3-point Likert scale in the concluding survey.

Anonymization was guaranteed by automatically assigning an ID to the survey response, with linkage implemented to compare the evolution of responses across the rounds. Adherence was ensured through email alerts during the steps of the Delphi process.

Consensus criteria and statistical analysis

The primary endpoint for concluding the Delphi process was consensus for at least half of the items. Consensus for a particular statement was defined as being at least 70% within the lowest or highest category (agree, neutral, or disagree) or within a single score on the Likert scale. Agreement without consensus was defined as being at least 50% within the lowest or highest category (agree, neutral, or disagree) or within a single score on the Likert scale.

Between-round stability was assessed using the McNemar change test for dichotomous variables. Permutation testing without replacement over 104 iterations was employed to approximate normality assumptions for Likert items. A p-value of 0.05 was considered significant. Analyses were performed using R Version 4.2.0 (R Core Team, Vienna, Austria).

Results

Panelists

Among 54 operators, fifty constituted the expert panel: 16 open vascular neurosurgeons, 13 interventional neuroradiologists, 12 dual trained neurosurgeons, 3 interventional neurologists, and 3 endovascular neurosurgeons. Ninety-three percent of panelists (26/28) performing open neurosurgical procedures have more than 10 years of experience. Eighty-two (26/32) percent of panelists performing endovascular procedures have more than 10 years of experience (Supplement Table 1).

Round 1

Among all the proposed parameters to define an aneurysm as complex (aneurysm dimension, dome/neck ratio, aspect ratio, neck geometry, sac morphology, the relation between

License CC BY-NC-ND 4.0

Table 1 Summary of the three-round Delphi process, conducted entirely through surveys

Round 1	Tied
Participants $n=50$ (85.5%, 57 invited)	Aneurysm dimension, dome/neck ratio, morphology, neck geometry, wall, and sac characteristics (including wall calcification, intraluminal thrombosis, blood blister-like or dissecting appearance), parent artery/collaterals status, planned treatment and previous treatments affects the aneurysm complexity
Statements $n=18$ items	Not tied
Open fields $n=2$	Unruptured status and patients' clinical status do not affect the aneurysm complexity. Aneurysm's aspect ratio, ruptured status, sac orientation, location, relation between neck surface and parent artery, presence of hematoma, vasospasm, the angle of bifurcation of the originating branches, and patient's age did not reach a consensus
End-points	
Consensus (> 70%) = 10/18	
Round 2	OS complex
Participants $n=47$	Fusiform or blood blister-like shape, dissecting aetiology, giant aneurysms (sac size ≥ 25 mm), broad neck encasing parent arteries, neck surface greater than ½ of the parent artery circumference, wall calcification, intraluminal thrombus, collateral branch originating from the sac, aneurysms located at the level of the anterior-inferior cerebellar artery (AICA), superior cerebellar artery (SCA), basilar trunk or basilar tip, treatments in the context of vasospasm and when a bypass (EC-IC or IC-IC) is planned
Statements OS $n=68$	OS no complex
Statements EVT $n=70$	Small aneurysms (sac size < 5 mm), small or medium neck (dome-neck ratio ≤ 1.33:1), saccular aneurysm with irregular shape, side wall aneurysms with a neck surface less than ½ of the parent artery circumference, sac orientation, aneurysms located at the level of the middle cerebral artery (MCA) or posterior communicating artery (PComA), and when a single clip is planned
End-points	EVT complex
Consensus OS (> 70%) = 39/68	Giant aneurysms (sac size ≥ 25 mm), very wide neck (dome/neck ratio ≤ 1:1) and collateral branch originating from the sac
Consensus EVT (> 70%) = 31/70	EVT no complex
	Small aneurysms (sac size < 5 mm), small or medium neck (dome-neck ratio ≤ 1.33:1), saccular aneurysm with irregular shape, side wall aneurysms, broad neck not encasing parent arteries, a neck surface less than ½ of the parent artery circumference, sac characteristics (wall calcification, intraluminal thrombus, any shape or aetiology), sac orientation, aneurysms located at the level of the internal carotid artery (ICA), posterior communicating artery (PComA) or basilar tip, and when coiling is planned
Round 3	Considerably influence on any treatment
Participants $n=42$	Dimension
Statements $n=7$	Morphology
Open fields $n=0$	Location
End-points	Neck geometry
Consensus (> 70%) = 1/7	
Agreement (> 50%) = 3/7	

License CC BY-NC-ND 4.0

the parent artery and neck surface, sac and wall characteristics, parent artery, and collateral branches characteristics, sac orientation, location, rupture or unruptured status, presence of vasospasm, type of planned treatment, and previous treatment), consensus (agreement of over 70% based on ratings) was reached for 10 out of 18 items.

The panelists agreed that the following parameters affect the complexity of the aneurysm: aneurysm dimension, dome/neck ratio, morphology, neck geometry, wall, and sac characteristics (including wall calcification, intraluminal thrombosis, blood blister-like, or dissecting appearance), parent artery/collaterals status, planned treatment, and previous treatments. They also agreed that the unruptured status and patients' clinical status do not affect the complexity of the aneurysm. Aneurysm aspect ratio, ruptured status, sac orientation, location, the relation between the neck surface and the parent artery, presence of hematoma, vasospasm, the angle of bifurcation of the originating branches, and the patient's age did not reach a consensus (Supplement Table 2).

Round 2

Among all statements requiring a Likert scale response (68 for open surgery and 70 for endovascular treatment), a consensus (agreement of over 70% based on ratings) was reached for 39 out of 68 items for open surgery and 31 out of 70 items for endovascular treatment. Results are summarized in Table 2 and reported in Supplement Table 3.

For the open surgery, panelists agreed that aneurysms meeting the following criteria are associated with complexity: fusiform or blood blister-like shape, dissecting aetiology, giant aneurysms (sac size ≥ 25 mm), broad neck encasing parent arteries, neck surface greater than half of the parent artery circumference, wall calcification, intraluminal thrombus, collateral branch originating from the sac, aneurysms located at the level of the anterior-inferior cerebellar artery (AICA), superior cerebellar artery (SCA), basilar trunk, or basilar tip, treatments in the context of vasospasm, and when a bypass (EC-IC or IC-IC) is planned. They also agreed that the following criteria are not associated with complexity for open surgery: small aneurysms (sac size < 5 mm), small or medium neck (dome-neck ratio ≤ 1.33:1), saccular aneurysm with an irregular shape, side wall aneurysms with a neck surface less than half of the parent artery circumference, sac orientation, aneurysms located at the level of the middle cerebral artery (MCA) or posterior communicating artery (PComA), and when a single clip is planned.

For the endovascular treatment, panelists agreed that aneurysms meeting the following criteria are associated with complexity: giant aneurysms (sac size ≥ 25 mm), a very wide neck (dome/neck ratio ≤ 1:1), and collateral branch originating from the sac. They also agreed that the following criteria are not associated with complexity for endovascular treatment: small aneurysms (sac size < 5 mm), small or medium neck (dome/neck ratio ≥ 1.33:1), saccular aneurysm with an irregular shape, side wall aneurysms, broad neck not encasing parent arteries, a neck surface less than half of the parent artery circumference, sac characteristics (wall calcification, intraluminal thrombus, any shape or aetiology), sac orientation, aneurysms located at the level of the internal carotid artery (ICA), posterior communicating artery (PComA), or basilar tip, and when coiling is planned.

Round 3

Among the seven items (applicable to both open and endovascular treatment) requiring a Likert scale response, agreement (consensus of over 50% based on ratings) was reached for four items. For both open surgery and endovascular treatment, panelists agreed that aneurysm dimension, morphology, location, and neck geometry significantly influence the complexity of the treatment. All the remaining items had consistent scores across the rounds (Supplement Fig. 1).

Discussion

The modified DELPHI methodology used in this study had the aim to assess the consensus extent among experts who are not independent of each other and typically already share common viewpoints of aneurysm management. DELPHI panel achieved consensus on several CIA parameters addressed in the survey. From the perspective of open surgery, the complexity of an aneurysm is defined by its location, size of the sac, and non-saccular shape (either blood blister-like or fusiform). With regard to the size and location, for example, in some neurosurgical series the likelihood of requiring retreatment was linked to both elements, being significantly higher for non-MCA aneurysms larger than 12 mm, compared to MCA aneurysms smaller than 12 mm. [18] In terms of shape, open surgery of blood blister-like aneurysms is associated with a higher risk of poor clinical outcomes, mortality, and periprocedural complications than endovascular treatment. [26] In the case of fusiform aneurysms, both approaches entail high mortality and complication rates, yet open surgery requires multiple and more intricate steps, such as direct clipping, trapping with bypass, proximal occlusion, resection with reanastomosis, transposition, aneurysmorrhaphy with thrombectomy, and wrappin, compared with the endovascular reconstruction or deconstruction of the artery [1, 15]. In addition, the dome/neck ratio holds more significance in endovascular than in surgical treatment. In randomized controlled trials (RCTs), coiling nearly doubled the treatment failure rate of clipping (24.2% vs. 14.5%) of wide-necked aneurysms [8], and single

License CC BY-NC-ND 4.0

Table 2 Characteristics tied with complexity of intracranial aneurysms. OS = open surgery, EVT = endovascular treatment

TIED TO COMPLEXITY OF INTRACRANIAL ANEURYSM			
		OS	EVT
Dimension	Giant (≥ 25 mm)	X	X
	Large (≥ 10 mm)		
	Medium (5–10 mm)		
	Small (< 5 mm)		
	Very small (< 3 mm)		
Dome-neck ratio	Small neck (2:1)		
	Medium neck (1.33:1)		
	Wide neck (1:1)		
	Beyond wide neck (< 1:1)		X
Morphology	Regular		
	Multilobate		
	Fusiform	X	
Neck geometry	Side-wall		
	Bifurcation-small neck		
	Bifurcation-wide neck	X	
Neck surface	Neck surface < 1/2 parent artery circumference		
	Neck surface > 1/2 parent artery circumference	X	
Sac features	Wall calcification	X	
	Intraluminal thrombus	X	
	Blood Blister-like	X	
	Dissecting aetiology	X	
Parent artery and collaterals	Parent artery focal stenosis		
	Collateral branch from sac	X	X
	Collateral branch from neck		
Location	Anterior circulation Proximal		
	Anterior circulation Distal		
	Posterior circulation Proximal	X	
	Posterior circulation Distal		
Ruptured status	Ruptured		
	Vasospasm	X	
Planned treatment	Single clip		
	Multiple clips		
	Bypass IC-IC	X	
	Bypass EC-IC	X	
	Intrasaccular devices		
	Coiling		
	Balloon assisted coiling/ID		
	Stent assisted coiling/ID		
	Flow-diverter ± coils/ID		

stent-assisted coiling did not demonstrate any advantage over coiling alone. [5] Consequently, endovascular treatments necessitate other strategies, such as Y-stent-assisted coiling or intrasaccular devices, resulting in high rates of long-term angiographic occlusion with a low incidence of treatment-related complications. [6, 19] However, these results need to be confirmed in RCTs.

Categorizing aneurysms under a broad definition of "complex" may be problematic. Most research or clinical trials do not explicitly classify aneurysms as "complex" or "non-complex", but they use variables associated to the aneurysm complexity, such as location, neck size, aneurysm size, and parent vessel attributes [3].This discrepancy indicates that the term "complex" is more often used in product names or to describe treatment procedures rather than as a clinical or academic classification. Consequently, there may not be a widely accepted or practical definition for "complex" aneurysms, particularly given the rapid advancements in

License CC BY-NC-ND 4.0

endovascular devices and microsurgical techniques. Why is the definition of a CAI clinically crucial? Firstly, in the context of medical communication, establishing a clear and accurate definition is essential to prevent misunderstandings and foster precise understanding among physicians, including neurosurgeons, neurointerventionalists, anesthesiologists, intensive care physicians, neuroradiologists, neurologists, and others. This clarity becomes paramount in the clinical assessment of cerebral aneurysms, where a classification based on complexity directly impacts treatment decisions. Secondly, the implications extend to the realm of medical research, as studies and investigations may specifically target categories of cerebral aneurysms identified as "complex." This targeted approach proves especially beneficial for the exploration of new medical devices or the comparative analysis of different therapeutic techniques. Thirdly, a well-defined classification system would directly benefit patients, allowing them to make well-informed decisions about their health. Currently, clinical decisions regarding the treatment of brain aneurysms are based on fragmented and incomplete evidence-based foundations. Determining the need for treatment should involve weighing the estimated risks associated with the disease, the treatment, and the patient. However, this is difficult with the currently available scoring systems, [10, 11, 14, 24] that do not consider the risks associated with the treatment. We can also argue that assigning a standard value to the risk of treatment may not fully encompass the complexities involved when patients are considering high-risk preventive interventions. Identifying variables that could fill this gap, enabling the comparison of treatment complexities, is perhaps useful in making informed decisions. Lastly, considering that individualized care necessitates rigorous scientific experience, identifying elements related to aneurysm complexity will help formulate hypotheses to be directly tested, avoiding conclusions based on outdated beliefs or fragile observational data. [21] In many centers, clipping is still preferred over coiling for large aneurysms, based on initial endovascular series, including surgically challenging patients, which indicated a high recanalization rate [22, 25]. Stent-assisted coiling is used for large or wide-necked aneurysms, although the STAT trial showed a higher efficacy of stenting for narrow-necked aneurysms compared to wide-necked ones [5] While we lack randomized experience for relatively old techniques and devices, new technologies, which should require the same prospective experience, are being used in clinical practice.

Limitations

The purpose of the DELPHI method is to establish a consensus on defining the complexity of brain aneurysms to develop data-driven recommendations. Therefore, a DELPHI consensus is by no means intended to replace evidence-based guidelines. This approach could have several limitations. First, the relatively small number of members in the expert panel could potentially have led to biased results, although efforts were made to represent a broad spectrum of specialties and geographic regions. Second, panelists involved in this DELPHI are not independent of each other and typically already share common viewpoints of aneurysm management. Third, the methodology of requiring > 50% agreement for further inclusion in Round 2 could potentially exclude parameters significant to only one specialty group. While the study aimed to identify commonalities across specialties, this approach might not fully capture the specific needs and perspectives of each group. Fourth, the panel consensus represents a snapshot in time, while technologies, particularly in the endovascular field, are constantly evolving. Hence, the results of this study will likely require updates as new devices or better evidence become available.

Conclusions

The definition of aneurysm complexity is associated with the type of treatment, whether open surgery or endovascular. For open surgery, complexity is determined by its location, size, neck geometry, collateral branches originating from the aneurysm sac and the type of treatment required. From an endovascular perspective, complexity is linked to size, dome-neck ratio ≤ 1:1, and collateral branches originating from the aneurysm sac. The guidance derived from these statements may improve the standardization and objectivity of CIA management.

Supplementary Information The online version contains supplementary material available at https://doi.org/10.1007/s00701-024-06182-z.

Authors contribution Conception and design [illegible]

Data acquisition: FD, MR, ER, FCA, ASA, https://doi.org/10.1007/s00 MC, RC, FTC, HD, GE, JTF, SF, AG, AEH, PJ, APJ, MK, VK, TK, GL, TRM, JM, PJM, EN, VMP, AR, LR, VR, AHS, RT, SIT, AT, PV, LV, NV, DW, HW, BX, SY, WHVZ, SP.

Data analysis and interpretation: FD, MR, SP.

Drafting the work: FD, MR, SP.

Critical revision: all authors.

Final approval: all authors.

Dr. Yoshimura reports research grants from Stryker, Siemens Healthineers, Bristol-Myers Squibb, Sanofi, Eisai, Daiichi Sankyo, Teijin Pharma, Chugai Pharmaceutical, HEALIOS, Asahi Kasei Medical, Kowa, CSL Behring; and lecturer fees from Stryker, Medtronic, JoDTNSon & JoDTNSon, Kaneka, Terumo, Biomedical Solutions, Boehringer-Ingelheim, Daiichi Sankyo, Bayer, Bristol-Meyers Squibb.

Dr Ameer E. Hassan—1. Consultant/Speaker: Medtronic, Microvention, Stryker, Penumbra, Cerenovus, Genentech, GE Healthcare, Scientia, Balt, Viz.ai, Insera therapeutics, Proximie, NeuroVasc, NovaSignal, Vesalio, Rapid Medical, Imperative Care, Galaxy Therapeutics, Route 92 and Perfuze. 2. Principal Investigator: COMPLETE study – Penumbra, LVO SYNCHRONISE – Viz.ai, Millipede Stroke Trial—Perfuze, RESCUE—ICAD—Medtronic. 3. Steering Committee/Publication committee member: SELECT, DAWN, SELECT 2, EXPEDITE II, EMBOLISE, CLEAR, ENVI, DELPHI, DISTALS. 4.DSMB—COMAND trial.

Francesco DIANA | Ph.D. Thesis | University of Limoges and University of Salerno | 2025 156
License CC BY-NC-ND 4.0

Dr Daniel C. Walsh: Consultant/Speaker for BBraun Aesculap, Stryker, Zeiss, GSK plc.

Dr Adnan H Siddiqui Current Research Grants: Co-investigator for NIH—1R01EB030092-01, Project Title: High Speed Angiography at 1000 frames per second; Mentor for Brain Aneurysm Foundation Carol W. Harvey Chair of Research, Sharon Epperson Chair of Research, Project Title: A Whole Blood RNA Diagnostic for Unruptured Brain Aneurysm: Risk Assessment Prototype Development and Testing. Financial Interest/Investor/Stock Options/Ownership: Adona Medical, Inc., Bend IT Technologies, Ltd., BlinkTBI, Inc, Cerebrotech Medical Systems, Inc., Cognition Medical, CVAID Ltd., E8, Inc., Endostream Medical, Ltd, Galaxy Therapeutics, Inc., Imperative Care, Inc., InspireMD, Ltd., InspireMD, Ltd., Instylla, Inc., IRRAS AB, Launch NY, Inc., NeuroRadial Technologies, Inc., NeuroTechnologyInvestors, Neurovascular Diagnostics, Inc., Peijia Medical, PerFlow Medical, Ltd., Q'Apel Medical, Inc., QAS.ai, Inc., Radical Catheter Technologies, Inc., Rebound Therapeutics Corp. (Purchased 2019 by Integra Lifesciences, Corp), RistNeurovascular, Inc. (Purchased 2020 by Medtronic), Sense Diagnostics, Inc., Serenity Medical, Inc., Silk Road Medical, Sim & Cure, SongBird Therapy, Spinnaker Medical, Inc., StimMed, LLC, Synchron, Inc., Three Rivers Medical, Inc.,Truvic Medical, Inc., Tulavi Therapeutics, Inc., Vastrax, LLC, Viseon, Inc. Consultant/Advisory Board: Apellis Pharmaceuticals, Inc., Boston Scientific, Canon Medical Systems USA, Inc., Cardinal Health 200, LLC, Cerebrotech Medical Systems, Inc., Cerenovus, Cordis, Corindus, Inc., Endostream Medical, Ltd, Imperative Care, InspireMD, Ltd., Integra, IRRAS AB, Medtronic, MicroVention, Minnetronix Neuro, Inc., Peijia Medical, Penumbra, Q'Apel Medical, Inc., Rapid Medical, Serenity Medical, Inc., Silk Road Medical, StimMed, LLC, Stryker Neurovascular, Three Rivers Medical, Inc., VasSol, Viz.ai, Inc. National PI/Steering Committees: Cerenovus EXCELLENT and ARISE II Trial; Medtronic SWIFT PRIME, VANTAGE, EMBOLISE and SWIFT DIRECT Trials; MicroVention FRED Trial & CONFIDENCE Study; MUSC POSITIVE Trial; Penumbra 3D Separator Trial, COMPASS Trial, INVEST Trial, MIVI neuroscience EVAQ Trial; Rapid Medical SUCCESS Trial; InspireMD C-GUARDIANS IDE Pivotal Trial.

Funding This research received no specific grant from any funding agency in the public, commercial or not-for-profit sectors.

Data availability Not applicable.

Code availability Not applicable.

Declarations

Ethics approval Not applicable.

Consent to participate All authors.

Consent for publication All authors.

Conflicts of interest/competing interests The authors report no conflict of interest concerning the materials or methods used in this study or the findings specified in this paper.

References

1. Anson JA, Lawton MT, Spetzler RF (1996) Characteristics and surgical treatment of dolichoectatic and fusiform aneurysms. J Neurosurg 84(2):185–193
2. Aydin K, Puthuran M, Onal Y et al (2023) The angiographic and clinical follow-up outcomes of the wide-necked and complex intracranial aneurysms treated with LVIS EVO–Assisted coiling. Neurosurgery 92(4):827–836
3. Becske T, Kallmes DF, Saatci I et al (2013) Pipeline for uncoilable or failed aneurysms: results from a multicenter clinical trial. Radiology 267(3):858–868
4. Beiderbeck D, Frevel N, von der Gracht HA, Schmidt SL, Schweitzer VM (2021) Preparing, conducting, and analyzing Delphi surveys: Cross-disciplinary practices, new directions, and advancements. MethodsX 8:101401
5. Boisseau W, Darsaut TE, Fahed R et al (2023) Stent-assisted coiling in the treatment of unruptured intracranial aneurysms: a randomized clinical trial. Am J Neuroradiol 44(4):381–389
6. Cagnazzo F, Limbucci N, Nappini S, Renieri L, Rosi A, Laiso A, di Carlo DT, Perrini P, Mangiafico S (2019) Y-Stent-Assisted coiling of wide-neck bifurcation intracranial aneurysms: a meta-analysis. Am J Neuroradiol 40(1):122–128
7. Chen S-Q, Li L, Gao B-L, Wu Q-W, Shao Q-J, Wang Z-L, Zhang K, Li T-X (2023) Safety and effect of pipeline flex embolization device for complex unruptured intracranial aneurysms. Sci Rep 13(1):4570
8. Darsaut TE, Findlay JM, Bojanowski MW et al (2023) A pragmatic randomized trial comparing surgical clipping and endovascular treatment of unruptured intracranial aneurysms. Am J Neuroradiol 44(6):634–640
9. Diana F, Pesce A, Toccaceli G, Muralidharan V, Raz E, Miscusi M, Raco A, Missori P, Peschillo S (2022) Microsurgical clipping versus newer endovascular techniques in treatment of unruptured anterior communicating artery-complex aneurysms: a meta-analysis and systematic review. Neurosurg Rev 45(2):1089–1100
10. Etminan N, Brown RD, Beseoglu K et al (2015) The unruptured intracranial aneurysm treatment score. Neurology 85(10):881–889
11. Fahed R, Darsaut TE (2017) The Delphi Oracle and the management of aneurysms. J Neurointerv Surg 9(e1):e1–e2
12. Fan F, Fu Y, Liu J et al (2022) Multiple Pipeline Embolization Devices for the Treatment of Complex Intracranial Aneurysm: A Multi-Center Study. Front Aging Neurosci. https://doi.org/10.3389/fnagi.2022.905224
13. Gómez-Amador JL, Valencia-Ramos CG, Sangrador-Deitos MV et al (2023) Roadmapping technique in the hybrid operating room for the microsurgical treatment of complex intracranial aneurysms. J Cerebrovasc Endovasc Neurosurg 25(1):50–61
14. Greving JP, Wermer MJH, Brown RD et al (2014) Development of the PHASES score for prediction of risk of rupture of intracranial aneurysms: a pooled analysis of six prospective cohort studies. Lancet Neurol 13(1):59–66
15. Griffin A, Lerner E, Zuchowski A, Zomorodi A, Gonzalez LF, Hauck EF (2021) Flow diversion of fusiform intracranial aneurysms. Neurosurg Rev 44(3):1471–1478
16. Guyatt GH, Oxman AD, Kunz R, Vist GE, Falck-Ytter Y, Schünemann HJ (2008) What is "quality of evidence" and why is it important to clinicians? BMJ 336(7651):995–998
17. Haverkamp C, Kaier K, Shah M, von zur Mühlen C, Beck J, Urbach H, Meckel S (2024) Cerebral aneurysms: Germany-wide real-world outcome data of endovascular or neurosurgical treatment from 2007 to 2019. J Neurointerv Surg 16(4):365–371
18. Jabbarli R, Pierscianek D, Wrede K, Dammann P, Schlamann M, Forsting M, Müller O, Sure U (2016) Aneurysm remnant after clipping: the risks and consequences. J Neurosurg 125(5):1249–1255
19. Pierot L, Szikora I, Barreau X et al (2023) Aneurysm treatment with the Woven EndoBridge (WEB) device in the combined population of two prospective, multicenter series: 5-year follow-up. J Neurointerv Surg 15(6):552–557
20. Ravina K, Rennert RC, Brandel MG, Strickland BA, Chun A, Lee Y, Carey JN, Russin JJ (2021) Comparative Assessment of

Francesco DIANA | Ph.D. Thesis | University of Limoges and University of Salerno | 2025
License CC BY-NC-ND 4.0

Extracranial-to-Intracranial and Intracranial-to-Intracranial In Situ Bypass for Complex Intracranial Aneurysm Treatment Based on Rupture Status: A Case Series. World Neurosurg 146:e122–e138
21. Raymond J, Darsaut TE (2023) Understanding categories or subgroups and a common clinical reasoning error: the example of aneurysm size and neck width. Neurochirurgie 69(6):101491
22. Raymond J, Roy D, Bojanowski M, Moumdjian R, L'Espérance G (1997) Endovascular treatment of acutely ruptured and unruptured aneurysms of the basilar bifurcation. J Neurosurg 86(2):211–219
23. Rennert RC, Nguyen VN, Abedi A, Atai NA, Carey JN, Tenser M, Amar A, Mack WJ, Russin JJ (2023) Combined open revascularization and endovascular treatment of complex intracranial aneurysms: case series. Front Neurol. https://doi.org/10.3389/fneur.2023.1102496
24. Rinkel GJE, Algra A, Greving JP, Vergouwen MDI, Etminan N (2017) PHASES and the natural history of unruptured aneurysms: science or pseudoscience? J Neurointerv Surg 9(6):618
25. Roy D, Raymond J, Bouthillier A, Bojanowski MW, Moumdjian R, L'Espérance G (1997) Endovascular treatment of ophthalmic segment aneurysms with Guglielmi detachable coils. AJNR Am J Neuroradiol 18(7):1207–1215
26. Tan H, Zhang T, Huang G, Li Z, Wang Z, Cheng M, Liu L, Liu L (2023) Endovascular intervention vs. microsurgery on the prognosis of anterior circulation blood blister-like aneurysm: a cohort study. Front Neurol. https://doi.org/10.3389/fneur.2023.1103138
27. Toccaceli G, Diana F, Cagnazzo F, Cannizzaro D, Lanzino G, Barbagallo GMV, Certo F, Bortolotti C, Signorelli F, Peschillo S (2020) Microsurgical Clipping Compared with New and Most Advanced Endovascular Techniques in the Treatment of Unruptured Middle Cerebral Artery Aneurysms: A Meta-Analysis in the Modern Era. World Neurosurg 137:451-464.e1
28. Togashi S, Shimizu H (2022) Complex intracranial aneurysms, pp 225–238. https://doi.org/10.1007/978-3-030-87649-4_12
29. Wang X, Han G, Wang H, Shang Y, Shi M, Wang X, Bao J, Wang Z, Tong X (2023) Cerebral revascularization for complex middle cerebral artery aneurysms: surgical strategies and outcomes in a single center. Neurosurg Rev 46(1):68
30. Xue T, Deng R, Gao B, Wang Z, Ma C, You W, Zhu Y, Chen Z, Wang Z (2021) Intraoperative indocyanine green video angiography (ICG–VA) with FLOW 800 software in complex intracranial aneurysm surgery. Chin Neurosurg J 7(1):28
31. Zhang J, He L, Xia X, Zhang L, Yu K (2023) Braided stent-assisted coil embolization versus laser engraved stent-assisted coil embolization in patients with unruptured complex intracranial aneurysms. Clinics 78:100202

Publisher's Note Springer Nature remains neutral with regard to jurisdictional claims in published maps and institutional affiliations.

Springer Nature or its licensor (e.g. a society or other partner) holds exclusive rights to this article under a publishing agreement with the author(s) or other rightsholder(s); author self-archiving of the accepted manuscript version of this article is solely governed by the terms of such publishing agreement and applicable law.

Authors and Affiliations

Francesco Diana[1,2,43] · Michele Romoli[3] · Eytan Raz[4] · Ronit Agid[5] · Felipe C. Albuquerque[6] · Adam S. Arthur[7] · Jürgen Beck[8] · Jerome Berge[9] · Hieronymus D. Boogaarts[10] · Jan-Karl Burkhardt[11] · Marco Cenzato[12] · René Chapot[13] · Fady T. Charbel[14] · Hubert Desal[15] · Giuseppe Esposito[16] · Johanna T. Fifi[17] · Stefan Florian[18] · Andreas Gruber[19] · Ameer E. Hassan[20] · Pascal Jabbour[21] · Ashutosh P. Jadhav[6] · Miikka Korja[22] · Timo Krings[23] · Giuseppe Lanzino[24] · Torstein R. Meling[25] · Jaques Morcos[26] · Pascal J. Mosimann[23] · Erez Nossek[27] · Vitor Mendes Pereira[28] · Andreas Raabe[29] · Luca Regli[16] · Veit Rohde[30] · Adnan H. Siddiqui[31] · Rokuya Tanikawa[32] · Stavropoula I. Tjoumakaris[33] · Alejandro Tomasello[1,2] · Peter Vajkoczy[34] · Luca Valvassori[35] · Nikolay Velinov[36] · Daniel Walsh[37] · Henry Woo[38] · Bin Xu[39] · Shinichi Yoshimura[40] · Wim H. van Zwam[41] · Simone Peschillo[42]

✉ Simone Peschillo
simone.peschillo@gmail.com

[1] Interventional Neuroradiology, University Hospital Vall d'Hebron, Barcelona, Spain

[2] Stroke Research Group, Vall d'Hebron Research Institute, Barcelona, Spain

[3] Neurology and Stroke Unit, Department of Neuroscience, Bufalini Hospital, Cesena, Italy

[4] Department of Radiology, New York University Langone Health, New York, NY, USA

[5] Division of Neuroradiology, JDMI, University Health Network, Toronto, Canada

[6] Department of Neurosurgery, Barrow Neurological Institute, St. Joseph's Hospital and Medical Center, Phoenix, AZ, USA

[7] University of Tennessee, Semmes-Murphey Neurologic and Spine Clinic, Memphis, TN, USA

[8] Department of Neurosurgery, Medical Center, University of Freiburg, Freiburg, Germany

[9] Interventional Neuroradiology Department, CHRU, Bordeaux, France

[10] Department of Neurosurgery, Radboud University Medical Centre, Nijmegen, Netherlands

[11] Department of Neurosurgery, Hospital of the University of Pennsylvania, Penn Medicine, Philadelphia, USA

[12] Department of Neurosurgery, Grande Ospedale Metropolitano Niguarda, Milan, Italy

[13] Department of Interventional Neuroradiology, Alfried Krupp Hospital Ruttenscheid, Essen, Germany

[14] Department of Neurosurgery, University of Illinois at Chicago, Chicago, IL, USA

[15] Department of Diagnostic and Therapeutic Neuroradiology, University Hospital of Nantes, Nantes, France

License CC BY-NC-ND 4.0

[16] Department of Neurosurgery, University Hospital of Zurich, University of Zurich, Zurich, Switzerland

[17] Department of Neurosurgery, Icahn School of Medicine at Mount Sinai, New York, NY, USA

[18] Department of Neurosurgery, Iuliu Hatieganu" University of Medicine and Pharmacy, Cluj County Clinical Emergency Hospital, Cluj-Napoca, Romania

[19] Department of Neurosurgery, Johannes Kepler University, Neuromed Campus, Kepler Universitätsklinikum, Linz, Austria

[20] Department of Neurology, Valley Baptist - University of Texas Rio Grande Valley, Harlingen, TX, USA

[21] Department of Neurosurgery, Thomas Jefferson Hospital, Philadelphia, PA, USA

[22] Department of Neurosurgery, University of Helsinki and Helsinki University Hospital, Helsinki, Finland

[23] Interventional and Diagnostic Neuroradiology, University of Toronto & Toronto Western Hospital, Toronto, ON, Canada

[24] Department of Neurologic Surgery, Mayo Clinic, Rochester, MN, USA

[25] Department of Neurosurgery, Rigshospitalet, Copenhagen, Denmark

[26] Vivian L. Smith Department of Neurosurgery, UTHealth Houston Neurosciences, Houston, TX, USA

[27] Department of Neurosurgery, New York University School of Medicine, New York, NY, USA

[28] Division of Neurosurgery, Departments of Surgery & Medical Imaging, St. Michael's Hospital, University of Toronto, Toronto, ON, Canada

[29] Department of Neurosurgery Inselspital, Bern University Hospital and University of Bern, Bern, Switzerland

[30] Department of Neurosurgery, University Medical Center Göttingen, Georg-August-University, Göttingen, Germany

[31] Department of Neurosurgery, Jacobs School of Medicine and Biomedical Sciences, University at Buffalo, Buffalo, NY, USA

[32] Department of Neurosurgery, Stroke Center, Sapporo Teishinkai Hospital, Sapporo, Hokkaido, Japan

[33] Department of Neurological Surgery, Thomas Jefferson University Hospital, Philadelphia, PA, USA

[34] Department of Neurosurgery, Charité-Universitätsmedizin Berlin, Berlin, Germany

[35] Neuroradiology Unit, Ospedale San Carlo, Milan, Italy

[36] Clinics of Neurosurgery, Vascular and Endovascular Neurosurgery, University Hospital Pirogov, Sofia, Bulgaria

[37] King's College Hospital NHS Foundation Trust, London, UK

[38] Department of Neurosurgery, Donald and Barbara Zucker School of Medicine at Hofstra/Northwell, Manhasset, NY, USA

[39] Department of Neurosurgery, Huashan Hospital, Fudan University, Shanghai, China

[40] Department of Neurosurgery, Hyogo Medical University, Nishinomiya, Japan

[41] Department of Radiology and Nuclear Medicine, School for Cardiovascular Diseases (CARIM), Maastricht UMC+, Maastricht, The Netherlands

[42] Endovascular Neurosurgery, Guido Guglielmi Endowed Chair in Endovascular Neurosurgery, Unicamillus International University of Health Sciences, Rome, Italy

[43] Department of Scienze della Vita, Della Salute e delle Professioni Sanitarie Link Campus University, Rome, Italy

License CC BY-NC-ND 4.0

Appendix 2. MARTA score

MARTA score

Neurosurgery

Associated Risks to the Treatment of unruptured intracranial Aneurysms (MARTA) Score: development and external validation

--Manuscript Draft--

Manuscript Number:	NEU-D-25-01686R2
Article Type:	Clinical Research
Section/Category:	Cerebrovascular
Corresponding Author:	Michele Romoli, MD, PhD Maurizio Bufalini Hospital: Ospedale M Bufalini di Cesena ITALY
Order of Authors:	Francesco Diana, MD
	Adnan H Siddiqui
	Vinay Jaikumar
	Ammad A. Baig
	Alejandro Tomasello
	David Hernandez
	Manuel Requena
	Marta De Dios Lascuevas
	Fuat Arikan
	Bin Xu
	Yujun Liao
	Eytan Raz
	Charlotte Chung
	Erez Nossek
	Nico Stroh-Holly
	Matthias Gmeiner
	Vittorio Civelli
	Francesco Arpaia
	Nicolas K Khattar
	Haydn A Hoffman
	Christopher M Nickele
	Adam S Arthur
	Fady Charbel
	Peter Vajkoczy
	Amina Sanchin
	Pascal Jabbour
	Giuseppe Lanzino
	Ryan C Ransom
	Andreas Raabe
	Thomas Petutschnigg

Powered by Editorial Manager® and ProduXion Manager® from Aries Systems Corporation

License CC BY-NC-ND 4.0

	Nicolay Velinov
	Jan-Karl Burkhardt
	Ameer E Hassan
	Hamzah Saei
	Andrea Salcuni
	Elia Manfrini
	Paolo Eusebi
	Adriano Bonura
	Michele Romoli
	Simone Peschillo
Manuscript Region of Origin:	SPAIN
Abstract:	Background and Objectives: Unruptured intracranial aneurysms (UIA) are increasingly detected and require careful management to prevent rupture. No externally validated score currently predicts procedural risk to guide treatment decisions. We developed and validated two predictive scores for complications after endovascular (EVT) or neurosurgical treatment (NT) of UIA using routinely collected clinical and aneurysmal features. Methods: We conducted a multicenter retrospective study including UIA patients treated with EVT or NT across 15 neurovascular centers (2014-2024). Predictive models were built using multivariable logistic regression, with variables derived from Delphi consensus. The primary outcome was a composite safety endpoint: new neurological deficits, mRS worsening (≥1 point or mRS 2–5 within 30 days), or procedural death. Internal validation used bootstrapping; external validation was performed temporally and institutionally. Model performance was assessed via AUROC and calibration. Final scores, named MARTA-EVT and MARTA-NT, were compared to existing models identified through systematic review. Results: Among 2647 patients (1907 EVT, 740 NT), procedural complications occurred in 6.3% (EVT) and 12.8% (NT). Independent predictors included age, baseline mRS, aneurysm location, size, morphology, and procedural factors. MARTA-EVT (AUROC=0.68, 95%CI=0.57–0.78) and MARTA-NT (AUROC=0.65, 95%CI=0.54–0.77) showed moderate discrimination and good calibration. MARTA-EVT outperformed existing models; MARTA-NT performed similarly to SAFETEA. Predictive models are available open-source: https://martascore.shinyapps.io/MARTA/. Conclusion: MARTA-EVT and MARTA-NT are validated tools for predicting procedural risks in UIA treatment and may support patient counseling and clinical decision-making.
Additional Information:	
Question	**Response**
Significance of the Work: Please include a brief statement summarizing the significance of the work and in particular how it differs from and advances existing literature.	Our findings emphasize the critical need for predictive models that align with modern neurovascular practices. By utilizing routinely collected clinical and aneurysmal characteristics, the MARTA scores bridge existing gaps in procedural risk stratification, providing clinicians and patients with a reliable, simple-to-use, and evidence-based tool for optimizing management strategies.
Compliance with Research Reporting Guidelines: *Neurosurgery* endorses several reporting guidelines and requires authors to submit their research articles in accordance with the appropriate guideline statement(s) and checklist(s). Completed applicable checklists and flow diagrams must be included with submissions.	Yes - Submission Adheres to Appropriate Reporting Guideline(s) and Applicable Checklists/Materials Are Included

Powered by Editorial Manager® and ProduXion Manager® from Aries Systems Corporation

License CC BY-NC-ND 4.0

Research articles that must be submitted according to the appropriate reporting guideline(s) include, but are not limited to: randomized trials, systematic reviews, meta-analyses of interventions, meta-analyses of observational studies, diagnostic accuracy studies, and observational epidemiological studies (eg, case series, cohort, case-control, and cross-sectional studies). Consult the EQUATOR Network, which maintains a useful, up-to-date list of guidelines as they are published, with links to articles and checklists: http://www.equator-network.org. Please confirm below that information is reported according to the relevant reporting guideline(s) and any required materials are included with the submission:	
Please indicate which reporting guideline(s) the study adheres to (eg, STROBE, PRISMA, CONSORT). as follow-up to "**Compliance with Research Reporting Guidelines**: *Neurosurgery* endorses several reporting guidelines and requires authors to submit their research articles in accordance with the appropriate guideline statement(s) and checklist(s). Completed applicable checklists and flow diagrams must be included with submissions. Research articles that must be submitted according to the appropriate reporting guideline(s) include, but are not limited to: randomized trials, systematic reviews, meta-analyses of interventions, meta-analyses of observational studies, diagnostic accuracy studies, and observational epidemiological studies (eg, case series, cohort, case-control, and cross-sectional studies). Consult the EQUATOR Network, which maintains a useful, up-to-date list of guidelines as they are published, with links to articles and checklists: http://www.equator-network.org. Please confirm below that information is	TRIPOD+AI

Powered by Editorial Manager® and ProduXion Manager® from Aries Systems Corporation

License CC BY-NC-ND 4.0

reported according to the relevant reporting guideline(s) and any required materials are included with the submission:"	
Patient anonymity and informed consent: It is the author's responsibility to ensure that patients' privacy is protected. Informed consent should be obtained in writing from the patient if there is concern that a patient's anonymity cannot be maintained in written text or with use of photographs or video.	I Agree
Funding Information:	

Powered by Editorial Manager® and ProduXion Manager® from Aries Systems Corporation

License CC BY-NC-ND 4.0

Associated Risks to the Treatment of unruptured intracranial Aneurysms (MARTA) Score: development and external validation

Abstract

Background and Objectives: Unruptured intracranial aneurysms (UIA) are increasingly detected and require careful management to prevent rupture. No externally validated score currently predicts procedural risk to guide treatment decisions. We developed and validated two predictive scores for complications after endovascular (EVT) or neurosurgical treatment (NT) of UIA using routinely collected clinical and aneurysmal features.

Methods: We conducted a multicenter retrospective study including UIA patients treated with EVT or NT across 15 neurovascular centers (2014-2024). Predictive models were built using multivariable logistic regression, with variables derived from Delphi consensus. The primary outcome was a composite safety endpoint: new neurological deficits, mRS worsening (≥1 point or mRS 2–5 within 30 days), or procedural death. Internal validation used bootstrapping; external validation was performed temporally and institutionally. Model performance was assessed via AUROC and calibration. Final scores, named MARTA-EVT and MARTA-NT, were compared to existing models identified through systematic review.

Results: Among 2647 patients (1907 EVT, 740 NT), procedural complications occurred in 6.3% (EVT) and 12.8% (NT). Independent predictors included age, baseline mRS, aneurysm location, size, morphology, and procedural factors. MARTA-EVT (AUROC=0.68, 95%CI=0.57–0.78) and MARTA-NT (AUROC=0.65, 95%CI=0.54–0.77) showed moderate discrimination and good calibration. MARTA-EVT outperformed existing models; MARTA-NT performed similarly to SAFETEA. Predictive models are available open-source: https://martascore.shinyapps.io/MARTA/.

Conclusion: MARTA-EVT and MARTA-NT are validated tools for predicting procedural risks in UIA treatment and may support patient counseling and clinical decision-making.

Running Title: MARTA score for IAs risk treatment assessment.

Key words

Intracranial aneurysm; endovascular treatment; clipping; treatment risk; score.

Abbreviation list

ACA= anterior cerebral artery; AChA= anterior choroidal artery; ACoA= anterior communicating artery; AICA= anterior inferior cerebellar artery; BA= basilar artery; BAC= balloon assisted coiling; EVT= endovascular treatment; FD= flow diverter(s); IA= intracranial aneurysm(s); ICA= internal carotid artery; ICA-T= internal carotid artery terminus; ID= intrasaccular device(s); MCA= middle cerebral artery; NT= neurosurgical treatment; OphA= ophthalmic artery; PCA= posterior cerebral artery; PICA= posterior inferior cerebellar artery; PComA= posterior communicating artery; UIA= unruptured intracranial aneurysm(s); SAC= stent assisted coiling; SAH= subarachnoid hemorrhage; SCA= superior cerebellar artery; VA= vertebral artery.

License CC BY-NC-ND 4.0

Introduction

Unruptured intracranial aneurysms (UIAs) are increasingly detected, requiring careful management to balance rupture risk against treatment complications. While ruptured IAs need urgent intervention to prevent re-rupture,[1] evidence on the safety and benefits of treating UIAs remains limited. Both endovascular (EVT) and neurosurgical treatments (NT) carry a risk of serious complications,[2-4] which must be weighed against rupture risk, life expectancy, and patient concerns.

Although rupture risk scores like UIATS[5] and PHASES[6] use accessible patient and aneurysm data, treatment risk scores are less developed, often lack external validation, or are limited to specific treatments.[7-12]

This study aimed to develop and validate the Morbidity and Mortality Associated Risk in the Treatment of unruptured intracranial Aneurysms (MARTA) score, using routinely collected patient, aneurysm, and treatment data to predict complications for EVT and NT.

Methods

Study design and population

This multicenter retrospective study, approved by the local ethics board (IRB PR(AG)72/2024), complied with the Helsinki Declaration. Informed patient consent was waived due to the observational design using anonymized data. The study followed the Transparent Reporting of a Multivariable Prediction Model for Individual Prognosis or Diagnosis + AI (TRIPOD + AI) Checklist.

We included all consecutive UIA patients treated with EVT or NT at 15 international tertiary referral neurovascular centres within 2014 and August 2024. We excluded patients with subarachnoid hemorrhage (SAH), previously treated UIAs, and unsuccessful treatment attempts. Aborted EVT and NT procedures were excluded to focus on complications arising from completed procedures, ensuring homogeneity in the outcome assessment.

Development cohorts were defined as all cases consecutively enrolled between 2014 and August 2024 (Table 1) and testing cohorts were restricted to patients enrolled at three neurovascular centers selected between January 1st 2020 and August 31st 2024, to ensure temporal and external validation (Supplemental content 1, Table 1 and Table 2).

Data sources and collected variables

Data were sourced from the MARTA Database, comprising prospectively collected patient records from high-volume centers (≥50 UIA treatments annually, with many exceeding 100 cases per year). Individual practitioner experience (e.g., years of practice or case volume) was not systematically collected due to the retrospective and anonymized nature of the data. Variables included demographics, comorbidities, aneurysm characteristics (size, location, morphology, neck geometry, sac features), and procedural details, standardized per Delphi consensus.[13] Aneurysms were classified as anterior (ICA, MCA, ACA) or posterior (vertebrobasilar) circulation.

Data sharing statement

Individual participant data will not be shared. Study protocol, statistical analysis plan, analytic code will be shared after publication and ending 12 months following article publication with

License CC BY-NC-ND 4.0

researchers who provide a methodologically sound proposal to achieve aims in the approved proposal. Proposals may be submitted up to 12 months following article publication.

Outcome

The primary outcome was a composite safety endpoint: new neurological deficits, modified Rankin Scale (mRS) worsening (≥1 point or mRS 2-5 within 30 days),[12] or procedural death. Neurologic complications were categorized as major (permanent or transient deficits requiring more than 1 month to recover and affecting the patient's quality of life - independently from changes in mRS) or minor (transient deficits resolving within 30 days). Outcomes were verified by principal investigators and a monitoring committee (Supplemental content 1, Table 3).

Systematic review

Following PRISMA and MOOSE guidelines (PROSPERO: CRD42025635940), we searched PubMed, EMBASE, and Cochrane Library for validated UIA treatment risk scores. Included studies had sample sizes >500, internal or external validation, and were published in English. Risk of bias was assessed using the Prediction Model Risk of Bias Assessment Tool (PROBAST). Validated scores were compared with MARTA.

Statistical analysis

Assuming a 10% complication rate and six predictors per score, we required at least 600 patients per treatment group. Missing data (<5%) were imputed after data pursuit. Logistic regression identified predictors of the primary outcome for EVT and NT separately, using variables from Delphi consensus[13] and prior reviews.[7,12] Model performance was evaluated via area under the receiver operating characteristic curve (AUROC) and calibration plots (LASSO-based regression models for EVT and NT). Bootstrapping provided internal validation, and external validation used a separate cohort. MARTA-EVT and MARTA-NT scores were developed from regression coefficients and Delphi consensus, tested against existing scores (SAFETEA, S-C-C) using the DeLong test. Analyses was conducted using R software (version 4.3.3), with dplyr, haven, pRoc packages and in-house built functions (MR).

Results

Study participants

We included 1907 UIA receiving EVT (1460 in the development cohort and 447 in the testing cohort) and 740 receiving NT (602 in the development cohort and 138 in the testing cohort). Table 1 summarizes the characteristics of the EVT and the NT development cohorts.

The mean age in the EVT cohort was 58.5 years, while in the NT cohort, it was 57.1 years. Most patients were women in both cohorts: 77.9% in the EVT cohort and 77.2% in the NT one. The observed prevalence of the composite primary outcome in the EVT development cohort was 6.3% (92 events/1460 patients; Supplemental content 1, Table 4). People developing the composite outcome had worse functional status (median mRS 1 vs 0, p<.001), higher prevalence of UIA at ICA-T, MCA, ACA and posterior circulation sites, larger aneurysms, and higher rates of complex saccular and neck features (e.g. 19.6% vs 9.1%, p=.002). The observed prevalence of the composite primary outcome in the NT cohort was 12.8% (77/602 patients, Supplemental content 1, Table 4). Procedural complications were higher in patients with higher

License CC BY-NC-ND 4.0

mRS at baseline, with ICA-T, ACA, posterior circulation aneurysm location, with larger, irregularly shaped, multilobar aneurysms, and in those with branches originating from the neck.

Model and score development and performance - EVT

Table 2 presents the results from a binary logistic regression model. Location, dimension, and branch from the sac were independent predictors of the primary outcome. Overall, the model had a relatively good accuracy for predicting the primary outcome after correction for optimism (c-statistic=0.78; 95%CI=0.75-0.84). The Grønnesby and Borgan test was not significant (p=0.40), indicating a good overall fit (Supplemental content 1, Figure 1). Sensitivity analysis using a LASSO-based logistic regression model showed stable calibration performance (Supplemental content 1, Figure 2).

Based on model coefficients and DELPHI items,[13] we developed through consensus the MARTA-EVT score, considering key operational aneurysmal and baseline clinical features (6 variables): age, baseline mRS, aneurysm location, aneurysm size, parent artery and collateral branch characteristics, and treatment approach (score range 2-13; Table 3 for score). MARTA-EVT had moderate discrimination ability in the testing cohort (AUROC=0.68, 95%CI=0.57-0.78; Figure 1, 1A).

The predicted probabilities of composite primary outcome stratified by the MARTA score for each risk group are presented in Figure 2, 2A. Primary outcome risk increases from low-risk group (MARTA-EVT≤4=2.4%) to medium-risk (MARTA 5-6=5.1%), high-risk (MARTA-EVT 7-8=9.2%) and critical-risk groups (MARTA ≥9=18.3). A post-hoc analysis using center-level procedural volume as a proxy for experience showed consistent model performance across high- and very high-volume centers (EVT: AUROC=0.67-0.69).

Model and score development and performance - NT

Table 4 presents a binary regression model for primary outcome prediction in the NT group. Overall, the model had a relatively high accuracy for the adjudication of the primary outcome after correction for optimism (c- statistic=0.73; 95%CI=0.67-0.78). The Grønnesby and Borgan test was not significant (p=0.38), indicating a good overall fit (Supplemental content 1, Figure 1). Sensitivity analysis using a LASSO-based logistic regression model showed stable calibration performance (Supplemental content 1, Figure 2).

Based on model coefficients and DELPHI-based items,[13] we developed the MARTA-NT score considering key operational aneurysmal and baseline clinical features (6 variables): age, baseline mRS, aneurysm location, aneurysm size, morphology, parent artery focal stenosis (score range 3-13; Table 3 for score). MARTA NT score had a moderate discrimination ability in the validation cohort (AUROC=0.65, 95%CI=0.54-0.77; Figure 1, 1B).

The predicted probabilities of composite primary outcome stratified by the MARTA score for each risk group are presented in Figure 2, 2B. In the NT group, the predicted probability progressively ingreased from low-risk group (MARTA-NT≤4= 4.2%) to medium (MARTA-NT=5-6; 13.7%), high (MARTA-NT=7-8; 29.6%) and critical-risk groups (MARTA-NT≥9; 75%). A post-hoc analysis using center-level procedural volume as a proxy for experience showed consistent model performance across high- and very high-volume centers (NT: AUROC=0.64-0.66).

License CC BY-NC-ND 4.0

Systematic review and score comparison

The systematic review retrieved 411 studies, of which 7 reached the final screening stage, and 2 were included in qualitative synthesis and quantitative comparison with MARTA score in the validation cohort (PRISMA flowchart in Supplemental content 1, Figure 3). Of the two studies reporting a potential predictive score for neurological complications, one had moderate risk of bias, and one had high risk of bias,[12] mainly related to participant selection and validation methods. When compared to other scores in patients treated with EVT, the MARTA EVT score had a significantly higher discrimination ability compared to SAFETEA ($p=0.002$) and S-C-C ($p<0.001$; Figure 1, 1A). In patients treated with a NT approach, the MARTA score had similar performance to SAFETEA (Figure 1, 1B).

Discussion

Using a large dataset encompassing 15 institutions, we developed and validated the Morbidity and Mortality Associated Risk in the Treatment of unruptured intracranial Aneurysms (MARTA), a simple scoring system for predicting complication risk in patients with UIA. The score was developed to address the need for an evidence-based assessment of the risk associated with treating UIA. The multidisciplinary approach, despite the incomplete understanding of the natural history of cerebral aneurysms, increasingly relies on predictive scores for rupture risk,[5,6] whereas operative risk continues to be defined arbitrarily. The MARTA scores demonstrated discrete discriminative ability, with approximately 68% accurate prediction of the primary outcome in people receiving EVT and 65% in people receiving NT. Notably, it relied solely on routinely collected parameters, including baseline mRS, aneurysm location and dimension, anatomical characteristics such as parent artery stenosis and collateral branches originating from the aneurysmal sac, and the selected treatment. MARTA performed significantly better than currently adopted prediction scores for EVT, whose external validity, in this large cohort, seems critically low. This is likely related to the current study larger training dataset and multicenter nature, as well as to the large-volume characteristics of all centers included. Of note, the MARTA scores share the same parameters used in scores evaluating the risk of rupture of IA, such as the PHASES[6] and the UIATS[5]. This makes the MARTA score user-friendly given that no unusual items are required for use. The MARTA score has many strengths that enhance its practicality and effectiveness. Despite its simplicity and ease of calculation, the score exhibits good discriminative ability, with prediction accuracy ranging of up to 68% in the cohorts investigated. Such predictive ability is based on a large and diverse population of patients with UIA undergoing elective embolization, whether endovascular (1907 patients), or microsurgical (740 patients). Given that the timeframe of the enrolment in our study spans a decade that witnessed critical technological advances in the EVT of aneurysms, MARTA score may be a more realistic reflection of modern neurovascular practice than previously available scores. We collected many clinical outcomes, including minor and major neurologic deficits, mRS at discharge, all types of ischemic and hemorrhagic complications related to treatment, therefore providing meaningful information on the rate of complications achieved in large volume specialized centers. Such information may help in modelling future trials and studies, and possibly may contribute to the adoption of cost-effective strategies. In our cohort, the MARTA score demonstrated a higher predictive value than other proposed predictive models, such as the SAFETEA[7] and S-C-C[12] scores. This

License CC BY-NC-ND 4.0

superior performance underscores its potential as a more reliable tool for predicting complication risk in patients with UIA. Beyond MARTA, this study also provides a first attempt for an external validation of SAFETEA and S-C-C scores, with external validation highlighting a predictive accuracy sufficiently low to discourage any implementation in clinical practice. An inherent limitation of the MARTA scores lies in their simplification of the complex interplay of variables involved in aneurysm pathology and treatment risk. While the full logistic regression models demonstrated higher predictive accuracy (c-statistic up to 0.78), the simplified scores were necessarily constructed by selecting a subset of variables based on consensus and statistical significance. This approach does not fully capture the interdependence between aneurysmal features, anatomical configurations, and clinical context. Aneurysms represent a multifactorial and anatomically intricate disease, where variables such as location, morphology, and vessel geometry are not isolated predictors, but elements of a dynamic pathophysiological system. By reducing this complexity to a sum of discrete, independently weighted factors, scoring systems may fail to account for important non-linear interactions or correlated risks. This trade-off between usability and precision is common in clinical tools; however, it highlights the need for complementary use of full predictive models, available at https://martascore.shinyapps.io/MARTA/, or AI-based tools, especially in borderline or complex cases where subtle combinations of features may critically influence outcomes.

Focusing on results of our cohort, we considered a composite safety outcome including any neurological deficit, mRS worsening at discharge, or death related to procedural complications. The overall rates of composite outcomes were lower in the EVT cohorts compared to the NT ones (EVT dev/test= 6.3/5.1% vs. NT dev/test= 12.8/15.9%). Also, major neurological complications, mRS worsening and mortality were lower in the EVT cohort (EVT dev/test= 2.5/1.6%, 3.4/3.4% and 0/0.5% vs. NT dev/test= 4.8/6.5%, 9.6/13% and 0.7/2.2% respectively). In the endovascular cohort, coiling with or without balloon assistance compared with other advanced endovascular treatments, was associated with higher complication risks. The overall complication rate associated with coiling (+ balloon assisted technique) was 16.3%, in line with previous reports, such as the ARETA study, including more than one thousand patients.[14] We can argue that the increased risk rate can be partially explained by the longer procedure time and the intrasaccular manipulation associated with coiling, compared with newer approaches such as intrasaccular devices, stent assisted coiling or flow diversion. We found that some locations, such as ICA-T, MCA, distal ACA or VA, an increasing aneurysm dimension, and some other characteristics, such as collateral branches originating from the aneurysmal sac were added value for the prediction of endovascular treatment complications in the logistic regression. In the neurosurgical cohort we found that some locations, such as posterior circulation or distal ACA, increased aneurysm size, shallow shape, and focal stenosis of the parent artery were added value for prediction of complications in the logistic regression. Finally, although morbidity and mortality rates are notably higher in the neurosurgical cohort, we emphasize that the score is not intended to compare EVT and NT. Instead, its purpose is to identify escalating risk levels within each approach, recognizing that certain variables are more relevant to one treatment modality than the other. Under these premises, MARTA scores have moderate predictive accuracy and may help in identifying specific aneurysmal features and delineate the a-priori risk related to treatment, therefore aiding in informing patients and multidisciplinary decision-making.

License CC BY-NC-ND 4.0

Limitations

To mitigate potential selection bias in treatment modality decisions, we employed a multicenter design across 15 high-volume neurovascular centers, standardized inclusion criteria, and outcome definitions, and developed separate predictive models for EVT and NT. Additionally, variable selection was guided by a Delphi consensus to ensure objectivity, and external validation was performed to enhance generalizability across diverse clinical settings. However, we acknowledge that individual clinician preferences may still influence treatment choices, which represents a potential limitation. First, our study is based on decentralized collection of prospective data from several tertiary referral neurovascular centers, therefore implying an intrinsic risk of selection bias. However, the stability of the score's performance in the validation cohort and the internal assessment through calibration confer robustness to our findings, potentially supporting their generalizability. Second, MARTA scores focus solely on treatment risks and does not account for variables associated with the risk of aneurysm rupture. The integration of such data in a single score might be useful in clinical practice. Third, certain aneurysm locations and morphologies may have been underrepresented, as well as some treatment strategies. Therefore, further studies are needed to provide extensive external validation for MARTA score and test the accuracy of MARTA against further developed scores to identify the most useful tool for patient management. Future studies could explore incorporating failed attempts to further refine risk prediction. Fourth, the exclusion of unsuccessful treatment attempts may limit the generalizability of the MARTA scores to the full spectrum of procedural risks, as aborted procedures represent a real-world risk in UIA treatment, even if a sensitivity analysis including these cases demonstrated no significant impact on model performance, supporting the robustness of our approach. Fifth, the lack of granular data on individual neurosurgeon and neurointerventionist experience, such as years of practice or case volume, which could influence treatment outcomes. While all participating centers were high-volume tertiary referral centers (≥50 UIA treatments annually), this may limit the generalizability of the MARTA scores to less experienced or lower-volume centers. Future validation studies in lower-volume or less experienced centers are needed to confirm the scores' broader applicability. Finally, it should be noted that more granular measures, including radiomics and neuroinflammatory status, may add to the currently simplified score, which therefore represents a platform on which to build for further steps.

Conclusions

This study highlights the predictive value of the MARTA score for neurological complications and clinical deterioration after EVT/NT for UIA. Clinicians can integrate this predictive model into a comprehensive framework to possibly aid in the process of informing patients and individualize the treatment approach, also using the open-source calculator made available at https://martascore.shinyapps.io/MARTA/. Further external validation is needed to confirm MARTA scores full generalizability.

References

License CC BY-NC-ND 4.0

1. Molyneux AJ, Kerr RS, Yu LM, Clarke M, Sneade M, Yarnold JA, Sandercock P; International Subarachnoid Aneurysm Trial (ISAT) Collaborative Group. International subarachnoid aneurysm trial (ISAT) of neurosurgical clipping versus endovascular coiling in 2143 patients with ruptured intracranial aneurysms: a randomised comparison of effects on survival, dependency, seizures, rebleeding, subgroups, and aneurysm occlusion. Lancet. 2005 Sep 3-9;366(9488):809-17. doi: 10.1016/S0140-6736(05)67214-5. PMID: 16139655.
2. Algra AM, Lindgren A, Vergouwen MDI, Greving JP, van der Schaaf IC, van Doormaal TPC, Rinkel GJE. Procedural Clinical Complications, Case-Fatality Risks, and Risk Factors in Endovascular and Neurosurgical Treatment of Unruptured Intracranial Aneurysms: A Systematic Review and Meta-analysis. JAMA Neurol. 2019 Mar 1;76(3):282-293. doi: 10.1001/jamaneurol.2018.4165. PMID: 30592482; PMCID: PMC6439725.
3. Kotowski M, Naggara O, Darsaut TE, Nolet S, Gevry G, Kouznetsov E, Raymond J. Safety and occlusion rates of surgical treatment of unruptured intracranial aneurysms: a systematic review and meta-analysis of the literature from 1990 to 2011. J Neurol Neurosurg Psychiatry. 2013 Jan;84(1):42-8. doi: 10.1136/jnnp-2011-302068. Epub 2012 Sep 25. PMID: 23012447.
4. Naggara ON, Lecler A, Oppenheim C, Meder JF, Raymond J. Endovascular treatment of intracranial unruptured aneurysms: a systematic review of the literature on safety with emphasis on subgroup analyses. Radiology. 2012 Jun;263(3):828-35. doi: 10.1148/radiol.12112114. PMID: 22623696.
5. Etminan N, Brown RD Jr, Beseoglu K, Juvela S, Raymond J, Morita A, Torner JC, Derdeyn CP, Raabe A, Mocco J, Korja M, Abdulazim A, Amin-Hanjani S, Al-Shahi Salman R, Barrow DL, Bederson J, Bonafe A, Dumont AS, Fiorella DJ, Gruber A, Hankey GJ, Hasan DM, Hoh BL, Jabbour P, Kasuya H, Kelly ME, Kirkpatrick PJ, Knuckey N, Koivisto T, Krings T, Lawton MT, Marotta TR, Mayer SA, Mee E, Pereira VM, Molyneux A, Morgan MK, Mori K, Murayama Y, Nagahiro S, Nakayama N, Niemelä M, Ogilvy CS, Pierot L, Rabinstein AA, Roos YB, Rinne J, Rosenwasser RH, Ronkainen A, Schaller K, Seifert V, Solomon RA, Spears J, Steiger HJ, Vergouwen MD, Wanke I, Wermer MJ, Wong GK, Wong JH, Zipfel GJ, Connolly ES Jr, Steinmetz H, Lanzino G, Pasqualin A, Rüfenacht D, Vajkoczy P, McDougall C, Hänggi D, LeRoux P, Rinkel GJ, Macdonald RL. The unruptured intracranial aneurysm treatment score: a multidisciplinary consensus. Neurology. 2015 Sep 8;85(10):881-9. doi: 10.1212/WNL.0000000000001891. Epub 2015 Aug 14. PMID: 26276380; PMCID: PMC4560059.
6. Greving JP, Wermer MJ, Brown RD Jr, Morita A, Juvela S, Yonekura M, Ishibashi T, Torner JC, Nakayama T, Rinkel GJ, Algra A. Development of the PHASES score for prediction of risk of rupture of intracranial aneurysms: a pooled analysis of six prospective cohort studies. Lancet Neurol. 2014 Jan;13(1):59-66. doi: 10.1016/S1474-4422(13)70263-1. Epub 2013 Nov 27. PMID: 24290159.
7. Algra AM, Greving JP, de Winkel J, Kurtelius A, Laban K, Verbaan D, van den Berg R, Vandertop W, Lindgren A, Krings T, Woo PYM, Wong GKC, Roozenbeek B, van Es ACGM, Dammers R, Etminan N, Boogaarts H, van Doormaal T, van der

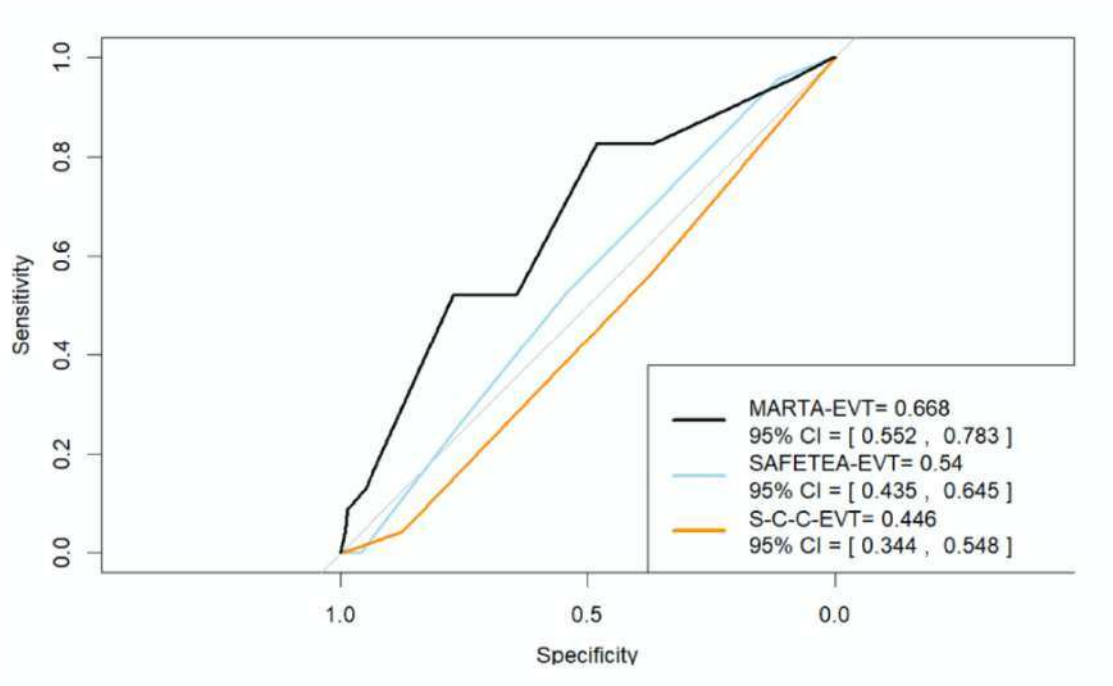
License CC BY-NC-ND 4.0

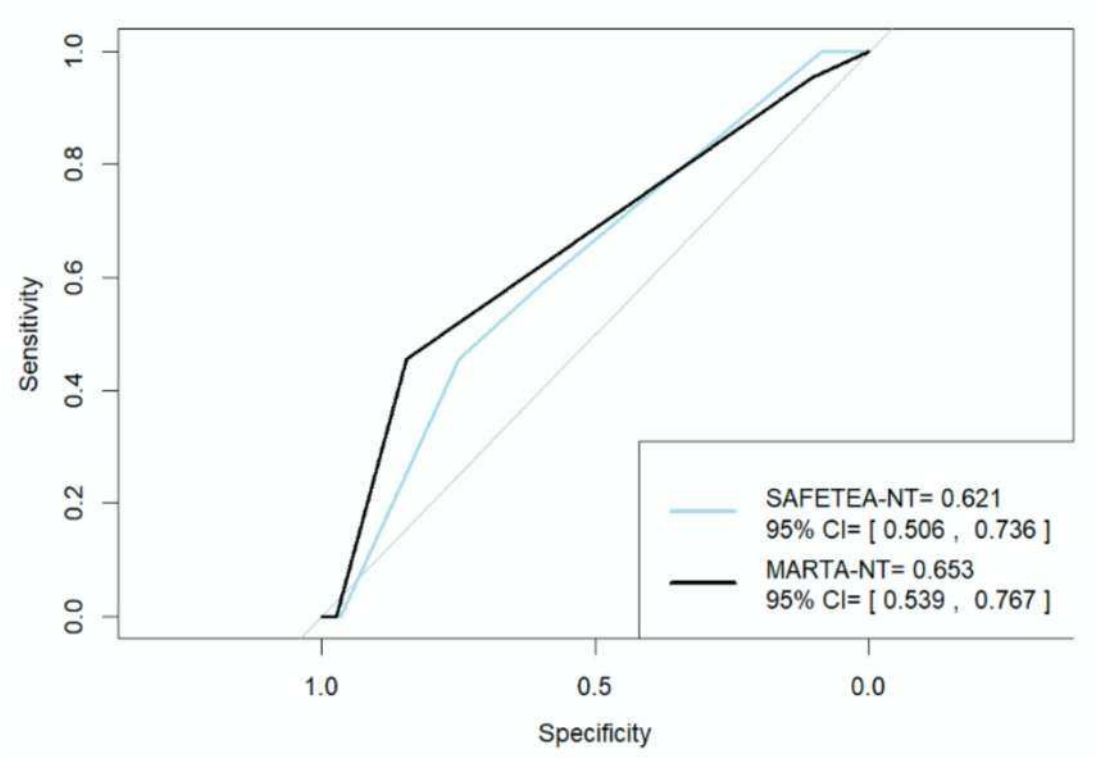
Zwan A, van der Schaaf IC, Rinkel GJE, Vergouwen MDI. Development of the SAFETEA Scores for Predicting Risks of Complications of Preventive Endovascular or Microneurosurgical Intracranial Aneurysm Occlusion. Neurology. 2022 Oct 17;99(16):e1725-e1737. doi: 10.1212/WNL.0000000000200978. PMID: 36240099.

8. Ji W, Liu A, Lv X, Kang H, Sun L, Li Y, Yang X, Jiang C, Wu Z. Risk Score for Neurological Complications After Endovascular Treatment of Unruptured Intracranial Aneurysms. Stroke. 2016 Apr;47(4):971-8. doi: 10.1161/STROKEAHA.115.012097. Epub 2016 Feb 11. PMID: 26869386; PMCID: PMC4819491.
9. Ogilvy CS, Carter BS. A proposed comprehensive grading system to predict outcome for surgical management of intracranial aneurysms. Neurosurgery. 1998 May;42(5):959-68; discussion 968-70. doi: 10.1097/00006123-199805000-00001. PMID: 9588539.
10. Newman WC, Neal DW, Hoh BL. A new comorbidities index for risk stratification for treatment of unruptured cerebral aneurysms. J Neurosurg. 2016 Sep;125(3):713-9. doi: 10.3171/2015.8.JNS14553. Epub 2016 Jan 8. PMID: 26745486.
11. Sweid A, Starke RM, Herial N, Chalouhi N, Das S, Baldassari MP, Alexander TD, Tjoumakaris S, Gooch MR, Hasan D, Rosenwasser RH, Romo V, Jabbour P. Predictors of Complications, Functional Outcome, and Morbidity in a Large Cohort Treated With Flow Diversion. Neurosurgery. 2020 Sep 15;87(4):730-743. doi: 10.1093/neuros/nyz508. PMID: 31858148.
12. Ji W, Liu A, Lv X, Kang H, Sun L, Li Y, Yang X, Jiang C, Wu Z. Risk Score for Neurological Complications After Endovascular Treatment of Unruptured Intracranial Aneurysms. Stroke. 2016 Apr;47(4):971-8. doi: 10.1161/STROKEAHA.115.012097. Epub 2016 Feb 11. PMID: 26869386; PMCID: PMC4819491.
13. Diana F, Romoli M, Raz E, Agid R, Albuquerque FC, Arthur AS, Beck J, Berge J, Boogaarts HD, Burkhardt JK, Cenzato M, Chapot R, Charbel FT, Desal H, Esposito G, Fifi JT, Florian S, Gruber A, Hassan AE, Jabbour P, Jadhav AP, Korja M, Krings T, Lanzino G, Meling TR, Morcos J, Mosimann PJ, Nossek E, Pereira VM, Raabe A, Regli L, Rohde V, Siddiqui AH, Tanikawa R, Tjoumakaris SI, Tomasello A, Vajkoczy P, Valvassori L, Velinov N, Walsh D, Woo H, Xu B, Yoshimura S, van Zwam WH, Peschillo S. Complex intracranial aneurysms: a DELPHI study to define associated characteristics. Acta Neurochir (Wien). 2024 Jul 11;166(1):294. doi: 10.1007/s00701-024-06182-z. PMID: 38990336.
14. Pierot L, Barbe C, Nguyen HA, Herbreteau D, Gauvrit JY, Januel AC, Bala F, Comby PO, Desal H, Velasco S, Aggour M, Chabert E, Sedat J, Trystram D, Marnat G, Gallas S, Rodesch G, Clarencon F, Soize S, Gawlitza M, Spelle L, White P. Intraoperative Complications of Endovascular Treatment of Intracranial Aneurysms with Coiling or Balloon-assisted Coiling in a Prospective Multicenter Cohort of 1088 Participants: Analysis of Recanalization after Endovascular Treatment of Intracranial Aneurysm (ARETA) Study. Radiology. 2020 May;295(2):381-389. doi: 10.1148/radiol.2020191842. Epub 2020 Feb 25. Erratum

License CC BY-NC-ND 4.0

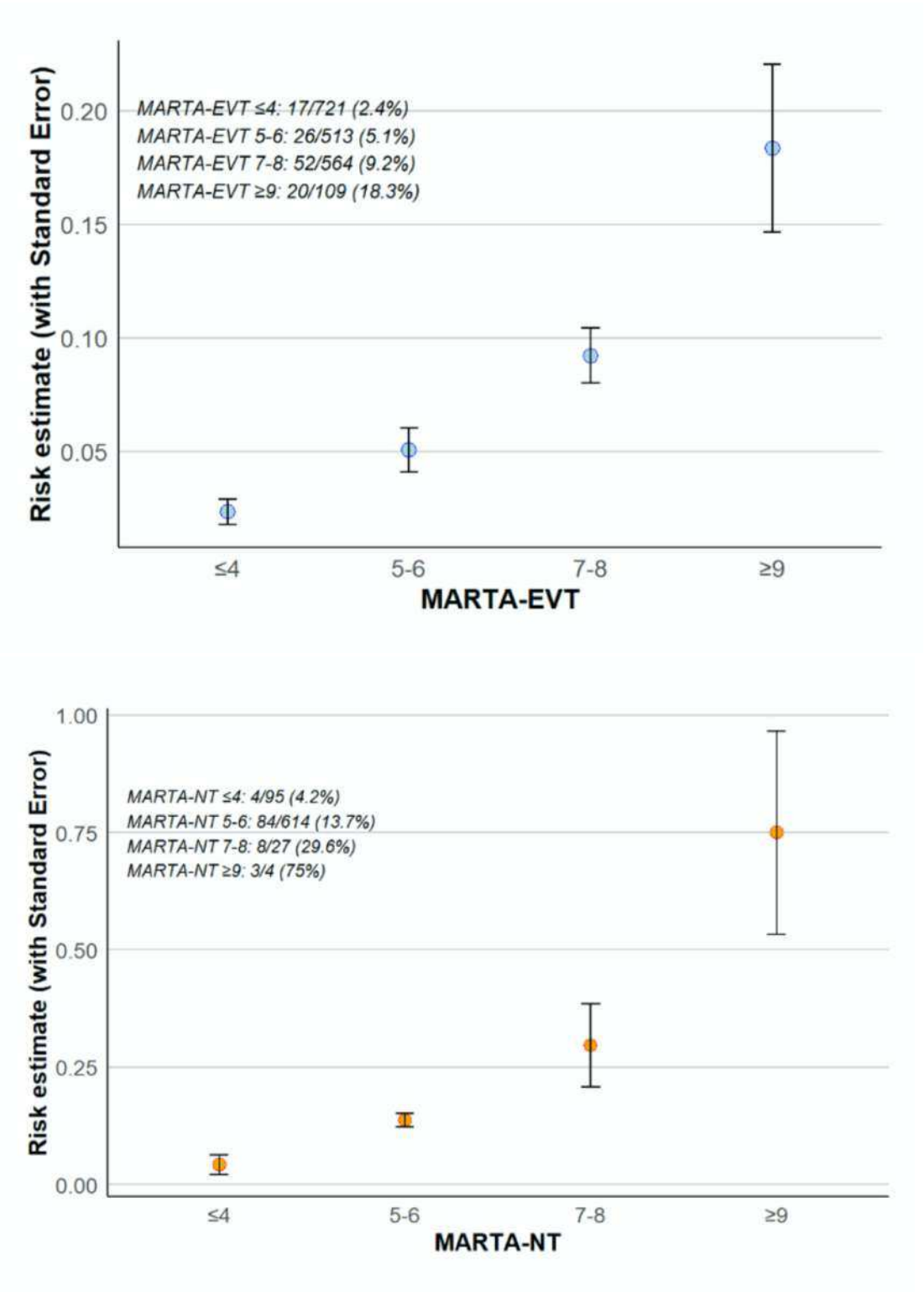
Figure 1





License CC BY-NC-ND 4.0

Figure 2



License CC BY-NC-ND 4.0

Appendix 3. IFD-assisted coiling

IFD-assisted coiling

brain sciences

MDPI

Article

Intrasaccular Flow Disruptor-Assisted Coiling of Intracranial Aneurysms Using the Novel Contour Neurovascular Systems and NEQSTENT: A Single-Center Safety and Feasibility Study

Francesco Diana [1], Marta de Dios Lascuevas [2,3], Simone Peschillo [4,5,*], Eytan Raz [6], Shinichi Yoshimura [7], Manuel Requena Ruiz [2,3], David Hernández Morales [2,3] and Alejandro Tomasello [2,3]

1 Neuroradiology, University Hospital 'San Giovanni di Dio e Ruggi d'Aragona', 84125 Salerno, Italy; francesco.diana@gmail.com
2 Neuroradiology, Vall d'Hebron Hospital Universitari, 08035 Barcelona, Spain; martalascuevas@gmail.com (M.d.D.L.); m.requenaruiz@gmail.com (M.R.R.); dhm050780@hotmail.com (D.H.M.); alejandrotomasello@gmail.com (A.T.)
3 Grupo de Recerca en Ictus, Vall d'Hebron Institut de Recerca, 08035 Barcelona, Spain
4 UniCamillus International Medical University, 00131 Rome, Italy
5 Endovascular Neurosurgery, Pia Fondazione Cardinale G Panico Hospital, 73039 Tricase, Italy
6 Department of Radiology, NYU Langone Health, New York, NY 10016, USA; eytan.raz@gmail.com
7 Department of Neurosurgery, Hyogo College of Medicine, Nishinomiya 663-8501, Japan; hyogoneuro@yahoo.co.jp
* Correspondence: simone.peschillo@gmail.com

check for updates

Citation: Diana, F.; de Dios Lascuevas, M.; Peschillo, S.; Raz, E.; Yoshimura, S.; Requena Ruiz, M.; Hernández Morales, D.; Tomasello, A. Intrasaccular Flow Disruptor-Assisted Coiling of Intracranial Aneurysms Using the Novel Contour Neurovascular Systems and NEQSTENT: A Single-Center Safety and Feasibility Study. *Brain Sci.* **2022**, *12*, 991. https://doi.org/10.3390/brainsci12080991

Academic Editor: Simona Lattanzi

Received: 6 July 2022
Accepted: 24 July 2022
Published: 26 July 2022

Publisher's Note: MDPI stays neutral with regard to jurisdictional claims in published maps and institutional affiliations.

Copyright: © 2022 by the authors. Licensee MDPI, Basel, Switzerland. This article is an open access article distributed under the terms and conditions of the Creative Commons Attribution (CC BY) license (https://creativecommons.org/licenses/by/4.0/).

Abstract: *Background:* Intrasaccular flow disruptors (IFD) have been introduced in the treatment of intracranial aneurysms (IAs) to overcome the low aneurysm occlusion rate and the high recanalization rate of the coiling technique. Among them, the Contour Neurovascular System (CNS) and the Neqstent (NQS) were designed to reconstruct the aneurysmal neck and both can be used as assisting coiling devices. We aimed to report our preliminary experience with the flow disruptor-assisted coiling (IFD-AC) technique. *Methods:* We performed a retrospective analysis of prospectively collected data of all patients with IAs treated with the IFD-AC. *Results:* Between February 2021 and April 2022, we treated 15 IAs with the IFD-AC: 10 ruptured and 5 unruptured. The IFD-AC was successfully performed in 13 cases, with a post-operative RROC 1 in 12 cases (92.3%) and RROC 2 in 1 case (7.7%). There was one ischemic event (6.7%) and no hemorrhagic complications. Twelve patients underwent a mid-term radiologic follow-up: Ten IAs (83.4%) presented an adequate occlusion, while 2 (16.7%) had a recurrence. *Conclusions:* The IFD-AC, both with the CNS and the NQS, seems a safe technique with promising efficacy profile. The IFD-AC has proved to be safe without antiplatelet therapy in ruptured cases. Further studies are needed to confirm our preliminary results.

Keywords: brain aneurysms; endovascular treatment; coiling; assisted coiling; intrasaccular devices; flow disruptor

1. Introduction

Endovascular treatment (EVT) of intracranial aneurysms (IAs) became the preferred therapeutic modality after the introduction of Guglielmi detachable coils over three decades ago [1–5]. However, coiling of IAs, even with the balloon-assisted technique, raised criticism due to the low post-operative complete occlusion rate, between 57.9% [6] and 76% [7], and the high recanalization rate, which occurs in 8–33.6% of cases [8–11]. Aneurysm recanalization is associated with bleeding or re-bleeding risks, between 2.7% and 11% [7,12,13], and these risks are proportional to the rate of incomplete occlusion [7].

New devices, called intrasaccular flow disruptors, were developed to overcome these limitations. Nevertheless, randomized controlled trials [14–18] and observational

License CC BY-NC-ND 4.0

studies [19,20] assessing their efficacy showed rates of adequate occlusion (≈80%) and complete occlusion (≈54%) at the long-term follow-up comparable to coiling.

The Contour Neurovascular System (CNS) and the Neqstent (NQS) are intrasaccular devices designed to reconstruct the aneurysmal neck with a dual-layer radiopaque nitinol memory mesh. The NQS, with 48 wires, is the coiling assisting device. The coiling microcatheter can be jailed, or it can cross the meshes. Differently, the CNS, with 144 wires, was conceived as intrasaccular flow disruptor, but it can be used as a coiling assisting device with the jailing technique (Figure 1B). In any case, there are no available data in the literature on the flow disruptor-assisted coiling neither with NQS nor with CNS. This study aimed to report the feasibility and safety of the intrasaccular flow disruptor-assisted coiling (IFD-AC) with the NQS and CNS in the treatment of ruptured and unruptured IAs.

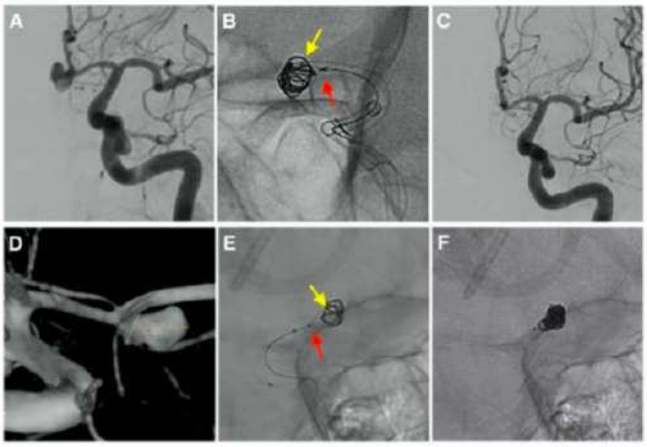


Figure 1. Cases of intrasaccular flow disruptor-assisted coiling (IFD-AC). (**A**–**C**) Case 15 performed with the CNS (red arrow) and a jailed coiling microcatheter (yellow arrow). (**D**–F). Case 12 performed with the NQS (red arrow), crossing its meshes with the coiling microcatheter (yellow arrow).

2. Materials and Methods

We performed a retrospective analysis of clinical and radiological data prospectively collected in the institutional database of Vall d'Hebron University Hospital of Barcelona. We included all patients with IA treated with the IFD-AC.

We collected baseline patients' clinical data, admission data, such as modified Rankin Scale (mRS), Hunt and Hess score, and Fisher score, aneurysms' characteristics, and procedural data (Table 1). We recorded procedural and post-procedural complications, radiological follow-up, done with CT angiography or Digital Subtracted Angiography, and clinical outcomes. The aneurysmal neck coverage of the intrasaccular device was classified as complete or incomplete, if part of the aneurysmal neck was uncovered. The aneurysm occlusion was quantified using the Raymond–Roy Class (RROC) [21]. Clinical outcome was measured with the mRS at the discharge and the 3-month follow-up.

The study was conducted in accordance with the Declaration of Helsinki and approved by the Institutional Ethics Committee of the University Hospital Vall d'Hebron (protocol code PR(AG)564/2021, date of approval 26 November 2021).

License CC BY-NC-ND 4.0

Table 1. Summary of baseline characteristics. ACoA: Anterior communicating artery; APT: Antiplatelet therapy; BA: Basilar artery; CNS: Contour Neurovascular System; DAP: Dual antiplatelets; EVD: External ventricular drainage; ICA: Internal carotid artery; OPhA: Ophthalmic artery; PCoA: Posterior communicating artery; SAP: Single antiplatelet.

		1	2	3	4	5	6	7	8	9	10	11	12	13	14	15
Patients	Sex	F	M	F	M	F	M	F	F	F	F	M	M	F	M	F
	Age	42	57	75	53	46	51	78	69	73	59	70	77	65	72	50
	1st treatment	Yes	Yes	Yes	Yes	Yes	No	Yes	Yes	Yes	Yes	Yes	Yes	Yes	Yes	Yes
	Baseline mRS	0	5	5	2	0	5	5	5	0	5	0	0	0	0	2
	SAH	Yes	Yes	Yes	Yes	Yes	Yes	Yes	Yes	Yes	Yes	No	No	No	No	No
	Hunt and Hess	2	4	5	2	1	5	5	5	2	3	0	0	0	0	0
	Fisher score	2	4	4	4	4	4	4	4	4	4	0	0	0	0	0
	Treatment timing, day	2	1	1	2	1	22	1	2	2	2	-	-	-	-	-
Aneurysms	Location	ICA-OPhA	ACoA	BA	BA	ICA-PCoA	ACoA	ACoA	ICA-supracl	ICA-supracl	ICA-supracl	ACoA	ACoA	ACoA	ICA-supracl	ACoA
	Neck Width, mm	3.5	7.2	4.4	3.5	3.4	5	4.5	6	1.4	3	5	3.3	2.6	3.4	2.4
	Equatorial Width, mm	11	8.5	6.2	7.5	5.7	6	6.4	11	2.7	3.5	6	4	5.2	5.2	4.9
	Height (mm)	17	6.6	8	6	4	7.7	7.4	15	2.7	5.4	5	3.4	3.2	6.8	5
Devices	Device	NQS	NQS	CNS	CNS	NQS	NQS	NQS	NQS	NQS	CNS	CNS	NQS	NQS	NQS	CNS
	Size	9	11	7	7	7	7	7	9	7	5	9	7	7	7	5
	APT pre-medication	No	No	No	No	No	No	No	No	No	No	DAP *	SAP *	DAP *	SAP *	SAP *

* DAPT: ASA 100 mg and Clopidogrel 75 mg five days before treatment. SAPT: ASA 100 mg one day before treatment.

License CC BY-NC-ND 4.0

Endovascular Procedure

All cases were performed under general anesthesia, with a trans-femoral or trans-radial artery approach. Patients with unruptured IAs were prepared with dual or single antiplatelet therapy before treatment (Table 1). We did not use antiplatelets in ruptured IAs. We used intraoperative heparin in all cases, administering weight-adjusted doses and monitoring the Activated Clotting Time with a target range of 200–250 s. We routinely infused 15 mg of Nimodipine through the line of the guiding catheter. No other specific intraoperative drug was used.

A 6F long sheath was navigated into the main target artery. A preliminary diagnostic angiography with a three-dimensional rotational angiogram was used for aneurysm sizing and selection of working projections. We followed the sizing algorithm recommended by Cerus Endovascular to select the intrasaccular device. We generally used a bi-axial system for the IFD-AC, except for two cases requiring an intermediate catheter (PhenomPlus 4F—120 cm and SofiaPlus 6F—115 cm). In 10 cases, we used the jailing technique: a 0.017-inch coiling microcatheter (Echelon 10—0.017″ID × 150 cm) was navigated into the aneurysmal sack, subsequently, a NQS or CNS was deployed at the aneurysmal neck through a 0.021-inch microcatheter (Phenom 21—0.021″ID × 160 cm) and detached after coiling (Figure 1A–C). In three cases, we used the coil-through technique. Hence, the NQS was deployed, and its meshes were crossed with the coiling microcatheter (Figure 1E,F).

At the end of the procedure, we performed a control Vaso-CT in all cases.

3. Results

Between February 2021 and April 2022, we treated 15 patients with IAs using the IFD-AC: 9 females and 6 males, whose mean age was 61.2 ± 11.6.

Ten patients (67%) presented with aneurysmal subarachnoid hemorrhage (aSAH). At the admission, the median Hunt and Hess score was 3.15 (range 1–5) and the median Fisher score was 4 (range 2–4). In nine of them, the IFD-AC was the first line approach, and it was done within 24/48 h from aneurysm rupture. In one case (Case 6), the IFD-AC was performed after 22 days to retreat an incomplete coiled anterior communicating artery aneurysm (ACoAa).

Five patients with incidental IAs underwent an elective treatment. All of them had a baseline mRS ≤ 2.

Treated IAs had a mean equatorial width of 6.7 ± 2.8 mm, a mean neck width of 3.9 ± 1.5 mm, and a height of 6.9 ± 4.1 mm. Seven of them were located on the ACoA, six on the internal carotid artery (ICA) and two on the basilar tip.

The IFD-AC was successfully performed in 13 cases (Table 2): nine with the NQS and four with the CNS. After deployment of the intrasaccular device, the aneurysmal neck coverage was complete in 11 patients (84.6%) and incomplete in two cases (15.4%).

After coiling, we achieved a complete occlusion (RROC 1) in 12 cases (92.3%), a small neck remnant (RROC 2) in one case (7.7%). We failed to perform the IFD–AC in two cases in which we could not detach the device because of anatomical factors. In case 8 (Figure 2A), the NQS detachment was hampered by stenosis of the parent artery. The device was deployed but protruding outside the aneurysmal neck and worsening the parent artery stenosis (Figure 2B). This configuration caused the slowing down of the blood flow to distal territories and the distal embolization of the parieto-occipital M3 branch of the right middle cerebral artery (Figure 2C). The NQS was removed with the consequent arterial flow restoration (Figure 2D). The distal embolism did not cause neurological deficits. In case 10 (Figure 2E,F), the CNS covered the origin of a fetal PCoA (Figure 2G). Consequently, it was removed, and the initial strategy was switched to a BAC without procedural complications (Figure 2H).

License CC BY-NC-ND 4.0

Table 2. Complications and outcomes. Com: Complete; CTA: CT-angiography; DSA: Digital subtracted angiography; Inc: Incomplete.

		1	2	3	4	5	6	7	8 *	9	10 *	11	12	13	14	15
Immediate outcome	Procedure success	Yes	Yes	Yes	Yes	Yes	Yes	Yes	No	Yes	No	Yes	Yes	Yes	Yes	Yes
	Neck coverage	Inc	Inc	Com	Com	Com	Com	Com	-	Com	-	Com	Com	Com	Com	Com
	Intrasaccular flow	No	No	No	No	No	No	No	Yes	No	Yes	No	No	No	No	No
	Final RROC	2	1	1	1	1	1	1	2	1	1	1	1	1	1	1
Operative-related complications	Access site	No	No	No	No	No	No	No	No	No	No	No	No	No	No	No
	IA perforation	No	No	No	No	No	No	No	No	No	No	No	No	No	No	No
	Ischemic stroke	No	No	No	No	No	No	No	Yes	No	No	No	No	No	No	No
	Morbidity	No	No	No	No	No	No	No	No	No	No	No	No	No	No	No
	Mortality	No	No	No	No	No	No	No	No	No	No	No	No	No	No	No
Unrelated complications	Vasospasm	No	No	No	No	Yes	No	No	Yes	Yes	Yes	No	No	No	No	No
	EVD	No	Yes	Yes	No	No	Yes	Yes	Yes	Yes	Yes	No	No	No	No	No
	VPS	No	No	No	No	No	No	Yes °	No	No	No	No	No	No	No	No
Clinical outcomes	Discharge mRS	0	1	2	1	3	4	4	6	4	6	0	0	0	0	2
	90-days mRS	0	0	0	0	0	2	4	0	5	6	0	0	0	0	0
Radiological outcomes	Imaging f-u	DSA	CTA	CTA	DSA	DSA	CTA	-	DSA	CTA	CTA	DSA	CTA	DSA	DSA	CTA
	F-u time, day	180	90	120	215	180	90	-	25	205	3	90	90	180	90	1
	RROC scale	3	2	2	2	1	1	-	1	1	1	1	1	1	3	1
	Retreatment	Yes °	No	No	No	No	No	No	No	No	No	No	No	No	No	No

* Case 8: deployment failed due to stenosis of the parent artery. The device protruded, inducing slowing of the distal flow and subsequent embolism to the distal parieto-occipital M3 segment. The NQS was removed with arterial flow restoration. Case 10: it was a wide-neck aneurysm encompassing the origin of a fetal PCoA. We opted for balloon-assisted coiling to protect the PCoA from CNS and coils protrusion. ° Case 7: VPS was positioned 72 days after treatment. ° Case 1: the patient was retreated due to aneurysm recurrence with a flow diverter.

License CC BY-NC-ND 4.0

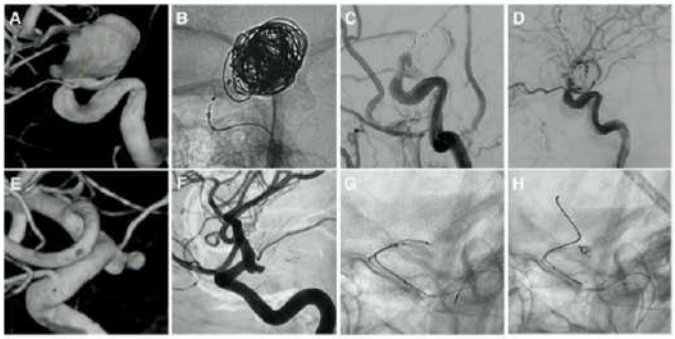


Figure 2. Cases of unsuccessful intrasaccular flow disruptor-assisted coiling. Case 8: **(A)** Supraclinoid ICA aneurysm with severe stenosis of the parent artery. **(B)** IFD-AC performed with the NQS. **(C,D)** Flow arrest completely resolved after NQS removal. Case 10: **(E,F)** Posterior communicating artery aneurysm. **(G)** Incomplete deployment of the NQS due to the arterial anatomy. **(H)** Treatment continued with a balloon-assisted coiling.

Regarding procedural complications, we recorded one (6.7%) minor ischemic event, which did not cause neurological deficits. There were no procedural hemorrhagic complications caused by aneurysm or vessel perforation, no disabling or deathly events.

Among 10 patients with aSAH, two developed significant arterial vasospasm (Case 5 and 8) requiring treatments with intra-arterial injection of Verapamil and mechanical dilatation with stent retriever. Seven patients received external ventricular drainage (EVD), switched to a ventriculoperitoneal shunt (VPS) in one case.

Four patients with SAH had an mRS ≤ 2 at the discharge (40%), while 7 (70%) at the three months follow-up. In-hospital mortality due to SAH complications was 20%. All patients with unruptured aneurysm had an mRS ≤ 2 at the discharge and at the 3-months follow-up.

Radiological follow-up was available in 12 of 13 patients successfully treated with the IFD-AC. Follow-up time ranged between 1 and 215 days. Aneurysm adequate occlusion was seen in 10 patients (83.4%): seven complete occlusions (RROC 1) and three with a small residual neck (RROC 2). Aneurysm recanalization (RROC 3) occurred in two patients (16.7%). Retreatment was done in one patient (Case 1) who underwent a NQS-AC with a final RROC 2. He was retreated with a flow diverter. We had no cases of aneurysm re-rupture.

4. Discussion

Intrasaccular flow disruption is a new endovascular approach to treat IAs, aiming to disrupt the intra-aneurysmal flow and to create intra-aneurysmal thrombosis. Intrasaccular flow disruptors have different shapes and sizes. The majority of them occupy the aneurysmal sac, such as the Woven-EndoBridge (MicroVention, Aliso Viejo, CA, USA), the Artisse, and the Medina Embolic Device (Medtronic, Irvine, CA, USA), while the CNS adapts to the lower half of the aneurysm, covering the neck. It is a circular, dual-layered structure of 2×72 nitinol wires with one radiopaque platinum marker. It is retrievable and electrolytically detached. It deploys through 0.021″ or 0.027″ microcatheters. It can also be used as an assisting coiling device, jailing a coiling microcatheter, although it has never been described before. The NQS device is derived from the CNS, made by 48 wires, developed to create an aneurysmal neck scaffolding for coils. This is, to date, the first series reporting results of the new IFD-AC technique, both with the NQS and the CNS.

The feasibility of the IFD-AC is mainly related to the device deployment. In this series, the IFD was successfully deployed in 13 cases (86.7%). This rate is relatively high if compared with the Cerus study [18] in which the CNS was successfully deployed at the first attempt in 21 of 32 patients (66%). Our technical failures were caused by anatomical factors which hamper the usage of the IFD. We can argue that parent artery stenoses, wide-neck

License CC BY-NC-ND 4.0

aneurysms encompassing the origin of a branch or aneurysms with a small neck unsuited for two parallel microcatheters are the main limitations of the IFD-AC technique.

The aneurysmal neck scaffolding created by the IFD is an important factor affecting the long-term outcome [22]. In our experience, the complete neck coverage was achieved 84.6% of cases.The improper positioning or orientation of the IFD creates unfavorable flow conditions [23,24], which affect the immediate and complete aneurysm occlusion. In our opinion the adjunctive coils of the IFD-AC technique can help to face this limitation (Figure 3A). Indeed, just one of the two cases with a residual uncovered neck resulted in a neck remnant after coiling and recurrence at the mid-term follow-up. Moreover, there are other specific cases in which the CNS may benefit from coiling. First, when the CNS is undersized to avoid protrusion in the parent artery. In this case, it has a flat configuration with a reduced grip on the aneurysmal wall. Coils can stabilize the CNS, avoiding its migration inside the sac (Figure 3B). Second, in ruptured cases, to ensure the immediate occlusion of the aneurysm.

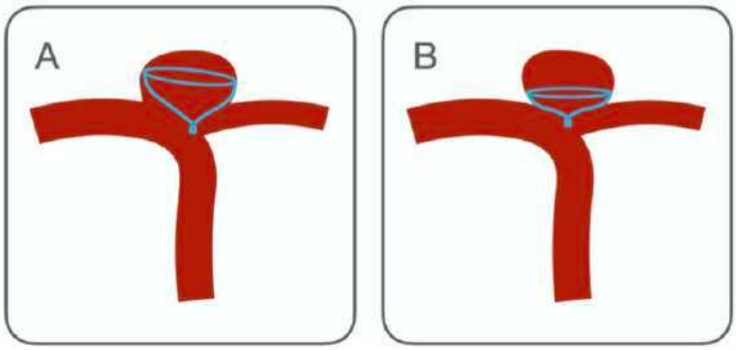


Figure 3. Contour Neurovascular System deployment configurations which may benefit of adjunctive coils. (**A**) CNS incomplete aneurysmal neck coverage. A condition similar to the "dog ear" remnant of the aneurysm clipping, representing a risk for aneurysm recanalization. (**B**) Aneurysmal sack encompassing the origin of an artery. This branch is at risk of being occluded by the CNS. In this case, the CNS is undersized, hence, it opens in a flat configuration, which reduces the anchoring of the device to the aneurysmal wall and increases the risk of intrasaccular migration.

We can infer the important role of the IFD-AC in ruptured aneurysms looking at the results of the SAC [25,26]. In ruptured cases the SAC has a high occlusion rate, but the overall complication rate is not negligible (≈20%), and the safety of the proper antiplatelet therapy needed for stenting has not been evaluated in the acute setting. The IFD-AC can keep advantages of the SAC, such as the aneurysmal neck scaffolding that increases coils packaging and trigger the aneurysmal neck endothelialization, and can overcome problems related to the antiplatelet therapy. Indeed, our preliminary experience suggests that the IFD-AC can be performed in ruptured aneurysms without significant embolic complications.

Aneurysm occlusion and recanalization rates are the main concerns of the endovascular treatment [6,12,15,16,27,28]. Among patients treated successfully with the IFD-AC the post-operative aneurysm complete occlusion rate was 92.3%, and the mid-term aneurysm complete occlusion rate was 70%. These are promising results if compared with the results of the Cerus study, in which the immediate complete occlusion rate was 7–10%, and the mid-term complete occlusion rate was 44% [18]. Aneurysm recurrence occurred in two cases, both treated with NQS-AC. There was no recurrence in the group of CNS-AC. Despite the small number of cases, we can speculate that the CNS in assisted coiling may increase the complete occlusion rate, compared to the NQS, due to its structure that allows

License CC BY-NC-ND 4.0

denser aneurysmal neck scaffolding and higher intrasaccular flow disruption effect. Further studies are needed to confirm this result.

Finally, the safety profile of the NQS and CNS seems acceptable and most likely comparable with other endovascular treatment options.

5. Limitations

This study has several limitations. First, the small sample size. The encouraging, clinical and radiological outcomes need to be re-assessed with larger sample sizes. Second, the role of intra-operative antiplatelets, both in ruptured and unruptured cases, need to be assessed in further studies. Third, we included aneurysms with different locations and thus different risk of recurrence [29]. Further studies are needed to assess treatment efficacy in different locations. Fourth, the efficacy of the IFD-AC needs to be assessed in studies with long-term follow-up.

6. Conclusions

The intrasaccular flow disruptor-assisted coiling with the Contour Neurovascular System and the Neqstent seems a safe technique for both ruptured and unruptured aneurysms. Our series demonstrated a promising efficacy profile. In ruptured cases, the intrasaccular flow disruptor-assisted coiling has proved to be safe without antiplatelet therapy. Further studies are needed to confirm our preliminary results.

Author Contributions: Conceptualization, F.D.; methodology, F.D. and M.d.D.L.; investigation, F.D. and S.P.; resources, M.d.D.L., M.R.R., D.H.M. and A.T.; data curation, M.d.D.L., M.R.R. and D.H.M.; writing—original draft preparation, F.D. and S.P.; writing—review and editing, E.R., S.Y., M.R.R., D.H.M., M.d.D.L. and A.T.; supervision, S.P. and A.T. All authors have read and agreed to the published version of the manuscript.

Funding: This research received no external funding.

Institutional Review Board Statement: The study was conducted in accordance with the Declaration of Helsinki, and approved by the Institutional Ethics Committee of the University Hospital Vall d'Hebron (protocol code PR(AG)564/2021, date of approval 26 November 2021).

Informed Consent Statement: Informed consent was obtained from all subjects involved in the study.

Data Availability Statement: All data relevant to the study are included in the article.

Conflicts of Interest: The authors declare no conflict of interest.

References

1. Guglielmi, G.; Viñuela, F.; Sepetka, I.; Macellari, V. Electrothrombosis of Saccular Aneurysms via Endovascular Approach. Part 1: Electrochemical Basis, Technique, and Experimental Results. *J. Neurosurg.* **1991**, *75*, 1–7. [CrossRef] [PubMed]
2. Guglielmi, G.; Viñuela, F.; Dion, J.; Duckwiler, G. Electrothrombosis of Saccular Aneurysms via Endovascular Approach. Part 2: Preliminary Clinical Experience. *J. Neurosurg.* **1991**, *75*, 8–14. [CrossRef] [PubMed]
3. Molyneux, A. International Subarachnoid Aneurysm Trial (ISAT) of Neurosurgical Clipping versus Endovascular Coiling in 2143 Patients with Ruptured Intracranial Aneurysms: A Randomised Trial. *Lancet* **2002**, *360*, 1267–1274. [CrossRef]
4. McDougall, C.G.; Spetzler, R.F.; Zabramski, J.M.; Partovi, S.; Hills, N.K.; Nakaji, P.; Albuquerque, F.C. The Barrow Ruptured Aneurysm Trial. *J. Neurosurg.* **2012**, *116*, 135–144. [CrossRef]
5. Wiebers, D.O. Unruptured Intracranial Aneurysms: Natural History, Clinical Outcome, and Risks of Surgical and Endovascular Treatment. *Lancet* **2003**, *362*, 103–110. [CrossRef]
6. Pierot, L.; Barbe, C.; Thierry, A.; Bala, F.; Eugene, F.; Cognard, C.; Herbreteau, D.; Velasco, S.; Chabert, E.; Desal, H.; et al. Patient and Aneurysm Factors Associated with Aneurysm Recanalization after Coiling. *J. Neurointerv. Surg.* **2021**, neurintsurg-2021-017972. [CrossRef]
7. Johnston, S.C.; Dowd, C.F.; Higashida, R.T.; Lawton, M.T.; Duckwiler, G.R.; Gress, D.R. CARAT Investigators Predictors of Rehemorrhage after Treatment of Ruptured Intracranial Aneurysms: The Cerebral Aneurysm Rerupture After Treatment (CARAT) Study. *Stroke* **2008**, *39*, 120–125. [CrossRef]

License CC BY-NC-ND 4.0

8. Ferns, S.P.; Sprengers, M.E.S.; van Rooij, W.J.; Rinkel, G.J.E.; van Rijn, J.C.; Bipat, S.; Sluzewski, M.; Majoie, C.B.L.M. Coiling of Intracranial Aneurysms: A Systematic Review on Initial Occlusion and Reopening and Retreatment Rates. *Stroke* **2009**, *40*, e523–e529. [CrossRef]
9. Benaissa, A.; Barbe, C.; Pierot, L. Analysis of Recanalization after Endovascular Treatment of Intracranial Aneurysm (ARETA Trial): Presentation of a Prospective Multicenter Study. *J. Neuroradiol.* **2015**, *42*, 80–85. [CrossRef]
10. Taschner, C.A.; Chapot, R.; Costalat, V.; Machi, P.; Courthéoux, P.; Barreau, X.; Berge, J.; Pierot, L.; Kadziolka, K.; Jean, B.; et al. Second-Generation Hydrogel Coils for the Endovascular Treatment of Intracranial Aneurysms: A Randomized Controlled Trial. *Stroke* **2018**, *49*, 667–674. [CrossRef]
11. Bendok, B.R.; Abi-Aad, K.R.; Ward, J.D.; Kniss, J.F.; Kwasny, M.J.; Rahme, R.J.; Aoun, S.G.; El Ahmadieh, T.Y.; El Tecle, N.E.; Zammar, S.G.; et al. The Hydrogel Endovascular Aneurysm Treatment Trial (HEAT): A Randomized Controlled Trial of the Second-Generation Hydrogel Coil. *Neurosurgery* **2020**, *86*, 615–624. [CrossRef]
12. Molyneux, A.J.; Kerr, R.S.C.; Yu, L.-M.; Clarke, M.; Sneade, M.; Yarnold, J.A.; Sandercock, P. International Subarachnoid Aneurysm Trial (ISAT) Collaborative Group International Subarachnoid Aneurysm Trial (ISAT) of Neurosurgical Clipping versus Endovascular Coiling in 2143 Patients with Ruptured Intracranial Aneurysms: A Randomised Comparison of Effects on Survival, Dependency, Seizures, Rebleeding, Subgroups, and Aneurysm Occlusion. *Lancet* **2005**, *366*, 809–817. [CrossRef]
13. McDougall, C.G.; Johnston, S.C.; Gholkar, A.; Barnwell, S.L.; Vazquez Suarez, J.C.; Massó Romero, J.; Chaloupka, J.C.; Bonafe, A.; Wakhloo, A.K.; Tampieri, D.; et al. Bioactive versus Bare Platinum Coils in the Treatment of Intracranial Aneurysms: The MAPS (Matrix and Platinum Science) Trial. *AJNR Am. J. Neuroradiol.* **2014**, *35*, 935–942. [CrossRef]
14. Pierot, L.; Costalat, V.; Moret, J.; Szikora, I.; Klisch, J.; Herbreteau, D.; Holtmannspötter, M.; Weber, W.; Januel, A.-C.; Liebig, T.; et al. Safety and Efficacy of Aneurysm Treatment with WEB: Results of the WEBCAST Study. *J. Neurosurg.* **2016**, *124*, 1250–1256. [CrossRef]
15. Pierot, L.; Gubucz, I.; Buhk, J.H.; Holtmannspötter, M.; Herbreteau, D.; Stockx, L.; Spelle, L.; Berkefeld, J.; Januel, A.-C.; Molyneux, A.; et al. Safety and Efficacy of Aneurysm Treatment with the WEB: Results of the WEBCAST 2 Study. *AJNR Am. J. Neuroradiol.* **2017**, *38*, 1151–1155. [CrossRef]
16. Fiorella, D.; Molyneux, A.; Coon, A.; Szikora, I.; Saatci, I.; Baltacioglu, F.; Sultan, A.; Arthur, A. WEB-IT Study Investigators Demographic, Procedural and 30-Day Safety Results from the WEB Intra-Saccular Therapy Study (WEB-IT). *J. Neurointerv. Surg.* **2017**, *9*, 1191–1196. [CrossRef]
17. Arthur, A.S.; Molyneux, A.; Coon, A.L.; Saatci, I.; Szikora, I.; Baltacioglu, F.; Sultan, A.; Hoit, D.; Delgado Almandoz, J.E.; Elijovich, L.; et al. The Safety and Effectiveness of the Woven EndoBridge (WEB) System for the Treatment of Wide-Necked Bifurcation Aneurysms: Final 12-Month Results of the Pivotal WEB Intrasaccular Therapy (WEB-IT) Study. *J. Neurointerv. Surg.* **2019**, *11*, 924–930. [CrossRef]
18. Liebig, T.; Killer-Oberpfalzer, M.; Gal, G.; Schramm, P.; Berlis, A.; Dorn, F.; Jansen, O.; Fiehler, J.; Wodarg, F. The Safety and Effectiveness of the Contour Neurovascular System (Contour) for the Treatment of Bifurcation Aneurysms: The CERUS Study. *Neurosurgery* **2021**, *90*, 270–277. [CrossRef]
19. Cortez, G.M.; Akture, E.; Monteiro, A.; Arthur, A.S.; Peterson, J.; Dornbos, D.; Jabbour, P.; Gooch, M.R.; Sweid, A.; Tjoumakaris, S.I.; et al. Woven EndoBridge Device for Ruptured Aneurysms: Perioperative Results of a US Multicenter Experience. *J. Neurointerv. Surg.* **2021**, *13*, 1012–1016. [CrossRef]
20. Da Ros, V.; Bozzi, A.; Comelli, C.; Semeraro, V.; Comelli, S.; Lucarelli, N.; Burdi, N.; Gandini, R. Ruptured Intracranial Aneurysms Treated with Woven Endobridge Intrasaccular Flow Disruptor: A Multicenter Experience. *World Neurosurg.* **2019**, *122*, e498–e505. [CrossRef]
21. Roy, D.; Milot, G.; Raymond, J. Endovascular Treatment of Unruptured Aneurysms. *Stroke* **2001**, *32*, 1998–2004. [CrossRef]
22. Cebral, J.R.; Chung, B.J.; Mut, F.; Chudyk, J.; Bleise, C.; Scrivano, E.; Lylyk, P.; Kadirvel, R.; Kallmes, D. Analysis of Flow Dynamics and Outcomes of Cerebral Aneurysms Treated with Intrasaccular Flow-Diverting Devices. *AJNR Am. J. Neuroradiol.* **2019**, *40*, 1511–1516. [CrossRef]
23. Hajirayat, K.; Gholampour, S.; Sharifi, I.; Bizari, D. Biomechanical Simulation to Compare the Blood Hemodynamics and Cerebral Aneurysm Rupture Risk in Patients with Different Aneurysm Necks. *J. Appl. Mech. Tech. Phy.* **2017**, *58*, 968–974. [CrossRef]
24. Gholampour, S.; Mehrjoo, S. Effect of Bifurcation in the Hemodynamic Changes and Rupture Risk of Small Intracranial Aneurysm. *Neurosurg. Rev.* **2021**, *44*, 1703–1712. [CrossRef]
25. Russo, R.; Bradac, G.B.; Castellan, L.; Gallesio, I.; Garbossa, D.; Iannucci, G.; Mardighian, D.; Menozzi, R.; Pitrone, A.; Romano, G.; et al. Neuroform Atlas Stent-Assisted Coiling of Ruptured Intracranial Aneurysms: A Multicenter Study. *J. Neuroradiol.* **2021**, *48*, 479–485. [CrossRef]
26. Mokin, M.; Primiani, C.T.; Ren, Z.; Piper, K.; Fiorella, D.J.; Rai, A.T.; Orlov, K.; Kislitsin, D.; Gorbatykh, A.; Mocco, J.; et al. Stent-Assisted Coiling of Cerebral Aneurysms: Multi-Center Analysis of Radiographic and Clinical Outcomes in 659 Patients. *J. Neurointerv. Surg.* **2020**, *12*, 289–297. [CrossRef]
27. Diana, F.; Pesce, A.; Toccaceli, G.; Muralidharan, V.; Raz, E.; Miscusi, M.; Raco, A.; Missori, P.; Peschillo, S. Microsurgical Clipping versus Newer Endovascular Techniques in Treatment of Unruptured Anterior Communicating Artery-Complex Aneurysms: A Meta-Analysis and Systematic Review. *Neurosurg. Rev.* **2021**, *45*, 1089–1100. [CrossRef]

License CC BY-NC-ND 4.0

28. Toccaceli, G.; Diana, F.; Cagnazzo, F.; Cannizzaro, D.; Lanzino, G.; Barbagallo, G.M.V.; Certo, F.; Bortolotti, C.; Signorelli, F.; Peschillo, S. Microsurgical Clipping Compared with New and Most Advanced Endovascular Techniques in the Treatment of Unruptured Middle Cerebral Artery Aneurysms: A Meta-Analysis in the Modern Era. *World Neurosurg.* **2020**, *137*, 451–464.e1. [CrossRef] [PubMed]
29. Liu, H.; Wang, D.; Leng, X.; Zheng, D.; Chen, F.; Wong, L.K.S.; Shi, L.; Leung, T.W.H. State-of-the-Art Computational Models of Circle of Willis with Physiological Applications: A Review. *IEEE Access* **2020**, *8*, 156261–156273. [CrossRef]

License CC BY-NC-ND 4.0

Appendix 4. FD with or without coils

Flow diverter with or without coils

Neurosurgical Review (2025) 48:519
https://doi.org/10.1007/s10143-025-03675-y

RESEARCH

Flow diverter with or without adjunctive coils in the treatment of large and giant intracranial aneurysms: a meta-analysis

Matias E. Sein[1] · Alejandro Ceciliano[2,3] · Fernando Navarro[2,3] · Silvina Molina[1] · Francisco Villasante[2,3] · Eduardo E. Tejado[1] · Manuel Requena[4,5] · David Hernandez[4,5] · Marta de Dios Lascuevas[4,5] · Alejandro Tomasello[4,5] · Francesco Diana[4,5,6]

Received: 24 August 2024 / Revised: 10 June 2025 / Accepted: 15 June 2025
© The Author(s), under exclusive licence to Springer-Verlag GmbH Germany, part of Springer Nature 2025

Abstract
To evaluate the available evidence on the efficacy and safety of flow diverters (FD) with or without adjunctive coils (C) for the treatment of large and giant aneurysms. A systematic review and meta-analysis of relevant studies in PubMed and selected articles up to December 2022 were conducted. The primary objective was to evaluate the rate of favorable occlusion O'Kelly Marotta (OKM) C-D at the last follow-up, while the secondary objective was to assess complication rates. A fixed-effects model was used, and relative risks (RR) and 95% confidence intervals (CI) were calculated. A total of 146 articles were identified, but only 10 were included in the meta-analysis. This included 541 controlled aneurysms out of a total of 680 large and giant aneurysms from 1,667 patients. We found no statistical differences in favorable OKM C-D outcomes with or without the adjunctive use of coils (RR 1.06 [0.96, 1.17]; $p=0.280$). However, FD+C presented fewer complications (RR 0.56 [0.33, 0.95]; $I^2=0\%$; $p=0.03$). No statistical differences were found for mortality (RR 0.86 [0.34, 2.18]; $I^2=0\%$; $p=0.75$). The use of adjunctive coils during treatment of large and giant aneurysms with FD seems to reduce the risk of procedural and delayed complications, while it does not increase the aneurysm occlusion rate.

Clinical trial number
Not applicable.

Keywords Cerebral aneurysm · Large · Giant · Flow diverters (FD) · Coils (C) · Meta-analysis

Abbreviations

C	coils
CI	Confidence intervals
CS	Case series
FD	Flow diverter
HR	Hazard Ratio
NOS	Newcastle-Ottawa Scale
OD	Odds Ratio
OKM	O´Kelly Marotta
PC	Prospective cohort
RC	Retrospective cohort
RR	Relative risks
SMD	Standardized mean difference

✉ Matias E. Sein
seinmatias@gmail.com

1 Interventional Neuroradiology, Italian Hospital, La Plata, Argentina

2 Interventional Neuroradiology, German Hospital, CABA, 155, 920, Berisso, Buenos Aires 1923, CP, Argentina

3 Interventional Neuroradiology, Austral Hospital, CABA, Buenos Aires, Argentina

4 Interventional Neuroradiology, Vall d'Hebron University Hospital, Barcelona, Spain

5 Stroke Research Group, Vall d'Hebron Research Institute, Barcelona, Spain

6 Department of Scienze della Vita, Della Salute e delle Professioni Sanitarie, Link Campus University, Rome, Italy

Published online: 20 June 2025

License CC BY-NC-ND 4.0

Introduction

Endovascular treatment (EVT) of large and giant aneurysms is challenging [1]. Coiling of such aneurysms has a high recanalization rate, even if assisted with balloon or stent [2, 3]. The introduction of flow diverters (FD) has changed the treatment of large and giant aneurysms, as well as those with wide necks, dissecting etiology, or fusiform shapes. Nevertheless, studies on FD in large and giant aneurysms are limited. Due to the delayed complete occlusion reported in these studies, some authors recommend adjunctive coiling with the aim to protect the dome, to reduce the intrasaccular flow velocity, and shear wall tension, promoting thrombus formation, early aneurysm occlusion, and reducing the risks of late rupture [2, 4–7]. Although efforts have been made to investigate the best therapeutic option, a consensus has not yet been established, and often it depends on the physician's preference [3]. Moreover, there is a concern about the complication rate related to the adjunctive coiling [3, 8, 9].

We aimed to provide a systematic review and meta-analysis to assess the efficacy and safety of FD with coils (FD+C), in comparison with FD alone for the treatment of large and giant aneurysms.

Materials and methods

Protocol and search strategy

This systematic review and meta-analysis followed the Preferred Reporting Items for Systematic Reviews and Meta-Analyses (PRISMA) guidelines, as well as the Cochrane manual [10].

We searched Medline electronic database until December 2022. Search terms included MeSH and Emtree terms as well as specific keywords for intracranial aneurysms and endovascular treatment with flow diverters, including: [("Intracranial Aneurysm"[Majr]) AND (large OR giant) AND coils AND (flow divert*)] OR [("Intracranial Aneurysm"[Majr]) AND (large OR giant) AND (flow divert*) AND (coils OR not coils)] OR [("Intracranial Aneurysm"[Majr]) AND (large OR giant) AND (flow divert*) AND (coil* OR not coil*)]. Additionally, manual searches were conducted in the reference lists of published articles to ensure the completeness of the bibliography.

We used the PICOS (Patient population, Intervention, Control, Outcome, Study design) framework for the inclusion criteria: (P) adult patients with large and giant intracranial aneurysms; (I) EVT with FD and coils; (C) EVT with FD alone; (O) adequate aneurysm occlusion rate, defined by the O'Kelly Marotta (OKM) grade C or D; secondary: procedural complication rates. Our search focused on interventional studies, either randomized or cohort studies (S).

We excluded non-English or Spanish language studies, unpublished studies, conference abstracts, studies including less than 5 patients, meta-analyses, comments, guidelines, technical notes, editorials, book chapters, and in vitro and animal studies.

Outcomes

The primary outcome was the adequate occlusion rate, defined by the O'Kelly Marotta (OKM) grade C or D. The OKM grading scale is a proposed method of assessing the degree of angiographic filling and contrast stasis in the setting of intracranial aneurysms treated by endovascular flow diversion [11].

Secondary outcomes were rates of procedure-related, hemorrhagic or ischemic complications, and mortality. Procedure-related complications ere defined as deployment complication, FD migration and acute thromboembolism. Hemorrhagic complications were defined as distal wire perforation, early and delayed aneurysm rupture, parenchymal hemorrhage aneurysm, while ischemic complications were defined as transient ischemic attack, minor and mayor cerebral infarction, delayed in-stent stenosis and mass effect.

Study selection

Two reviewers independently (SME and NF) assessed the titles and abstracts of the articles identified through the search strategy, as well as data extraction. All relevant publications were evaluated by these reviewers, who also determined the final inclusion of studies in the meta-analysis. Concordance between reviewers was assessed using the Covidence program. Disagreements were resolved through consensus in meetings with all authors.

The extracted data included authors, publication year, study design, number of treated patients, large and giant aneurysms treated with FD with or without coils, and the number of uncontrolled aneurysms.

Data extraction and quality assessment

The same reviewers independently extracted data from the included trials. Data extraction was performed using a standardized form to collect this information. The quality of included studies was assessed using the Newcastle-Ottawa Scale (NOS) for cohort studies, which evaluates studies based on three main aspects: selection, comparability, and determination of the outcome of interest [12, 13]. The scale sets a maximum score of 9 points, considering studies of

License CC BY-NC-ND 4.0

high quality if the score is ≥7 points. All eligible studies were included regardless of their assessed quality.

Statistical analysis

This meta-analysis was conducted using the Review Manager program (RevMan 5.4), Jamovi for Microsoft Windows, version 1.6 [Computer Software], and Open Meta Analyst. For each dichotomous outcome, the cumulative incidence (event rate) and the 95% confidence interval (CI) were calculated. Relative risks (RR) for comparison were also calculated using the Mantel-Haenszel method. Due to no heterogeneity among studies, a fixed-effects model was used for all analyses. Publication bias was assessed using a funnel plot based on Egger's regression test. Statistical significance was identified with a p-value < 0.05.

Results

Selected studies and quality assessment

The initial literature search yielded 144 articles, and 2 articles were selected from the manual search. After reviewing abstracts and titles, 107 articles were excluded, and 39 articles were selected for full-text examination. In total, 10 studies were included (8 retrospective cohort studies, 1 prospective study, and 1 case series) (Fig. 1; Table 1). Among them, 7 studies (70%) had a low risk of bias, while 3 studies (30%) had a high risk of bias. Subsequently, bias risk graphs were generated for each included article, presented as an overall percentage (Supplementary Fig. 1) and individually (Supplementary Fig. 2).

Study characteristics and descriptive summary

These 10 studies included a total of 1667 patients, of whom 680 had large and giant aneurysms [1–6, 14–17]. Out of these, 541 aneurysms with controls were included in the study. Among the treated aneurysms, 291 (53.8%) were treated with FD + C, and 250 (46.2%) were treated with FD. Only 3 articles (30%) discriminated aneurysm size concerning the therapeutic approach, with 48 classified as large and 15 as giant. Table 1 provide a summary of the included studies.

Primary outcome

Among all included patients, the overall adequate occlusion rate (OKM C-D) was 83.9% (453/541; 95% CI 80.8%-87%; I^2:0%; p:0.21). When dichotomized by therapeutic modality, the rate was 85.6% (249/291; 95% CI 81.5%-89.6%) in the FD + C group, while 81.6% (204/250; 95% CI 76.8%-86.4%) in the FD group (Supplementary Fig. 3) [1–6,

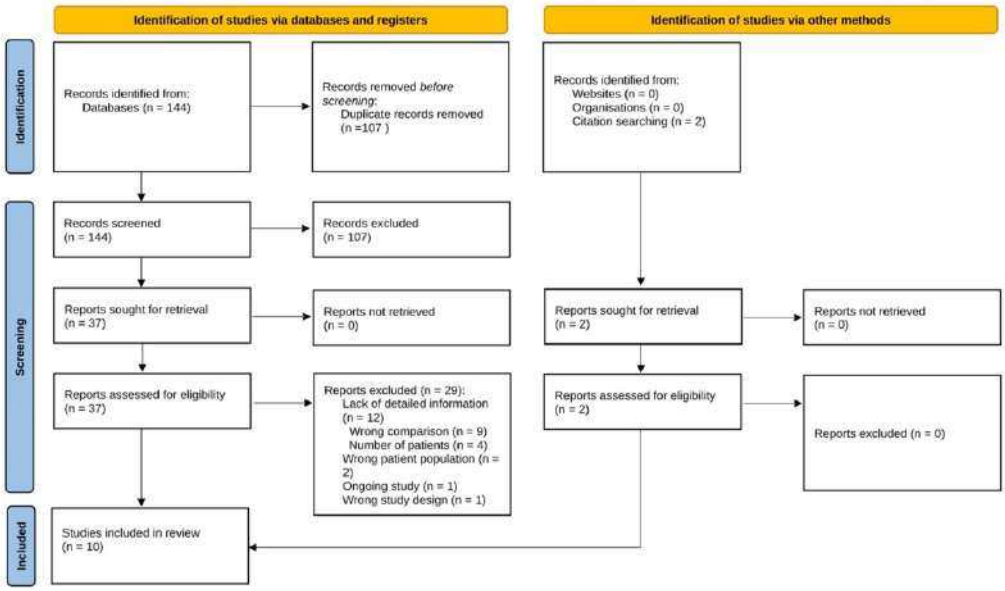


Fig. 1 Prisma flow chart of the search and screening process

License CC BY-NC-ND 4.0

Table 1 Reference data of the articles included. CS (case series), RC (retrospective cohort), PC (Prospective cohort), NOS (Newcastle-Ottawa Scale) low risk of bias *. High risk of bias †. FD (Flow diverter)

Study	Year	Study design	Flow diverter specific	Specific of large and giant aneurysms	NOS	N° of patiens	N° of large and giant intracranial aneurysms	N° of uncontrolled aneurysms	N° of aneurysms treated with more than 1 FD	Group	Controlled aneurysms			O'Kelly Marotta Classification	
											Total	Large	Giant	C	D
Chalouhu et al.	2013	RC	No	Yes	9*	160	40	5	13	FD	32	-	-	-	27
										FD+C	3	-	-	-	3
Meckel et al.	2013	RC	Yes	Yes	6†	10	10	-	9	FD	3	-	3	1	1
										FD+C	7	2	5	3	4
Carneiro et al.	2014	CS	Yes	Yes	6†	8	8	-		FD	2	-	-	-	2
										FD+C	6	-	-	-	3
Zhou et al.	2014	PC	Yes	Yes	7*	28	28	3	5	FD	8	-	-	1	6
										FD+C	17	-	-	5	12
Peschillo et al.	2017	RC	Yes	Yes	9*	44	44	1	8	FD	26	23	3	4	17
										FD+C	18	14	4	1	16
Tejada et al.	2019	RC	Yes	Yes	6†	9	9	-	1	FD	8	8	-	-	8
										FD+C	1	1	-	-	1
Choi et al.	2020	RC	No	Yes	9*	112	39	1		FD	33	-	-	9	17
										FD+C	5	-	-	1	2
Lv et al.	2020	RC	No	No	7*	80	41	-	7	FD	16	-	-	-	16
										FD+C	25	-	-	-	25
Kandemirli et al.	2022	RC	Yes	Yes	9*	45	45	-	1	FD	24	-	-	5	15
										FD+C	21	-	-	-	17
Wang et al.	2022	RC	Yes	No	9*	1171	416	-		FD	98	-	-	-	75
										FD+C	188	-	-	-	156
Total	-	-	-	-	-	1667	680	10	44		541	48	15	30 (6.6)	423 (93.4)

License CC BY-NC-ND 4.0

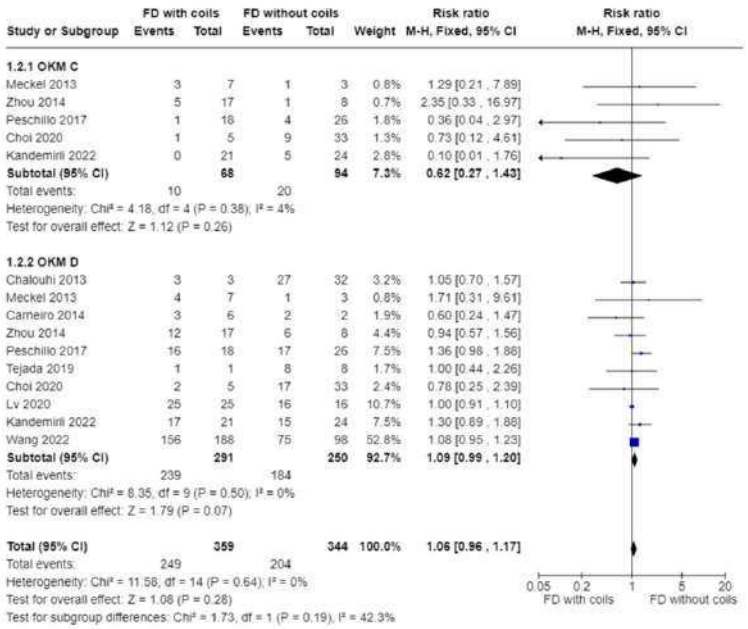


Fig. 2 The comparison of large and giant aneurysms treated with Flow Diverter with or without coil coadjuvant

14–17]. Meta-analysis of included studies demonstrated no statistically significant differences between groups (RR 1.06 [0.96, 1.17]; I^2:0%; p:0.28) (Fig. 3).

Subgroup analysis of OKM grades did not show statistical differences between groups: in the OKM C subgroup RR 0.62 [0.27, 1.43]; I^2:4%; p:0.26, and in the OKM D subgroup RR 1.09 [0.99, 1.20]; I^2:0%; p:0.07 (Fig. 4). Egger's regression was performed for each subgroup (p:0.12 for the OKM C subgroup and p:0.96 for the OKM D subgroup), showing no publication bias. The funnel plots show that we need more studies (Supplementary Fig. 4).

Secondary outcome

The overall complication rate was 10.7% (47/418; 95% CI 7.8%-13.7%; I^2:0%; p:0.10).

When dichotomizing by therapeutic modality, the complication rate was 5% (14/169; 95% CI 1.9%-8%; I^2:0%: p:0.35) in the FD+C group, and 8.4% (33/249; 95% CI 5.2%-11.7%; I^2:0%; p: 0.08) in the FD group.

The rate of device-related complications was 4.3% (5/70; 95% CI 0%-8.7%; I^2:0%: p:0.51) in the FD+C group and 19.3% (15/71; 95% CI 10.5%-28.1%; I^2:0%; p: 0.59) in the FD group. Hemorrhagic complications were 6.3% (4/49; 95% CI 0%-12.9%; I^2:0%: p:0.57) in the FD+C group and 6.2% (6/85; 95% CI 1.1%-11.2%; I^2:0%; p: 0.70) in the FD group. Ischemic complications were 5.1% (5/50; 95% CI 0%-10.6%; I^2:0%: p:0.06) in the FD+C group and 7.2% (12/93; 95% CI 2.2%-12.2%; I^2:0%; p: 0.04) in the FD group (Supplementary Figs. 5 and 6). Meta-analysis of included studies demonstrated lower complications rate for the FD+C group (RR 0.56 [0.33, 0.95]; I^2:0%; p:0.03). (Fig. 4)

Subgroup analysis did not show statistically significant differences between groups for FD-related complications (RR 0.46 [0.20, 1.05]; I^2:0%; p:0.06), although a trend in favor of FD+C. Also, hemorrhagic complications (RR 1.00 [0.30, 3.34]; I^2:0%; p:1.00) and ischemic complications (RR 0.51 [0.22, 1.22]; I^2:0%; p:0.45) were not statistically different between groups. Egger's regression for each subgroup (p:0.86 for the FD-related subgroup, p:0.26 for hemorrhagic complications, and p:0.90 for ischemic complications) showed no publication bias. (Supplementary Fig. 7)

Only 5 articles reported mortality rates. The overall mortality rate was 9.8% of treated patients (17/172; 95% CI 5.4%-14.3%; I^2:0%; p:0.72): 11.1% (6/54; 95% CI 2.7%-19.5%) in the FD+C group and 9.3% (11/118; 95% CI 4.1%-14.6%) in the FD group (Supplementary Fig. 8). No statistical differences were found for any proposed therapy (RR 0.86 [0.34, 2.18]; I^2:0%; p:0.75), (Fig. 4). Egger's regression (p:0.29) showed no publication bias. (Supplementary Fig. 9).

License CC BY-NC-ND 4.0

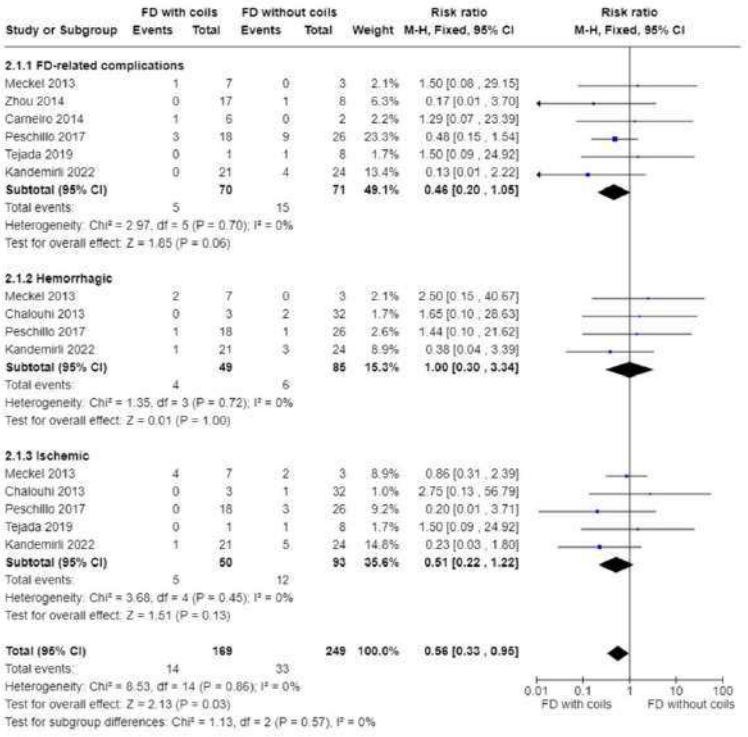


Fig. 3 The comparison of complications

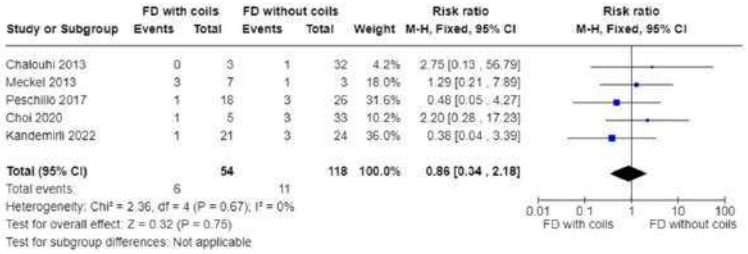


Fig. 4 Mortality comparison

Discussion

In this meta-analysis, we provide insights into the efficacy and safety of flow diverter treatment with or without coiling of large and giant intracranial aneurysms. The aim was to address the question of which treatment is safer and more effective, given the complexity of such aneurysms and the varying conclusions that should be found in the literature. We found that the adjunctive coiling of the aneurysm did not statistically increase the adequate occlusion rate (OKM C-D). However, the treatment with FD+C was associated with lower complication rates, especially device-related and ischemic complication rates.

Several meta-analyses have attempted to evaluate outcomes and complications with the use of FD, such as the study presented in 2013 by Brinjikji and colleagues [18]. They included 1451 patients with 1654 intracranial aneurysms treated with FD, reporting a complete occlusion rate of 76% (95% CI [70%,81%]) at 6 months, a procedure-related morbidity of 5% (95% CI [4%, 7%]), and a mortality of 4% (95% CI [3%, 6%]). A more recent meta-analysis in 2021 by Jia-Lin Xia and colleagues compared the treatment of unruptured aneurysms with FD versus coil embolization,

License CC BY-NC-ND 4.0

including 8 studies with 839 patients treated with FD and 2734 with coils. They found a higher rate of complete occlusion at 6 months with the use of FD (OR 0.28 [0.09, 0.85]; I2:82%; p:0.02) [19]. In subgroup analysis, FD treatment was associated with significantly higher complete occlusion rates at 6 months for large or giant aneurysms (OR 0.12 [0.07, 0.21]; I^2:0%; p:<0.01), while no differences were observed in non-large/giant aneurysm groups (OR 1.10 [0.46, 2.60]; I^2:18%; p:0.83). In 2022, Li and colleagues compared FD treatment with conventional coil treatment, including 18 studies with 1001 patients treated with FD and 1133 with coils [20]. They found that the FD group had larger aneurysms (standardized mean difference [SMD] 0.22 [0.03, 0.41]; p: 0.02). Angiographic results for FD treatment indicated a higher rate of complete occlusion (OR 2.55 [1.70, 3.83]; I^2:68%; p:<0.01) and lower rates of recurrence (OR 0.24 [0.12, 0.46]; I^2:36%; p:<0.01) and retreatment (OR 0.31 [0.21, 0.47]; I^2:30%; p:<0.01). There was a higher risk of complications in the FD group compared to the endovascular coil group (OR 1.4 [1.01, 1.96]; p:0.04).

In our study, we found that 83.9% (453/541; 95% CI 80.8%-87%; I^2:0%; p:0.21) had a favorable occlusion rate OKM C-D, consistent with findings presented by Shehata, like the PEDESTRIAN study, and better than those presented by Brinjikji [18, 21, 22]. When dichotomized by therapeutic modality, the FD+C had a favorable occlusion of 85.6% (249/291; 95% CI 81.5%-89.6%), while the FD-only group was 81.6% (204/250; 95% CI 76.8%-86.4%), and the comparison was inconclusive (RR 1.06 [0.96, 1.17]; I^2:0%; p:0.28).This aligns with Sweid and colleagues' findings, although their final recommendation is the combined use for large and giant aneurysms [23]. When analyzing subgroups, we note a statistically significant trend for OKM D in favor of FD without coadjuvant coils (RR 1.09 [0.99, 1.20]; I^2:0%; p:0.07). Als, we highlight that few articles discriminated aneurysm size, limiting statistical power (33.3%).

The PEDESTRIAN study, presented in 2021, reported long-term follow-up on 835 patients with 1000 aneurysms treated with the Pipeline flow diverter [22]. They obtained a low rate of overall complications, including 3.6% (30/835) for stroke (mostly caused by stent thrombosis) and 1.8% (23/835) for hemorrhagic complications. The overall morbidity rate, including subarachnoid hemorrhage, was 2.7% (23/835). The all-cause mortality rate was 4.6% (38/835), with a neurological mortality rate of 3.1% (26/835). Cox logistic regression identified aneurysm size as the only significant predictive factor for neurological death (HR 6.37 [95% CI: 2.41–16.81]; $p=0.01$). These findings do not align with the results of this study.

On the contrary, our results coincide with those presented by Sweid, who reported similar hemorrhagic complications between groups (5.5% for coadjuvant coils and 4.8% for FD-only, without statistical significance, p:0.81) as well as ischemic complications (12% for coadjuvant coils and 6.3% for FD-only, without statistical significance, p: 0.21) [23].

Regarding complications, we found that the coadjuvant use of coils resulted in fewer general complications (RR 0.56 [0.33, 0.95]; I^2:0%; p:0.03). However, subgroup analysis (related to FD, hemorrhagic, and ischemic complications) was inconclusive, although complications related to FD showed a trend favoring the use of coils (RR 0.46 [0.20, 1.05]; I^2:0%; p:0.06).

Limitations

This study has some limitations. There are no RCT studies, and among the observational studies, most are retrospective. Most of the articles present treatments up to the ophthalmic segment, potentially introducing a bias in the distal and posterior circulation. Some articles used different dimension to define large aneurysms, and it could have an effect in the occlusion rate. Additionally, a specific type of FD was not analyzed, despite known differences. Some articles did not use the OKM classification, requiring adaptation to the mentioned classification, and there was no standardized follow-up time, so the last follow-up was mentioned. The articles that used coils as coadjuvant do not specify the quantity used and do not reference light or dense packing. Despite these limitations, we can draw important conclusions.

Conclusion

In large and giant aneurysms, the use of FD with adjunctive coils seems to not to increase the rate of adequate aneurysm occlusion compared to FD alone. However, our results demonstrated a trend in favor of the adjunctive coiling, in reducing the periprocedural and ischemic risks.

Supplementary Information The online version contains supplementary material available at https://doi.org/10.1007/s10143-025-03675-y.

Acknowledgements Not applicable.

Author contributions Conception and design of the work: SM, AT, FD.Data acquisition: SEM, AC, FN, SM, FV, EET.Data analysis and interpretation: SEM, FD, AT.Drafting the work: SEM, AC, FN, SM, FV, EET.Critical revision: all authorsFinal approval: all authors.AT and FD are both senior Authors.

Funding Not applicable.

Data availability No datasets were generated or analysed during the current study.

License CC BY-NC-ND 4.0

Declarations

Disclosures The materials or methods used in this study or the findings specified in this paper.

Human Ethics and Consent to Participate declarations Not applicable.

Consent to participate The nature of this study, a metanalysis, does not need a patients' consent.

Competing interests The authors declare no competing interests.

References

1. Zhou Y, Yang P, Fang Y, Xu Y, Hong B, Zhao W, Li Q, Zhao, Huang Q, Liu J (2014) A novel flow-diverting device (Tubridge) for the treatment of 28 large or giant intracranial aneurysms: a single-center experience. AJNR Am J Neuroradiol 35:2326–2333. https://doi.org/10.3174/AJNR.A3925
2. Kandemirli SG, Baltacioglu F, Jesser J, Kizilkilic O, Islak C, Möhlenbruch M, Kocer N (2022) Flow Redirection endoluminal device (FRED) with or without adjunctive coiling in treatment of very large and giant cerebral aneurysms. Clin Neuroradiol 32:471–480. https://doi.org/10.1007/S00062-021-01061-X
3. Choi JH, Lee KS, Kim B, soo, Shin YS (2020) Treatment outcomes of large and giant intracranial aneurysms according to various treatment modalities. Acta Neurochir (Wien) 162:2745–2752. https://doi.org/10.1007/S00701-020-04540-1
4. Tejada JG, Lopez GVV, Koovor JME, Riley K, Martinez M (2019) Mid-term follow-up of staged bilateral internal carotid artery aneurysm treatment with pipeline embolization. Interv Neuroradiol 25:664–670. https://doi.org/10.1177/1591019919853586
5. Peschillo S, Caporlingua A, Resta MC, Paul Peluso JP, Burdi N, Sourour N, Diana F, Guidetti G, Clarençon F, Bloemsma GC, Maria F, Di, Donatelli M, Resta M (2017) Endovascular treatment of large and giant carotid aneurysms with Flow-Diverter stents alone or in combination with coils: A multicenter experience and Long-Term Follow-up. Oper Neurosurg (Hagerstown) 13:492–502. https://doi.org/10.1093/ONS/OPX032
6. Wang C, Luo B, Li T, Maimaitili A, Mao G, Song D, Wang Y, Feng W, Wang Y, Shi H, Wan J, Liu J, Guan S, Zhao Y, Zhang H (2022) Comparison of the pipeline embolisation device alone or combined with coiling for treatment of different sizes of intracranial aneurysms. Stroke Vasc Neurol 7:345–352. https://doi.org/10.1136/SVN-2021-001258
7. Jing L, Zhong J, Liu J, Yang X, Nikhil P, Meng H, Wang S, Zhang Y (2016) Hemodynamic effect of flow diverter and coils in treatment of large and giant intracranial aneurysms. World Neurosurg 89:199–207. https://doi.org/10.1016/J.WNEU.2016.01.079
8. Raymond J, Darsaut TE (2011) An approach to recurrent aneurysms following endovascular coiling. J Neurointerv Surg 3:314–318. https://doi.org/10.1136/JNIS.2011.004788
9. Szikora I, Berentei Z, Kulcsar Z, Marosfoi M, Vajda ZS, Lee W, Berez A, Nelson PK (2010) Treatment of intracranial aneurysms by functional reconstruction of the parent artery: the Budapest experience with the pipeline embolization device. AJNR Am J Neuroradiol 31:1139–1147. https://doi.org/10.3174/AJNR.A2023
10. Moher D, Liberati A, Tetzlaff J, Altman DG, Altman D, Antes G, Atkins D, Barbour V, Barrowman N, Berlin JA, Clark J, Clarke M, Cook D, D'Amico R, Deeks JJ, Devereaux PJ, Dickersin K, Egger M, Ernst E, Gøtzsche PC, Grimshaw J, Guyatt G, Higgins J, Ioannidis JPA, Kleijnen J, Lang T, Magrini N, McNamee D, Moja L, Mulrow C, Napoli M, Oxman A, Pham B, Rennie D, Sampson M, Schulz KF, Shekelle PG, Tovey D, Tugwell P (2009) Preferred reporting items for systematic reviews and meta-analyses: the PRISMA statement. PLoS Med 6. https://doi.org/10.1371/JOURNAL.PMED.1000097
11. O'Kelly CJ, Krings T, Fiorella D, Marotta TR (2010) A novel grading scale for the angiographic assessment of intracranial aneurysms treated using flow diverting stents. Interventional Neuroradiol 16:133–137. https://doi.org/10.1177/159101991001600204
12. Stang A (2010) Critical evaluation of the Newcastle-Ottawa scale for the assessment of the quality of nonrandomized studies in meta-analyses. Eur J Epidemiol 25:603–605. https://doi.org/10.1007/S10654-010-9491-Z
13. Wells G, Shea B, O'Connell D, Peterson J, Welch V, Losos M, Tugwell P (2000) The Newcastle–Ottawa scale (NOS) for assessing the quality of non-randomized studies in metaanalysis. Appl Eng Agric 18:727–734
14. Carneiro A, Rane N, Küker W, Cellerini M, Corkill R, Byrne JV (2014) Volume changes of extremely large and giant intracranial aneurysms after treatment with flow diverter stents. Neuroradiology 56:51–58. https://doi.org/10.1007/S00234-013-1304-0
15. Chalouhi N, Tjoumakaris S, Starke RM, Gonzalez LF, Randazzo C, Hasan D, McMahon JF, Singhal S, Moukarzel LA, Dumont AS, Rosenwasser R, Jabbour P (2013) Comparison of flow diversion and coiling in large unruptured intracranial saccular aneurysms. Stroke 44:2150–2154. https://doi.org/10.1161/STROKEAHA.113.001785
16. Meckel S, McAuliffe W, Fiorella D, Taschner CA, Phatouros C, Phillips TJ, Vasak P, Schumacher M, Klisch J (2013) Endovascular treatment of complex aneurysms at the vertebrobasilar junction with flow-diverting stents: initial experience. Neurosurgery 73:386–394. https://doi.org/10.1227/01.NEU.0000431472.71913.07
17. Lv X, Jiang C, Wu Z, Jiang W, Wang G (2020) Complex cerebral aneurysms: intra-luminal reconstruction using pipeline flow-diverting stent and the obliteration mechanism. Neuroradiol J 33:91–97. https://doi.org/10.1177/1971400919894879
18. Brinjikji W, Murad MH, Lanzino G, Cloft HJ, Kallmes DF (2013) Endovascular treatment of intracranial aneurysms with flow diverters: a meta-analysis. Stroke 44:442–447. https://doi.org/10.1161/STROKEAHA.112.678151
19. Xia JL, Li GL, Liu HE, Feng-Fei X, Gu XD (2021) Flow-diverting device versus coil embolization for unruptured intracranial aneurysm: A meta-analysis. Medicine 100:e26351. https://doi.org/10.1097/MD.0000000000026351
20. Li S, Zeng C, Tao W, Huang Z, Yan L, Tian X, Chen F (2022) The safety and efficacy of flow diversion versus conventional endovascular treatment for intracranial aneurysms: A Meta-analysis of Real-world cohort studies from the past 10 years. AJNR Am J Neuroradiol 43:1004–1011. https://doi.org/10.3174/AJNR.A7539
21. Shehata MA, Ibrahim MK, Ghozy S, Bilgin C, Jabal MS, Kadirvel R, Kallmes DF (2022) Long-term outcomes of flow diversion for unruptured intracranial aneurysms: a systematic review and meta-analysis. J Neurointerv Surg. https://doi.org/10.1136/JNIS-2022-019240
22. Lylyk I, Scrivano E, Lundquist J, Ferrario A, Bleise C, Perez N, Lylyk PN, Viso R, Nella-Castro R, Lylyk P (2021) Pipeline embolization devices for the treatment of intracranial aneurysms, Single-Center registry: Long-Term angiographic and clinical outcomes from 1000 aneurysms. Neurosurgery 89:443–449. https://doi.org/10.1093/neuros/nyab183
23. Sweid A, Atallah E, Herial N, Saad H, Mouchtouris N, Barros G, Gooch MR, Tjoumakaris S, Zarzour H, Hasan D, Chalouhi

Francesco DIANA | Ph.D. Thesis | University of Limoges and University of Salerno | 2025
License CC BY-NC-ND 4.0

N, Rosenwasser RH, Jabbour P (2018) Pipeline-assisted coiling versus pipeline in flow diversion treatment of intracranial aneurysms. J Clin Neurosci 58:20–24. https://doi.org/10.1016/j.jocn.2018.10.081

Publisher's note Springer Nature remains neutral with regard to jurisdictional claims in published maps and institutional affiliations.

Springer Nature or its licensor (e.g. a society or other partner) holds exclusive rights to this article under a publishing agreement with the author(s) or other rightsholder(s); author self-archiving of the accepted manuscript version of this article is solely governed by the terms of such publishing agreement and applicable law.

License CC BY-NC-ND 4.0

Appendix 5. Article Rosuvastatin

Rosuvastatin

Original research

Rosuvastatin for intracranial aneurysms treated with flow diverters: preclinical study in rabbits

Francesco Diana ,[1,2,3] Géraud Forestier ,[4] Romain Chauvet,[4,5] Marie Laure Perrin,[6] Maxime Baudouin ,[7] Jonathan Cortese ,[4,8] Alexis Belgacem,[4] Voahirana Ratsimnazafy,[9] Marine Coulomb,[10] Margot D'Arrigo,[10] Edouard Lefebvre,[10] Sylvain Dulaurent,[10] Nicolas Picard,[10] Heloise Daverat,[6] Gregory Sasselina,[6] Daphnee Chandellier,[6] Jérémy Mounier,[4] Claude Couquet,[4] Caroline Croguennec,[4] Ludovic Micallef,[4] Aurelien Le Flahec,[4] Nicolas Dubois,[4] Michele Romoli ,[11] Charbel Mounayer,[12] Sylvia M Bardet ,[6] Francesco Di Salle,[3] Faraj Terro,[6] Aymeric Rouchaud [6,12]

► Additional supplemental material is published online only. To view, please visit the journal online (https://doi.org/10.1136/jnis-2025-024237).

For numbered affiliations see end of article.

Correspondence to
Dr Francesco Diana; francesco.diana.md@gmail.com

Received 20 August 2025
Accepted 8 October 2025

Check for updates

© Author(s) (or their employer(s)) 2025. No commercial re-use. See rights and permissions. Published by BMJ Group.

To cite: Diana F, Forestier G, Chauvet R, *et al*. *J NeuroIntervent Surg* Epub ahead of print: [*please include* Day Month Year]. doi:10.1136/jnis-2025-024237

ABSTRACT

Background Flow diverters (FDs) revolutionized cerebral aneurysm treatment by promoting aneurysm sac sealing but have limitations, including thromboembolic complications and incomplete occlusion. Rosuvastatin enhances endothelialization via endothelial progenitor cell mobilization and nitric oxide bioavailability, potentially improving FD healing. This study assessed the effect of rosuvastatin on FD endothelialization in a rabbit aneurysm model.

Methods Twenty-two rabbits with elastase-induced aneurysms underwent FD implantation in the right subclavian artery. In the same animals, FDs were placed in the descending aorta to assess side branch patency. Thirteen rabbits received rosuvastatin plus aspirin (Rosu+ASA; 10 mg/kg/day each) and nine received aspirin alone (ASA; 10 mg/kg/day). Two weeks post-implantation, aneurysm occlusion (O'Kelly-Marotta scale), side branch patency (high frequency optical coherence tomography), and histological/MPM strut coverage were evaluated. Rosuvastatin serum concentration was correlated with endothelial cell coverage.

Results Complete aneurysm occlusion (OKM D) occurred in 11/13 (84.6%) of Rosu+ASA vs 6/9 (66.6%) of ASA animals. Patency of branches ≥1 mm was higher with Rosu+ASA (17/18 (94.4%) vs 9/13 (46.1%), PP=0.007), as was patency of branches <1 mm (21/22 (95.4%) vs 11/15 (73.4%), P=0.036). The composite outcome (complete occlusion+patent branches) favored Rosu+ASA (10/13 (76.9%) vs 2/9 (22.2%), P=0.011). Histology showed a trend toward greater strut coverage and neointimal thickness in Rosu+ASA (P=0.1). Rosuvastatin serum concentration strongly correlated with endothelial cell coverage (r=0.92, P=0.02).

Conclusion In rabbit FD models, rosuvastatin therapy seems to improve aneurysm occlusion, preserving side branch patency. We also found an association between drug levels and endothelial cells covering the FD. These findings support further investigations.

WHAT IS ALREADY KNOWN ON THIS TOPIC

⇒ Flow diverters (FDs) treat cerebral aneurysms by redirecting blood flow and promoting sac occlusion but are limited by perioperative thrombotic or hemorrhagic complications and incomplete aneurysm occlusion. Rosuvastatin enhances endothelialization by mobilizing endothelial progenitor cells (EPCs), increasing nitric oxide bioavailability, and reducing thrombotic states. However, its specific effects on FD endothelialization were previously unexplored.

WHAT THIS STUDY ADDS

⇒ In a rabbit aneurysm model, rosuvastatin (combined with aspirin) increased complete aneurysm occlusion rates, significantly improved patency of side branches covered by FDs, showed a trend toward greater strut coverage and neointimal thickness especially at the aneurysm neck. Moreover, rosuvastatin serum levels were correlated with endothelial cell coverage on the FD.

HOW THIS STUDY MIGHT AFFECT RESEARCH, PRACTICE OR POLICY

⇒ These findings could guide future preclinical and clinical research on statin use in FD-treated aneurysms, potentially leading to pharmacological protocols to enhance occlusion rates and reduce thromboembolic risks. This study highlights the need for clinical trials to optimize FD therapy.

INTRODUCTION

Flow diverters (FDs) have introduced a significant change in the endovascular reconstructive treatment of cerebral aneurysms. These metal stents function by redirecting the blood flow into the parent artery and promoting the sealing of the aneurysm sac, reducing the blood inflow and outflow within it.[1 2] However, FDs have some limitations. First, there is a risk of thrombotic or hemorrhagic complications,

J NeuroIntervent Surg: first published as 10.1136/jnis-2025-024237 on 28 October 2025. Downloaded from http://jnis.bmj.com/ on November 2, 2025 by guest. Protected by copyright, including for uses related to text and data mining, AI training, and similar technologies.

License CC BY-NC-ND 4.0

responsible for a perioperative morbidity-mortality rate of 7.1%.[3 4] Second, 20.1% of aneurysm occlusion failures still occur due to the proteolytic activity within the intra-aneurysmal thrombus, the persistent aneurysmal flow, and inflammation caused by the metal struts.[5 6] All these events alter the aneurysm healing process, the FD colonization by endothelial progenitor cells, and the neotissue coverage across the aneurysm neck which is a critical step for curing intracranial aneurysms after FD implantation.[7]

Rosuvastatin, a statin used to treat high cholesterol, has been shown to enhance endothelialization by promoting the mobilization and differentiation of endothelial progenitor cells (EPC). It increases nitric oxide bioavailability and reduces Endothelial Tissue Factor and Plasminogen Activator Inhibitor-1, favoring a non-thrombotic state.[8–10] Studies demonstrate that rosuvastatin improves endothelial function and accelerates re-endothelialization of blood vessels, including after coil embolization and stent implantation, through EPC promotion.[11–13] These effects could suggest a potential role for rosuvastatin in enhancing the endothelialization of FDs, which is critical for long-term vascular repair. The aim of our study was to assess in an animal model the effect of rosuvastatin on bare metal FD endothelialization.

MATERIALS AND METHODS

Study design

This study includes an efficacy and a security analysis in a rabbit model with elastase-induced aneurysms.

For the efficacy study, aneurysms have been induced with the elastase model at the origin of the right common carotid artery (RCA), and FDs have been implanted 4 weeks after in the right subclavian artery, covering the neck of the aneurysm.

In the same rabbits, a security study was conducted with implantation of an FD in the sub-renal descending aorta covering lumbar arteries, to assess the follow-up patency of these small arteries considered to have collateral branches and perform histological analysis of strut coverage.

A total of 22 rabbits were included in the study and randomly assigned to one of two groups. Thirteen rabbits were allocated to the test group, receiving rosuvastatin plus aspirin (Rosu+ASA, both at a dosage of 10 mg/kg/day), and nine to the control group, receiving aspirin alone (ASA at a dosage of 10 mg/kg/day). The initial aim was to include 15 rabbits in each group (n=30 total). However, four rabbits died after aneurysm creation (before random assignment to each study group) due to brain ischemia following right common carotid artery (RCA) ligation; these were excluded from the study as they did not enter the treatment phase. This left 26 rabbits available for randomization, and we adjusted our plan to allocate 13 rabbits to each group. After FD implantation, an additional four rabbits in the ASA group were euthanized in accordance with Good Laboratory Practice (GLP) regulations due to procedure-related complications: three developed right inferior limb paralysis (likely related to vascular access issues), and one developed paraparesis. An autopsy on the last rabbit revealed thrombosis of the aortic FD. A flowchart depicting animal enrollment, randomization, dropouts, and reasons for exclusion is provided in figure 1.

Rabbits were euthanized 2 weeks after stent implantations.

The outcomes assessed were: (1) the 2 weeks aneurysm occlusion rate with the O'Kelly-Marotta scale[14] (1); (2) the 2 weeks patency of branches covered by FD with the high frequency optical coherence tomography (HF-OCT); (3) FD coverage with the histological staining, including Hematoxylin and Eosin stain for endothelial cells and Multiphoton Microscopy (MPM) for endothelial cells and collagen fibers; (4) the correlation between rosuvastatin serum concentration and endothelial cells covering the FD (figure 1 for protocol).

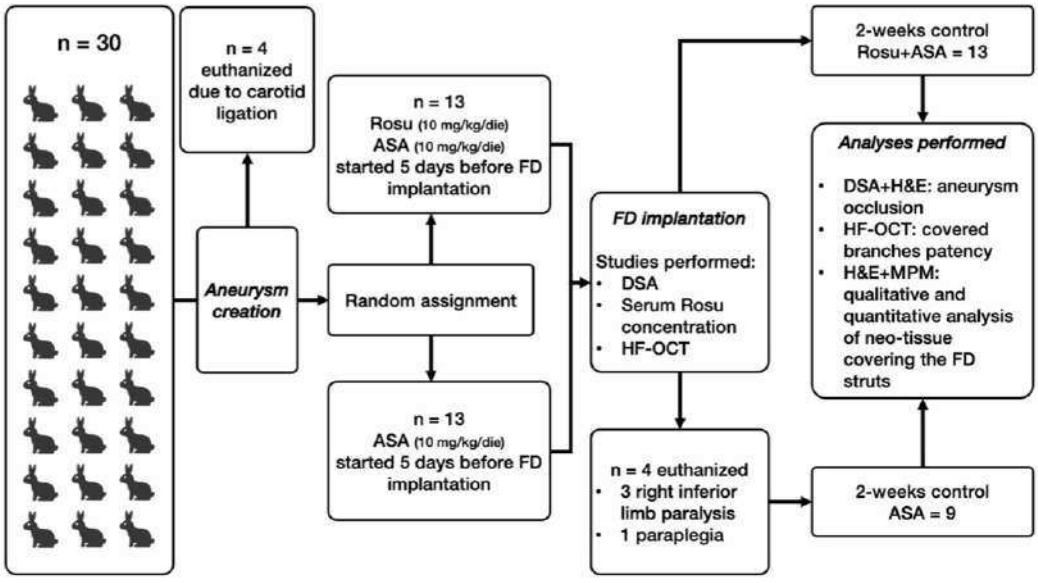


Figure 1 Study protocol. DSA, digital subtraction angiography; FD, flow diverter; H&E, hematoxylin-eosin; HF-OCT, high frequency optical coherence tomography; MPM, multiphoton microscopy; ROS, rosuvastatin; ASA, aspirin.

J NeuroIntervent Surg: first published as 10.1136/jnis-2025-024237 on 28 October 2025. Downloaded from http://jnis.bmj.com/ on November 2, 2025 by guest. Protected by copyright, including for uses related to text and data mining, AI training, and similar technologies.

License CC BY-NC-ND 4.0

Animal care

This study was conducted using New Zealand White rabbits, weight 3.0 to 3.5 kg. Food and water were provided as much or as often as necessary. All animal care and experimental procedures were conducted in accordance with the 2013 French legislation and European Community guidelines (Directive 2010/63/UE for the Care and Use of Laboratory Animals). The study received approval from the regional Ethical and Animal Care Committee, and followed the ARRIVE 2.0 guidelines for animal studies. For each procedure, general anesthesia was administered using intramuscular injection of 0.5 mg/kg of acepromazine (Vetranquil 1%), 20 mg/kg of ketamine, and 4.5 mg/kg of xylazine (Rompun). Postoperative analgesia was assured with buprenorphine 0.02 to 0.04 mg/ kg per 6 hours, administered with pain systematic evaluation before and after the administration. Animals were euthanized under general anesthesia during the last procedure using a lethal injection of pentobarbital (60 mg/kg) followed with bilateral thoracotomy.

Rosuvastatin and aspirin administration

Rosuvastatin was prepared from powdered Rosu Arrow 20 mg tablets. Aspirin was prepared from ASPIRIN Bayer 500 mg. Both drugs were administered as an aqueous solution. The tablets were pulverized using a RM 200 RETSCH mortar grinder for 3 minutes with a crushing force setting of 3. The resulting powder was dissolved in 3 mL of water and administered orally via gavage at approximately 14:30 daily. Five days before FD implantation, rabbits were premedicated with aspirin and rosuvastatin or aspirin alone according to the randomization group, and this medication regimen was continued until the final procedure.

Aneurysm creation

Aneurysm creation procedures were performed as previously described.[15] Under controlled laboratory conditions, each selected rabbit underwent a surgical exposure of the right common carotid artery. The procedure involved careful isolation of the artery, transverse arteriotomy of the isolated artery, and the retrograde introduction of a 5F sheath. Under fluoroscopy a 4F Fogarty balloon was inflated at the origin of the right common carotid artery to isolate it from the rest of the circulation, and the elastase was injected for 30 minutes. The sheath was then removed, and the common carotid artery was ligated a few centimeters distal to the origin. Aneurysms were treated 3 weeks after aneurysm creation. All endovascular procedures were performed with an Artis Icono (Siemens Healthineers, Germany). Baseline characteristics of aneurysms and parent vessels were reported in online supplemental table 1.

FD implantation and angiographic evaluation

Under controlled laboratory conditions, each selected rabbit underwent surgical exposure of the right common femoral artery. The procedure involved careful isolation of the artery, transverse arteriotomy of the isolated artery, and the introduction of a 6F sheath. Under fluoroscopy a 6F guide catheter (Envoy 6F, Codman Neuro, Raynham, MA) was advanced over a 0.35-inch guidewire in the right subclavian artery. A run and a 3D acquisition were acquired to confirm the aneurysm and to select the FD according to subclavian artery diameters. With a 0.21-inch microcatheter (Headway21, MicroVention, California, USA), a bare metal FD (Silk Vista, Balt, France) was deployed (online supplemental table 2). After FD implantation HF-OCT imaging was acquired with the HF-OCT (Spryte Medical, Bedford, MA, USA), with a 100 mm/s pull-back speed, generating 540 frames/pull-back with simultaneous intra-arterial iodine contrast injection at a rate of 3–6 mL/s for a total volume of 16–24 mL to clear the blood from the vessel. Then, FD implantation and HF-OCT acquisition were repeated at the level of the descending aorta.

Two weeks later, through a 6F sheath introduced in the surgically exposed left common femoral artery, we performed a digital subtraction angiography (DSA) control of the subclavian FD (efficacy control) and an HF-OCT control of the aortic FD (safety control). Aneurysm occlusion was evaluated with the the O'Kelly-Marotta (OKM) scale: OKM A defined as total filling of the sac (>95%), OKM B as subtotal filling (5–95%), OKM C as entry remnant (<5%) and OKM D as no filling (0%). OKM D and C were defined as adequate occlusion. In the HF-OCT, covered branches (lumbar arteries) were defined patent when no neotissue was observed over the FD at the level of the ostium, stenotic when ≥50% of the neotissue covered the FD over the ostium or occluded when neotissue completely occluded the ostium. We assessed the effect on different sized branches, analyzing the patency of covered arteries smaller or bigger than 1 mm. We also assessed a composite efficacy/safety outcome including the complete aneurysm occlusion with all side branches covered by the FD patent.

Rosuvastatin concentration assessment

Each rabbit of the Rosu+ASA group started the rosuvastatin therapy 5 days before the FD implantation. Before implanting the FD, a blood sample was collected in dry tubes using the marginal ear vein of the rabbit. on arrival at the Pharmacology-Toxicology laboratory, the samples were centrifuged at 13 000 rpm for 10 minutes. The supernatant (150 µL) was then transferred into vials for analysis. Samples were immediately frozen at −20°C until further analysis.

The sample analysis was performed using the LC-MS/MS Sciex Qtrap 5500 system (Marlborough, MA, USA). Injection of 5 µL of the supernatant allowed for the quantification of the serum concentration of rosuvastatin. The method used was validated following the Quick Easy Cheap Effective Rugged Safe (QuEChERS) protocol, ensuring effective extraction and precise analysis.

We assessed the correlation between the rosuvastatin serum concentration, and the percentage of collagen (Collagen SHG+) and endothelial surface (Nucleus DAPI+surface) covering the aortic FD after 2 weeks, obtained with the MPM.

Histology and MPM

After the 2 weeks imaging procedure, all the animals were euthanized followed by retroperitoneal exposure of the aorta for harvesting. Histomorphological and MPM analyses were performed as previously described.[16–18]

For histomorphological analysis, fixed specimens were dehydrated in a graded series of ethanol and then embedded in methyl methacrylate. Transversal (in the case of stented-descending aorta branch) or longitudinal (FD-treated aneurysm; across the neck) tissue sections (10 µm) across the aneurysm neck were performed with a diamond wire saw or with a laser microtome (SC3M facility from the Inserm/Nantes Université/ONIRIS UMR1229 RMeS Laboratory and SFR Bonamy). Tissue sections were stained with hematein and eosin (H&E). Stained tissue sections were digitized using the Hamamatsu NanoZoomer 2.0-RS digital slide scanner (Hamamatsu Photonics, Hamamatsu City, Shizuoka, Japan) at a 40x magnification (ie, 227 nm/pixel). For quantitative tissue strut coverage, we used QuPath software (v0.5.1). Several parameters were determined including, the

J Neurointervent Surg: first published as 10.1136/jnis-2025-024237 on 28 October 2025. Downloaded from http://jnis.bmj.com/ on November 2, 2025 by guest. Protected by copyright, including for uses related to text and data mining, AI training, and similar technologies.

License CC BY-NC-ND 4.0

percentage of strut cover (SC), the mean neointimal thickness (NIT, µm), neointimal coverage ratio, neointima-to-media ratio in the regions outside the neck. To assess the overall quality of stent coverage, we determined the percentage of struts covered (SC) by neotissue, regardless of the morphology of the tissue or the neointimal thickness. We then analyzed the extent of quantitative stent coverage by measuring the exact values (µm) of mean neointimal thickness (NIT) (online supplemental table 3) for histological analysis protocol.

For MPM, the samples were stained with DAPI and imaged using a custom-built multiphoton microscope (Olympus BX61WI/FV1200MPE, Hamburg, Germany) equipped with a Ti:sapphire femtosecond laser (810 nm excitation). A 25×water immersion objective (NA 1.05, 2 mm WD) was used for deep tissue imaging (up to 400 µm). Images (512×512 pixels) were acquired at 4 µm z-steps, covering a 500×500 µm field of view in 4–8 different zones. SHG (collagen), red autofluorescence (elastin or mesenchymal-like cells), and DAPI (nuclei) were detected on dedicated Photomultiplier Tubes. All images were corrected for background and processed identically. Collagen quantification and directionality was based on SHG signal z-projections in five zones and analyzed with FIJI using the "Analyze Particles" and "Directionality" (scored from 0 – no direction to 3 – unique and homogeneous direction) plugins, as previously described.[17]

Statistical analysis

Data are presented in numbers (percentage) for discrete variables and mean±SD for continuous variables. Inter-rater agreements were calculated with Fleiss' kappa. A Fisher's exact test was used to evaluate qualitative variables as appropriate. All statistical analyses were performed using one-way analysis of variance (ANOVA) and Tukey's multiple comparisons tests based on the mean and SD. P-values ≤0.05 were considered statistically significant, with the degree of significance indicated as follows: * for P≤0.05, ** for P≤0.01, and *** for P≤0.001. All statistics were performed using R software (v3.6.1) or Prism GraphPad software.

RESULTS

In all rabbits included in the analysis, FDs were successfully implanted. All FDs were patent immediately after implantation. Thirteen rabbits were included in the Rosu+ASA group and nine in the ASA group.

Aneurysm occlusion

The 2 weeks DSA control showed a higher not statistically significant complete aneurysm occlusion rate in the Rosu+ASA group compared with the ASA group (OKM D 11/13 (84.6%) vs 6/9 (66.6%), P=0.323; table 1). An OKM C was observed in two cases in both groups (15.4% vs 22.2%), and in one case of the control groups there was a sac remnant (OKM B). An adequate occlusion was higher in the Rosu+ASA group (OKM C-D 13/13 (100%) vs 8/9 (88.8%); table 1). Examples of the DSA control can be seen in online supplemental file 1).

Branches covered by the FD and strut coverage

With the HF-OCT done immediately after the FD implantation at the level of the descending aorta we identified 40 covered branches in the Rosu+ASA group and 28 in the ASA group (table 1). Examples of the HF-OCT control can be seen in online supplemental figure 2).

Table 1 DSA and HF-OCT outcomes

		Rosu+ASA	ASA	P value
DSA – aneurysm occlusion				
Aneurysms number, n		**13**	**9**	
Aneurysm status, n (%)	OKM D	11 (84.6%)	6 (66.6%)	0.323
	OKM C	2 (15.4%)	2 (22.2%)	
	OKM B	0	1 (11.1%)	
	OKM A	0	0	
HF-OCT – side branches and distal end of the FD				
Basal HF-OCT - covered branches <1 mm, n		**22**	**15**	
Control HF-OCT, n (%)	Patent	21 (95.4%)	11 (73.4%)	0.036
	Stenotic	0	2 (13.3%)	
	Occluded	1 (4.6%)	2 (13.3%)	
Basal HF-OCT - covered branches ≥1 mm, n		**18**	**13**	
Control HF-OCT, n (%)	Patent	17 (94.4%)	6 (46.1%)	0.007
	Stenotic	0	4 (30.8%)	
	Occluded	1 (5.6%)	3 (23.1%)	
Basal HF-OCT - FD distal end malapposed, n		**14**	**9**	
Control HF-OCT	Endothelialized	9 (64.3%)	7 (77.8%)	0.421
	No endothelialized	5 (35.7%)	2 (22.2%)	
Composite outcome		**13**	**9**	
Aneurysm occlusion and patent covered branches	Yes	10 (76.9%)	2 (22.2%)	0.011
	No	3 (23.1%)	7 (77.8%)	

ASA, aspirin; DSA, digital subtraction angiography; FD, flow diverter; HF-OCT, high frequency optical coherence tomography; OKM, O'Kelly-Marotta; Rosu, rosuvastatin.

J NeuroIntervent Surg: first published as 10.1136/jnis-2025-024237 on 28 October 2025. Downloaded from http://jnis.bmj.com/ on November 2, 2025 by guest. Protected by copyright, including for uses related to text and data mining, AI training, and similar technologies.

License CC BY-NC-ND 4.0

Thirty-seven covered branches had an ostium diameter smaller than 1 mm (22 in the Rosu+ASA group and 15 in the ASA group). The 2 weeks HF-OCT control showed a significantly higher patency rate in the Rosu+ASA group compared with the ASA group (21/22 (95.4%) vs 11/15 (73.4%); P=0.036). Stenosis and occlusion were also lower in the Rosu+ASA group compared with ASA group (0/22 vs 2/15 (13.3%) and 1/22 (4.6%) vs 2/15 (13.3%)).

Thirty-one covered branches had an ostium diameter ≥1 mm (18 in the Rosu+ASA group and 13 in the ASA group). The 2 weeks HF-OCT control showed a significantly higher patency rate in the Rosu+ASA group compared with the ASA group (17/18 (94.4%) vs 6/13 (46.1%); P=0.007). Stenosis and occlusion were also lower in the Rosu+ASA group (0/18 vs 4/13 (30.8%) and 1/18 (5.6%) vs 3/13 (23.1%)).

Composite outcome

The composite outcome, including all rabbit models with the aneurysm completely occluded and all covered branches patent, was significantly higher with rosuvastatin therapy (10/13 (76.9%) vs 2/9 (22.2%); P=0.011).

Histomorphological analysis FD/stent coverage by neotissue

In stented aortas, examination of H&E-stained sections showed that in both the ASA group and the Rosu+ASA group, the stent struts were generally covered with well-organized tissue, with no evidence of persistent inflammatory cells, residual fibrin, or red blood cells, indicating advanced healing (Supplemental figure 2). All samples exhibited good stent apposition (figure 3A,B). Both groups demonstrated excellent coverage rates, with a trend toward improved strut coverage in the Rosu+ASA group compared with the ASA group, in both SC (97.9–100% in the Rosu+ASA group vs 83.3–100% in the ASA group; Figure 3C) and NIT (55.9–145 µm (median: 107 µm) in the Rosu+ASA group vs 35.7–138 µm (median: 95.4 µm) in the ASA group; Figure 3D).

In FD-treated aneurysms (figure 3E), histology confirmed the data obtained by DSA, indicating that the Rosu+ASA group showed a better rate of successful aneurysm occlusion compared with the ASA group. Assessment of the percentage of strut coverage (SC) in FD-treated aneurysms, both in zones adjacent to the neck (proximal and distal) and at the neck itself (figure 3F), confirmed the data obtained in aortas and indicated that at the neck, as well as in adjacent zones, NIT tended to be higher (figure 3G) in the Rosu+ASA group compared with the ASA group (figure 2B). In the zones adjacent to the neck, this tendency was confirmed when analyzing the neointima-to-media ratio (figure 3H).

MPM in stented aorta: endothelial cells and collagen

The percentage of the luminal surface covered by DAPI+nuclei, assessed by MPM (figure 2A), was not statistically different between groups (ASA 30.62% vs Rosu+ASA 32.90%, p=0.149), suggesting comparable cellular colonization. Collagen coverage, quantified via SHG signal (figure 2E), did not show statistical difference between groups (ASA 44.98% vs Rosu+ASA 41.99%, P=0.286), indicating that both treatments led to similar levels of extracellular matrix (ECM) deposition. Collagen fiber alignment (figure 2G) was not statistically different between groups (ASA 1.978 vs Rosu+ASA 1.677, P=0.132), suggesting that overall collagen organization remained largely unaffected by rosuvastatin co-treatment.

Rosuvastatin concentration and endothelialization

Rosuvastatin serum concentration was successfully measured in each rabbit of the Rosu+ASA group (µg/L). The Pearson correlation coefficient between Rosu serum concentration and endothelial cells coverage (Nucleus DAPI+surface) of FD was r=0.92, indicating a strong statistically positive relationship (P=0.02). The Pearson correlation coefficient between Rosu serum concentration and collagen surface (Collagen SHG+) on FD was r=−0.51, indicating no relationship. Finally, the Pearson correlation coefficient between Rosu serum concentration and collagen directionality (Collagen dir Score) was r=−0.53, indicating no relationship (figure 4).

DISCUSSION

In this preclinical study on a rabbit model, we aimed to assess the safety and efficacy of the rosuvastatin therapy on bare metal FD endothelialization. Rabbit models with elastase-induced aneurysms reliably replicate key anatomical, hemodynamic, and histopathological features of human aneurysms, allowing for translational research in device development and pathophysiology studies.[19 20] We report four key findings associated with rosuvastatin therapy: (1) a trend toward a higher aneurysm occlusion rate, (2) a significantly lower occlusion rate of side branches covered by the FD, (3) a trend toward a higher strut coverage by the neotissue, (4) a direct correlation between the rosuvastatin serum concentration and the endothelial cells covering the FD, without neointimal hyperplasia.

These results provide important preclinical evidence on the effect of the rosuvastatin therapy on the treatment of intracranial aneurysms with FD, paving the way for further research. Rosuvastatin promotes endothelialization through several mechanisms supported by both in vitro and in vivo studies. It enhances the mobilization and function of EPC, which is critical for endothelial repair and neovascularization. In animal models, rosuvastatin increases circulating EPC, improves their incorporation at sites of vascular injury, and accelerates re-endothelialization, effects that are mediated in part by upregulation of CXCR4 and activation of the SDF-1α/CXCR4 axis, as well as by eNOS-dependent pathways.[12 21–23] At the cellular level, rosuvastatin increases eNOS expression and activity, leading to greater nitric oxide bioavailability, which is essential for endothelial health and repair.[24–26]

Our histological analysis revealed that both ASA and Rosu+ASA groups achieved advanced healing with well-organized tissue covering stent struts, yet the Rosu+ASA group consistently showed higher strut coverage and neointimal thickness, both in stented aortas and FD-treated aneurysms, accompanied by a higher rate of complete aneurysm occlusion. These morphological results align with our observation of a strong correlation between serum rosuvastatin levels and the percentage of endothelial cell coverage on the FD, that are consistent with prior studies on vascular injury and aneurysm models, which have shown that rosuvastatin improves endothelial repair scores and promotes more uniform and integrated endothelial coverage, likely through enhanced EPC proliferation, migration, and tube formation.[12 22 23] Moreover, a study by Liu P *et al*,[12] confirmed that rosuvastatin upregulates VEGF-A expression, thereby supporting endothelial cell viability and function and contributing to improved endothelialization of vascular stents and grafts. Additionally, rosuvastatin reduces oxidative stress and inflammation, further supporting endothelial cell survival and function.[27–29] These findings suggest that rosuvastatin may influence the rate of neointimal hyperplasia and the risk of

J Neurointervent Surg: first published as 10.1136/jnis-2025-024237 on 28 October 2025. Downloaded from http://jnis.bmj.com/ on November 2, 2025 by guest. Protected by copyright, including for uses related to text and data mining, AI training, and similar technologies.

License CC BY-NC-ND 4.0

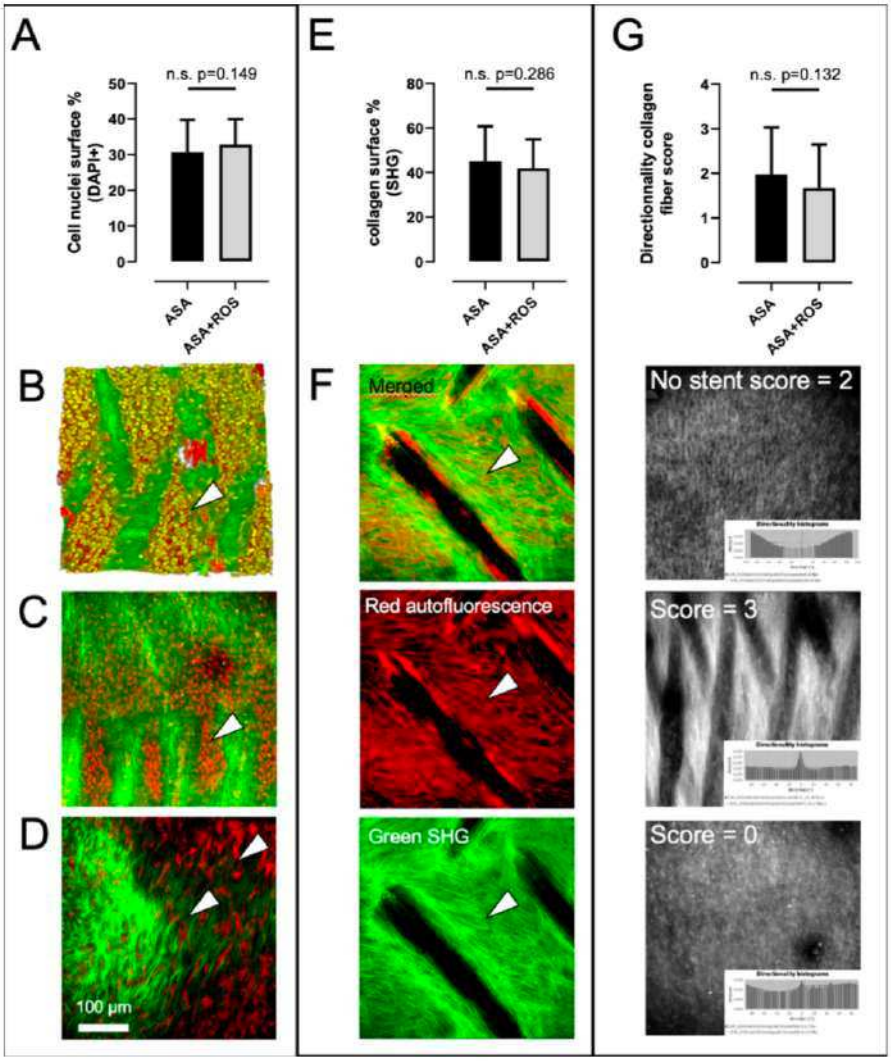


Figure 2 Multiscale analysis of neotissue formation and extracellular matrix remodeling following flow-diverter stent (FD) implantation in rabbit arteries. (A) Quantification of endothelial cell coverage by multiphoton microscopy (MPM), based on the surface area occupied by DAPI- nuclei. No significant difference between treatment groups (n.s., P=0.149). (B–D) MPM images showing 3D reconstructions of the vascular wall at distinct depths. DAPI-stained nuclei are pseudo-colored yellow (arrowheads indicate endothelial cells in B and C), SHG-positive collagen appears green, and red autofluorescence highlights endothelial cells in C and mesenchymal-like cells in D. (E) Collagen surface area (%) assessed from SHG signal in MPM images; no significant difference was observed between groups (n.s., P=0.286). (F) Multichannel MPM views showing neotissue bridging between stent struts. Top: merged image (SHG green+red autofluorescence); middle: red channel only; bottom: SHG signal only. Arrowheads highlight aligned collagen bundles and adjacent smooth muscle-like cells. (G) Collagen fiber directionality scores derived from SHG image analysis showed no significant difference (n.s., P=0.132). The right column presents representative images ranging from score 0 (disorganized fibers) to score 3 (highly aligned), including a "no stent" control with minimal orientation. Data are presented as mean±SD or individual values. Statistical comparisons were performed using appropriate nonparametric tests. Scale bar: 100 µm.

in-stent stenosis. Further clinical studies might assess the effect of rosuvastatin therapy on neointimal hyperplasia.

We did not find any association between rosuvastatin therapy and the percentage of collagen fibers. Collagen fibers, along with mesenchymal-like cells such as fibroblasts and myofibroblasts, play a key role in ECM remodeling, an essential component of neotissue formation. MPM imaging provided valuable insight into the structural organization of the neotissue covering the

J Neurointervent Surg: first published as 10.1136/jnis-2025-024237 on 28 October 2025. Downloaded from http://jnis.bmj.com/ on November 2, 2025 by guest. Protected by copyright, including for uses related to text and data mining, AI training, and similar technologies.

License CC BY-NC-ND 4.0

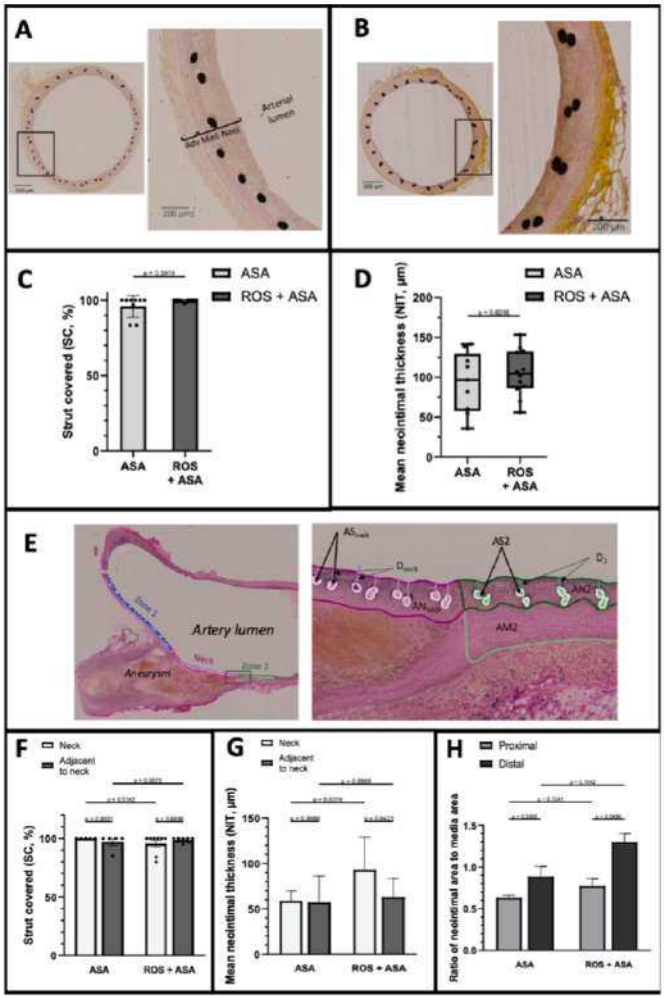


Figure 3 Effects of rosuvastatin on strut coverage by neotissue. (A) and (B), Representative images of H&E-stained transverse sections (diamond wire saw) of stented aortas from the ASA group (A) and the ROS+ASA group (B). Both groups show comparable and uniform strut coverage (SC). (C) Histogram representation of the mean percentage of struts covered in each group. Data are expressed as mean±SD. (D) Box-and-whisker plots (median; 25th and 75th percentiles) showing the mean neointimal thickness (NIT) in the ASA and ROS+ASA groups. (E) Illustrations of the zones delineated for the quantitative analysis of stent/flow diverter (FD) coverage in the subrenal aorta (A, H&E-stained transverse section) and in FD-treated aneurysms (B, H&E-stained longitudinal section), using QuPath software (v0.5.1). Neol: neointima; Med : media; Adv : adventitia. Zone 2 is proximal to the aneurysm neck; Zone 1 is distal. Dneck: distance from the device strut to the arterial lumen at the neck. D2: distance from the strut to the arterial lumen in Zone 2 (proximal to the neck). ASneck: area of the strut at the neck site. AS2: area of the strut in Zone 2. AM2: area of the media in Zone 2. See text for details. For FD-treated samples, (F) Percentage of SC, (G) mean of NIT both, in zones adjacent to the neck and at the neck itself, and the ratio of neointima-to-media in zones adjacent to the neck (P values are indicated, ANOVA test).

FD. Our observations suggest that neotissue formation follows a dual process. The development of a cohesive tissue scaffolding populated by mesenchymal-like cells including fibroblasts, myofibroblasts, and smooth muscle cells (figure 3D,F). Superficially, the formation of a continuous monolayer of endothelial cells covering the contours of the stent struts, indicating that endothelialization is guided by the mechanical topography of the device (figure 3B,C). This layered structure highlights the distinct yet complementary roles of endothelial and mesenchymal components in the maturation of neotissue following stent implantation.

Other statins, including atorvastatin, pravastatin, and simvastatin, have also been shown to promote endothelialization.[23 30–35] This suggests that the pro-endothelial effects of statins are a class

J NeuroInterv Surg: first published as 10.1136/jnis-2025-024237 on 28 October 2025. Downloaded from http://jnis.bmj.com/ on November 2, 2025 by guest. Protected by copyright, including for uses related to text and data mining, AI training, and similar technologies.

License CC BY-NC-ND 4.0

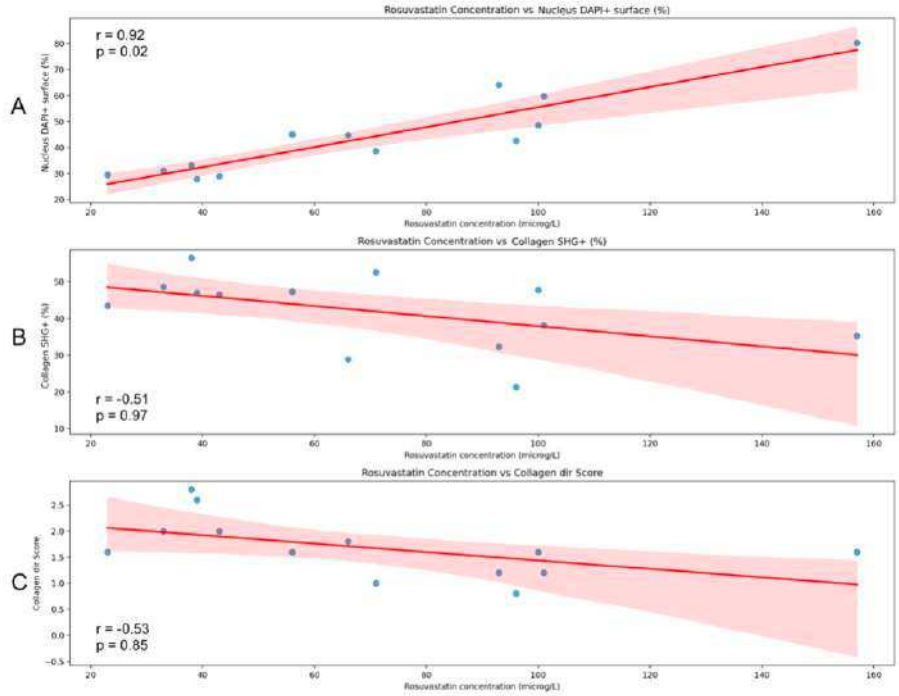


Figure 4 Pearson's correlation between ROS concentration and DAPI-positive nuclei endothelial cells (A), Collagen SHG-positive fibers (B), and collagen directionality score (C).

effect, although the degree of efficacy and the specific molecular pathways involved may differ among individual agents. The enhancement of endothelialization is recognized as one of the key pleiotropic benefits of statins, extending beyond their lipid-lowering properties.[30 35] In our study, we specifically chose to investigate rosuvastatin because clinical data indicate that it has superior efficacy in improving endothelial function compared with other statins, along with a stronger anti-inflammatory profile in endothelial cells.[23 35–38]

The complete occlusion rate of intracranial aneurysms treated with FD is approximately 77–83% at 1 year, with rates increasing to 87–90% at 2 years and up to 96% at 5 years based on pooled meta-analyses and large cohort studies. These rates are consistent across various device types and aneurysm locations, with some variation depending on aneurysm size, morphology, and follow-up duration.[39] Statin effect on FD treatment occlusion rate has been assessed by Salih *et al*,[40] in a propensity score-matched analysis, comparing occlusion rates in patients on statin therapy and those not on statins after treatment with the Pipeline Embolization Device (PED). They showed a higher, but not statistically significant, complete occlusion with statin (79.6% vs 67.4%). Our results confirm the trend toward a higher occlusion rate with statin therapy (84.6% vs 66.6%), without statistical significance (P=0.3). A key limitation of the study by Salih *et al*, is its retrospective, observational design. Although the authors applied propensity score matching to reduce confounding, residual bias cannot be excluded. Specifically, patients who were already on statin therapy prior to the intervention may differ systematically from those who were not, in terms of vascular risk profiles, comorbidities, or healthcare access. Moreover, the potential impact of statins on aneurysm healing and flow diverter efficacy may be influenced by underlying lipid profiles. Patients with hyperlipidemia could experience different molecular and inflammatory responses to statin therapy compared with normolipidemic individuals, which may affect endothelialization and aneurysm occlusion. The study does not account for these biological differences, nor does it stratify outcomes based on baseline lipid levels, which could be a significant modifier of statin effects in this context. Prospective randomized studies are needed to eliminate this bias.

The thromboembolic complication rate associated with the treatment of intracranial aneurysms using FD ranges between 3% and 6% in large series and meta-analyses, with specific risk profiles depending on aneurysm location and whether collateral branches are covered.[41] When focusing on the risk related to the coverage of collateral branches, the literature consistently shows that the risk of clinically significant thromboembolic complications remains below 5%, even though angiographic evidence of branch occlusion or narrowing is more common (e.g., ACA 66.6%, PComA 44.3%, MCA-M2 39.2%). Collateral circulation appears to mitigate the clinical impact of branch occlusion, whereas the risk of symptomatic ischemia increases when covering perforators or branches lacking robust collateral supply.[42] In our study, we observed a significant lower rate of branch occlusion (94.4% vs 46.1% for ≥1 mm arteries and 95.4% vs 73.4% for <1 mm arteries) and stenosis (30.8% vs 23.1% for ≥1 mm arteries and (0 vs 13.3% for <1 mm arteries) in side branches covered by the FD in patients treated with

J NeuroIntervent Surg: first published as 10.1136/jnis-2025-024237 on 28 October 2025. Downloaded from http://jnis.bmj.com/ on November 2, 2025 by guest. Protected by copyright, including for uses related to text and data mining, AI training, and similar technologies.

License CC BY-NC-ND 4.0

rosuvastatin. Finally, when we included both efficacy (aneurysm complete occlusion) and safety (patency of covered side branches) outcomes in a composite measure, we observed a significant effect of the rosuvastatin therapy (76.9% vs 22.2%; P=0.011). These findings suggest that rosuvastatin may exert a protective effect by reducing thromboembolic complications related to side branch coverage and may also promote enhanced aneurysm healing, stabilizing and controlling the process involved in the neotissue development, potentially reducing the incidence of neointimal hyperplasia.

Limitations

Our study does have some limitations. First, although the rabbit model is realistic, the different arterial wall composition between arteries of the human intracranial circulation and peripheral arteries of an animal model might affect the results. Additionally, although the elastase-induced rabbit aneurysm model reliably replicates histopathological and hemodynamic features of human intracranial aneurysms, it is a sidewall-stump model created at the origin of the right common carotid artery. This configuration may not fully replicate the complex flow dynamics of human bifurcation aneurysms, potentially limiting the generalizability of our findings to such clinical scenarios. Second, we had a limited size cohort; further investigation with a larger number of specimens is required to confirm our results. Third, in our study we used only aspirin rather than a dual antiplatelet therapy to treat the rabbit aneurysms, based on evidence that the antiplatelet regimen does not affect FD integration into the arterial wall and thromboembolic complications in animal models,[43] and cardiology studies suggesting no clinically significant interaction between statins and P2Y12 inhibitors, such as clopidogrel.[44–46] The double antiplatelet therapy generally used in humans for the FD treatment might affect our results. Finally, even if rosuvastatin therapy seems effective and safe in the treatment with FD, translating the therapy into clinical practice might not achieve the same results.

CONCLUSION

In rabbit aneurysm models with implanted FDs, the adjunctive administration of rosuvastatin seems to enhance the efficacy of the FD treatment, increasing the aneurysm occlusion rate, and the safety of the procedure, reducing the occlusion of the side branches covered by the FD. Further studies are needed to confirm our results and to assess the safety and efficacy of the rosuvastatin therapy in clinical studies.

Author affiliations
[1]Interventional Neuroradiology, Vall d'Hebron University Hospital, Barcelona, Spain
[2]Department of Life, Health and Health Professions Sciences, Link Campus University, Rome, Italy
[3]Department of Medicine, Surgery and Dentistry, Scuola Medica Salernitana, Section of Neurosciences, Salerno, Italy
[4]Plateform EMIS, CHU Limoges, Limoges, France
[5]Vascular surgery, CHU Dupuytren 2, Limoges, France
[6]CNRS, XLIM, UMR 7252, University Limoges, Limoges, France
[7]Radiology, CHU Limoges, Limoges, France
[8]Bicetre Hospital Interventional Neuroradiology, Le Kremlin-Bicetre, Île-de-France, France
[9]Institute of Epidemiology and Global Health - Michel Dumas, OmegaHealth; Inserm, U1094; IRD, UMR270; EpiMaCT (Epidemiology of chronic diseases in tropical zone), CHU Limoges, Department of Pharmacy, University of Limoges, Limoges, France
[10]Service de Pharmacie, CHU Limoges, Limoges, France
[11]Neurology and Stroke Unit, Maurizio Bufalini Hospital, Cesena, Emilia-Romagna, Italy
[12]Interventional Neuroradiology, CHU Limoges, Limoges, France

Social media Francesco Diana, LinkedIn @fdianamd

Acknowledgements The authors acknowledge Balt for supporting us by providing the flow diverters used in the study, the SC3M facility from the Inserm/Nantes Université/ONIRIS UMR1229 RMeS Laboratory and SFR Bonamy and the PLATINOM platform (www.unilim.fr\platinom). The PLATINOM platform benefits from the support of the Nouvelle Aquitaine region and the European Union (FEDER - PILIM project) as well as the National Research Agency under the "Programme d'Investissements d'Avenir" (Equipex NANOFUTUR ANR-21-ESRE-0012 and ADD4P ANR-21-ESRE-0007).

Contributors FD and AR contributed to the conception and design of the studies. All authors contributed to acquisition of the data, the interpretation of the data. FD, SMB, FT and AR drafted the work and revised it for significant intellectual content. All authors approved the final version of the manuscript; agree to be accountable for all aspects of the work, including its accuracy and integrity. AR is the guarantor of the study.

Funding The authors have not declared a specific grant for this research from any funding agency in the public, commercial, or not-for-profit sectors.

Competing interests FD is a consultant for Medtronic, Balt, and received an educational grant from Medtronic. JC received an educational grant from Balt, Medtronic, Phenox, Microvention, the Philippe Foundation, the French Society of Radiology and the French Society of Neuroradiology; and received honoraria for lectures from Balt. CM received honoraria for lectures from Balt. AR received honoraria for lectures from Balt.

Patient consent for publication Not applicable.

Ethics approval All animal care and experimental procedures were conducted in accordance with the 2013 French legislation, European Community guidelines (directive 2010/63/UE for the Care and Use of Laboratory Animals) and the ARRIVE 2.0 guidelines. The study received approval of the regional Ethical and Animal Care Committee and French Ministry of Higher Education and Research (APAFIS #37873-2022070114322309).

Provenance and peer review Not commissioned; externally peer reviewed.

Data availability statement All data relevant to the study are included in the article or uploaded as supplementary information.

Supplemental material This content has been supplied by the author(s). It has not been vetted by BMJ Publishing Group Limited (BMJ) and may not have been peer-reviewed. Any opinions or recommendations discussed are solely those of the author(s) and are not endorsed by BMJ. BMJ disclaims all liability and responsibility arising from any reliance placed on the content. Where the content includes any translated material, BMJ does not warrant the accuracy and reliability of the translations (including but not limited to local regulations, clinical guidelines, terminology, drug names and drug dosages), and is not responsible for any error and/or omissions arising from translation and adaptation or otherwise.

ORCID iDs
Francesco Diana https://orcid.org/0000-0002-3245-917X
Géraud Forestier https://orcid.org/0000-0003-4797-9693
Maxime Baudouin https://orcid.org/0000-0001-7240-220X
Jonathan Cortese https://orcid.org/0000-0002-1616-9113
Michele Romoli https://orcid.org/0000-0001-8009-8543
Sylvia M Bardet https://orcid.org/0000-0002-0217-6910
Aymeric Rouchaud https://orcid.org/0000-0003-0902-3375

REFERENCES

1 Kallmes DF, Ding YH, Dai D, *et al*. A new endoluminal, flow-disrupting device for treatment of saccular aneurysms. *Stroke* 2007;38:2346–52.
2 Kallmes DF, Brinjikji W, Cekirge S, *et al*. Safety and efficacy of the Pipeline embolization device for treatment of intracranial aneurysms: a pooled analysis of 3 large studies. *J Neurosurg* 2017;127:775–80.
3 Rouchaud A, Brinjikji W, Lanzino G, *et al*. Delayed hemorrhagic complications after flow diversion for intracranial aneurysms: a literature overview. *Neuroradiology* 2016;58:171–7.
4 Gory B, Berge J, Bonafé A, *et al*. DIVERSION Investigators. Flow Diverters for Intracranial Aneurysms: The DIVERSION National Prospective Cohort Study. *Stroke* 2019;50:3471–80.
5 Kulcsár Z, Houdart E, Bonafé A, *et al*. Intra-aneurysmal thrombosis as a possible cause of delayed aneurysm rupture after flow-diversion treatment. *AJNR Am J Neuroradiol* 2011;32:20–5.
6 Cebral J, Ollikainen E, Chung BJ, *et al*. Flow Conditions in the Intracranial Aneurysm Lumen Are Associated with Inflammation and Degenerative Changes of the Aneurysm Wall. *AJNR Am J Neuroradiol* 2017;38:119–26.
7 Ravindran K, Casabella AM, Cebral J, *et al*. Mechanism of Action and Biology of Flow Diverters in the Treatment of Intracranial Aneurysms. *Neurosurg* 2020;86:513–9.
8 Liu Y, Wei J, Hu S, *et al*. Beneficial effects of statins on endothelial progenitor cells. *Am J Med Sci* 2012;344:220–6.

J NeuroIntervent Surg: first published as 10.1136/jnis-2025-024237 on 28 October 2025. Downloaded from http://jnis.bmj.com/ on November 2, 2025 by guest. Protected by copyright, including for uses related to text and data mining, AI training, and similar technologies.

License CC BY-NC-ND 4.0

9 Lapergue B, Mohammad A, Shuaib A. Endothelial progenitor cells and cerebrovascular diseases. *Prog Neurobiol* 2007;83:349–62.
10 Zampetaki A, Kirton JP, Xu Q. Vascular repair by endothelial progenitor cells. *Cardiovasc Res* 2008;78:413–21.
11 Walter DH, Rittig K, Bahlmann FH, *et al*. Statin therapy accelerates reendothelialization: a novel effect involving mobilization and incorporation of bone marrow-derived endothelial progenitor cells. *Circulation* 2002;105:3017–24.
12 Liu P, An Q, Chen X, *et al*. Rosuvastatin for enhancement of aneurysm neck endothelialization after coil embolization: promotion of endothelial progenitor cells in a rodent model. *J Neurosurg* 2016;124:1265–74.
13 Sheu JJ, Hsiao HY, Chung SY, *et al*. Endothelial progenitor cells, rosuvastatin and valsartan have a comparable effect on repair of balloon-denudated carotid artery injury. *Am J Transl Res* 2019;11:1282–98.
14 O'kelly CJ, Krings T, Fiorella D, *et al*. A novel grading scale for the angiographic assessment of intracranial aneurysms treated using flow diverting stents. *Interv Neuroradiol* 2010;16:133–7.
15 Altes TA, Cloft HJ, Short JG, *et al*. ARRS Executive Council Award. Creation of saccular aneurysms in the rabbit: a model suitable for testing endovascular devices. American Roentgen Ray Society. *AJR Am J Roentgenol* 1999;349–54.
16 Verhaegen C, Kautbally S, Zapareto DC, *et al*. Early thrombogenicity of coronary stents: comparison of bioresorbable polymer sirolimus-eluting and bare metal stents in an aortic rat model. *Am J Cardiovasc Dis* 2020;10:72–83.
17 Bardet SM, Cortese J, Blanc R, *et al*. Multiphoton microscopy for pre-clinical evaluation of flow-diverter stents for treating aneurysms. *J Neuroradiol* 2021;48:200–6.
18 Cortese J, Rasser C, Even G, *et al*. CD31 Mimetic Coating Enhances Flow Diverting Stent Integration into the Arterial Wall Promoting Aneurysm Healing. *Stroke* 2021;52:677–86.
19 Zeng Z, Kallmes DF, Durka MJ, *et al*. Hemodynamics and anatomy of elastase-induced rabbit aneurysm models: similarity to human cerebral aneurysms? *AJNR Am J Neuroradiol* 2011;32:595–601.
20 Brinjikji W, Ding YH, Kallmes DF, *et al*. From bench to bedside: utility of the rabbit elastase aneurysm model in preclinical studies of intracranial aneurysm treatment. *J NeuroInterv Surg* 2016;8:521–5.
21 Chiang KH, Cheng WL, Shih CM, *et al*. Statins, HMG-CoA Reductase Inhibitors, Improve Neovascularization by Increasing the Expression Density of CXCR4 in Endothelial Progenitor Cells. *PLoS One* 2015;10:e0136405.
22 Zhou J, Cheng M, Liao YH, *et al*. Rosuvastatin Enhances Angiogenesis via eNOS-Dependent Mobilization of Endothelial Progenitor Cells. *PLoS ONE* 2013;8:e63126.
23 Schroeter MR, Humboldt T, Schäfer K, *et al*. Rosuvastatin reduces atherosclerotic lesions and promotes progenitor cell mobilisation and recruitment in apolipoprotein E knockout mice. *Atherosclerosis* 2009;205:63–73.
24 Geng J, Xu H, Yu X, *et al*. Rosuvastatin protects against oxidized low-density lipoprotein-induced endothelial cell injury of atherosclerosis in vitro. *Mol Med Rep* 2019;19:432–40.
25 Enomoto S, Sata M, Fukuda D, *et al*. Rosuvastatin prevents endothelial cell death and reduces atherosclerotic lesion formation in ApoE-deficient mice. *Biomed Pharmacother* 2009;63:19–26.
26 Landsberger M, Jantzen F, Könemann S, *et al*. Blockade of geranylgeranylation by rosuvastatin upregulates eNOS expression in human venous endothelial cells. *Biochem Biophys Res Commun* 2005;PMID:1005–9.
27 Zhao Z, Wang X, Lu M, *et al*. Rosuvastatin Improves Endothelial Dysfunction in Diabetes by Normalizing Endoplasmic Reticulum Stress via Calpain-1 Inhibition. *Curr Pharm Des* 2023;PMID:2579–90.
28 Woźniak E, Broncel M, Niedzielski M, *et al*. The effect of lipid-lowering therapies on the pro-inflammatory and anti-inflammatory properties of vascular endothelial cells. *PLoS One* 2023;PMCID:e0280741.
29 Tian XY, Wong WT, Xu A, *et al*. Rosuvastatin improves endothelial function in db/db mice: role of angiotensin II type 1 receptors and oxidative stress. *Br J Pharmacol* 2011;164:598–606.
30 Wolfrum S, Jensen KS, Liao JK. Endothelium-dependent effects of statins. *Arterioscler Thromb Vasc Biol* 2003;23:729–36.
31 Martínez-González J, Badimon L. Influence of statin use on endothelial function: from bench to clinics. *Curr Pharm Des* 2007;13:1771–86.
32 Ii M, Losordo DW. Statins and the endothelium. *Vascul Pharmacol* 2007;46:1–9.
33 Khaidakov M, Wang W, Khan JA, *et al*. Statins and angiogenesis: is it about connections? Biochem Biophys Res Commun. *Epub* 2009;PMID:543–7.
34 Meyer N, Brodowski L, Richter K, *et al*. Pravastatin Promotes Endothelial Colony-Forming Cell Function, Angiogenic Signaling and Protein Expression In Vitro. *J Clin Med* 2021;10:183.
35 Margaritis M, Channon KM, Antoniades C. Statins as regulators of redox state in the vascular endothelium: beyond lipid lowering. *Antioxid Redox Signal* 2014;20:1198–215.
36 Rawlings R, Nohria A, Liu PY, *et al*. Comparison of effects of rosuvastatin (10 mg) versus atorvastatin (40 mg) on rho kinase activity in caucasian men with a previous atherosclerotic event. *Am J Cardiol* 2009;103:437–41.
37 Woźniak E, Broncel M, Niedzielski M, *et al*. The effect of lipid-lowering therapies on the pro-inflammatory and anti-inflammatory properties of vascular endothelial cells. *PLoS One* 2023;18:e0280741.
38 Thondapu V, Kurihara O, Yonetsu T, *et al*. Comparison of Rosuvastatin Versus Atorvastatin for Coronary Plaque Stabilization. *Am J Cardiol* 2019;123:1565–71.
39 Shehata MA, Ibrahim MK, Ghozy S, *et al*. Long-term outcomes of flow diversion for unruptured intracranial aneurysms: a systematic review and meta-analysis. *J Neurointerv Surg* 2023;15:898–902.
40 Salih M, Young M, Filo J, *et al*. Effect of Statin on Radiographic and Clinical Outcomes of Intracranial Aneurysms Treated With Pipeline Embolization: A Propensity Score-Matched Analysis. *Neurosurgery* 2023;93:1000–6.
41 Ramirez-Velandia F, Filo J, Enriquez-Marulanda A, *et al*. Timing, type, and impact of thromboembolic events caused by flow diversion: a 10-year experience. *J Neurosurg* 2024;142:78–87.
42 Liu J, Cao F, Zhenmei N, *et al*. Flow-diverter stents in intracranial aneurysm treatment: impact on covered cerebral artery branches. *Int J Surg* 2024;110:53–65.
43 Forestier G, Cortese J, Bardet SM, *et al*. Comparison of arterial wall integration of different flow diverters in rabbits: The CICAFLOW study. *J Neuroradiol* 2024;51:236–41.
44 Geisler T, Zürn C, Paterok M, *et al*. Statins do not adversely affect post-interventional residual platelet aggregation and outcomes in patients undergoing coronary stenting treated by dual antiplatelet therapy. *Eur Heart J* 2008;29:1635–43.
45 Serebruany VL, Midei MG, Malinin AI, *et al*. Absence of interaction between atorvastatin or other statins and clopidogrel: results from the interaction study. *Arch Intern Med* 2004;164:2051–7.
46 Bhindi R, Ormerod O, Newton J, *et al*. Interaction between statins and clopidogrel: is there anything clinically relevant? *QJM* 2008;101:915–25.

J NeuroIntervent Surg: first published as 10.1136/jnis-2025-024237 on 28 October 2025. Downloaded from http://jnis.bmj.com/ on November 2, 2025 by guest. Protected by copyright, including for uses related to text and data mining, AI training, and similar technologies.

License CC BY-NC-ND 4.0

Appendix 6. Article P8RI-coated Silk Vista versus Pipeline Vantage (Shield)

P8RI-coated Silk Vista OCT

Original research

Comparative assessment of early neointimal formation: P8RI-coated Silk Vista versus Pipeline Vantage (Shield) in a rabbit model using optical coherence tomography

Jonathan Cortese [1,2,3,4] Géraud Forestier [1] Sylvia M Bardet [1,3] Maxime Baudouin [1,5] Romain Chauvet,[1,6] Marie Laure Perrin,[1,3] Alexis Belgacem,[1] Francesco Diana [1,7,8] Voahirana Ratsimbazafy,[9,10] Marine Coulomb,[9,10] Margot D'Arrigo,[9,10] Edouard Lefebvre,[9,10] Sylvain Dulaurent,[9,10] Gregory Sasselina,[1] Daphnee Chandellier,[1] Jérémy Mounier,[1] Claude Couquet,[1] Caroline Croguennec,[1] Ludovic Micallef,[1] Aurélien Le Flahec,[1] Nicolas Dubois,[1] Laurent Spelle [2,4] Charbel Mounayer,[1,11] Faraj Terro,[3,12] Aymeric Rouchaud [1,3,5]

► Additional supplemental material is published online only. To view, please visit the journal online (https://doi.org/10.1136/jnis-2025-024213).

For numbered affiliations see end of article.

Correspondence to
Dr Jonathan Cortese; jon.cortese@live.fr

Received 13 August 2025
Accepted 13 October 2025

Check for updates

© Author(s) (or their employer(s)) 2025. No commercial re-use. See rights and permissions. Published by BMJ Group.

To cite: Cortese J, Forestier G, Bardet SM, *et al*. *J NeuroIntervent Surg* Epub ahead of print: [*please include* Day Month Year]. doi:10.1136/jnis-2025-024213

ABSTRACT

Background Several coating strategies have been recently introduced to reduce thrombogenicity of flow diverters (FDs), while the P8RI coating focuses on stimulating endothelial cells for faster arterial healing. This study aims to evaluate early neointimal growth over the FD struts by comparing these two strategies in an animal model.

Methods Bare Silk Vista (bare-SV), P8RI Silk Vista (P8RI-SV), and Pipeline Vantage with Shield technology (Shield-PV) were implanted in rabbits to treat elastase-induced aneurysms (n=6, 10, and 7, respectively) and in the aorta (n=6, 7, and 4, respectively). At 5 and 28 days, the devices were imaged with optical coherence tomography (OCT) to evaluate the stent-coverage ratio. Conventional histology and multiphoton microscopy were also performed.

Results The aneurysm occlusion rate was similar in all three groups (P=0.577). On OCT images, the stent-coverage ratio on day 5 and day 28 (overall and at each location) was significantly higher with P8RI-SV compared with both bare-SV and Shield-PV (Kruskal-Wallis P<0.0001, Dunn post-test P<0.001 for both timepoints). Histological and multiphoton microscopy evaluations confirmed that the struts of P8RI-SV were covered by well-organized neointima expressing a high rate of collagen at the aneurysm neck and in the aorta, compatible with an advanced stage of tissue remodeling and stabilized neointima.

Conclusion P8RI-SV demonstrated higher rates of neointimal formation covering the FD struts compared with bare-SV and Shield-PV at day 5 and day 28 in rabbits. These results confirm faster and improved arterial healing with P8RI coating; however, further studies are needed to evaluate the clinical benefits in patients.

WHAT IS ALREADY KNOWN ON THIS TOPIC

⇒ Surface modifications with specialized coatings have been proposed to reduce the thrombogenicity of flow diverters, but they have shown little to no effect on endothelialization and intimal healing. The P8RI coating is designed to address both by promoting rapid integration of the Silk Vista device into the intima of the parent vessel while inhibiting platelet and leukocyte activation.

WHAT THIS STUDY ADDS

⇒ The Silk Vista P8RI, Silk Vista bare, and Pipeline Vantage devices were implanted in a rabbit model to evaluate neointimal coverage of the struts at two time points (5 and 28 days) using optical coherence tomography imaging.

HOW THIS STUDY MIGHT AFFECT RESEARCH, PRACTICE OR POLICY

⇒ Our results suggest that the P8RI coating promotes faster and more robust neointimal formation compared with the Shield coating (Vantage) and the uncoated Silk Vista. The use of P8RI could enhance the safety and efficacy of the Silk Vista device, while its capacity for rapid arterial healing may allow for a reduced duration of dual antiplatelet therapy.

INTRODUCTION

In recent years, two main limitations have emerged with the use of flow diverters (FDs) for the endovascular treatment of unruptured aneurysms: a high rate of thromboembolic events leading to life-threatening complications or neurological disabilities, and an incomplete occlusion rate of over 20% at 1 year, despite indications extended to smaller aneurysms.[1–3]

These drawbacks stem from the metallic structure of FDs, prompting exploration into the concept of camouflaging the struts with coating or biomimetic surface modifications. Inspired by research on coronary stents,[4] the first commercially available FD with surface modification was the Pipeline Flex embolization device with Shield technology

J NeuroIntervent Surg: first published as 10.1136/jnis-2025-024213 on 23 October 2025. Downloaded from http://jnis.bmj.com/ on October 24, 2025 by guest. Protected by copyright, including for uses related to text and data mining, AI training, and similar technologies.

License CC BY-NC-ND 4.0

(Medtronic, Irvine, CA), using phosphorylcholine. This modification, covalently bound to the device, mimics cell membrane surfaces to reduce thrombogenicity, as demonstrated in preclinical experiments.[5–8]

Another approach was recently proposed using P8RI (P8RI-coated Silk Vista (P8RI-SV), Balt, Montmorency, France), a peptide derived from the juxtamembrane extracellular CD31 sequence. It mimics CD31 functions as: (1) a key co-receptor in fostering appropriate biological responses to mechanical stresses, ensuring the maintenance of endothelial main physiological functions; and (2) a co-inhibitor of platelet and leukocyte activation.[9] It has been shown to reduce platelet and leukocyte activation in vitro and improve arterial healing after stenting in vivo.[10] In other words, the P8RI biofunctionalized coating targeting CD31 would: (1) reduce platelet adhesion and stent thrombosis risk; (2) limit leukocyte entrapment and proteolytic activity, lowering the risk of secondary rupture; and (3) promote endothelialization and de novo arterial tissue formation, accelerating aneurysm exclusion and healing.

Optical coherence tomography (OCT) serves as an intravascular high-definition imaging technique using near-infrared light reflection, enabling the real-time monitoring of neointima and thrombus formation on the surface of an implanted device. Several studies have demonstrated the correlation between OCT imaging and the histological examination with coronary stents,[11] and with FDs.[12]

The purpose of this study was to compare the rate of neointimal formation between the P8RI-SV and the Pipeline Vantage with Shield technology (Shield-PV; Medtronic, Irvine, CA), and the bare Silk Vista (bare-SV; Balt, Montmorency, France) in a rabbit aneurysm model and in a normal aorta.

METHODS

P8RI-coated Silk Vista

P8RI peptides were covalently grafted onto the commercially available SV (Balt), as previously described.[10]

Animal care

We used female white New Zealand rabbits, weight 3.0–3.9 kg. All animal care and experimental procedures were conducted in accordance with the 2013 French legislation and European Community guidelines (directive 2010/63/UE for the Care and Use of Laboratory Animals). The study received approval of the regional Ethical and Animal Care Committee and French Ministry of Higher Education and Research (APAFIS#37873 –2022070114322309 v2). For each procedure, general anesthesia was obtained using an intramuscular injection of ketamine (17 mg/kg), xylazine (4 mg/kg), and acepromazine (0.85 mg/kg). Local anesthesia was assured by subcutaneous injection of lidocaine (6 mg/kg).

FD implantation

In this study, the elastase-induced arterial aneurysm of the right common carotid artery model was used following a previously described method.[13 14] A total of 23 elastase-induced aneurysms were randomly treated with either a P8RI-SV (n=10), a bare-SV (n=6), or a Shield-PV (n=7) 3 weeks after aneurysm creation. A second FD, identical to the first one, was implanted in the abdominal aorta covering at least one lumbar artery (n=7 P8RI-SV, n=6 bare-SV, and n=4 Shield-PV). The implanted devices are presented in online supplemental table 1. Group size discrepancy is due to device availability. The bare-SV group was also used as a control group in a preliminary experiment.[15] One day before FD implantation, animals were premedicated with aspirin (40 mg by mouth, daily),[10 16] which was continued until the final procedure.

Following device implantation, digital subtraction angiography (DSA) and DynaCT were acquired to evaluate device placement and deployment (Icono, Siemens, Erlangen, Germany). DSA and OCT (Dragonfly Catheter, St Jude Medical, Westford, MA) were performed on day 5 and day 28. Aneurysm occlusion was assessed for all subjects using the Raymond Roy occlusion classification three-point scale, including: grade 1, complete occlusion; grade 2, near-to-complete occlusion; and grade 3, incomplete occlusion.[17] At 28 days following implant, subjects were euthanized under general anesthesia during the last procedure, using a lethal injection of T61 (200 mg/mL embutramide, 50 mg/mL mebezonium iodide, and 5 mg/mL tetracaine hydrochloride).

Primary analysis: OCT imaging

OCT images were acquired with a 10 mm/s pullback speed, generating 540 frames/pullback with simultaneous intra-arterial iodine contrast injection at a rate of 3–6 mL/s for a total volume of 16–24 mL. The entire stent length was imaged, obtaining around 200 images per stent. OCT image analysis was performed with Ilumien Optis post-processing software (Abbott, Lake County, IL). For FDs implanted at the aneurysm location, 15 cross-sectional images at regular intervals per pullback were analyzed, including five images at the level of the neck, five images proximal to the neck, and five images distal to the neck. For FDs implanted in the aorta, 15 cross-sectional images at regular intervals per pullback were analyzed; if an ostium was noted, the next image without an ostium was chosen instead.

To assess stent coverage with neointimal formation, we used a four-point grading scale to classify each strut, as previously described: type 1, bare/uncovered strut; type 2, protruding/uncovered strut; type 3, protruding embedded/covered strut; and type 4, smooth embedded/covered.[11 18] The stent-coverage ratio was used as the number of stent struts covered by neointima/total stent struts. Stent-excellent coverage ratio was also used as the number of stent struts covered and embedded in a smooth neointima/total stent struts. The stent-coverage ratio represents the speed progression of endothelialization and tissue growth over the stent struts, while stent-excellent coverage represents complete arterial healing.[6]

To determine neointimal growth, several endpoints were evaluated. The endoluminal surface was automatically detected by the imaging system and manually corrected when necessary. Stent struts were manually traced and positioned in the center of the stent strut which showed a bright 'blooming' appearance. The following parameters were measured: lumen area (defined as contours of the vessel lumen), stent area (identified by circumferential area limited by the contours of the struts), neointimal area (stent area − lumen area), and neointimal ratio ([mean stent area − mean lumen area]/mean stent area). The neointimal ratio could show the volume of neointimal formation.[19] Mean parent artery diameter and the FD-to-artery oversizing ratio are also given as they may influence OCT-derived metrics. Analyses were performed by three readers (JC, GS, DC); all were blinded for the type of FD.

Secondary analysis: conventional histology and multiphoton microscopy

Conventional histology: aneurysm site

Immediately after euthanizing, all FDs at the aneurysm and aorta segments were harvested and fixed in 4% paraformaldehyde.

J NeuroInterv Surg: first published as 10.1136/jnis-2025-024213 on 23 October 2025. Downloaded from http://jnis.bmj.com/ on October 24, 2025 by guest. Protected by copyright, including for uses related to text and data mining, AI training, and similar technologies.

License CC BY-NC-ND 4.0

Conventional histomorphological analysis was conducted following previously established protocols on the FD implanted at the aneurysm location.[16 20] Fixed specimens were dehydrated through a graded ethanol series and embedded in methyl methacrylate. Longitudinal sections (~10 µm thick) were obtained across the aneurysm neck using a laser microtome (TissueSurgeon, LLS ROWIAK GmbH, Hannover, Germany). Sections were subsequently stained with hematoxylin and eosin (HE) or Masson's trichrome. High-resolution digitization of the stained slides was performed using the Hamamatsu NanoZoomer 2.0-RS digital scanner (Hamamatsu Photonics, Hamamatsu City, Shizuoka, Japan) at 40× magnification (corresponding to 227 nm/pixel).

For quantitative assessment, several regions were selected on each stained section outside the aneurysm neck, each encompassing six neointima-covered struts. In each region, the areas of the neointima (used as an indirect measure of thickness), media, and struts were manually delineated and quantified using FIJI software.[21] Since neointimal formation involves the dedifferentiation of smooth muscle cells into myofibroblast-like phenotypes and their migration from the media to the luminal surface,[22] we hypothesized that neointimal thickness might correlate with medial thickness. Therefore, the neointimal area was normalized to the medial area by calculating the neointima-to-media area ratio. At the aneurysm neck, tissue coverage occurs circumferentially around the struts, making it difficult to delineate precisely the neotissue layer. To estimate neotissue thickness in this region, the distance from the center of each strut to the luminal border of the parent artery was measured, and the mean value was calculated for each stained section. Cellularity of strut-covered tissue (or cell recolonization) was measured with the area occupied by nuclei (stained with hematoxylin) as an indicator of cell density. This area was normalized to the total surface of the neointima and expressed as a percentage (% cellular occupancy = [nuclear area/total neointimal area] × 100).

Multiphoton microscopy: aorta site

Multiphoton microscopy was performed on the explanted stented aorta luminal surface after being cut longitudinally, following previously described protocols.[23] A detailed methodology can also be found in the legend of the online supplemental figures. Multiphoton microscopy allows for increased penetration depth into biological tissue with a working distance of 400 µm that yields high-resolution three-dimensional (3D) images of the neointimal wall. The nuclei of the samples were stained with DAPI (4',6-diamidino-2-phenylindole) (D9542, Sigma-Aldrich) in Live Cell Imaging Solution (A14291DJ, Molecular Probes).

Quantification and orientation of collagen fibers and cell recolonization were assessed, as described previously.[10 23] All images were background-corrected and median-filtered equally across samples. The images were segmented, rendered to 3D volumes, and measured with Imaris software (Bitplane AG, Switzerland). Collagen fiber orientation was calculated using the OrientationJ plugin to FIJI (National Institutes of Health) software. Collagen quantification was performed after z-projection of the 3D raw images, splitting channels (Red Green Blue (RGB)), and establishing threshold ranges to better distinguish collagen fibers from the rest of the sample (artifacts or debris) and the image background. Collagen area (%) was quantified using the 'Analyze Particles' command. Cell recolonization using endothelial cell quantification was measured using the signals corresponding to DAPI staining on both photomultiplier tubes (red and green=yellow pseudocolors), and the images were rendered to 8-bit grayscale (binary contrast enhancement). Five to eight zones of each stent were assessed. For each image, a threshold intensity procedure was carried out so that the fluorescent nuclei would appear as black objects on a white background. Then, particles were analyzed to assess the circular areas of the pixels, and the cell nuclei were quantified using automated counting performed with ImageJ analysis software.

Statistical analysis

Data are expressed as frequency (%) for categorical variables and as mean±SD or as median (IQR) for continuous variables depending on their distribution. The Kruskal-Wallis test with Dunn's post-test was used for skewed data. Normally distributed variables were analyzed with one-way analysis of variance (ANOVA) with Tukey post-test. The Fisher exact test was performed for categorical variables. A value of $P<0.05$ was considered statistically significant. Statistical analysis and graphic representations were performed using the GraphPad Prism version 10.0.0 for Windows, GraphPad Software (Boston, MA).

RESULTS

Angiographic outcome

The average height, width, and neck of the elastase-induced aneurysms were similar in all three groups; the parent artery mean diameters and FD-to-artery oversizing ratio were also similar in all three groups (table 1). One Shield-PV placed at the aneurysm location was found occluded at the distal end at day 5 due to fish-mouthing and was excluded from the DSA and OCT analyses. It should be noted that this device was not oversized (FD-to-artery oversizing ratio=1.0). Two subjects, both with one P8RI-SV at the aneurysm site and one at the aorta, died at day 5 after the OCT control due to anesthesia. Of note, both stents were patents, and aneurysms were occluded; both were included for the day 5 comparison.

On day 28, similar rates of complete/near-complete occlusion were observed in the P8RI-SV (6/8, 75%) and Shield-PV (5/6, 83%) groups compared with bare-SV (3/6, 50%; P=0.577). Finally, none of the covered lumbar arteries occluded in all the groups, and besides the occluded Shield-PV, one Shield-PV at the aneurysm site demonstrated signs of intimal hyperplasia (online supplemental figure 1).

Overall stent coverage (aorta and aneurysm site)

In total, 1110 cross-sectional images were included, of which 38 (from 16 different stents) were finally excluded from the analysis due to artifacts. OCT assessment enabled the observation of the speed of neointimal formation covering the FD struts (figure 1). Overall (aorta and aneurysm site) stent-coverage ratio at day 5 was significantly higher with the P8RI-SV (84% (69–93)) compared with both bare-SV (63% (46–82)) and Shield-PV (67% (50–83)) (Kruskal-Wallis $P<0.0001$, Dunn post-test $P<0.0001$ for both, bare-SV vs Shield-PV P=0.485). At day 28, overall stent-coverage ratio was raised in all groups and remained significantly higher with P8RI-SV (93% (81–100)) compared with both bare-SV (72% (56–92)) and Shield-PV (76% (59–96)) (Kruskal-Wallis $P<0.0001$, Dunn post-test $P<0.0001$ for both, bare-SV vs Shield-PV P=0.766).

Finally, reflecting healed arterial tissue, overall stent-excellent coverage ratio at day 28 was also significantly higher with P8RI-SV (79% (56–96)) compared with both bare-SV (39% (14–68)) and Shield-PV (60% (38–90)) (Kruskal-Wallis $P<0.0001$, Dunn post-test $P<0.0001$ and P=0.002, respectively, bare-SV vs Shield-PV $P<0.0001$).

J NeuroInterv Surg: first published as 10.1136/jnis-2025-024213 on 23 October 2025. Downloaded from http://jnis.bmj.com/ on October 24, 2025 by guest. Protected by copyright, including for uses related to text and data mining, AI training, and similar technologies.

License CC BY-NC-ND 4.0

Table 1 Angiographic and OCT analysis

					P value post-test analysis		
	Bare-SV	Shield-PV	P8RI-SV	P value	Bare vs Shield	Bare vs P8RI	Shield vs P8RI
Aneurysm height (mm)	7.6±2.5	8.5±1.7	9.9±4.4	0.395	–	–	–
Aneurysm neck (mm)	3.9±1.1	4.4±1.2	3.8±1.5	0.648	–	–	–
Aneurysm width (mm)	2.9±0.6	3.50±0.3	3.6±0.8	0.290	–	–	–
Mean parent artery diameter*	3.36±0.31	3.43±0.49	3.47±0.36	0.789	–	–	–
FD-to-artery oversizing ratio*	1.20±0.11	1.17±0.14	1.17±0.14	0.880	–	–	–
Aneurysm occlusion, n	3 (50%)	5 (83%)	6 (75%)	0.577	–	–	–
Lumbar artery patent, n	6 (100%)	4 (100%)	7 (100%)	1	–	–	–
Aorta at day 5							
Neointimal ratio	0.0099±0.016	0.0100±0.022	0.0110±0.012	0.88	–	–	–
Stent-coverage (%)	50 (32–68)	58 (38–76)	72 (54–86)	**<0.0001**	0.562	**<0.0001**	**<0.001**
Stent-excellent coverage (%)	0 (0–12)	6 (0–51)	14 (0–35)	**<0.0001**	**0.005**	**<0.0001**	1
Aorta at day 28							
Neointimal ratio	0.0256±0.02	0.0408±0.02	0.0495±0.03	**<0.0001**	**<0.001**	**<0.0001**	0.078
Stent-coverage (%)	81 (58–95)	87 (71–100)	100 (87–100)	**<0.0001**	0.083	**<0.0001**	**0.009**
Stent-excellent coverage (%)	57 (21–85)	83 (59–100)	90 (76–100)	**<0.0001**	**<0.001**	**<0.0001**	0.359
Aneurysm site at day 5							
Neointimal ratio	0.0271±0.01	0.0537±0.03	0.0319±0.02	**<0.0001**	**<0.0001**	0.253	**<0.0001**
Stent-coverage (%)	78 (58–87)	75 (58–91)	87 (80–97)	**<0.0001**	1	**<0.0001**	**<0.0001**
Stent-excellent coverage (%)	36 (2–49)	49 (34–61)	58 (40–80)	**<0.0001**	**<0.001**	**<0.0001**	**0.012**
Aneurysm site at day 28							
Neointimal ratio	0.0179±0.02	0.0364±0.03	0.0284±0.02	**<0.0001**	**<0.0001**	**0.002**	**0.030**
Stent-coverage ratio (%)	68 (53–89)	64 (53–87)	89 (77–97)	**<0.0001**	1	**<0.0001**	**<0.0001**
Stent-excellent coverage (%)	19 (12–42)	46 (27–73)	70 (45–84)	**<0.0001**	**<0.0001**	**<0.0001**	**<0.001**

Bold P values denote statistical significance.
*Aneurysm site.
FD, flow diverter; OCT, optical coherence tomography; PV, Pipeline Vantage; SV, Silk Vista.

OCT analysis at the aorta site

Complete results of OCT analysis of the FD implanted in the aorta are presented in table 1. At day 5, we observed a similar rate of neointimal ratio (P=0.88) in all three groups. Rate of stent coverage was significantly higher with P8RI-SV compared with bare-SV and Shield-PV (P<0.0001 and P<0.001, respectively), while stent-excellent coverage ratio was similar between Shield-PV and P8RI-SV (P=1) and both were significantly higher than bare-SV (P=0.005 for Shield-PV vs bare-SV and P<0.0001 for P8RI-SV vs bare-SV).

At day 28, P8RI-SV presented a significantly higher rate of neointimal ratio, stent coverage, and stent-excellent coverage when compared with bare-SV (all P<0.0001) and a significantly higher rate of stent coverage when compared with Shield-PV (P<0.0001).

OCT analysis at the aneurysm site

Complete results of OCT analysis of the FD implanted at the aneurysm site are also presented in table 1. On day 5, Shield-PV presented a higher rate of neointimal ratio than both bare-SV and P8RI-SV (P<0.0001 all). However, the stent-coverage ratio was similar between bare-SV and Shield-PV (P=1), with both stent-coverage ratio and stent-excellent coverage ratio significantly higher in the P8RI-SV group compared with bare-SV (P<0.0001, both) and Shield-PV (P<0.0001 and 0.012, respectively).

On day 28, Shield-PV presented a significantly higher neointimal ratio compared with P8RI-SV and bare-SV (P=0.030 and P<0.0001, respectively). Stent-coverage and stent-excellent coverage ratios were again significantly greater with P8RI-SV compared with bare-SV (P<0.0001, both) and Shield-PV (P<0.0001 and P<0.001, respectively).

Histological and multiphoton microscopy comparisons

HE and Masson's trichrome stainings of tissue sections showed that the struts of P8RI-SV were covered by well-organized neotissue (figure 2, online supplemental figure 2), both at the aneurysm neck and in arterial regions away from it. In contrast, the struts of bare-SV and Shield-PV were covered by tissue often infiltrated by immune cells.

Histological quantification of neointimal thickness at the aneurysm neck showed a trend toward increased neotissue formation with P8RI-SV compared with the other two devices, bare-SV and Shield-PV (online supplemental figure 3). A trend toward higher collagen content within the neointima tended to be higher in aneurysms treated with the P8RI-SV stent compared with those treated with bare-SV or P8RI-SV (online supplemental figure 4). Multiphoton microscopy quantification of neointimal thickness (aorta sites) based on collagen signal from second harmonic generation showed no statistically significant difference ($F_{(2, 24)} = 1861$ and P=0.180) between the three groups (bare-SV 42.95±8.41 µm and Shield-PV 47.02±16.91 µm), although there was also a trend toward greater thickness in the P8RI-SV group (57.33±9.53 µm) (online supplemental figure 5). None of these results achieved statistical significance. Finally, cell

J NeuroIntervent Surg: first published as 10.1136/jnis-2025-024213 on 23 October 2025. Downloaded from http://jnis.bmj.com/ on October 24, 2025 by guest. Protected by copyright, including for uses related to text and data mining, AI training, and similar technologies.

License CC BY-NC-ND 4.0

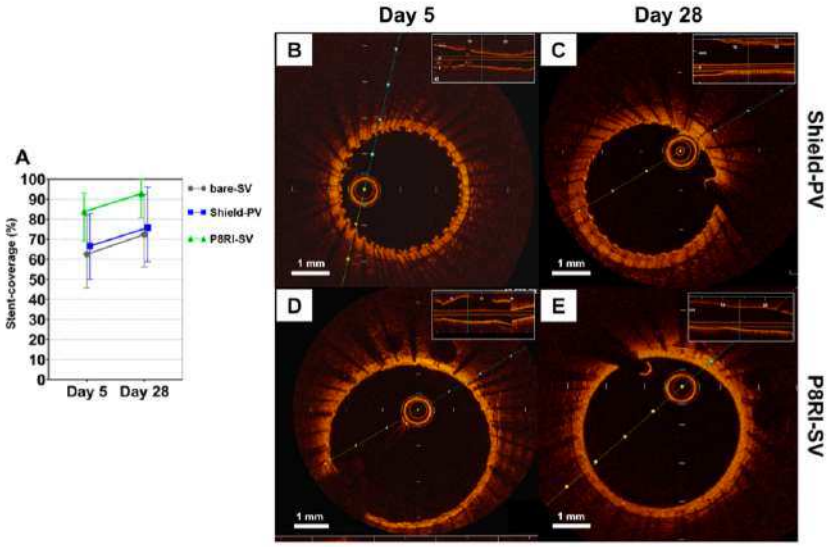


Figure 1 OCT analysis. (A) Overall stent-coverage ratio at day 5 and day 28. (B–E) Example of OCT images of flow diverters implanted in the aorta. (B and C) Shield-PV on day 5 (B) and on day 28 (C). (D and E) P8RI-SV on day 5 (D) and on day 28 (E). The struts of the Shield-PV present a delay of tissue coverage compared with the P8RI-PV. Small images on the top right corner of each panel represent the longitudinal reconstruction of the OCT acquisition. OCT, optical coherence tomography; PV, Pipeline Vantage; SV, Silk Vista.

recolonization (DAPI+cells) in luminal views of rabbit aorta captured in 3D with multiphoton microscopy showed significant differences in one-way ANOVA ($F_{(2, 34)} = 5.196$ and $P=0.0107$) between treatments (especially between P8RI-SV and Shield-PV; $P=0.0091$) (online supplemental figure 6). Cellular recolonization was similar in all three groups at the aneurysm location (online supplemental figure 7).

DISCUSSION

In the present preclinical study, using OCT evaluation, we found that P8RI-SV provides a higher rate of neointimal coverage compared with bare-SV and Shield-PV ($P<0.0001$) at day 5 and day 28. This illustrates the key functional advantage of the P8RI coating for FDs in aneurysm embolization. The OCT analysis demonstrated that all three devices exhibited moderate to high coverage at day 5, with similar increases in all three groups at day 28, but with P8RI remaining significantly higher at both time points. This pattern suggests that P8RI stimulates early endothelialization and tissue formation over the struts, leading to faster arterial healing without raising the risk of covered branch occlusion. These results are aligned with previous studies on Silk Vista with P8RI coating.[10 15] Also consistent with our observations, previous studies found similar speed of neointimal growth at early time points for Pipeline Flex devices and PV implanted in rabbits and pigs.[19 24]

Concerns were raised with the Shield coating regarding the risk of delayed endothelialization due to initial protein adsorption onto metallic strut being inhibited.[25] Furthermore, platelets play a positive role in the amplification of angiogenesis where arterial tissue healing is needed.[26] Matsuda *et al* found Flex Pipeline embolization device (PED) with Shield showed a similar neointimal volume to bare Flex PED.[19] Contradictory findings were found by Caroff *et al* who observed less neointimal formation with Flex PED with Shield.[12] Finally, two recent publications showed no significant delay of neointimal growth with Shield-PV compared with bare FDs.[16 24] Here, we found an overall similar rate of neointimal formation with the Shield-PV when compared with the bare-SV at day 5 and day 28.

OCT has become an important tool for the evaluation of clot burden or neointimal formation in preclinical studies testing stents. With a high resolution (10–20 µm limited sensitivity), OCT can detect early tissue formation over the device struts. Interest in achieving complete neointimal coverage increased in parallel with concerns regarding delayed aneurysm occlusion and late thromboembolic complications. OCT offers detailed assessment strut by strut of the tissue coverage after FD implantation. In coronary stenting studies, including major trials using OCT, coverage is evaluated as a binary outcome strut by strut and has been used as a primary endpoint.[27] It is considered a surrogate for the completeness of neointimal healing, which is believed to be protective against stent thrombosis.[28] Furthermore, coverage assessed by OCT correlates with histological neointimal healing and endothelialization after FD implantation in animal models.[29] Moreover, it has the advantage that it can be repeated at different time points without the need to sacrifice the subject. In a previous study, we confirmed that the tissue formation over the struts observed at day 5 was in fact neointima.[15]

Area assessment of neointimal growth is also accurately provided using OCT. Although it is traditionally used for hyperplasia evaluation in cardiology research,[27] it has been used to monitor neointimal growth in FD research in animal models.[12 19 24] However, higher volume or surface of neotissue formation does not necessarily correlate with better healing as it leads to intimal hyperplasia and in-stent stenosis.[12 30] Conversely, a delayed endothelialization may lead to unorganized thrombus formation and intimal hyperplasia. Here, we found a similar

J NeuroIntervent Surg: first published as 10.1136/jnis-2025-024213 on 23 October 2025. Downloaded from http://jnis.bmj.com/ on October 24, 2025 by guest. Protected by copyright, including for uses related to text and data mining, AI training, and similar technologies.

License CC BY-NC-ND 4.0

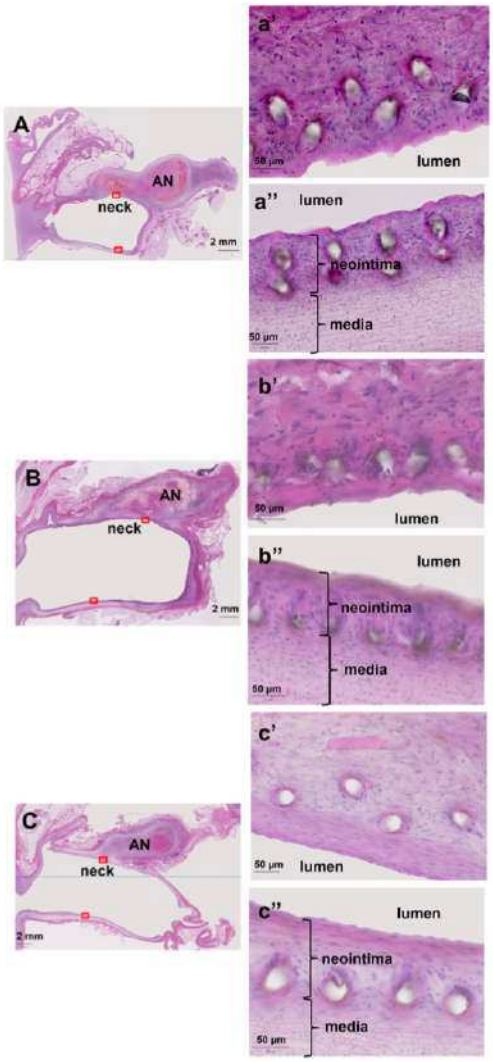


Figure 2 Hematoxylin and eosin staining of whole longitudinal sections across the necks of aneurysms treated with the different flow diverters. Bare-SV (A), Shield-PV (B), and P8RI-SV (C). High-magnification views of regions within the aneurysm neck and arterial wall outside the neck (a', a", b', b", c', c") show well-organized cell layers covering the struts in P8RI-SV-treated aneurysms (c', c"), in contrast to bare-SV (a', a") and Shield-PV (b', b"), where the tissue covering the struts consists of dispersed cells with no clearly defined layers, and in some cases, infiltration by immune cells. AN, aneurysm; PV, Pipeline Vantage; SV, Silk Vista.

neointimal ratio at the aorta site at day 5, while neointimal coverage was significantly higher at day 28 for P8RI-SV. Conversely, at the aneurysm site, Shield-PV expressed a significantly higher level of neointimal ratio at day 5 and neointimal ratio at day 28. However, it should be noted that one case of Shield-PV at the aneurysm site presented objective signs of hyperplasia, influencing these outcomes.

As expected following OCT imaging, histological assessment confirmed that the P8RI-SV struts were covered by well-organized neointima. In contrast, the struts of bare-SV and Shield-PV were covered by loosely organized tissue, often infiltrated by immune cells. Histological quantification showed a trend toward increased neotissue formation with a higher rate of collagen with P8RI-SV compared with the other two devices. These findings suggest that P8RI-SV promotes the formation of a more stable and higher-quality neotissue, potentially reducing blood flow disturbances, neointimal hyperplasia, and thrombus formation. It also supports the efficacy and rapidity of cellular recruitment on the surface of P8RI-SV stents. The lack of statistical significance may be attributed to the limited number of slices analyzed per sample and the presence of hyperplasia in the Shield-PV group. An increase in collagen content within this tissue may reflect a transition from a proliferative to a maturation phase, like the process of wound healing. This tissue remodeling is characterized by increased extracellular matrix deposition, contributing to vascular stabilization and potentially limiting excessive neointimal hyperplasia. In this context, collagen deposition, particularly of organized fibrillar types, may serve as a marker of neointimal stabilization rather than pathological fibrosis.[31] These findings suggest that P8RI-SV may promote a more advanced stage of tissue remodeling, favoring stabilization of the neointima and potentially reducing the risk of excessive hyperplastic response.

This study has some limitations. Experiments were performed in healthy rabbits, and we acknowledge that animal models are imperfect predictors of the human response. Also, small sample size and early control may be responsible for a lack of power, preventing the detection of a difference for the aneurysm occlusion rate; therefore, any potential impact on clinical outcomes, including antiplatelet therapy duration, remains to be established. Finally, as this study focused on neointima formation, we did not assess the antithrombotic and anti-inflammatory properties of the P8RI coating, which were previously evaluated in two preclinical studies.[10 15]

CONCLUSION

To summarize, in a rabbit model, we demonstrated that the P8RI-SV enabled faster and greater neointimal formation as compared with bare-SV and Shield-PV. These findings are of potential interest for achieving higher aneurysm occlusion rates and enabling earlier discontinuation of antiplatelet therapy in clinical practice; however, further studies are warranted to determine whether this biological effect translates into clinical benefits.

Author affiliations
[1]EMIS Research Laboratory, CHU Limoges, Limoges, France
[2]NEURI Vascular Center, Hôpital Bicêtre NEURI, Le Kremlin-Bicêtre, France
[3]CNRS, XLIM, UMR 7252, University of Limoges, Limoges, France
[4]INSERM U1195, Paris-Saclay University Faculty of Medecine, Le Kremlin-Bicetre, France
[5]Interventional neuroradiology, Centre Hospitalier Universitaire de Limoges, Limoges, France
[6]Vascular Surgery, CHU Limoges, Limoges, France
[7]Interventional Neuroradiology, Vall d'Hebron University Hospital, Barcelona, Spain
[8]Vall d'Hebron Research Institute, Barcelona, Spain
[9]Pharmacy, University-hospital of Limoges, Limoges, France
[10]Inserm U1094, IRD U270, EpiMaCT - Epidémiologie des maladies chroniques en zone tropicale, Institut d'Epidémiologie et de Neurologie Tropicale, OmegaHealth, University of Limoges, Limoges, France

J NeuroIntervent Surg: first published as 10.1136/jnis-2025-024213 on 23 October 2025. Downloaded from http://jnis.bmj.com/ on October 24, 2025 by guest. Protected by copyright, including for uses related to text and data mining, AI training, and similar technologies.

License CC BY-NC-ND 4.0

[11]Interventional Neuroradiology, CHU Limoges, Limoges, France
[12]Cell Biology, CHU Limoges, Limoges, France

Acknowledgements Balt sponsored the study. Histological analyses were performed within the PLATINOM platform, supported by the European Regional Development Foundation and the French government with the New Aquitaine region (FEDER-PILIM 2015-2020 and 2021-2027). We thank Yann Launay for his help in environmental electronic microscopy images capture.

Contributors JC, GF, SMB, MLP, VR, JM, CC, LS, CM, FT, AR contributed to the conception and design of the studies. All authors contributed to the acquisition of the data and the interpretation of the data. JC, GF, SMB, FT, MLP, FT, and AR drafted the work and revised it for significant intellectual content. All authors approved the final version of the manuscript, and agreed to be accountable for all aspects of the work, including its accuracy and integrity. JC is the guarantor.

Funding The authors have not declared a specific grant for this research from any funding agency in the public, commercial, or not-for-profit sectors.

Competing interests JC received an educational grant from Balt, Medtronic, Phenox, Microvention, the Philippe Foundation, the French Society of Radiology, and the French Society of Neuroradiology; and received honoraria for lectures from Balt. CM received honoraria for lectures from Balt. LS is a consultant for Microvention, Balt, Phenox, Stryker, Medtronic. AR received honoraria for lectures from Balt.

Patient consent for publication Not applicable.

Ethics approval Not applicable.

Provenance and peer review Not commissioned; externally peer reviewed.

Data availability statement Data are available upon reasonable request.

Supplemental material This content has been supplied by the author(s). It has not been vetted by BMJ Publishing Group Limited (BMJ) and may not have been peer-reviewed. Any opinions or recommendations discussed are solely those of the author(s) and are not endorsed by BMJ. BMJ disclaims all liability and responsibility arising from any reliance placed on the content. Where the content includes any translated material, BMJ does not warrant the accuracy and reliability of the translations (including but not limited to local regulations, clinical guidelines, terminology, drug names and drug dosages), and is not responsible for any error and/or omissions arising from translation and adaptation or otherwise.

ORCID iDs
Jonathan Cortese https://orcid.org/0000-0002-1616-9113
Géraud Forestier https://orcid.org/0000-0003-4797-9693
Sylvia M Bardet https://orcid.org/0000-0002-0217-6910
Maxime Baudouin https://orcid.org/0000-0001-7240-220X
Francesco Diana https://orcid.org/0000-0002-3245-917X
Laurent Spelle https://orcid.org/0000-0002-6748-8528
Aymeric Rouchaud https://orcid.org/0000-0003-0902-3375

REFERENCES

1 Ghaith AK, Greco E, Rios-Zermeno J, *et al*. Safety and efficacy of the pipeline embolization device for treatment of small vs. large aneurysms: a systematic review and meta-analysis. *Neurosurg Rev* 2023;46:284.
2 Gory B, Berge J, Bonafé A, *et al*. Flow Diverters for Intracranial Aneurysms: The DIVERSION National Prospective Cohort Study. *Stroke* 2019;50:3471–80.
3 Shehata MA, Ibrahim MK, Ghozy S, *et al*. Long-term outcomes of flow diversion for unruptured intracranial aneurysms: a systematic review and meta-analysis. *J Neurointerv Surg* 2023;15:898–902.
4 Lewis AL, Stratford PW. A Review on Phosphorylcholine-Coated Stents. *J Long Term Eff Med Implants* 2017;27:233–52.
5 Hagen MW, Girdhar G, Wainwright J, *et al*. Thrombogenicity of flow diverters in an ex vivo shunt model: effect of phosphorylcholine surface modification. *J Neurointerv Surg* 2017;9:1006–11.
6 Matsuda Y, Jang D-K, Chung J, *et al*. Preliminary outcomes of single antiplatelet therapy for surface-modified flow diverters in an animal model: analysis of neointimal development and thrombus formation using OCT. *J Neurointerv Surg* 2019;11:74–9.
7 Starke RM, Thompson J, Pagani A, *et al*. Preclinical safety and efficacy evaluation of the Pipeline Vantage Embolization Device with Shield Technology. *J Neurointerv Surg* 2020;12:981–6.
8 Zoppo CT, Mocco J, Manning NW, *et al*. Surface modification of neurovascular stents: from bench to patient. *J Neurointerv Surg* 2024;16:908–13.
9 Andreata F, Syvannarath V, Clement M, *et al*. Macrophage CD31 Signaling in Dissecting Aortic Aneurysm. *J Am Coll Cardiol* 2018;72:45–57.
10 Cortese J, Rasser C, Even G, *et al*. CD31 Mimetic Coating Enhances Flow Diverting Stent Integration into the Arterial Wall Promoting Aneurysm Healing. *Stroke* 2021;52:677–86.
11 Guagliumi G, Sirbu V. Optical coherence tomography: high resolution intravascular imaging to evaluate vascular healing after coronary stenting. *Cathet Cardiovasc Intervent* 2008;72:237–47.
12 Caroff J, Tamura T, King RM, *et al*. Phosphorylcholine surface modified flow diverter associated with reduced intimal hyperplasia. *J Neurointerv Surg* 2018;10:1097–101.
13 Altes TA, Cloft HJ, Short JG, *et al*. Creation of Saccular Aneurysms in the Rabbit. *AJR Am J Roentgenol* 2000;174:349–54.
14 Cortese J, Bayraktar EA, Oliver AA, *et al*. Creating elastase aneurysms in rabbits: a video primer. *J Neurointerv Surg* 2025;17:1133.
15 Cortese J, Forestier G, Bardet SM, *et al*. Preclinical in vitro and in vivo results of the new Silk Vista flow diverter with P8RI coating. *J Neurointerv Surg* 2025;17:775–81.
16 Forestier G, Cortese J, Bardet SM, *et al*. Comparison of arterial wall integration of different flow diverters in rabbits: the CICAFLOW study. *J Neuroradiol* 2024;51:236–41.
17 Mascitelli JR, Moyle H, Oermann EK, *et al*. An update to the Raymond–Roy Occlusion Classification of intracranial aneurysms treated with coil embolization. *J Neurointerv Surg* 2015;7:496–502.
18 Murase S, Suzuki Y, Yamaguchi T, *et al*. The relationship between re-endothelialization and endothelial function after DES implantation: comparison between paclitaxel eluting stent and zotarolims eluting stent. *Cathet Cardiovasc Intervent* 2014;83:412–7.
19 Matsuda Y, Chung J, Lopes DK. Analysis of neointima development in flow diverters using optical coherence tomography imaging. *J Neurointerv Surg* 2018;10:162–7.
20 Janot K, Boulouis G, Forestier G, *et al*. WEB shape modifications: angiography–histopathology correlations in rabbits. *J Neurointerv Surg* 2024;16:302–7.
21 Schindelin J, Arganda-Carreras I, Frise E, *et al*. Fiji: an open-source platform for biological-image analysis. *Nat Methods* 2012;9:676–82.
22 Déglise S, Bechelli C, Allagnat F. Vascular smooth muscle cells in intimal hyperplasia, an update. *Front Physiol* 2022;13:1081881.
23 Bardet SM, Cortese J, Blanc R, *et al*. Multiphoton microscopy for pre-clinical evaluation of flow-diverter stents for treating aneurysms. *J Neuroradiol* 2021;48:200–6.
24 Zoppo CT, Epshtein M, Gounis MJ, *et al*. Longitudinal healing flow diverting stents with phosphorylcholine surface modification. *J Neurointerv Surg* 2024;16:582–6.
25 Lewis AL, Stratford PW. Phosphorylcholine-coated stents. *J Long Term Eff Med Implants* 2002;12:231–50.
26 Patzelt J, Langer HF. Platelets in angiogenesis. *Curr Vasc Pharmacol* 2012;10:570–7.
27 Guagliumi G, Costa MA, Sirbu V, *et al*. Strut coverage and late malapposition with paclitaxel-eluting stents compared with bare metal stents in acute myocardial infarction: optical coherence tomography substudy of the Harmonizing Outcomes with Revascularization and Stents in Acute Myocardial Infarction (HORIZONS-AMI) Trial. *Circulation* 2011;123:274–81.
28 Gutiérrez-Chico JL, Alegría-Barrero E, Teijeiro-Mestre R, *et al*. Optical coherence tomography: from research to practice. *Eur Heart J Cardiovasc Imaging* 2012;13:370–84.
29 Murata A, Wallace-Bradley D, Tellez A, *et al*. Accuracy of optical coherence tomography in the evaluation of neointimal coverage after stent implantation. *JACC Cardiovasc Imaging* 2010;3:76–84.
30 Mühl-Benninghaus R, Haußmann A, Simgen A, *et al*. Transient in-stent stenosis: a common finding after flow diverter implantation. *J Neurointerv Surg* 2019;11:196–9.
31 Abraham LC, Dice JF, Finn PF, *et al*. Extracellular matrix remodeling--methods to quantify cell-matrix interactions. *Biomaterials* 2007;28:151–61.

J Neurointervent Surg: first published as 10.1136/jnis-2025-024213 on 23 October 2025. Downloaded from http://jnis.bmj.com/ on October 24, 2025 by guest. Protected by copyright, including for uses related to text and data mining, AI training, and similar technologies.

License CC BY-NC-ND 4.0

License CC BY-NC-ND 4.0

Rosuvastatine pour les anévrismes intracrâniens traités par dispositif de diversion de flux: étude préclinique chez le lapin

Les anévrismes intracrâniens (AI), touchant 2-3% des adultes, peuvent provoquer une hémorragie sous-arachnoïdienne grave. Les divertisseurs de flux (DF) traitent les AI, mais présentent des risques de thromboembolie et d'occlusion incomplète (jusqu'à 20%). Les statines pourraient améliorer les résultats des DF par des effets vasculaires.

Dans un modèle de lapin, des anévrismes induits par élastase ont été traités par DF. Les lapins ont reçu de la Rosuvastatine plus Aspirine (Rosu+ASA, n=13) ou Aspirine seule (ASA, n=9). Après deux semaines, l'occlusion des anévrismes, la perméabilité des branches et l'endothélialisation ont été évaluées. Rosu+ASA a montré une meilleure occlusion (84.6% vs 66.6%), une perméabilité accrue (≥1 mm: 94.4% vs 46.1%, p=0.007) et un meilleur résultat composite (76.9% vs 22.2%, p=0.011). La couverture endothéliale était corrélée aux niveaux de Rosuvastatine (r=0.92, p=0.02). La Rosuvastatine a amélioré l'efficacité des DF, suggérant des études supplémentaires.

Mots-clés : Anévrismes intracrâniens ; diversor de flux ; rosuvastatine ; endothélialisation.

La Rosuvastatina nel trattamento degli aneurismi cerebrali con flow diverter : studio preclinico in modello animale

Gli aneurismi intracranici (IAs) colpiscono il 2-3% degli adulti e possono rompersi, causando emorragia subaracnoidea, che ha elevata morbilità e mortalità. I flow diverter (FDs) permettono di trattare gli IAs ricostruendo il vaso parente, ma hanno complicazioni quali il tromboembolismo e l'occlusione incompleta raggiunge il 20% in alcuni casi. Le statine possono migliorare incrementare l'efficacia dei FDs migliorandone l'endotelizzazione. Modelli di aneurisma creati con elastasi in conigli, sono stati trattati con FDs. Ai conigli sono stati somministrati Rosuvastatina ed Aspirina (Rosu+ASA, n=13) o solo Aspirina (ASA, n=9). Dopo due settimane, sono stati valutati occlusione degli aneurismi, pervietà dei rami coperti dai FD ed endotelializzazione dei FD. Il gruppo Rosu+ASA ha mostrato un'occlusione degli aneurismi più elevata (84.6% vs 66.6%), una maggiore pervietà dei rami (≥1 mm: 94.4% vs 46.1%, p=0.007) e un outcome composito superiore (76.9% vs 22.2%, p=0.011). L'endotelizzazione del FD è risultata fortemente correlata con i livelli sierici di Rosuvastatina (r=0.92, p=0.2). La Rosuvastatina ha migliorato efficacia e sicurezza dei FDs.

Parole chiavi : Aneurismi cerebrali ; flow diverter ; rosuvastatina ; endotelizzazione.

Rosuvastatin for intracranial aneurysms treated with flow diverter: preclinical study in rabbits

Intracranial Intracranial aneurysms (IAs), affecting 2-3% of adults, can rupture, causing subarachnoid hemorrhage with high morbidity and mortality. Flow diverters (FDs) treat IAs by reconstructing arteries but face challenges like thromboembolism and incomplete occlusion (up to 20%). Statins may enhance FD outcomes via vascular effects like improved endothelial repair. In a rabbit model, elastase-induced aneurysms were treated with FDs. Rabbits received Rosuvastatin plus Aspirin (Rosu+ASA, n=13) or Aspirin alone (ASA, n=9). After two weeks, aneurysm occlusion, branch patency, and endothelialization were assessed. Rosu+ASA showed higher occlusion (84.6% vs 66.6%), better branch patency (≥1 mm: 94.4% vs 46.1%, p=0.007), and a superior composite outcome (76.9% vs 22.2%, p=0.011). Endothelial coverage correlated with Rosuvastatin levels (r=0.92, p=0.02). Rosuvastatin improved FD efficacy, suggesting potential for further study.

Keywords: intracranial aneurysms ; flow diverter ; rosuvastatin ; endothelialization.